Universidade de Lisboa

Faculdade de Farmácia

Anti-tumor immunity induced by a novel nanoparticulate vaccine: a mechanistic approach

Eva Zupančič

Orientadores: Prof. Doutora Helena F. Florindo
Prof. Doutor João Nuno Moreira
Prof. Doutora Mafalda Videira

Tese especialmente elaborada para a obtenção do grau de doutor no ramo de Farmácia, especialidade de Tecnologia Farmacêutica

2016

Universidade de Lisboa

Faculdade de Farmácia

Anti-tumor immunity induced by a novel nanoparticulate vaccine: a mechanistic approach

Eva Zupančič

Orientadores: Prof. Doutora Helena F. Florindo
Prof. Doutor João Nuno Moreira
Prof. Doutora Mafalda Videira

Tese especialmente elaborada para a obtenção do grau de doutor no ramo de Farmácia, especialidade de Tecnologia Farmacêutica

Júri
Presidente: Prof. Doutora Matilde Castro
Vogais: Prof. Doutor Steffen Jung
Prof. Doutora Julijana Kristl
Prof. Doutor Bruno Sarmento
Prof. Doutor Antonio Almeida
Prof. Doutora Helena F. Florindo

This research work was funded by Fundação para a Ciência e a Technologia (FCT), Ministério da Educação e Ciência, Portugal for the PhD Grant SFRH/BD/78480/2011 and Research projects UTAP-ICDT/DTP-FTO/0016/2014 and ENMed/0003/2015, under the framework of EuroNanoMed-II; iMed.ULisboa grant UID/DTP/04138/2013. In Israel, the Jung's laboratory is supported by the European Research Council (340345). Eva Zupančič is also grateful to the EMBO for the Short Term Fellowship (ASTF 277-2015) and to the EACR for a Travel Grant.

2016

This thesis was supervised by:

Prof. Dr. Helena F. Florindo (supervisor)
Assistant Professor
Research Institute for Medicines (iMed.ULisboa), Faculty of Pharmacy, Universidade de Lisboa, Lisbon, Portugal.

Prof. Dr. João Nuno Moreira (co-supervisor)
Assistant Professor
Center for Neuroscience and Cell Biology (CNC) and Faculty of Pharmacy (FFUC), University of Coimbra, Portugal

Prof. Dr. Mafalda Videira (co-supervisor)
Assistant Professor
Research Institute for Medicines (iMed.ULisboa), Faculty of Pharmacy, Universidade de Lisboa, Lisbon, Portugal.

This work was developed at:

Research Institute for Medicines (iMed.ULisboa), Faculty of Pharmacy, Universidade de Lisboa, Lisbon, Portugal.
&
Prof. Steffen Jung's laboratory at the Department of Immunology, Faculty of Biology, the Weizmann Institute of Science, Rehovot, Israel.

This research work was funded by Fundação para a Ciência e a Technologia (FCT), Ministério da Educação e Ciência, Portugal for the PhD Grant SFRH/BD/78480/2011 and Research projects UTAP-ICDT/DTP-FTO/0016/2014 and ENMed/0003/2015, under the framework of EuroNanoMed-II; iMed.ULisboa grant UID/DTP/04138/2013. In Israel, the Jung's laboratory is supported by the European Research Council (340345). Eva Zupančič is also grateful to the EMBO for the Short Term Fellowship (ASTF 277-2015) and to the EACR for a Travel Grant.

Declaration

This doctoral research work was carried out under the supervision of Prof. Helena F Florindo from the Department of Galenic Pharmacy and Pharmaceutical Technology at the Research Institute for Medicines (iMed.ULisboa), Faculty of Pharmacy, Universidade de Lisboa, Lisbon, Portugal.

I declare that it summarizes my independent research.

Eva Zupančič

To my loving family

Preface

“But for man, no rest and no ending. He must go on, conquest beyond conquest. First this little planet and all its winds and ways, and then all the laws of mind and matter that restrain him. Then the planets about him, and, at last, out across immensities to the stars. And when he has conquered all the deep space, and all the mysteries of time, still, he will be beginning." by Herbert George Wells in the Things to come (1936).

These words best describe the dynamic process of science and moreover, present the keystone of a breakthrough research and outstanding researchers. First we need to study the past, then improve and fight for our present, which will give us an opportunity to build and nurture a better future.

For the last 100 years, we have been facing a tremendous progress in nanotechnology, and more recently in immunology and cancer immunotherapy. In fact, nanomedicine is currently an emerging field with the successful application of nanotechnology to develop personalized tools to diagnose, prevent or treat specific pathological conditions. In addition, the recent stunning results obtained at clinical level with the use of T-cell therapy and immunecheckpoint inhibitors in patients presenting advanced stages of leukemia, melanoma, and lung cancers, have prompt the scientific community to critical role of the immune system in the destruction of those malignant cells. However, I believe that the up-to-date development procedure of nanosystems based on trial-by-error does not allow to control the overall physicochemical properties of these nanocarriers and thus may be underlying their premature failure at preclinical settings. Therefore, the present research project aims to combine both cancer immunotherapy and nanotechnology to develop a novel nanotechnology-based system to successfully modulate the activity and proliferation of immune cells, overcoming the tumor-stroma immunosuppressive microenvironment.

This research work was developed between September 2012 and August 2016, mainly in two research laboratories: Prof. Florindo laboratory at Research Institute for Medicines (iMed.ULisboa), Faculty of Pharmacy, University de Lisbon, Lisbon, Portugal and Prof. Jung laboratory at the Department of Immunology, Faculty of Biology, Weizmann institute of Science, Rehovot, Israel.

Under the supervision of Prof. Helena F. Florindo, I have developed, optimized and extensively characterized novel immunotherapeutic delivery systems for the delivery of both antigens and adjuvants to single targeted immune cells. Different types of NP have been developed in order to best attain the most efficient parameters for cancer immunotherapeutics.

The effect of multiple experimental parameters, such as nature of protein association (adsorbed vs. encapsulated) and polymers and surfactant concentrations on particle size, polydispersity index, zeta potential, encapsulation efficiency and integrity of the protein, surfactant residual amount, and integrity of the polymer after the formulation process were fully addressed. The effect of the optimal nanodelivery system on the viability of dendritic and cancer cells was also studied in order to ensure the safety of the system.

The effect of the optimized nanoparticulate vaccine on immune cells, both *in vitro* an *in vivo*, were performed at Prof. Steffen Jung's laboratory, at the Weizmann institute of Science, Rehovot, Israel. Professor Steffen Jung is a collaborator of Prof. Helena Florindo's laboratory and in his laboratory, I gained an extensive knowledge about the complexity of immune response in steady state conditions. Moreover, having in consideration the promising data obtained regarding the effect in the proliferation of different subpopulations of immune cells, it was possible to assess the immunotherapeutic potential of developed vaccine on the melanoma tumor-bearing mice. Different techniques were developed and explored to accomplish those goals, namely lymph node isolation, dendritic cell plasticity characterization and determination of T cell proliferation and activation.

Apart from those two research groups, existing collaborations with other laboratories and institutions were important to achieve the major goals of this multidisciplinary project. Prof. Carlos Afonso and Dr. Catarina Rodrigues from the Bioorganic chemistry group at iMed.ULisboa synthesized fluorophore-grafted polymer (PLGA-Rho) that was used for the *in vitro* and *in vivo* uptake studies. Prof. Ana S. Viana from Chemistry and Biochemistry Center, Sciences Faculty, Universitdade de Lisboa, Portugal provided further insight on the physicochemical characterization and diameter distribution of nanoparticle by atomic force microscopy. Prof. João Pinto and Dr Maria Paisana from the Innovative platforms for non-parental delivery systems at iMed.ULisboa provided the assistance with DSC and FTIR for more detailed physicochemical characterization of developed nanoparticate vaccine. Prof. Lea Eisenbach from Department of Immunology, Faculty of Biology, Weizmann institute of Science, provided a B16.MO5 melanoma cell. These melanoma cells are transfected with the Ovalbumin gene and therefore allowed to evaluate the specific nature of the enhanced immune response. Prof. Zelig Eshhar, from Department of Immunology at the Weizmann institute of Science, Rehovot, also supported the assessment of the efficacy of our nanovaccines, using specific tumor associated antigens. Finally, Prof. Ronit Satchi-Fainaro and PhD student Eilam Yeini from the Department of Physiology and Pharmacology, Sackler School of Medicine, Tel Aviv University, Israel, helped with the simultaneously cytokines

and chemokines immunoassay in the serum of melanoma-bearing mice after the treatment with the nanoparticulate vaccine.

The results reported in this PhD thesis were only possible due to this highly interdisciplinary environment.

Abstract

Biodegradable polymeric nanoparticles (NP) are promising tools for tumor eradication. Different nanovaccines based on the aliphatic-polyester (poly(lactic-co-glycolic acid) (PLGA) have been developed and optimized to investigate how different methods for antigen association to nanoparticulate carriers affect antigen uptake by antigen presenting cells (APC) and the generation and nature of antigen-specific immune responses. The different experimental parameters have been tested in order to predict the effect of the nature of protein association (adsorbed vs. entrapped) and polymers/surfactant concentrations, on NP average mean diameter, polydispersity index, surface charge, encapsulation efficiency, protein integrity and surfactant residual amount. This development procedure allowed for the rational identification of particle composition and experimental conditions that led to the antigen-associated nanocarrier presenting the ideal product specifications previously identified for optimal immune cell modulation, having in consideration literature evidences and our previous data.

We used PLGA and pegylated (PEG)-PLGA as a matrix polymer. When preparing NP with double-emulsion solvent-evaporation technique, we used α-lactalbumin (LALBA) as an antigen, glycol chitosan (CS) to increase the viscosity of the internal aqueous phase (IP) and polyvinyl alcohol (PVA) or Pluronic F127 (PF127) to stabilization the interphase of double emulsion. Various concentrations of surfactants has been used (2, 4, 5, 8, 10, 12 % v/v) to best meet the criteria of the most optimal nanoparticulate delivery system. We aimed for NP below 200 nm, polydispersity index (PDI) under 0.2 and ζ potential close to neutrality.

The formulations with 10 % v/v PVA solution in IP and 0.3 % v/v PVA or PF127 in external aqueous phase (EP) presented stable and repetitive NP formulations with desired physiochemical properties. The highest encapsulation efficacy (EE) values were obtained for the formulation prepared with PVA (EntrapLALBA(PVA)), reaching 80 % of the integrated protein, while NP with PF127 (EntrapLALBA(PF127)) presented around 70 % EE. As regards the protein adsorbed, NP formulations prepared with PVA (AdsLALBA(PVA)) or PF127 (AdsLALBA(PF127), reached the values of 40 % and 50 %, respectively.

Dynamic light scattering (DLS) and laser doppler velocimetry (LDV) were used to determine average particle size, polydispersity (PDI) and ζ potential, respectively. EntrapLALBA(PVA) presented the average size of 171 nm with PDI around 0.15 and ζ potential 0.51 mV. EntrapLALBA(PF127) had 185 nm with PDI 0.17 and ζ potential 0.37 mV. On the other side AdsLALBA(PVA) and AdsLALBA(PF127) presented slightly bigger

size 188 nm and 195 nm, respectively, with more negative ζ potential, -1,89 and -1,42 mV, respectively. NP size, PDI and geometry were also confirmed by atomic force microscopy (AFM).

Protein integrity was confirmed by sodium dodecyl sulfate-polyacrylamide gel electrophoresis (SDS-PAGE). Fourier transform infrared spectroscopy (FTIR) was further used to study the interaction of protein adsorption onto surfaces of polymeric NP. The presence of bands at the wavelengths 1662 cm^{-1} and 1562 cm^{-1}, that are specific for primary amides and amines, were detected in formulations AdsLALBA(PVA) and AdsLALBA(PF127), where LALBA was adsorbed onto the surface of the NP. While in NP EntrapLALBA(PVA) and EntrapLALBA(PF127) this bands were absent indicating the protein incorporation into the polymeric matrix. Differential scanning calorimetry (DSC) showed that the formulation process did not alter the structure of the polymers used in the preparation of NP.

The ability of the optimal formulations for systemic delivery and activation of DC was further evaluated *in vitro* and *in vivo* on bone marrow derived dendritic cells (BMDC). Similar activation and maturation profile of APC were obtained after the internalization of NP with antigen entrapped (EntrapNP) or adsorbed onto NP surface (AdsNP) evaluated at 3, 6, 16 and 24 h (ImageStream^{TM} and flow cytometry). The DC-NP interaction increased with the incubation time, presenting internalization values between 50-60% and 30-40%, *in vitro* and *in vivo*, respectively. Interestingly, MHCII was upregulated after the immunization with AdsNP and MHCI after the vaccination with EntrapNP, suggesting more efficient cross-presentation.

To evaluate the activation of antigen-specific immune response, we replaced LALBA for ovalbumin (OVA). It is a highly immunogenic model antigen for which, in immunology, we have well-established animal models that can help to study the effect of the antigen on immune system without any unspecific immune response. Phenotype, frequency and efficacy of immune cell stimulation induced by NP loaded with OVA (EntrapNP or AdsNP) and with/without TLR ligands (CpG and Monophosphoryl Lipid A (MPLA)) were characterized and their specificity clarified by the engrafted OT-I ($CD8^+$) and OT-II ($CD4^+$) T cells. EntrapNP with OVA and adjuvants presented the strongest antigen-specific cytotoxic immune response, following NP with AdsOVA-Ajds. Moreover, long-lasting memory of cytotoxic T lymphocytes (CTL), was evaluated 8 weeks after a single immunization in response to the different ways of antigen delivery, PBS, OVA in solution, OVA & Adjs in solution and NP AdsOVA, AdsOVA-Adjs, EntrapOVA, or EntrapOVA-Adjs. Immunizations where we used

antigen alone did not induce efficient CTL reactivation. Overall, Entrap OVA-Adj NP presented the most robust immune response in inducing the memory, followed by AdsOVA-Adjs NP and OVA & Adjs in solution.

To explore whether the immunization with formulated NP results in efficient cross-priming, an *in vivo* killing assay in steady-state conditions was performed. 24 h prior to immunization, animals were engrafted with $CD8^+$ (OT-I) cells. 5 days p.i., mice were injected with an equal mix of targeted and untargeted CD45.1 splenocytes. Targeted cells were pulsed with OVA peptide, SIINFEKL, and labeled with higher dose of CFSE ($CFSE^{hi}$) while un-targeted control cells were labeled with a lower dose of CFSE ($CSFE^{low}$). The *in vivo* clearance of both type of grafted cells was evaluated 16 h later in LN and spleens by flow cytometry. All NPs, with or without adjuvants, generated the most efficient in vivo killing activity towards the SIINFEKL-pulsed cells, as shown by the disappearance of the $CFSE^{hi}$ peak of cells. Indicating the successful induction of cross-priming and activation of antigen-specific CTL that could potentially lead to a broad and effective immune response pivotal in case of tumor rejections.

To test the efficacy of the therapeutic vaccine and to have a good read-out of the antigen-specific T cells, we used B16.MO5 melanoma-bearing mice using different vaccination schedules, single and three time immunization with OVA and adjuvants- loaded NP. The groups immunized with PBS and Empty NP served as a control and presented similar tumor growth. All treated groups showed a significant reduction in tumor growth. EntrapOVA-Adjs NP (3x immunization) presented the slowest tumor growth (more than 12x smaller final tumor volume), followed by the group immunized with AdsOVA-Adjs NP (3x immunization) (more than 9x smaller final tumor volume) and single vaccination with EntrapOVA-Adjs NP (more than 8x smaller final tumor volume). The highest amount of tumor infiltrating lymphocytes (TILs) at the tumor site was detected for EntrapOVA-Adjs NP (3x immunization), suggesting the best remission and survival prognosis of the treated group.

Two inflammatory cytokines (TNF-α and IFN-γ) produced by TILs were quantified in tumor microenvironment. 4-time high levels of TNF-α upon 3-time immunizations were detected in tumor microenvironment which kept the tumor growth under control. On the other side in the spleens, repeated vaccination prevented upregulation of both inflammatory markers, TNF-α and IFN-γ, indicating absence of systemic inflammation.

Overall, the present work shows that the design of safe but efficacious nanoparticulate cancer vaccines requires a deep understanding of NP biological effect on immune cells, both under steady-state and cancerous environment. A detailed characterization of the immune

cell-related pathways modulated by the optimal antigen-loaded NP and their correlation with the nature and anti-tumor efficacy of the induced immune response was performed *in vivo* in healthy and pathological conditions, showing that the nature of antigen delivery is crucial for a specific T cell activation and targeted cytotoxic effect.

Keywords

Cancer vaccine, nanoparticles (NP), PLGA, PLGA-PEG, antigen presenting cells (APC), dendritic cells (DC), melanoma.

Resumo

A demonstração do reconhecimento de células tumorais por células imunológicas evidenciou que o desenvolvimento de estratégias de vacinação poderá contribuir para a eliminação de células malignas, sem que se verifiquem os efeitos adversos associados aos tratamentos convencionais. No entanto, os antigénios associados a tumores (TAAs) identificados são na sua grande maioria fracamente imunogénicos, requerendo portanto a sua mistura com adjuvantes para que se obtenha uma resposta imunológica anti-tumoral forte. das nanoparticlas (NP) na interação com as células alvo e consequentes efeitos biológicos.

Este trabalho tem como principais objectivos: 1) desenvolvimento de sistemas de transporte biodegradáveis e estáveis, com propriedades físico-químicas adequadas ao transporte de antigénios a células imunológicas; 2) manutenção da estabilidade a longo prazo da integridade do antigénio incorporado nas NP; 3) estudos de internalização das nanopartículas por células dendríticas (DC) primárias; 4) caracterização da internalização in vivo destas nanopartículas e o seu efeito na expressão de marcadores de activação e moléculas co-estimulatórias à superfície das membranas de DCs nos nódulos linfáticos; 5) determinação da activação e proliferação de linfócitos T, in vivo, a diferentes tempos após a administração de nanopartículas; 6) caracterização da activação e expansão dos linfócitos T citotóxicos (CTL) in vivo, após a imunização de ratinhos com a vacina desenvolvida; 7) avaliação da resposta imunológica subjacente à activação de linfócitos T de memória e 8) caracterização das respostas imunológicas induzidas pelos antigénios associados à NP no modelo de ratinho B16.MO5.

NP de ácido láctico-co-glicólico peguilhadas (PLGA-PEG) foram preparadas pelo método da dupla emulsão com evaporação de solventes, utilizando ovalbumina (OVA) como antigénio modelo. O Glicolquitosano (CS) e o Pluronic F127 (PF127) foram utilizados de forma a que as NP desenvolvidas apresentassem as especificações adequadas à sua utilização em imunoterapia contra o cancro (diâmetro médio inferior a 200 nm, PDI inferior a 0,2 e carga de superfície perto de zero). Estas NP apresentaram um diâmetro médio (dm) de 167 nm, com um índice de polidispersão (PDI) de 0,167 e um potencial zeta perto da neutralidade (-1,66 mV), o que é desejável para evitar a captura destes nanosistemas pelos macrófagos. A eficiência de encapsulação (EE) e a capacidade de carga (LC) destas NPs foi de 57,5 % e 29 μg/mg, respectivamente. As NP modificadas pelo PF127 apresentaram um dm (180 nm com PDI 0,180) e um potencial zeta (1,78 mV) ligeiramente superiores, mas EE e LC inferiores (32 % e 16 μg/mg). Nenhuma destas formulações afetou a viabilidade de DC.

Consequentemente, procedeu-se à optimização da formulação utilizando α-lactalbumina (LALBA) como antigénio. Este foi o antigénio escolhido uma vez que se trata de uma proteína expressa em níveis muito elevados na maioria dos carcinomas mamários humanos, nomeadamente em 67 % de carcinomas mamários primários e 62 % das suas metástases, incluindo as encontradas nos nódulos linfáticos (LN), ossos, fígado, pulmão, pele e tecido subcutâneo. Além disso, LALBA apenas se encontra presente nas células epiteliais mamárias durante a lactação.

As formulações preparadas com 10 % PVA na fase interna e 0,3 % de PVA (formulação F3) ou PF127 (formulação F12) na fase externa demonstraram originar NP estáveis, com as especificações definidas como alvo. Os valores de EE mais elevados foram obtidos para a formulação preparada com PVA (EntrapLALBA(PVA)), atingindo os 80 % do valor da proteína inicialmente utilizado na formulação. Quando o PF127 foi utilizado (EntrapLALBA(PF127)), a EE foi cerca de 70 %. De qualquer forma, importa referir que independentemente do tensioativo utilizado para garantir a estabilidade da formulação, os valores de EE referidos encontram-se muito acima daqueles mencionados em estudos recentemente publicados pela comunidade científica. No que diz respeito à adsorção da proteína, atingiram-se valores de 40 ou 50 % para as formulações preparadas com PVA (AdsLALBA(PVA)) ou PF127 (AdsLALBA(PF127), respectivamente. No que diz respeito às imagens das NP obtidas por Microscopia de Força Atómica (AFM), estas evidenciaram um dm 30 nm menor do que o diâmetro hidrodinâmico determinado por DLS. Importa referir que não foram observadas diferenças entre as formulações EntrapLALBA(PVA) e EntrapLALBA(PF127), e entre as AdsLALBA(PVA) e AdsLALBA(PF127), tendo em conta os resultados obtidos por DLS. A análise das NP por Espectroscopia no infravermelho por transformada de Fourier (FTIR) permitiu evidenciar a presença da LALBA à superfície das NP AdsLALBA(PVA) e AdsLALBA(PF127), enquanto que as bandas 1662 cm^{-1} e 1562 cm^{-1}, características de aminas primárias e grupos $–NH_2$, respectivamente, se encontram ausentes no caso das NP que incorporam a proteína dispersa na sua matriz. Os estudos de calorimetria diferencial de varrimento (DSC) permitiram verificar que o processo de formulação não alterou a estrutura dos polímeros utilizados na preparação das NP. Além disso, não foram igualmente observadas interações específicas entre a proteínas e os polímeros nas diferentes formulações de NP desenvolvidas. Ainda assim, foi possível verificar uma maior temperatura de transição vítrea (Tg) nas NP AdsLALBA, comprovando-se portanto a presença desse antigénio à superfície destes transportadores.

A extensão e perfil de internalização das NP AdsLALBA(PVA), AdsLALBA(PF127), EntrapLALBA(PVA) e EntrapLALBA(PF127) por DC primárias in vitro foram avaliados a 3, 6, 16 e 24 h (ImageStream^{TM}). A interação DC-NP aumentou com o tempo de incubação, apresentando valores de internalização entre 50-60 %. Estes valores foram superiores para EntrapOVA(PF127) quando comparados com NP AdsOVA(PF127). Estas NP foram administradas a ratinhos C57BL/6 e os LN inguinais e popliteais foram isolados 16 h após a imunização A análise destas suspensões celulares por citometria de fluxo permitiu avaliar a expressão de marcadores de expressão de DC, nomeadamente MHCI e MHCII, bem como moléculas co-estimuladoras CD80 e CD86. As DC de animais tratados com NP EntrapOVA(PVA) e AdsOVA(PVA) apresentaram níveis de CD86 significativamente mais elevados do que os apresentados pelas DC de animais imunizados com as outras NP de teste, não tendo sido observadas diferenças entre os transportadores que incorporam a proteína ou aqueles cujos antigénios se encontram adsorvidos à sua superfície. O marcador MHCII apenas se encontrou aumentado significativamente nas DC de animais imunizados com NP AdsOVA(PVA), em comparação com os controlos.

Observou-se que as DC que capturaram NP AdsOVA(PVA) apresentavam valores de CD80, CD86, MHCI e MHCII significativamente maiores do que aquelas que incorporaram NP AdsOVA(PF127). Do mesmo modo, NP EntrapOVA(PVA) induziram um aumento significativo na expressão de MHCI e MHCII, quando comparados com os valores apresentados por estas células obtidas de LN de animais imunizados com as NP EntrapOVA(PF127). Desta forma, observou-se que o tensioativo utilizado na formulação desta vacina teve impacto na ativação de APC.

De forma a completar a caracterização da resposta imunológica induzida pelas NP, procedeu-se ao estudo do seu efeito na proliferação dos linfócitos T. Para tal, células OT-I e OT-II marcadas com CFSE foram administradas por via intravenosa (i.v.) a ratinhos, os quais foram posteriormente imunizados com NP EntrapOVA(PVA), EntrapOVA-CpG(PVA), AdsOVA(PVA), and AdsOVA-CpG(PVA). Três dias após o tratamento dos animais, observou-se que as células $CD4^+$ OT-II e $CD8^+$ OT-I T proliferaram extensivamente nos animais tratados com NP EntrapOVA(PVA). Esta proliferação foi a mais acentuada nos animais tratados com a combinação do antigénio e adjuvante dispersos na matriz da mesma NP (EntrapOVA-CpG(PVA)).

As NP Entrap e Ads(PVA) foram selecionadas para avaliar o seu efeito modelador da resposta imunológica em ratinhos saudáveis, bem como em modelos tumorais de melanoma que expressam OVA (B16MO5).

Avaliaram-se os níveis dos marcadores de ativação CD25, CD69 e CD44. Os linfócitos T de animais imunizados com NP EntrapOVA apresentaram valores de $CD25^+CD4^+$ e $CD25^+CD8^+$ 3-4 vezes superiores aos controlos, 48 h após o tratamento dos animais. Verificou-se igualmente um aumento gradual da expressão dos marcadores CD44, bem como do aumento do número total de linfócitos T, essencial para o desenvolvimento de uma resposta imunológica adaptativa eficaz.

Posteriormente avaliou-se a estimulação de CTL de memória, 8 semanas após a imunização de ratinhos C57BL/6 saudáveis com PBS, OVA em solução, OVA & Adjs em solução e NP AdsOVA, AdsOVA-Adjs, EntrapOVA, ou EntrapOVA-Adjs, previamente inoculados com células OT-I. Apenas foi observada uma proliferação acentuada de OT-I nos animais imunizados com NP EntrapOVA-Adjs.

OVA e os adjuvantes CpG e MPLA foram incorporados em NP e estas induziram uma resposta imunológica anti-tumoral eficaz no modelo de ratinho B16MO5 após a administração de uma ou três doses desta vacina. Os animais tratados com três doses das NP EntrapOVA-Adjs apresentaram o crescimento do tumor mais lento, seguidos por aqueles tratados com três doses de NP AdsOVA-Adjs e uma dose de NP EntrapOVA-Adjs. Também a administração de três doses de NP AdsOVA-Adjs ou EntrapOVA-Adjs tiveram um efeito significativo na infiltração de linfócitos no estroma tumoral, o que foi demonstrado pela análise histológica de amostras de massa tumoral coradas com hematoxilina e eosina (H&E) e por imunohistoquímica.

Observou-se que a imunização com três doses das NP AdsOVA-Adjs ou EntrapOVA-Adjs induziram a expressão de receptores antigénio 4 associado a linfócitos T citotóxicos (CTLA-4) isolados do baço e LN, sendo estes significativamente mais elevados para aqueles tratados com NP AdsOVA-Adjs.

A resposta anti-tumoral induzida pelas NP foi confirmada mesmo sem que se tenha procedido à transferência de OT-I, evidenciando portanto a indução de uma resposta imunológica adaptativa especificamente induzida pela vacina desenvolvida.

Palavras-chave

Vacinas contra tumores, nanoparticulas (NP), PLGA, PLGA-PEG, células dendríticas (DC), melanoma.

Acknowledgments

The choice of moving abroad to do my PhD was not easy to make. But as Mark Twain once wrote “Twenty years from now you will be more disappointed by the things that you didn't do than by the ones you did do. So throw off the bowlines. Sail away from the safe harbor. Catch the trade winds in your sails. Explore. Dream. Discover.”

Now, at the time of finishing my doctoral project, I can say that although sometimes it has been challenging and hard, the curiosity and passion for science gave me energy and drove me to continue this journey. In these four years I have had the opportunity to meet and interact with many people, to whom I would like to thank for their mentorship, support, encouragement and friendship.

I would like to give my sincere gratitude to my supervisor Prof. Helena F. Florindo for giving me the opportunity to work in her laboratory and combining two fields, nanotechnology and cancer treatment. She leads a laboratory with a broad knowledge and understanding in multiple fields of research while being a real person. She has provided me with a solid foundation, as I was starting to lay down the building blocks of my research career. Next to our constructive discussions throughout my work, I could also appreciate her motivation, support, trust and also the encouragement to continue my researcher career. For this, and many more, I will always be deeply grateful.

I am grateful to my co-supervisors Prof. João Nuno Moreira and Prof. Mafalda Videira for their support and encuragements through the years. I am thankfull to Prof. Moreira for hosting me in his laboratory at the Center for Neuroscience and Cell Biology (CNC) in Coimbra where I had the opportunity to learn how to do orthotopicly inoculation breast cancer cells into the mammary gland.

I would like to express my sincere thanks to Prof. Steffen Jung for hosting me in his laboratory at the Department of Immunology at the Weizmann Institute of Science. I am extremely honored and grateful for having been supervised by such an outstanding scientist and to have the opportunity to work in a such dynamic team. I deeply appreciate his generosity, availability, guidance, fruitful discussions, valuable expertise and broad knowledge in immunology. Moreover, I am grateful for all the extra collaborations with Prof. Lea Eisenbach, Prof. Zelig Eshhar, and Prof. Guy Shackar that he enabled.

I would like to express the deepest appreciation to the dean Prof. Matide de Castro and ex-dean Prof. José Morais for endorsement of my doctoral project at the Faculty of Pharmacy at the University of Lisbon.

I am deeply grateful to Prof. Rogério Gaspar, former leader of our group Nanomedicines and Drug Delivery Systems for building such a dynamic team and also for teaching and showing me how to develop critical thinking research skills and spirit.

I am grateful to researcher Dr Liana C Silva from the group Intracellular trafficking modulation for advanced drug delivery research at iMed.ULisboa for accepting me into her group when I first arrive to Portugal in 2011. Under her supervision I learned how to prepare liposomes to mimic the cell membranes of healthy individuals or patients with Niemann Pick diseases type C, which are enriched with the sphingosine and to characterize their biophysical properites.

I would also like to thank all the researchers that help me with a realization of this doctoral project. I am thankful to Prof. Carlos Afonso and Dr Catarina Rodrigues from the Biorganic chemistry group at iMed.ULisboa for synthesizing the fluorophore-grafted polymer (PLGA-Rho) that was used for *in vitro* and *in vivo* uptake studies.

I would like to thank Prof. Ana S. Viana from the Chemistry and Biochemistry center, Sciences Faculty, University of Lisbon, Portugal that helped me with further insight on the physicochemical characterization and diameter distribution of nanoparticle by atomic force microscopy.

I am grateful to Prof. João Pinto and Dr Maria Paisana from the Inovative platforms for non-parental delivery systems at iMed.ULisboa for their assistance with DSC and FTIR which enabled a more detailed physicochemical characterization of developed nanoparticulate vaccine.

I am thankful also to Ana Salgado, form the Galenic Pharmacy and Pharmaceutical technology department at iMed.ULisboa for her help with protein quantification in formulated nanoparticles.

I would like to acknowledge Dr Ziv Porat from Flow Cytometry unit, Biological Services Department, Weizmann Institute of Science, Rehovot, Israel for his help and the patience with all the Multispectral imaging flow-cytometry analysis.

I am deeply thankful to Prof. Lea Eisenbach from Department of Immunology, Faculty of Biology, Weizmann Institute of Science, Rehovot, Israel for Ovalbumin transfected B16.MO5 melanoma cells that allowed me to study and characterize the antigen-specific immune response. Moreover, I appreciate her guidance, generosity, valuable expertise and broad knowledge in the field of cancer immunotherapy.

I would like to thank Prof. Zelig Eshhar from Tel-Aviv Sourasky Medical Center, Tel Aviv and from the Department of Immunology at the Weizmann institute of Science,

Rehovot, Israel, the father of the CAR T-cell therapy, for providing breast cancer mouse model. From his group, I would also like to thank to Dr Tova Waks and Dr Anat Globerson-Levin for helping me with the inoculation of orthotopic tumor into a mammary gland and for their guidance along the experiment.

I am sincerely grateful to Prof. Ronit Satchi-Fainaro and PhD student Eilam Yeini from the Department of Physiology and Pharmacology, Sackler School of Medicine, Tel Aviv University, Israel, for their help, availability, and support with the cytokines and chemokines analysis in the serum of tumor-bearing mice after the treatment with the nanoparticulate vaccine.

I would like to sincerely thank all my colleagues and Intracellular trafficking modulation for advanced drug delivery research group members at the iMed.ULisboa; Dr Joana Silva, Dr Ana Raquel Varela, Dr Ana Saraiva, Natércia Rodrigues, Andreia Giro dos Santos, Ana Carreira, Carina Peres, João Conniot, Vanessa Sainz, Nuno Martinho, Ana Matos, Ester Ventura, Dr Liana Moura, for all the fruitful group meetings, and special moments we spent together in the lab or outside. With your help I have learned a lot about the Portuguese culture, habits, good food, and language. Muito Obrigada! A special thanks goes out to my PhD colleague Joana Silva, who was always willing to give an advice or suggestion when I needed.

I would also like to acknowledge my colleagues from Steffen Jung's laboratory at the Weizmann Institute of Science, Dr Caterina Curato, Dr Yohai Wolf, Dr Sigalit Boura-Halfon, Diana Varol, Biana Bernshtein, Zhana Moshayev, Eyal David, Jung-Seok Kim, Yuan Xia, Mor Gross, Anat Shemer, Nina Cortese, Yifat Segal-Hayou, Shira Tabachnick, Dr Louise Maor, and Yaara Biess for constructive discussions, questions, suggestions and doubts at our group meetings. With your help I learned a lot about GUT macrophages, BAT and microglia. It has been fun! You accepted me right away and made me feel really welcome. I am especially thankful to the Postdoc fellow Caterina Curato for all the time we spend together and all the knowledge that she shared with me, from the basics of FACS to the complexity and plasticity of DC and T cells. I will be forever thankful for all her time, help, support, advices and constructive discussion regarding both of our research projects and most importantly for genuine friendship that we build along the way. I have learned so much from her!

I would like to acknowledge all my friends from Slovenia, and those I meet in Portugal and Israel during all these experiences around Europe. I am thankful for friendships, all the good times, positive vibes, visits and support.

Finally, my biggest thanks go to my family. I am deeply grateful to my mother Janja and father Marjan for giving me roots to grow and wings to fly. Roots to know where my home is and the people that love me the most, and wings to go from the nest and practice what they have taught me through the years. I am thankful for teaching me persistence and dedication. Also for their unconditional and endless love, kindness, friendship, unlimited support and encouragements and their continuous examples of passion and devotion to knowledge, education, pharmaceutical science and medicine. My upbringing is why I am the person I am today. THANK YOU!!!

My sister Pija and cousins Tajda and Aljaž, I am deeply grateful for all the Skype chats, visits and trips that we took especially over the years that I have been abroad. Your endless support, positive energy, light spirit glimmer with realism kept me motivated to follow my goals and dreams.

I am sincerely grateful to my aunt Anita and uncle Mitja for their unconditional love, endless support, encouragements, friendship, and understanding. I am deeply grateful for the support and help especially in the times of troubles, when everything seemed to be impossible.

I would like to sincerely thank my boyfriend Menno. First, for his patience and willingness to travel around the Europe to shorten our distance. Secondly, for his uplifting positive energy, unconditional love, continuous encouragement, motivation and support in conquering my dreams.

List of abbreviations and acronyms

AFM	Atomic force microscopy
APC	Antigen-presenting cells
BMDC	Bone marrow derived dendritic cells
BSA	Bovine serum albumin
CD1	Cluster of differentiation 1
CEA	carcinoembryonic antigen
CLR	C-type lectin receptors
CTL	Cytotoxic T lymphocytes
CTLA-4	Cytotoxic T-lymphocyte-associated-antigen 4
CFSE	Carboxyfluorescein diacetate succinimidyl ester
DCM	Dichloromethane
DC	Dendritic cells
DC-SIGN	Dendritic cell-specific intracellular adhesion molecule-3 grabbing non-integrin
DD	Diferential display
DDW	Double Destilated Water
DDSs	Drug delivery systems
DLS	Dynamic light scattering
DMSO	Dimethilsulfoxide
PBS	Phosphate buffer sline
DCS	Differential scanning calorimetry
dsRNA	Double stranded RNA
DT	Diptheria and Tetanus
EE	Encapsulation efficiency
EMA	European Medicines Agency
EPR	Enhanced permeability and retention
ER	Endoplasmic reticulum
FAP	Fibroblast-activating protein
FDA	Food and Drug Administration
FITC	Fluorescein isothiocyanate
FTIR	Fourier transform infrared spectroscopy
GA	Glycolide/glycolic acid
GM-CSF	Granulocyte macrophage colony-stimulating factor
GMP	Good manufacturing practices
HLA	Human leukocyte antigen
HPLC	High-performance liquid chromatography
HPV	Human papillomavirus

IFN	Interferon
IL	Interleukin
imDC	Immature dendritic cells
LALBA	α-lactalbumin
LC	Loading capacity
LDV	Laser Doppler Velocimetry
LN	Lymph nodes
LPS	Lipopolysaccharide
LUV	Uni-lamellar vesicles
mDC	Mature dendritic cells
MF	Myofibroblasts
MHC	Major histocompatibility complex
MHCp	MHC-peptide complex
MLV	Multi-lamellar vesicles
MPLA	Monophosphoryl lipid A
MP	Microparticles
MPS	Mononuclear phagocytic system
MTT	3-(4,5-dimethylthiazol-2-yl)-2,3-(4,5-dimethylthiazol-2-yl)-2,5-diphenyltetrazolium bromide
MUC1	Human milk mucin
NF-κB	Nuclear factor-κB
NK	Natural killer
NKT	Natural killer T
NOD	Nucleotide oligomerization domain
NP	Nanoparticles
ODN	Oligodeoxynucleotides
OVA	Ovalbumin
PAMPs	Pathogen-associated molecular patterns
PAP	Prostatic acid phosphatase
PAT	Process analytical technologies
PBMCs	Peripheral blood mononuclear cells
PCL	Polycaprolactone
PD-1	Programmed death-1
pDC	Plasmacytoid DC
PDI	Polydispersity Index
PEG	Poly(ethylene glycol)
PEG-b-PLGA	Poly(D,L-lactic-co-glycolide-b-ethylene glycol)
PEI	Polyethylenimine
PF127	Plurinic® F127
PGA	Polyglycolide/polyglycolic acid

PLA	Polylactide/polylactic acid
PLGA	Poly(lactic-co-glycolide) or poly(lactic-co-glycolic) acid
PRRs	Pattern recognition receptors
R-PLGA	Rhodamine 6G derivative-grafted poly(lactic-co-glycolide)
PSA	Prostate specific antigen
PSMA	Prostate specific membrane antigen
PVA	Polyvinyl alcohol
QbD	Quality by design
RES	Reticuloendothelial system
RIG	Retinoic-acid inducible gene
RLRs	Retinoic-acid inducible gene-like receptors
s.c.	Subcutaneous
scFv	Single-chain Fv antibody
siRNA	Small interfering RNA
ssRNA	Single-stranded RNA
SUV	Small uni-lamellar vesicles
TAA	Tumor associated antigens
TAP	Transporter associated with antigen processing
TCR	T cell receptor
TGF	Tumor growth factor
TIL	Tumor infiltrating lymphocytes
***T*g**	Glass transition temperatures
TGF	Tumor growth factor
Th	T helper
TLR	Toll-like receptors
***T*m**	Melting temperature
TME	Tumor microenvironment
TNF	Tumor necrosis factor
Tregs	Regulatory T cells
VEGF	Vascular endothelial growth factor
VLP	Virus-like particles
W/O	Water-in-oil
W/O/W	Water-in-oil-in water

List of figures

Chapter 1

List of tables

Objectives of the doctoral thesis

The overall goals of this PhD research work were the development and characterization of a novel immunotherapeutic nanoparticulate delivery system. Of particular interest were the determination of vaccine efficiency *in vivo* under steady-state conditions and finally the characterization of the anti-tumor immune response in tumor-bearing mice.

Specific aims:

1. Development of high reproducible and stable biodegradable polymeric nanoparticulate delivery systems with desired physicochemical characteristics for optimal immune cell targeting.
2. Integrity of NP-entrapped protein and long-term stability of developed nanoparticulate vaccine.
3. *In vitro* time-dependent internalization studies of antigen-loaded nanoparticles by bone marrow derived dendritic cells (BMDC).
4. *In vivo* characterization of NP uptake, and effect on the activation markers and co-stimulatory molecule expressed on DC at draining lymph nodes
5. Determination of T cell activation and proliferation at different time points after NP immunization
6. *In vivo* cytotoxic T lymphocyte (CTL) assay for the characterization of the effective activation and priming of antigen-specific CTL
7. Evaluation of the long-lasting CTL memory achieved after NP administration
8. Characterization of anti-tumor immune response in Ovalbumin transfected melanoma B16.MO5 bearing-mice.

The following chapters describe and discuss the major achievements of the research work pursued in order to achieve the above mentioned goals of this PhD research project.

Table of contents

Chapter 1

Chapter 1 - Translational peptide-associated nanosystems: promising role as cancer vaccines

(General introduction)

Eva Zupančič[a,b], Carina Peres[a], Ana I Matos[a], João Lopes[a], João N Moreira[b,c], Rogério S Gaspar[a], Helena F Florindo[a*]

[a]Research Institute for Medicines (iMed.ULisboa), Faculty of Pharmacy, Universidade de Lisboa, Lisbon, Portugal.

[b]Center for Neuroscience and Cell Biology (CNC), Unniversity of Coimbra, Portugal

[c]Faculty of Pharmacy (FFUC), University of Coimbra, Coimbra, Portugal

Review manuscript published in Bentham Science Journal Current Topics in Medicinal Chemistry. 2016;16(3):291-313 PMID: 26126909

Graphical abstract

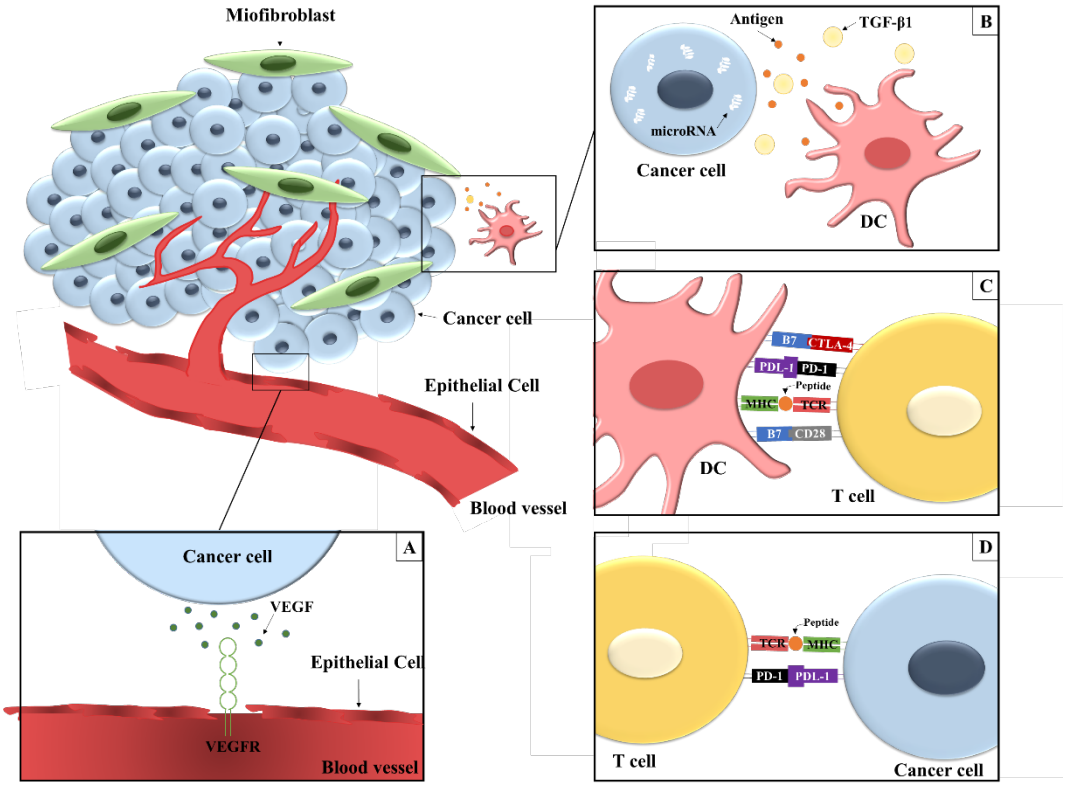

Examples of promising targets within tumor microenvironment to tackle an integrative and combined immune-mediated anti-tumor effect. A) In tumor microenvironment (TME), cancer cells overexpress VEGF. This growth factor is one of the major contributors to angiogenesis, which allows the tumor progression and metastasis; B) DC and tumor cells overexpress TGF-β1 in TME which influence all leukocyte populations; C) In lymph nodes, the immune-checkpoint receptors CTLA-4 and PD-1 play important roles in cancer progression, inhibiting T cell activation; D) in TME, the latter also contribute to the inhibition of T cell activation.

Abstract

Cancer is a heterogeneous disease that results from a multi-step process, being characterizedby uncontrolled proliferation, invasion and metastasis. The understanding that tumor cells can be recognized by host immune cells has highlighted the potential advantages of using vaccination purposes to eliminate cancer cells, while avoiding severe side effects associated to conventional cancer treatments. Interesting outcomes have been obtained with the new identified tumor associated antigens (TAA), including recombinant proteins and peptides. However, these molecules are weakly immunogenic, demanding the concomitant use of adjuvants to boost and achieve a strong tumor-specific immune response. Different classes of nanosystems have been used to protect and deliver several vaccine components. *In vitro* and preclinical studies have emphasized their promising role to attain a prolonged eradication of cancer cells,

including metastasis. However, some studies support the co-entrapment of multiple adjuvants and TAA within a single particulate carrier, while others indicate that stronger immune responses were obtained using a mixture of nanocarriers entrapping different combinations of TAA and adjuvants. These apparently contradictory results may be related to nanocarrier physicochemical properties, which have a profound impact on their interaction with targeted cells and consequent biological effects.

This review discusses the application of nanoscale systems as cancer vaccines, highlighting the particular characteristics of tumor biology and immunology that have been used to guide the design of these nanodelivery tools. We also aim to explore the major weaknesses that have prevented their wide application in the clinic to overcome the delivery, efficacy and safety issues associated to biological entities.

Keywords: cancer vaccines; dendritic cells; immune modulation; nanosystems; peptide antigens; targeting; tumor microenvironment;

Introduction

Cancer is still one of the leading causes of death worldwide, despite considerable improvements in treatment and diagnosis approaches. In fact, the majority of tumors are known to be heterogeneous, phenotypically and functionally diverse with several biological subtypes, which seem to be one of the major causes for the impaired outcomes of diverse anti-tumor strategies [1, 2]. The main goal of cancer therapy is to promote the eradication of malignant cells, while preventing the damage to healthy tissues. However, conventional strategies for cancer treatment (chemotherapy, surgery, and radiotherapy) are not specifically directed to tumor cells [3, 4]. As a result, those can lead to severe side effects and limited effectiveness, thus compromising patient quality of life. Several studies have been dedicated to the development of effective and targeted cancer treatments to improve patient overall survival rate, while avoiding off-target toxic effects. Recent advances in distinct but complementary fields, as nanotechnology, tumor immunology, biotechnology, and cancer biology have led to alternative forms of cancer treatment [5-7]. Immunotherapeutic strategies, in particular cancer vaccines, are one of the most challenging but promising tools that take advantage of patient's own immune system to foster the successful eradication of cancer cells. Cancer vaccines are envisioned to be administered after the detection of disease, thus being considered as therapeutic rather than prophylactic vaccines [8-10]. They have many theoretical advantages over other conventional therapies like low toxicity, high specificity, and continued anti-tumor effect attributed to immunologic memory, which protects individuals from an eventual recurrence [11, 12]. Effective cancer vaccines present the ability to target defined antigens expressed on tumor cell membrane and to induce specific and long-lasting anti-tumor immune responses [12, 13]. Most used tumor associated antigens (TAA) are proteins which peptide epitopes are recognized by T cells in combination with major histocompatibility complex (MHC) class molecules, by activating antigen presenting cells (APC), namely dendritic cells (DC). Therefore, different vaccination approaches have been devoted to explore the use of single or multiple peptides of different TAA, as antigens to potentiate the induction of an effective immune response directed specifically towards tumor cells overexpressing those entities [4]. In fact, most of soluble antigens are weakly immunogenic requiring their combination with adjuvants to induce effective anti-tumor immunity [14, 15].

The use of nanodelivery systems as adjuvants has been extensively explored, offering several advantages over traditional vaccines. These carriers have been shown to protect and

entrap considerable amounts of multiple antigens, especially low immunogenic peptide molecules [16, 17]. In addition, these vehicles have the ability to potentiate the recognition, capture, processing and presentation of peptide epitopes to effector T cells [18, 19]. On the other hand, increasing knowledge on tumor immunology has provided deeper insight into the complex interplay between cancer and immune cells within tumor microenvironment (TME), which can be used in a rational manner to guide the successful development of effective nanotechnology-based cancer vaccines [20-22].

On the other hand, different cell-targeting peptides have been explored to attain the site-specific delivery of different cargoes (e.g. drugs, oligonucleotides) to distinct cells within tumor site, such as stroma, fibroblasts and tumor blood cells [23]. These targeting moieties hold various advantages over monoclonal antibodies or their fragments, such as low immunogenicity, size and easy production process [24]. Besides being out of the scope of this review, interesting recent studies point out the promising use of these non-immunogenic peptide-based alternative therapies to attain the eradication of the disseminated form of this malignant disease through the activation of multiple effector mechanisms [25].

This review presents an overview of the tumor immunology, highlighting the critical immune cells and immune-related pathways essential for the induction of a cytotoxic immune response against cancer cells. In addition, we will discuss the development of effective cancer vaccines and elucidate the advantages of different nanosystems as platforms for the delivery of tumor peptide antigens, but also to modulate and regulate multiple TME signaling pathways towards an integrative approach to overcome tumor immune evasion and consequent proliferation.

1. General immune response

The immune system is divided into two branches, the innate and the adaptive immunity that usually act together. The innate immunity represents the first line of host defense by surveying the local microenvironment to provide “danger” signals to trigger a swift and non-antigen-specific response. Moreover, it plays a crucial role in the initiation and subsequent direction of adaptive immune responses through the secretion of pro-inflammatory cytokines by innate immune cells, as monocytes, macrophages and neutrophils (Figure 1) [26, 27]. The adaptive immune response allows for a versatile and long-lasting specific host defense. In contrast to innate immunity, this antigen-specific immune response will only be achieved after several days, due to the clonal expansion of effector T and B cells (Figure 1) [27, 28]. The generation of effective antigen-specific adaptive immunity requires antigen

presentation to selected T cells, which activation will trigger their differentiation to provide various effector mechanisms to eliminate any cell that will express the specific antigens, such as microorganisms and tumor cells [28, 29].

APC are essential regulators of the innate immune response, acting as a key bridge between the two branches of the immune system. These cells are involved in the uptake of antigens and presentation of epitope peptides to naïve T cells, resulting in the activation of innate and adaptive immunology or tolerance to self-antigens, due to their ability to deliver activating signals [28]. The three types of APC (DC, B cells and macrophages) differentially express MHC class and costimulatory molecules, being involved in different immune response pathways [10, 30]. B cells contribute to adaptive immunity by secreting antibodies and constitutively expressing MHC class II molecules, and through the expression of costimulatory molecules only upon their activation. Macrophages can also mediate innate immune responses directly and make a crucial contribution to the effector phase of the adaptive immune response over the expression of the MHC class II and costimulatory molecules [10, 27].

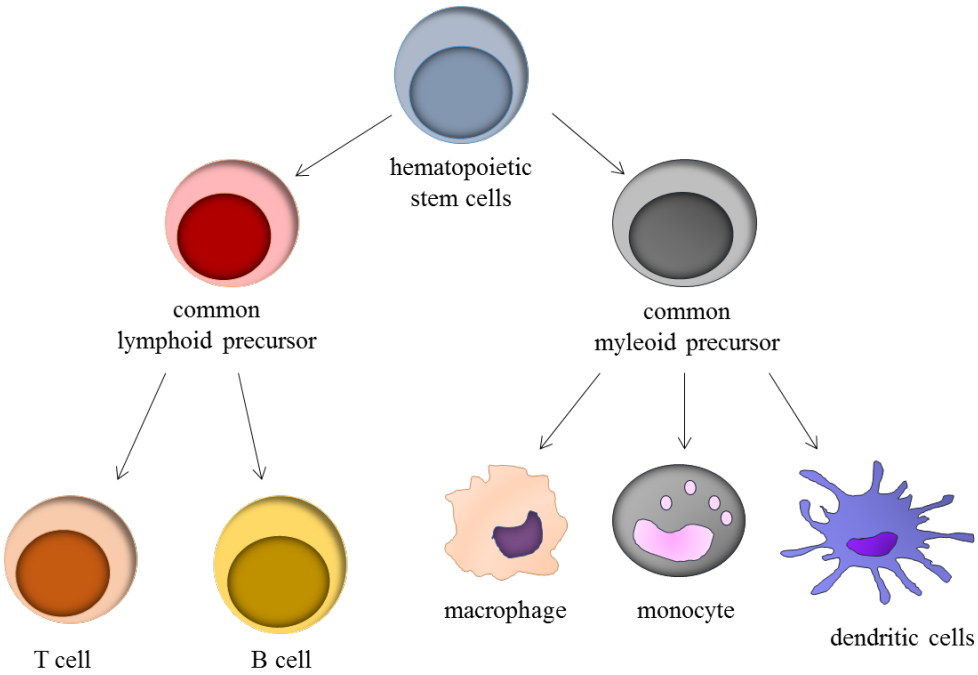

Figure 1: Two main lineages of white blood cells. The myeloid lineage gives rise to effector cells of the innate immune response (DC, monocytes, macrophages). The lymphoid lineage originates cells of the adaptive immune response (T cells and B cells).

1.1. Dendritic cell biology

DC are classified according to their developmental origin, anatomical location, surface antigens, cytokine activators, and immune response final outcome [17, 31, 32].

DC are divided in two major populations, referred to as conventional DC (cDC) and plasmacytoid DC (pDC) [32]. cDC are further subdivided in Langerhans cells and myeloid DC (mDC). Langerhans cells are found in oral, respiratory and genital mucosa, and in epidermis, being named dermal, submucosal or interstitial DC depending on their anatomic location [33, 34]. Moreover, mDC are the only DC subset that presents the ability to cross-present antigens [35]. Their protective tumor immunity was previously demonstrated in several studies by the cross-presentation of antigens, leading to an effective induction of antigen-specific $CD8^+$ T cell responses [36] and secretion of interleukin (IL)-12 [37, 38]. Despite the differences between DC subtypes, they are all able to express high quantities of MHC molecules [32]. The plasmacytoid pathway generates the major subset of DC, the pDC. These APC were found in blood and lymphoid organs [39], where they induce a strong innate immune response by secreting high amounts of type 1 interferons (IFN) [40, 41], which facilitate T cell activation, expansion, and survival for disease-free survival. Combined stimulation of pDC and mDC seems to prime T helper 1 (Th1) effector cells, resulting in the generation of more potent and strong immune responses [39, 41].

All DC subtypes go through three stages of differentiation: DC precursors, immature DC (iDC), and mature DC [42]. Precursors and iDC are produced continuously in the bone marrow and are delivered through the blood to peripheral tissues for screening the presence of "danger" signals. Upon encountering foreign antigens, DC detect pathogen-associated molecular patterns (PAMPs) by pattern recognition receptors (PRRs) expressed at their surface, promptly triggering the innate immune system by inducing the production of multiple inflammatory molecules, namely cytokines and chemokines [26, 27, 43]. In fact, the recognition of PAMPs by iDC leads to their migration towards the afferent lymph nodes, where these APC undergo a maturation process. Once mature, DC have low ability to capture antigens, but present a potent immunostimulatory capacity for priming T cells due to their capacity to efficiently present processed antigen-MHC molecule complexes [27, 32]. Additionally, mature DC synthesize high levels of IL-12, enhancing both innate (Natural killer cells, (NK cells)) and adaptive (B and T cells) immunities [28, 44].

On the other hand, DC can also lead to antigen-specific tolerance or anergy, through the development of IL-10 secreting inducible regulatory T cells (Tregs), which present a strong capacity to suppress lymphocyte responses and to prevent autoimmunity [36].

1.2. DC critical role to overcome tumor-mediated mechanisms of immune evasion

Cancer cells have the ability to evade the immune system through multiple mechanisms, which involve the manipulation of tumor-immune microenvironment cells and signaling pathways, impairing antigen presentation by APC, and promoting immune suppressive mechanisms. In theory, vaccinated patients could mount an immune response able to either eliminate the tumor or keep it under constant restraint, prolonging patient survival [45, 46].

DC are central players in tumor immunology and present the unique ability to migrate from the site of infection to the draining lymph nodes to activate the effector immune cells, determining tolerance/immunity balance. Therefore DC-based targeting strategies can be exploited against autoimmune and infectious diseases, as well as cancer [36, 47].

Maturation of DC is critical for the tumor-specific immune response. Processed peptide fragments are coupled to MHC class I or MHC class II molecules, being then translocated to the DC surface and presented to naïve T lymphocytes ($CD8^+$ or $CD4^+$ T cells) [48, 49].

Two main pathways for antigen presentation have been categorized for peptide loading-processes onto MHC molecules to activate specific subsets of T cells. These pathways are the MHC class I for the presentation of endogenous antigen, and MHC class II for processing and presenting antigens from exogenous origin.

Extracellular antigens are taken up through endocytosis by APC. In the endosomes and lysosomes, proteins are degraded to generate peptides of 10 to 30 amino acids (aa) in length. These peptides then interact with MHC class II molecules to form a stable MHC class II-peptide complex that is then transported to cell surface for expression and potential interaction with the T cell receptor (TCR) on $CD4^+$ T cells [50, 51]. MHC class II molecules are exclusively expressed by APC. Even though, the fate of exogenous antigen is not limited to MHC class II molecules. An alternative antigen presentation pathway is the "cross-presentation", in which Ds, namely mDC, present antigens onto MHC class I molecules. This mechanism activates $CD8^+$ T cells to generate an immune response [52, 53].

Intracellular antigens are translocated into the endoplasmic reticulum (ER) from the cytoplasm, through the proteasomes, where they are cleaved into peptides of 8-12 aa in length. The peptides in the ER are bound to MHC class I molecules and resultant complexes will be then transported from the ER to the cell surface, where they interact with the TCR of $CD8^+$ T cells [50, 54], which proliferate and differentiate into cytotoxic T lymphocytes

(CTL). However, MHC class I molecules are not exclusively expressed by these APC, being also found in all nucleated cells [50, 55].

Once $CD4^+$ T cells have recognized and bind to MHC class II molecules, they become activated and secret cytokines that can stimulate B cells, macrophages and CTL. These immune cells do not secret cytokines, being rather fundamental to recognize and eradicate cells overexpressing those targeted antigens, such as tumor cells [56].

iDC are highly motile cells, continuously sampling antigens through peripheral tissues and lymph nodes. In the absence of any costimulatory signal, T cells will not be activated, becoming tolerant or anergic. Naïve T lymphocytes in the DC-T cell synapse, require three signals to become activated: first signal arises from the interaction between the TCR on naïve T cell and the MHC molecule in the presence of a foreign antigen [57]; second signal stems from co-stimulatory molecules expressed on mature DC, such as CD80, CD86, and CD40, interacting with the cognate receptors on T cells, CD28 and CD40L, respectively [58]; and a third signal that directly affects T cells, through cytokines and chemokines, like IL-12 and IFN (IFN-α/β/γ), produced by DC. These signals enable DC to translate pathogenic signals to naïve T cells and trigger adaptive immune responses by promoting T cell migration, differentiation, survival and acquisition of effector functions [49, 59, 60].

The activation of naïve T cells ensures the induction of appropriate immune responses, either cellular or humoral. The cellular response is characterized by the generation of CTL, which are critical for the generation of an optimal anti-tumor immunity able to mediate tumor destruction. In fact, $CD8^+$ T cells principally recognize endogenous intracellular antigens presented by MHC class I molecules. Once activated, these T cells can directly kill infected or malignant cells, but also acquire a long-lasting memory phenotype, allowing a fast response if a second contact with those antigens occur under repeated infections or cancer recurrence [61, 62]. Theoretically, this should be best achieved by targeting the TAA to DC that would efficiently present processed epitopes loaded onto MHC class I molecules for effective $CD8^+$ T cell priming. However, recent findings indicate that both $CD4^+$ and $CD8^+$ T cells need to be involved [63]. $CD4^+$ T cells seem to be required for the optimal activation of $CD8^+$ T cells, but also for an effective generation of memory T cell populations. In fact, $CD8^+$ T lymphocytes fail to maintain functionality *in vivo* mostly because of the absence of $CD4^+$ T cell help. Therefore, to ensure optimal killer T cell immunity, $CD8^+$ T cells need to be differentiated into effector CTL and memory T cells, while $CD4^+$ T cells need to proliferate and differentiate into effective helpers, which is fundamental to activate antigen-specific effectors and attract innate immune cells [64-66].

Classically, the effector $CD4^+$ T cells were thought to differentiate into Th1 and Th2 cells, but other subsets have been recently described as Th17, Th9 and Tregs [67]. Even if both Th1 and Th2 cells showed to mediate anti-cancer function, IFN-γ-secreting Th1 cells appeared to be more effective [67].

Most conventional vaccines result in the production of antibodies and stimulation of Th cell-mediated immune responses, rather than activation CTL. This could be best accomplished by providing additional adjuvants to potentiate DC activation [68, 69].

2. Cancer vaccines as an immunotherapeutic strategy

Immunotherapeutic strategies take advantage of patient's own immune response by activating *in vivo* immune effectors against specific TAA to overcome the tolerance to tumor cells. Within cancer therapy, cancer vaccines are one of the most challenging but promising tools. Prophylactic cancer vaccines are envisioned to prevent the development of cancer in certain high-risk individuals [8, 13, 17]. U.S. Food and Drug Administration (FDA) and European Medicines Agency (EMA) have approved Gardasil® and Cervarix®, two preventable cancer vaccines expected to, confer protection against HPV infection [70, 71]. There is also an approved prophylactic vaccine for hepatitis B virus infection, to prevent liver cancer [72].

The FDA has recently approved one therapeutic cancer vaccine, Provenge®, as an alternative treatment for metastatic prostate cancer patients [73]. This is a cellular based approach, in which APC are isolated by leukapheresis and cultured *ex vivo* with the antigen prostatic acid phosphatase (PAP) and the protein granulocyte-macrophage colony-stimulating factor (GM-CSF). These *ex vivo* cultured cells will be then administered back to the patient to stimulate the immune system to destroy cells that overexpressed this particular antigen [74, 75].

Despite the antigenic variations between healthy and malignant cells, tumors have also evolved various immune escape mechanisms to evade destruction by the immune system [29, 76]. The activation of DC seems to be the limiting step for the induction of selective and strong anti-tumor immune responses. *Ex vivo* manipulation of DC, as that described for Provenge®, is a personalized type of cell therapy, being thus a very complex, time consuming and costly approach. In addition, these *ex vivo* DC have poor migratory capacity and limited clinical efficacy [77]. Thus, *in vivo* targeting of DC is highly desirable and should involve the administration of the most immunogenic TAA along with the most effective adjuvants, to prime host tumor-specific immune effector mechanisms [13, 78, 79].

An important step for vaccine development has been and still is the identification of TAA. These antigenic entities may be derived from proteins usually expressed on cell surface, secreted or exclusively present at intracellular level. Ideally, these TAA should be mutated or exclusively confined to malignant cells, being thus absent or minimally expressed by normal cells [13, 80]. Unfortunately, certain TAA can also be found in healthy cell populations, being recognized as "self" antigens by immune cells thus rendering them tolerant. In addition, their presence at non-malignant tissues can not only compromise cancer vaccine efficacy but also result in important side effects [81, 82]. Therefore, antigens are chosen based on their ability to induce robust anti-tumor immunity, including cellular ($CD4^+$ and $CD8^+$ T cell) and humoral (B cell) immune responses, while ensuring the establishment of long-lasting T cell memory [83, 84].

TAA can be classified in different categories according to their function or expression pattern in different tissues [80, 85]: (i) Antigens specific for certain tumors, such as the melanocyte differentiation antigens (e.g. Mart1/Melan A, gp100, tyrosinase) or prostate-expressed antigens (e.g. prostate specific antigen (PSA) and prostate specific membrane antigen (PSMA)). (ii) Cancer testis antigens are promising TAA (e.g. MAGE melanoma antigen, carcinoembryonic antigen (CEA) and alphafetoprotein (AFP)) for the induction of specific anti-tumor immune responses. This is a family of proteins present at different tumor cells, being absent from all other normal adult tissues, except germ cells and placenta. (iii) Overexpressed oncogenes or mutated tumor suppressor genes (HER-2, MUC1, Ras, p53).

In either case, these antigens tend to be poorly immunogenic, and thus a single antigen may not be sufficient to induce an immune response capable of destroying cancer cells, due to tumors' heterogeneity and phenotypic diversity [4]. As a result, multivalent vaccines are expected to induce more effective cytotoxic immune response against multiple targeted cancer cells in comparison to single-antigen containing vaccine [14].

The safety of these peptide-based cancer vaccines has been demonstrated in many trials, which have highlighted several of their advantages. Aside from their low cost and relatively easy manufacture process, they exhibit low toxicity/immunogenicity compare to proteins and whole-cell lysate [14]. Moreover, peptide vaccines are quite flexible in terms of chemical modifications performed to improve their immunization efficiency. Some of those alterations include the introduction of specific D-amino acids [86] or peptide sequences [87], the fusion of two or more functionalized peptides [88] or the conjugation of peptides with chemotherapeutic agents [4, 89]. Even though, due to their size, peptides can be rapidly

degraded and eliminated from the blood circulation, being thus inefficiently taken up by APC when used *in vivo* [90].

In fact, these vaccines containing TAA in solution have low *in vivo* stability and often require multiple administrations. In addition, soluble antigens have low membrane permeability and get rapidly degraded by enzymes once internalized [91]. Several studies have shown that the administration of a single antigen tends to elicit strong Th2 responses, while activates only 1-5% of circulating $CD8^+$ T cells [14, 92, 93]. On the other hand, the co-administration of a single antigen with an adjuvant, often led to more prominent Th1 immune responses [17]. As so, both antigen and adjuvants are essential for an efficient activation of DC, otherwise the tolerance or anergy to the antigen may be induced [14, 15, 47]. In fact, most of cancer vaccines under clinical trials are based on the administration of various TAA combined with adjuvants in solution to boost anti-tumor immune responses (e.g. IFN-α2b, GM-CSF, IL-2) [47, 94, 95].

3. Nanoscale systems as fundamental tools for cancer vaccines

To overcome antigen low specificity and unresponsiveness in many patients, an ideal cancer vaccine formulation should comprise not only antigens and adjuvants, but also a delivery system able to modulate antigen presentation pathways. In fact, optimal tumoricidal activity of cancer vaccines can be only attained when both $CD4^+$ and $CD8^+$ T cell responses are efficiently induced [35, 63].

Nanosized carriers have been widely explored as promising platforms for cancer vaccination [96, 97]. These nanodelivery systems present a large surface area to volume ratio, which physicochemical properties (e.g. size, surface charge and hydrophobicity) can be exploited to impart desired *in vivo* behavior and interaction with different cells within TME [98, 99]. In addition to their nanoscale size, these nanoparticulate systems are able to entrap, encapsulate or embed considerable amounts of different types of molecules, including drugs, polypeptides, proteins and oligonucleotides [100]. In the field of cancer immunotherapy, particulate nanosystems have been investigated to offer protection and prolonged release of single or multiple TAA and immune-stimulatory molecules to immune cells, for optimal presentation in a targeted and prolonged manner [13, 47, 101]. The nature of antigen association (adsorbed/conjugated onto nanocarrier surface or entrapped within matrix) is defined by antigen solubility and stability [102]. Additionally, similarly to the structure/composition of each class of nanomedicines (Figure 2), it will have a considerable effect on the payload release profile [103].

Generally, TAA carried by nanosystems have the ability to escape degradation in the endosomes and reach the cytosol in higher concentrations than those antigens administered in the soluble form. These loaded antigens will be thus presented by MHC class I molecules more effectively and for longer periods of time, leading to effective antigen recognition and to the activation of humoral and/or cellular immune responses fundamental for the successful eradication of cancer cells [17, 104]. Moreover, different studies have reported the successful co-entrapment of cancer antigens and adjuvants into the same particulate delivery system, which is critical for the efficient activation and subsequent maturation of DC [105, 106].

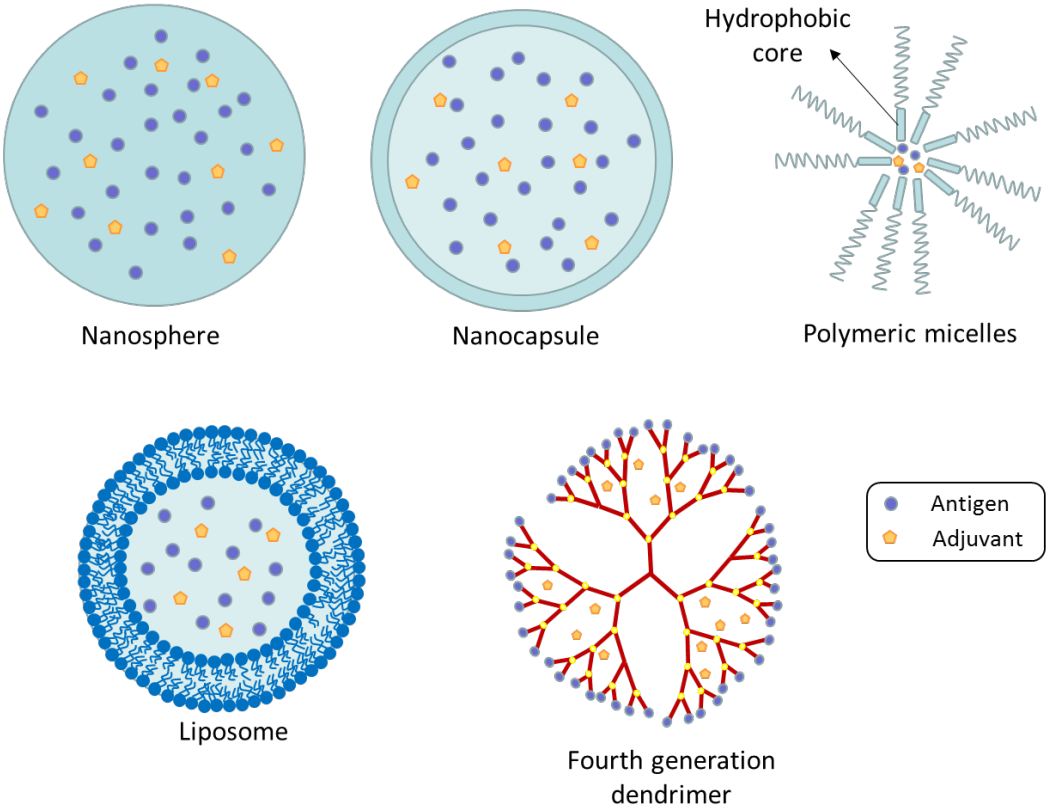

Figure 2: Examples of nanosystems for peptide delivery to potentiate anti-tumor immune responses. Polymeric nanoparticles are defined as submicron spherical nanosystems. Depending upon the formulation method, nanospheres or nanocapsules can be obtained. Nanospheres are systems in which antigens and adjuvants are physically and uniformly dispersed in polymer matrix, while in the case of nanocapsules antigens and adjuvants are encapsulated in polymer and surrounded by a polymer membrane. Hydrophilic and hydrophobic molecules can be entrapped inside the polymer or adsorbed to the surface. Polymeric micelles are self-assembled into this spherical entities formed by amphiphilic block-copolymers. The hydrophobic core is oriented inwards, while the hydrophilic regions of the polymer chains are oriented outwards the aqueous medium. Liposomes are self-assembled nanocarriers made of phospholipids and can be classified according to their size and lamellarity. Lipid bilayer membranes can incorporate hydrophobic compounds, while hydrophilic molecules can be incorporated in enclose aqueous core. Dendrimers are multi-branched three-dimensional globular structures of well-defined

molecular weight polymers, formed by a hydrophobic central core, inner void space and symmetrical branches of repeating monomer units, resulting with a hydrophobic central core and a hydrophilic surface.

The composition, formulation methodologies, and consequent morphology, size, and surface physicochemical properties of nanomedicine-based systems, have a profound impact on NP nanocarrier interaction with cell membranes, determining their ability to overcome these physiological barriers, but also to favor specific biophysical intracellular events [107, 108].

Nanocarriers can be prepared from a variety of materials, which will ultimately determine their biological outcome. Their selection depends on formulation process and route of administration, being intimately linked and dictated by the expected physicochemical properties (size, surface charge, hydrophobicity) and immunotherapeutic effects [109, 110].

Extensive research works have shown that the ideal dimensions of nanosystems for local intratumoral administration should be in the range of 10–100 nm [109]. On the other hand, nanocarriers within 100 to 500 nm are efficiently taken up by DC after being administered through the subcutaneous administration route. Even though, carriers with sizes between 200 nm and 500 nm will be taken up by DC and then delivered to lymph nodes, while nanoparticles smaller than 200 nm will arrive at lymphoid organs through the lymph drainage within hours after their administration [35]. These carriers are known to avoid the reticuloendothelial system (RES), such as liver and spleen, presenting then a prolonged circulation time in blood [111].

Modification of surface characteristics is often required to target specific cells. One promising approach encompasses nanosystem functionalization with specific ligands, such as peptides, proteins or antibodies, which will have a considerable effect on *in vivo* biodistribution of nanocarriers [36, 112]. These ligands can provide selectivity and higher binding efficiency to cell surface receptors, minimizing the accumulation of nanomedicines at off-target cells.

Different studies have reported the successful use of different classes of nanosystems for the delivery of cancer peptide antigens and/or immune-modulators to activate strong, selective and long-lasting anti-tumor humoral and cellular immune responses [101] (Table 1).

3.1. Peptide-loaded polymeric nanoparticles and micelles

Polymeric nanoparticles (NP) have been explored to achieve a sustained release profile for antigens and adjuvants over prolonged periods of time [101, 113]. These molecules

can be encapsulated by a polymer membrane (nanocapsules) or be dispersed into the polymer matrix (nanospheres) (Figure 2). As they normally present a uniform size with narrow polydispersity index, these nanocarriers are highly stable, capable of displaying a predicted controlled drug release [99, 114].

On the other hand, polymeric micelles are self-assembled spherical nanocarriers formed of amphiphilic block-copolymers composed by hydrophilic and hydrophobic monomers. In aqueous solution, the block-copolymers assemble into a core–shell structure. The hydrophobic parts of their chains form a hydrophobic core, while the hydrophilic regions of the polymer chains are oriented outwards the aqueous medium [115, 116].

Biodegradable synthetic and/or natural homopolymers or copolymers are commonly used in the preparation of these polymeric nanoscale systems. The aliphatic polyesters, as poly(lactic acid) (PLA), poly(glycolic acid) (PGA), poly (lactic and glycolic acid) (PLGA), and poly(ε-caprolactone) (PCL) are among the most studied polymers for drug delivery purposes, being FDA approved biomaterials suitable for the delivery of vaccine formulations via several routes of administration, including oral, nasal, dermal and parenteral [117, 118].

Polymeric nanosystems possess many advantages over other types of nanocarriers. Aliphatic polyesters comprise several requirements needed for the formulation of optimal delivery systems for human use. In fact, these materials are nontoxic, nonimmunogenic, biocompatible, biodegradable, and have been investigated as successful and cost-effective formulation components under Good Manufacturing Practices (GMP) scale-up processes [109, 119, 120].

PLGA-based nanoscale carriers are able to protect loaded antigens from immediate degradation or premature elimination, and present the ability to control antigen release rate. This property can be tailored towards a specific need, being indeed predicted by the molecular weight and specific ratio of lactic and glycolic acid monomers [121, 122]. Additionally, chemical modification of aliphatic polyester with targeting ligands has allowed the delivery and subsequent active cellular uptake of entrapped entities, including TAA and adjuvants, to wide spectrum of specific cell types within tumor site [98, 109, 123].

Silva and colleagues (2014) developed untargeted NP and mannose-grafted NP to target CD206 DC surface receptors using a mixture of three aliphatic polyesters [17, 124]. The first ones were composed by PLGA, PEG-b-PLGA and PEG-b-PCL, in a 70:15:15 w/w ratio. Mannose was conjugated to the PEG-b-PCL copolymer used for the formulation of the CD206-targeted polymeric PLGA/PCL nanosystem. These NP were able to entrap different combinations of MHC class I (Melan-A:26; ELAGIGILTV and gp100:209; IMDQVPFSV)

and class II (gp100:44-59; WNRQLYPEWTEAQRLD) restricted melanoma associated antigens (MAAs) and two TLR ligands, Polyinosinic-polycytidylic acid (Poly(I:C)) and 20-deoxyribo (cytidinephosphate-guanosine (CpG)-oligodeoxynucleotide (ODN). The subcutaneous administration of these cancer antigens and adjuvants co-entrapped in those NP improved immune responses in a B16F10 melanoma metastatic model, in both prophylactic and therapeutic settings. These results support their use as a promising component of a multiple immunotherapeutic approach to improve or even achieve the complete eradication of tumor cells. The most significant tumor growth rate reduction was observed in the group treated with the combination of mannose-NP containing MHC class I and MHC class II restricted peptides entrapped in different carriers, but in association with both TLR ligands, suggesting the importance of the activation of both $CD4^+$ and $CD8^+$ T cells in the efficacy of the anti-tumor immune response against this metastatic cancer model [125].

Similarly, Ma *et al.* (2012) also reported that a multivalent vaccine based on PLGA NP co-entrapping three peptides (MART-1:27–35, gp100:154–162 and gp100: 209–217) generated stronger cytotoxic activity in a murine melanoma model than those NP containing only two of those peptides (MART-1:27–35 and gp100:154–162). Moreover, they have also studied the difference of the CTL cytotoxicity through DC after their activation with PLGA-NP encapsulating peptides or pulsed with free peptides. NP encapsulating peptide induce a significantly stronger anti-tumor response even though the peptide dose was lower [126]. A comparable observation has also been previously suggested by Clawson (2010), when he and his coworkers observed that Hp91 conjugated onto the surface of PLGA-NP induced a more prominent activation of DC that the peptide in solution [127].

The anti-tumor effect of PLGA-NP co-encapsulating the tyrosinase-related protein 2 peptide (TRP2: 180–188; SVYDFFVWL) and the 7-acyl lipid A, a TLR4 ligand, was assessed in a murine melanoma B16 tumor model. The therapeutic anti-tumor effect was induced by antigen-loaded NP, with or without the 7-acyl lipid A. In the absence of the adjuvant, antigen-loaded NP showed higher number of activated $CD8^+$ T cell in lymph nodes. On the other hand, NP co-encapsulating both antigen and adjuvant led to higher number of activated $CD8^+$ T cells in the spleen, showing stronger migration abilities. Moreover, increased levels of inflammatory cytokines were also shown at the TME [128].

Tan *et al.* (2014) developed lipid-coated NP, using PLGA, 1,2-dioleoyl-sn-glycero-3-phosphocholine phospholipid (DDPC) and 1,2-distearyl-sn-glycero-3-phosphoethanolamine-N-PEG 2000 (DSPE-PEG). These NP were able to entrap various combinations of MHC I class restricted peptides (TRP2: 180–188; SVYDFFVWL, gp100: 25–33; KVPRNQDWL and

p15E: 604–611; KSPWFTTL) with a TLR4 ligand, the monophosphoryl lipid A (MPLA). The authors assessed the ability of these different nanoparticulate systems to prevent tumor growth in a B16 murine tumor model. The main goal of this study was to compare the anti-tumor effect obtained with the administration of a single particulate carrier encapsulating one type of antigen, with the one induced by a mixture of NP carrying each a different peptide. The mice immunized with NP loaded with a single peptide seem to induce a more pronounced antigen-specific T cell response. Interestingly, these formulations were not able to alter tumor-growth, in contrast to the combination of multiple NP containing different single antigens, which induced a significant suppression of tumor growth [129].

Wu and colleagues (2010) prepared pH responsive polymeric micelles with the tumor targeting AP peptide (CRKRLDRN) that binds to IL-4 receptors, which are highly expressed in breast tumor cells. Micelles were loaded with the doxorubicin and the fluorescence dye TRITC, to evaluate micelles binding affinity both *in vitro* and *in vivo*. These carriers presented a pronounced anti-cancer therapeutic efficacy in a MDA-MB-231 human breast tumor-bearing mice, which was significantly different from that obtained in animals treated with either the drug in solution or encapsulated in micelles without the AP protein [130].

3.2. Peptide-loaded liposomes

Liposomes have been studied extensively as carriers particularly for anti-cancer therapies. These are lipid (natural or synthetic) composed self-assembled vesicles within the range of 50 to 1000 nm (Figure 2) [131, 132].

As mentioned for polymeric nanosystems, liposomes also present the ability to protect the therapeutic agents from degradation, thus prolonging their biological half-life. In addition, these carriers are easily functionalized with targeting ligands to deliver payloads to the site of action, which can promote (immune) therapeutic efficacy, but also and equally important, reduce important side effects [133]. However, unlike polymeric nanosystems, liposomes have the ability to carry hydrophilic molecules in an aqueous core and simultaneously incorporate or embed hydrophobic compounds inside the lipid bilayer [134]. These features, together with their biocompatibility and biodegradability, make liposomes unique delivery systems [135].

Several types of liposomes can be prepared by different preparation methods, depending on the required application, size, lamellarity and final amount of the encapsulated antigen [136]. Liposomes can be classified into multi-lamellar vesicles (MLV), large uni-lamellar vesicles (LUV), and small uni-lamellar vesicles (SUV), depending on their size and

number of bilayers. MLV, are usually composed of 5-25 lipid bilayers, presenting dimensions above 500 nm. Liposomes with only one bilayer, such as LUV are generally larger than 100 nm, whereas SUV present smaller sizes [133, 137].

Cruz et al. (2011) prepared liposomes using a lipid mixture of egg phosphatidylcholine/ phosphatidylglycerol/palmitoyl peptide (EPC/PG/palmitoylpeptide) at 80:20:10 molar ratio. Targeted liposomes were prepared by conjugating Fc fragment of human IgG conjugated to DSPE-PEG-Mal added to lipid mixture. These targeted liposomes were able to effectively bind to human DC, inducing a stronger immunological response than the untargeted system [138]. The same lipid composition was used to co-entrap a soluble cancer-testis peptide antigen (NY-ESO-187-111, with the sequence LLEFYLAMPFATPMEAELARRSLAQ) with an immunostimulatory peptide adjuvant (Palm-IL-1 and MAP-IFN-γ). Similarly, the most potent immunological response was presented by liposomes which surface was modified by targeting moieties for human DC via Fc receptor. These results suggest that this targeted vaccine strategy is a promising tool to improve immunotherapeutic outcomes against cancer disease, but also in other immunocompromised states [139].

MUC1 is a glycoprotein widely overexpressed on distinct types of cancers, such as lung cancer, breast cancer, prostate cancer and colorectal cancer. L-BLP25 is a peptide liposomal vaccine, containing 25-aminoacid sequence of MUC1 (STAPPAHGVTSAPDTRPAPGSTAPP), corresponding to the exposed core peptide of MUC1 protein. Sangha et al. 2007 studied the effect of that liposomal vaccine in combination with the adjuvant MPLA. This delivery system was used to facilitate the uptake of the antigenic peptide by APC, leading to an antigen-specific T cell immune response that acts on MUC1-expressing tumors both in preclinical MUC1-transgenic lung cancer mouse model and patients [140].

Sarkar and colleagues formulated 1,2-dipalmitoyl-sn-glycero-3-phosphatidyl- choline (DPPC) liposomes to entrap a 20 aminoacid MUC1 peptide containing a GalNAc-O-Thr (Tn) conjugated to a TLR2 ligand, Pam3Cys, which works as adjuvant and lipid anchor in the liposomes. Mice immunized with this liposome-based vaccine demonstrated increased T cell proliferation, compared to non-treated mice [141].

Mansourian and coworkers encapsulated HER-2 derived peptide, p5 peptide, in liposomes formulated using various lipids (dioleoyl phosphatidylethanolamine (DOPE) and/or fusogenic 1,2- dioleoyl-3-trimethylammonium-propane (DOTAP)) and in combination with the adjuvant CpG-ODN to obtain the most optimal *in vivo* immune response. This study

reports the increased delivery of p5 by DOTAP-cholesterol-DOPE liposomes admixed with CpG-ODN. Moreover, tumor sizes and animal survival rates support the successful induction of both $CD8^+$ and $CD4^+$ T cell-mediated immune responses [142].

3.3. Dendrimers

Dendrimers are multi-branched three-dimensional globular structures of well-defined molecular weight polymers, formed by a hydrophobic central core, inner void space and symmetrical branches of repeating monomer units (Figure 2). Moreover, their biocompatibility, nanometric size, narrow polydispersity index, long-term circulation, and possibility of presenting multiple functional groups at the periphery, makes dendrimers promising new platforms for peptide-based vaccine delivery [143-145]. Dendrimer synthesis methodology can be divergent, which starts from the core element in the center outwards; or convergent, beginning from the peripheral branching units towards the center. Both strategies will lead to a structure that presents a hydrophilic surface and a hydrophobic central core [145, 146]. TAA and immune-modulators can be encapsulated into the hydrophobic inner cavities, while targeting moieties will be conjugated to the terminal functional groups of dendrimers to interact with specific molecules expressed on targeted cells.

Liu et al. (2013) created a highly promising vaccine candidate to treat HPV-related cancers. These researchers conjugated the HPV peptide antigen E744−62 (8Q epitope; QAEPDRAHYNIVTFCCKCD) to the polyacrylate polymer, leading to a peptide conjugated dendrimer that reduced or eradicated tumor growth in a mouse model for cervical cancer (TC-1) after a single immunization. Moreover, in this study no additional adjuvants were used [147].

4. Nanothechnological-based startegies for immune cells and tumor microenvironmental targeting

As previously mentioned, conventional cancer therapies do not specifically target the tumor, leading to several and severe side effects. Thus, nanocarrier-based cancer vaccines have emerged as an alternative therapeutic strategy and have already shown promising results [113]. This targeted immunotherapy is being explored to overcome the heterogeneity of malignant cells and the immune suppression induced by both the tumor and its microenvironment. The main goal of this therapeutic strategy is not only to target and kill tumor cells in a specific manner, but also to alert the immune system to eliminate residual cancer cells [148].

There are two main mechanisms for the targeted delivery of peptide-loaded nanovehicles to tumors: (i) passive targeting, through leaky vasculature surrounding the tumors; and (ii) active targeting, by grafting specific ligands of different cells within TME (e.g. tumor cells or angiogenic endothelial cells) to the nanocarrier surface [149]. In contrast to normal cells, cancer cells present anatomical defectiveness, in addition to functional abnormalities. Unpaired angiogenesis is responsible for the unique pathophysiological characteristics of tumor blood vessels. They present irregular shape, and are highly disorganized and dilated with a high number of pores, resulting in enlarged gap junctions between endothelial cells [149, 150]. This compromised architecture and regulation of tumor blood vessels allow the selective migration and accumulation of molecules up to 400 nm diameter into the surrounding tumor region within tumor interstitium due to the "Enhanced Permeability and Retention (EPR) effect" [102, 151].

In addition, it has been shown that nanoparticles persist in the tumor for a period during which occurs their local disintegration and consequent release of entrapped agents, as drugs, immunoadjuvants or antigens [152, 153]. However, passive targeting suffer from limitations, since not all tumors exhibit a considerable EPR effect, and the vascular permeability may not be similar within a single tumor [151]. One strategy followed to overcome this limitation aims to modify the nanocarrier surface with targeting moieties to recognize and bind overexpressed molecules at immune or cancer cells. Antibodies and their fragments, but also other proteins, peptides, nucleic acid based ligands, and small molecules are some of the most used recognition ligands for the specific delivery of nanocarriers [150]. However, to achieve high specificity and a considerable effect on the biodistribution of these surface-modified nanosystems, those receptors should be highly expressed on tumor cells, but absent on normal cells, minimizing their accumulation in healthy tissues. Targeted cells will internalize nanovaccines by receptor-mediated endocytosis, promoting the accumulation of higher amount of TAA and/or adjuvants and immune modulators, thus improving their biological effect. Delivery system strategies aiming to achieve immunomodulation are now part of the pharmaceutical companies' pipeline [154]. The importance of this immunological framework, resulting from nanomedicines potential for selective immune system stimulation, has recently become apparent with a massive number of scientific publications and awarded patents related to vaccines [155].

Table 1. Examples of peptide-associated nanosystems for sustained and targeted delivery of antigens and adjuvants for cancer immunotherapy.

Class of nanomedicine	Peptide antigen/ Adjuvant(s)	Composition	Immune-mediated response	REF
Self-assemble micelles	Entrapped OVA cytotoxic T-cell epitope (EQLESIINFEKLTE)	Dipalmitic acid tail (diC_{16}) associated to peptide antigen N-terminus	Subcutaneous administration of diC16-OVA micelles and controls (PBS, OVA in PBS, OVA+ incomplete Freud's adjuvant (IFA) on days 0, 1 and 20). Cancer cells expressing OVA were inoculated on days 30 diC16-OVA micelles were able to decrease tumor growth rate compared to controls.	[156]
Lipid vesicles	OVA	Conjugation of recombinant hexahistidine-tagged forms of single chain antibody fragments (ScFv) to CD11c and DEC-205 DC receptors onto highly metastatic murine melanoma (B16-OVA) plasma membrane vesicles (B16-OVA-derived PMV) incorporating a novel metal-chelating lipid (3(nitrilotriacetic acid)-ditetradecylamine; NTA3-DTDA)	*In vitro* and *in vivo* targeting of DC by modified PMV; Stimulation of strong B16-OVA-specific CTL responses, prominent protection against tumor growth and prolonged disease-free survival	[157]
Dendrimers	PAn DR (PADRE) + OVA encoded plasmid	Polyamidoamine (PAMAM) dendrimers	Administration of a single dose of PADRE-conjugate dendrimers and OVA encoding plasmid by subcutaneous administration protected animals against tumor growth for 25 days.	[158, 159]
Dendrimers	MHC class II-targeting peptides	DNA (pcDNA3-tyrosine-related protein-2 (*TRP2*) and pcDNA3-gp70) conjugated with Generation 5 polyamidoamine (G5-PAMAM) cross-linked with PADRE epitope (aKXVAAWTLKAAaZC) and HemoAgglutinin HA:110–120 (SFERFEIFPKEC)	Subcutaneous injection of DNA-peptide-dendrimer complexes, followed by dermal electroporation, transfected APC, mostly DC, *in vivo* directly in the lymph nodes, induced T cell immunity and humoral response, and reduced tumor growth in a B16F10 melanoma model.	[160]
Liposomes	Entrapped influenza hemaglutinin peptide HA 307-319-C (PKYVKQNTLKLAT-C) peptide conjugated onto liposomal surface through diacylated and triacylated lipopeptides that (TLR2 agonists)	Egg yolk L-α-phosphatidylcholine (PC), L-α-phos- phatidyl-DL-glycerol (PG) and cholesterol (75/20/50 molar ratio) SUV conjugated with thiol-reactive functionalized lipopeptides (TLR2 agonists)	The conjugation of thiol carrying HA 307-319-C peptide epitope onto liposomes previously functionalized with thiol-reactive lipopeptides did not induced maturation of DC *in vitro*. On the other hand, the incorporation of those lipopeptides into SUV did not change the immunostimulatory capacity of these lipopetides, being able to stimulate DC *in vitro* and induce their effective maturation	[161]
Liposomes	luteinizing hormone-releasing hormone (LHRH)-tetanus toxoid	EPC/ phosphatidylglycerol (PG)/palmitoyl-peptide	The encapsulation of peptide and specific targeting to DC receptors, as FCy, significantly increase	[138]

	peptide	(80/20/10 molar ratio), containing 1% DSPE-PEG-Mal to conjugate Fc fragments of human IgG	antigen uptake and T-cell response *in vitro*	
Liposomes	TLR agonists (zymosan (TLR2), R848 (TLR7/8), poly(I:C) (TLR3), LPS (TLR4) and CpG (TLR9)); Antigens (OVA8 peptide SIINFEKL, and trp-2, peptide SVYDFFVWL (B16 melanoma) and gp61–80 peptide (lymphocytic choriomeningitis virus (LCMV))	cationic lipid octadecenolyoxy[ethyl-2-heptadecenyl-3 hydroxyethyl] imidazolinium chloride and cholesterol	TLR9 or TLR3-complexed liposomes encapsulating antigens induced strong $CD8^+$ and $CD4^+$ T cell responses and IFN-α production after administered by i.p. route. Trp-2 –loaded TLR-complexed liposomes significantly reduced melanoma tumor growth, demonstrating a therapeutic anti-tumor activity.	[162]
Liposomes	CTL epitope SIINFEKL Co-encapsulated with the TLR3 ligand poly(I:C)	Antigen and adjuvant loaded cationic liposomes composed of DOTAP and DOPC	Immunogenicity of formulated liposomes was determined *in vitro* and *in vivo. In vitro*, liposomes were efficient in the delivery of antigen to DC, while *in vivo* activation of $CD8^+$ T cell immune response was triggered. The activation of CTL by liposomes was 25 fold stronger than the CTL activation induced by adjuvant and antigen in solution.	[163]
Liposomes	CTL epitope peptide derived from human ErbB2 (p36-71: CG-TYLPTNASL), Th peptide epitope from influenza haemagglutinin (HA 307-319: PKYVKQNTLKLAT-C) associated with TLR2/1 (Pam3CAG) or TLR2/6 agonists (Pam2CAG and Pam2CGD)	Liposomes were prepared by mixing phospholipids (PC, PG), cholesterol, anchor (DPGMal or DPGBr*) and DOG(Man)2 in a 75/20/50/5/3 molar ratio.*(maleimide or bromoacetyl) CTL and Th peptide epitopes were conjugated to DPGMal or DPGBr anchors of mannosylated liposomes loaded with various adjuvants.	*In vivo* studies showed that either prophylactic or therapeutic vaccination was successful in a BALB/c mouse model challenged with renal carcinoma cells expressing human ErbB2. Both type of liposomes (Pam3CAG/DPGMal or DPGBr/ErbB2/HA) triggered an efficient tumor eradication in 100% of mice.	[164]
Liposomes	Glycosylated (SAPDT(α-D-GalNAc)RPAP) or nonglycosylated (SAPDTRPAP) MUC1 peptide, Th peptide epitope (KLFAVWKITYKDT) with immunoadjuvant Pam_3CysSK_4 (TLR2 ligand)	Covalent linkage of peptides and adjuvant on the surface of the liposomes composed of egg phospatidylcholine, phosphatidylglycerol, and cholesterol.	Both glycosylated and non-glycosylated vaccine induced CTL immune response. Immunity triggered by glycosylated tripartite vaccine had significantly better results regarding tumor prevention.	[165]
Liposomes	HPV16 E6- and E7-derived peptides. (E6 8–19, (MFQDPQERPRKL); E6 49-57,(VYDFAFRDL); E6 66–74 (PYAVCDKCL); E6 82-90, (EYRHYCYSL); E6 87-95 (CYSLYGTTL); E6 98-106, (QYNKPLCDL) and E7 10–20, (IVLHLEPQNEI); E7 51–	Oligomannose-coated liposomes containing HPV16 E6- and E7-derived peptides	*In vitro* studies on HPV-16 positive cervical carcinoma patient's peripheral blood mononuclear cells (PBMCs) showed the highest immunogenicity for E6-derived peptide (E6 66-74). Moreover, this study also demonstrates that oligomannose-coated liposomes containing peptides are more efficient than vaccination with DNA in standard liposomes.	[166]

	60, (HYNIVTFCCK); E7 83-93, (LMGTLGIVCPI))			
Liposomes	CTL epitope peptides (Hantaan nucleocapsid protein (HTN M6; SVIGFLAL) or HPV E7 (QAEP- DRAHYNIVTF), MPLA	Phosphatidyl-b-oleoyl-g-palmitoyl ethanolamine (POPE), cholesterol hemisuccinate (CHOH), and monophosphoryl lipid A (MPLA) (POPE/CHOH/MPL 7:3:0.01 molar ratio)	pH-sensitive liposomes were able to reduce melanoma tumor growth and induce antigen-specific CTL immune response for 6 weeks.	[167]
Liposomes and lipid vesicles	P17 (ICAM-4: 37-58) and P18 (ICAM-4: 149-177) and one 12-mer cyclic peptide (P30) to bind to CD11c/CD18 at DC	Antigen-loaded liposomes (DS-PC, cholesterol, DSPEPEG750, NTA3-DTDA and tracer lipid OG488-DHPE (molar ratio 46.5:46.5:5:1:1)) B16-OVA-derived PMV engrafted with peptides	*In vitro* and *in vivo* strong binding to $CD11c^+$ and $CD11b^+$ cells; Intravenous administration of liposomes induced humoral immune responses and T cells, while liposomes were able to protect against tumor growth in both lung and subcutaneous B16-OVA tumor models	[168]
Polymeric nanoparticles	Murine melanoma antigenic peptides (hgp100:25-33 (KVPRNQDWL) and TRP2:180-188 (SVYDFFVWL)), MPLA	PLGA nanoparticles	Intradermal administration of peptide-loaded PLGA NP were able to induce prolonged antigen-specific immune responses. The subcutaneous administration of co-encapsulted TRP 180e188 peptide and MPLA in PLGA NP prevented B16 tumor growth	[169]
Polymeric nanoparticles	short peptide (Hp91; DPNAPKRPPSAFFLFCSE)	Hp91-loaded PLGA NP and PLGA NP functionalization with Hp91 peptide	The incorporation of Hp91 peptide strongly stimulated DC *in vitro*, in comparison to free antigen; however antigen delivered at NP surface was 4-fold stronger than Hp91-loaded PLGA NP.	[127]
Nanoparticles	EphA2 peptide	L-phenylalanine (Phe)-conjugated poly(Y -glutamic acid) (Y-PGA-Phe NP)	Amphiphilic peptide-immobilized prevented MC38 tumor cells growth and successfully induced an antigen-specific cytotoxic immune response *in vivo*. This formulation did not elicit severe side effects, in contrast to the mixture of this peptide antigen with complete Freund Adjuvant (CFA)	[170]

4.1. Nanosystems as fundamental tools for *in vivo* DC targeting

Attentions have been focused on the development of novel DC-based cancer vaccines to provide durable anti-tumor immunity and avoid tumor progression [171]. As previously mentioned, DC represent the sentinels of the immune system and are known as the most potent APC able to modulate the adaptive immunity [172]. DC can process TAA into the MHC class I and MHC class II pathways to interact with $CD8^+$ and $CD4^+$ T cells, respectively [173]. Moreover, DC populations present the unique capacity to efficiently cross-present antigens, in particular human $BDCA3C^+$ (CD141C) blood mDC [174, 175] and murine $CD8\alpha^+$/$DEC205^+$ DC [176], which is essential for the development of anti-tumor cytotoxic

immune responses [177]. DC have also been presented as immunocompetent in initial stages of tumor progression [178]. In this regard, new nanovaccine-based strategies have been designed to selectively target DC, enhancing the antigen uptake efficiency and consequently, the activation of cellular motility to secondary lymphoid tissues (spleen, lymph nodes and mucosal lymphoid system) for further activation of naïve T cells [179, 180].

To overcome the disadvantages of individual ex vivo DC-based approaches (section 3.), peptide-based vaccines have been suggested to deliver antigens directly to DC *in vivo* [77]. However, their weak immunogenicity has demanded for their combination with delivery nanosystems to increase their recognition and uptake by DC, but also to modulate antigen-presentation pathway [102, 181].

Passive targeting of DC can be achieved by directing nanovaccines to DC-rich locals, such as lymph nodes and peripheral tissues, as skin. For this purpose, nanovehicle size and coating are important physicochemical factors playing crucial roles in the interaction and internalization by DC, affecting the subsequent processing of antigens via MHC class I, MHC class II or cross-presentation pathways [182]. Tolerance can also be induced if the maturation stimulus is given too late after antigen capture by DC. On the other hand, antigens will not be efficiently presented if they reach already mature DC, being important to highlight that the time period at which antigen and adjuvant reach DC is crucial, affecting the overall immune outcome. [183]. It has been well established that nanosize is among the most crucial factors that determine the antigen delivery, internalization and processing by lymph-node-resident immature DC instead of only peripheral immature DC, providing a more potent immune-stimulation [184, 185]. As previously described, small nanovaccines (< 100 nm) are directly transported to DC at lymph nodes, into the lymphatic system by interstitial flow; larger carriers (>500 nm) are predominantly internalized by skin iDC (dermis, epidermis and to a lesser extent subcutis), draining subsequently to the lymph nodes; and intermediate sized nanovaccines (100-500 nm) follow both pathways [186]. Nanosized vaccine delivery vehicles may be also preferable to induce cytotoxic immune responses by cross-presentation pathway, extremely important for cancer immunotherapy [187]. Moreover, studies have shown that DC preferentially internalize particles within viral-sized range, whereas those presenting dimensions similar to bacteria are preferentially ingested by macrophages [188]. Nanosystem surface properties constitute additional and important factors that influence the kinetic of uptake by DC. The improvement in bloodstream circulation half-life of nanosized systems has been achieved through the “PEGylation” process. This consists in coating nanosystems surface with hydrophilic PEG molecules by conjugation, grafting or adsorption, especially to

avoid their immediate recognition as non-self, and consequent capture and destruction [17, 102, 189].

However, besides the ability inherent to nanosystems to act as an intrinsic "danger signal" inducing DC maturation and consequently adaptive immune responses, in vivo studies have demonstrated that delivery vehicles alone are not sufficiently strong to activate a sustained immunity [185]. Therefore, DC maturation stimuli are critical for the induction of potent anti-tumor immune responses [171].

The active targeting of DC may facilitate nanovaccine uptake and DC maturation, being a relevant alternative to have in consideration while developing an effective cancer vaccine strategy [186]. To improve the efficacy but also the specificity of interaction with DC, nanosystem surface have been decorated with bioactive ligands, including peptides, antibodies, proteins, polysaccharides, glycolipids, glycoproteins, and lectins, which particularly bind to DC-surface receptors [17, 190, 191]. Moreover, the delivery of both cancer antigens and adjuvants within the same platform, to a single DC population is expected to improve immune outcome [192].

In mammals, TLR are the most studied class from the broad spectrum of PPRs predominantly expressed on DC, and can be divided into surface bound receptors (TLR1, 2, 4, 5, 6 and also TLR10 in humans and TLR11 in mice) and intracellular receptors present in the endosomes (TLR3, 7, 8 and TLR9) [193-195]. TLR identify PAMPs and are involved in the initiation, promotion and execution of immune response through DC activation and maturation. This process results in the secretion of co-stimulatory molecules (CD80, CD86 and CD40), chemokines and inflammatory cytokines (IL-6 and TNF-α) required to potentiate TAA presentation through MHC class I pathway to $CD8^+$ T cells, increasing cancer immunotherapeutic efficacy [17, 43, 196, 197]. Extracellular TLR recognize bacterial invaders, but also fungi and some enveloped viruses, while intracellular TLR recognize nucleic acids from viral or bacterial pathogens [17].

The discovery of TLR and their crucial role in orchestrating both innate and adaptive immune responses have led to the development of an entire class of potent immunomodulatory adjuvants, namely the TLR ligands [198]. Therefore the use of TLR agonists as vaccine adjuvants is an attractive strategy to be explored in the design of these nanotherapeutic systems [199].

CpG DNA motifs present in bacterial and viral genomes can be incorporated into liposomal [200, 201] and polymeric [202] nanosized vehicles acting directly on DC maturation by binding intracellular TLR9 [203-206]. Also, poly(I:C) adjuvant, mimicking a

double stranded RNA (dsRNA) produced by most viruses during replication, can bind to TLR3 and have been associated to stronger anti-tumor immune responses [102, 206, 207]. This receptor still contributes to the initiation of immune responses against the induction of dsRNA replication in infected cells [208]. Co-administration of TLR3 and TLR9 ligands within the same liposome demonstrated an enhancement in cross-presentation of loaded exogenous TAA, being associated with stronger anti-tumor immune responses [209]. In addition, MPLA ligand can also be delivered when associated with liposomal [140] or polymeric [169] nanosystems to target TLR4, which recognizes components of bacterial cell wall, similarly to TLR2 [183, 210, 211]. It has been recently shown that IL-6 secreted by TLR4-activated DC is capable of reversing the Treg suppressive effects, activating T cell functions [212]. Otherwise, mouse TLR7 and its homologous human TLR8 can recognize imidazoquinoline-like molecules and viral single-stranded RNA (ssRNA) [213]. The ability of Imiqiuimod and Resiquimod to activate respectively the homologous of TLR9, TLR7 and TLR8, involved in viral recognition, is also being currently tested in clinical trials [214]. The administration of other TLR agonists such as Flt3L or CD40L also showed to enhance DC activation and maturation *in vivo* [215]. Moreover, different DC populations express distinct sets of TLR. Consequently different TLR ligands will induce the activation of different DC. TLR1–6 and TLR8 ligands activate human mDC [216], while TLR7 and TLR9 ligands activate exclusively pDC in lymph nodes [217]. Furthermore, the same TLR ligand can induce different cytokines according to the DC subset, which influence T cell response [218]. TLR9 ligand only activates pDC present on lymph nodes. As a result, and despite the active targeting with TLR9 ligand, carriers within nanometer dimensions can directly reach the draining lymph nodes to be efficiently taken up by pDC over the exclusive peripheral DC [187]. Additionally, a combination of different TLR ligands, such as TLR3 and TLR7, can be co-delivered by a singular nanosystem to DC, being expected a synergistic effect of sustained secretion of cytokines (IL-6 and IL-12) and development of higher resistance to Treg-mediated immune suppression by $CD4^+$ and $CD8^+$ T cells, unlike those obtained in the presence of a single TLR ligand [219]. The delivery of TLR ligands and TAA by the same nanosystems may not only alert the immune system by potentiating the presentation of TAA via MHC I to $CD8^+$ T cells, but also allow for a sustained TLR signaling and TAA release in DC, reducing the need for high doses or repeated administrations of those compounds, consequently, limiting their toxicity and/or the non-specific immune activation [220, 221]. The effective dose of TLR for *in vivo* T cell activation can be reduced until 100 fold when delivered in nanosystems [202]. In this regard, the combination of TLR ligands with TAA

may have a massive impact on the efficacy of cancer vaccines for melanoma, lymphoma, glioblastoma, breast, prostate, ovarian and lung cancers. This combination can in fact act as a potent immune modulator, as well as a safe and effective vaccine adjuvant through the induction of Th1 immune responses [17].

Among the most expressed receptors by DC, C-type lectin receptors (CLR) are characterized by the presence of carbohydrate binding domains involved in the recognition and internalization of many glycosylated self-antigens and pathogens, such as viruses, bacteria, and fungi, making them popular targets for cancer vaccine delivery [17]. Targeting antigens to CLR was demonstrated to enhance humoral and cellular immunity against tumors [222]. CLR, such as DEC-205, DC-SIGN, CLEC9A, mannose receptor (CD206), Dectin-1, Langerin and DCIR2, can recognize binding and endocytosis ligands with a terminal sugar, such as mannose, fucose and N-acetylglucosamine conjugated onto nanosystem surface [171, 223, 224]. These receptors have been proposed as another promising approach for DC-active targeting on cancer immunotherapy due to their particular engagement in antigen internalization, processing and loading on MHC class I or MHC class II molecules [225, 226]. Among others, the active targeting of mannose receptor has been reported to increase vaccine effectiveness by promoting the TAA cross-presentation pathway and consequent induction of effective $CD8^+$ T cell-mediated immune responses [227].

Other effective approach for DC targeting is based on Fc receptor (FcR). Nanosystems can be functionalized with IgG, IgA or IgE Fc fragments against FcγRIIa (CD32a) [191], FcαRIa (CD89a) and FcεRI, respectively, inducing the activation of DC to directly prime CTL responses [228].

On the other hand, other ligands or cytokines can be conjugated onto the surface of nanodelivery platforms to enhance T-cell immunity. DC-specific antibodies, such as anti-CD11c (myeloid marker), anti-CD40 [229] and anti-DEC-205 [230] have been used to modify nanosystem surface, not only to enhance the specificity of DC targeting *in vivo*, but also to foster their uptake, promote antigen processing and consequent DC effective maturation [157]. Recent studies have indicated that $CD8^+$ T cell effectors may be generated by triggering CD40 on APC, not requiring the simultaneous stimulation by MHC II-related Th cells via CD40 ligands [231].

Notwithstanding, polymer "PEGylation" has also been used as a fundamental strategy to stabilize the conjugation process [232], where functional ligands are attached to the surface of nanosystems via terminal ends of PEG-grafted polymers, for targeting specific organs or subcellular organelles [233-235].

4.2. Targeting and modulation of tumor microenvironment

Despite improvements made on peptide-associated nanosystems for cancer vaccines, most of the clinical trials have shown that only a small number of these candidates induced an effective tumor regression [16]. As previously described, the immune system has the ability to recognize, eliminate, and protect the body from tumor cells by mounting robust innate and adaptive immune responses. However, tumor is able to induce sophisticated immune escape mechanisms where both cancer cells and immune cell populations are involved, explaining this poor clinical outcome [236]. Contrarily to stroma healthy cells that acts as a barrier against cancer development, the presence of tumor cells induces crucial stroma alterations with the recruitment of fibroblasts and immune cells, matrix remodeling, and development of vascular networks, leading to the formation of the TME and supporting tumorigenesis [237]. Different cytokines, chemokines and growth factors can be found within TME extracellular matrix, which along with tumor stromal cells (immune suppressor cells, myofibroblasts (MFs), and endothelial cells) account for the complexity of this tumor-stromal interplay [238, 239]. TME constitutes a physical barrier to tumor-targeting molecules, but it also has a major role in tumor immunosuppression, growth, invasion and angiogenesis [240, 241]. Thus, stromal TME cells constitute a promising target for integrative, targeted and immune-mediated anti-tumor approaches. Therefore, improved clinical outcomes would benefit from the successful modulation of tumor associated cytokine network and cell communication within TME, which could be promoted by the use of those NP to stromal targeted cells, avoiding off-targeted effects [242].

An effective strategy to modulate the heterogeneous population and signaling pathways within tumor site requires a combinatory approach involving, namely chemotherapy, vaccination and cancer-immune network modulation within TME. The association of these approaches presenting complementary mechanisms of action may be the key to overcome the multiple factors and mechanisms involved in the promotion of pro-tumorigenic behavior and dissemination [243-245]. To improve or even achieve the complete eradication of tumor cells, it is essential to follow an integrative strategy able to i) prime the immune system potentiating antigen presentation; ii) regulate immunosuppressive processes and tumor-related pathways within TME to prevent the inhibition of anti-tumor responses; iii) suppress the development of tumor vascular networks (angiogenesis), and iv) downregulate proliferation of malignant cells [246].

TME key population MFs are directly implicated in the suppression of anti-tumor immune responses and thus in the subsequent invasion and metastasis. MFs present common features on primary and metastatic tumors, thus being less likely to acquire mutations than tumor cells. MFs highly express fibroblast-activating protein (FAP), which has not yet been found in normal tissues or cells. In adults, FAP expression seems to be limited to pathologic sites, constituting a promising target within stromal environment [247]. MFs are the major source of collagen deposits within stroma and are also deeply involved in drug resistance and in the evasion of effective anti-tumor immune responses through several MF-derived factors [248]. Tumor growth factor- β1 (TGF- β1), a cytokine essentially secreted by DC and tumor cells, is able to induce i) the differentiation of fibroblasts into MFs; ii) the promotion of tumor angiogenesis; but also iii) tolerance against tumor cells, playing a key role in tumor-induced immunosuppression [199]. This immune suppressive cytokine affects all populations of leukocytes in a stimulatory or inhibitory manner. For instance, TGF- β1 decreases DC' maturation and antigen presentation capacity, but can also affect monocytes and macrophages by decreasing their phagocytic and effector functions, compromising their consequent ability to present antigens (Figure 3). Moreover, this cytokine decreases $CD4^+$ T cells effector function and even convert the latter into immunosuppressive Treg cells [242, 249]. Cancer patients present high levels of TGF-β1 in the plasma and at the invasive fronts of human cancer tissues, being thus commonly related to tumor metastasis and poor prognosis [250]. Recent studies have demonstrated that blocking the TGF-β1 signaling pathway may represent an attractive therapeutic strategy for the treatment of human cancer, by directly increasing the efficacy of both immunosurveillance and current immunotherapeutic strategies [251]. A strategy for disrupting this tumor-promoting pathway is silencing TGF-β1 by small interfering RNA (siRNA) [252]. siRNA is a promising technique in oncotherapy that can selectively inhibit target gene expression, and therefore overcome the limitations presented by other therapies [253]. To the best of our knowledge, there is only one study that reports the use of TGF-β1 siRNA loaded-nanoparticles to enhance an anti-tumor immune therapeutic effect. Accordingly, Xu et al. (2014) developed a mannose-modified lipid-calcium-phosphate NP to co-deliver Trp2 peptide and CpG to DC. The efficacy of that vaccine in a metastatic B16F10 melanoma model was significantly improved when combined with a TGF-β1 siRNA liposome-protamine-hyaluronic acid nanoparticle [6].

In addition to proliferation, angiogenesis is one of the main features of tumor tissues. This process is driven due to hypoxic conditions in tumor, where cells take advantage of the formation of new blood vessels from pre-existing vasculature to progress and satisfy their

need in nutrient and oxygen [254]. Studies performed in breast cancer patients have showed a positive correlation between angiogenesis and the degree of metastasis, as well as the tumor recurrence, and shorter survival rates, which reveal the importance of this process in tumor growth, progression and metastasis [255, 256]. In a pathological condition such as cancer, angiogenesis is mediated by the release of molecules by both healthy (endothelial cells, epithelial cells, mesothelial cells and leucocytes) and transforming cells [257], being the vascular endothelial growth factor (VEGF) considered as one of the most important pro-angiogenic factor and one of the major contributors to this process. This molecule was found overexpressed in various human cancers, including breast [258], prostate [259], liver [260], colorectal [261] and gastric cancers [262]. Different studies have shown that blocking VEGF signaling pathway, by blocking its receptor (VEGFR) or decreasing VEGF expression, allows reducing tumor associated angiogenesis and blood vessel-dependent metastasis (Figure 3) [263]. Many VEGFR inhibitors have been developed and tested so far, including small-molecule inhibitors, anti-VEGF monoclonal antibodies, and aptamers that strongly antagonizes the VEGF-VEGFR binding with high specificity [264-266]. Nevertheless, several limitations have been associated with these strategies, including unfavorable pharmacokinetics, poor tumor accumulation, and undesired interaction with the immune system [267]. Another strategy that has been exploit for disrupting this angiogenic pathway, but still at less extension, is the silencing of VEGF using siRNA. However, the *in vivo* use of naked siRNA to targeted tissues and cells remains a challenge due to the fragile nature of the molecule, which can be rapidly degraded by nucleases in plasma, its renal elimination, and limited penetration across the capillary endothelium. Moreover, siRNA molecules are too large (~13 kDa) and too negatively charged to enter cells by a passive diffusion mechanism, leading to an inefficient cellular uptake [268, 269]. Polymeric NP are a valuable approach to enable the protection of those biomolecules from degradation and potentiate their cytoplasm delivery providing their escape from endo-lysosomal compartments [270-273].

The activation of T cells is critical to the immune surveillance of tumors, being specially regulated by a balance between co-stimulatory signals and immune checkpoints. Most of the immune checkpoints, defined as a set of immune inhibitory pathways, are essential to preserve the quality and amplitude of physiological immune responses and prevent autoimmunity under normal physiological conditions [237]. However, the secretion of immune-checkpoint proteins and their receptors can be deregulated in tumors. The overexpression of inhibitory ligands and receptors that regulate CTL effector functions in tissues has been extensively reported particularly on tumor cells or on non-transformed cells

in the TME [274]. Thus, blockade of immune checkpoints seems an important target to improve human cancer therapeutics and a powerful approach to enhance the anti-tumor immunity. Antagonist monoclonal antibodies (mAbs) can be manufactured to readily block immune checkpoints through the lymphocyte inhibitory receptors targeting, attaining the amplification of antigen-specific T cell responses and consequently a sustained endogenous anti-tumor activity [275]. In the context of clinical cancer immunotherapy, cytotoxic T-lymphocyte-associated-antigen 4 (CTLA-4; also known as CD152) and programmed cell death protein 1 (PD-1; also known as CD279) are the two immune-checkpoint receptors most actively studied, showing different mechanisms to regulate anti-tumor immunity in order to enhance the potential to produce durable clinical responses [276]. CTLA-4 receptor plays a critical role acting as a signal damper through the regulation of T cell early activation. CTLA-4 is a homolog of CD28 with 100-fold greater affinity for CD80/CD86 ligands. The binding of this competitive ligand interrupts the second signal, suppressing T cell activation and consequently contributing to the tumor growth [277]. Blockade of CTLA-4 with mAbs such as Ipilimumab and Tremelimumab, recently approved by the FDA for use as first-line or second-line therapy for patients with advanced melanoma, was associated with enhancement of T cell responses and tumor destruction [278, 279]. PD-1 is associated with the inhibition of anti-tumor T cell responses, being expressed by the majority of tumor infiltrating lymphocytes, in response to the common overexpression of their ligands, such as B7-H1 (PD-L1) or B7-DC (PD-L2), by tumor and stromal cells [280]. Thus, the inhibition of the interaction PD-1-ligands with mAb, such as anti-PD-1 monoclonal antibody BMS-936558 (also known as MDX-1106 and ONO-4538), can enhance T cell responses and mediate preclinical anti-tumor activity, in cancer immunotherapy (Figure 3) [281].

On the other hand, miRNAs are important gene expression regulators. They are short oligonucleotides (18-22 nucleotides) involved in multiple pathways related to the development and differentiation of cells, and in the pathogenesis of cancer [282]. These molecules are misregulated in cancer, being up or down-regulated depending on miRNA and cancer type. For example, the downregulation of the pigment-cell-enriched miRNA-211 was detected in melanoma cells and it has been associated to their invasiveness due to its key role in the tumor progression [283]. Thus, this melanoma tumor-suppressing miRNA constitutes an important target, being expected to provide therapeutic benefit [282]. Similarly, recent evidence revealed that miRNA-21 is overexpressed both in stromal fibroblasts and colorectal cancer cells, enhancing the tumor cells invasiveness. However, despite the important outcome expected by using miRNA to regulate tumor progression *in vivo*, their biological effect

depends on the development of cell-specific delivery approaches that are currently underexplored [284, 285]. As it was mentioned for siRNA, nanocarriers are promising systems to overcome cellular barriers and modulate intracellular trafficking to increase their bioavailability in the cytoplasm [269, 286].

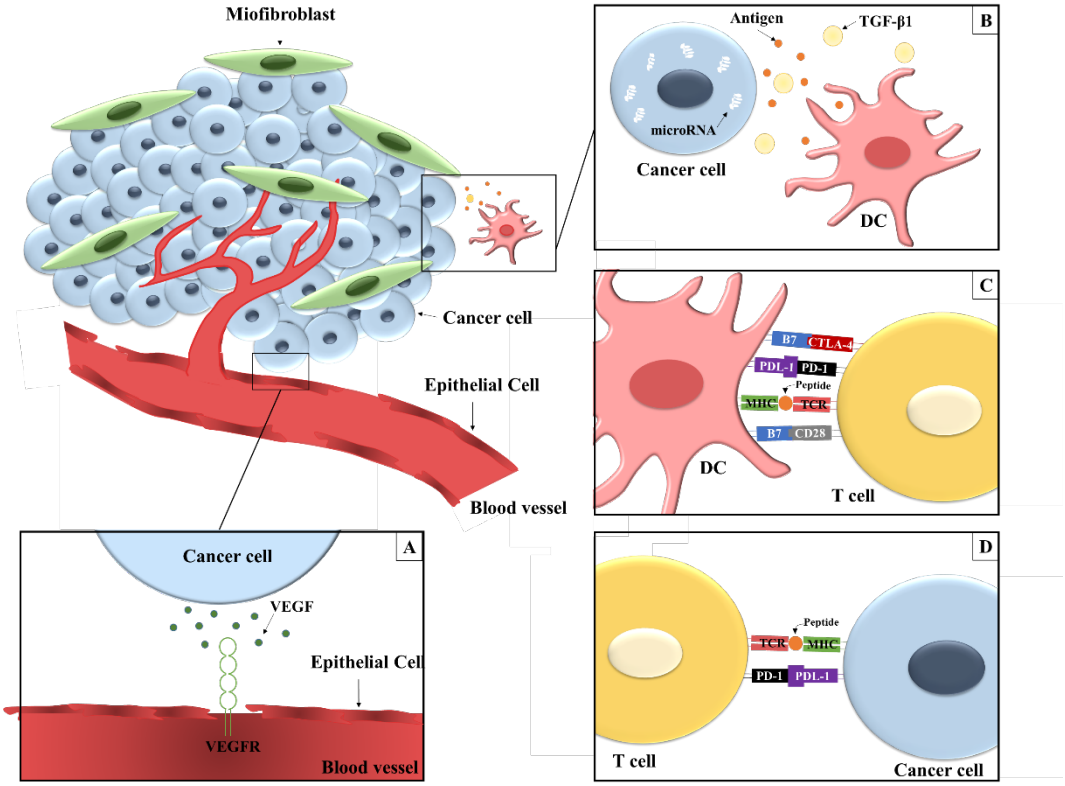

Figure 3: Examples of promising targets within tumor microenvironment to tackle an integrative and combined immune-mediated anti-tumor effect. A) In tumor microenvironment (TME), cancer cells overexpress VEGF. This growth factor is one of the major contributors to angiogenesis, which allows the tumor progression and metastasis; B) DC and tumor cells overexpress TGF-β1 in TME which influence all leukocyte populations; C) In lymph nodes, the immune-checkpoint receptors CTLA-4 and PD-1 play important roles in cancer progression, inhibiting T cell activation; D) in TME, the latter also contribute to the inhibition of T cell activation. Examples of promising targets within tumor microenvironment to tackle an integrative and combined immune-mediated anti-tumor effect.

5. Translation of peptide-loaded nanosystams into the market

It has long been recognized that nanomedicines could significantly benefit transversely all pharmaceutical areas. The broad applicability of the nanotechnology in areas where significant biomedical advances were obtained, explains why nanomedicines have emerge as a promising tool for developing more effective pharmaceutical products. The substantial role of nanotechnologies has been confirmed by the number of filled patents in the biomedical field [154, 287]. In fact, the significant repercussions in the future of patients' access to

innovative therapeutic strategies will only be possible by pursuing industrial property strategies, including inventions, patents, trademarks, industrial designs, and geographic indications of source.

Higher targeted specificity, superior efficiency in the clinical outcomes and a better understanding of the role, modulation and regulation of the pathophysiology dynamics at the molecular level, could enable nanomedicines to achieve a disease control with an unprecedented precision. Even though, no particulate-based cancer vaccines have been registered for clinical usage.

From a technological point of view, the lack of control of nanomaterials' intrinsic properties and formulation process, especially related to the random conjugation of those high affinity ligands to nanocarrier surface, constitute an important drawback responsible for NP' low reproducibility and consequent limited translation into clinical use. The need for a detailed characterisation of NP-cell interaction has thus been increasingly recognized within research community and pharmaceutical companies as a crucial step to provide efficient drug delivery, avoiding its future failure in clinical settings [154, 155].

An important part of the strategy has to take into consideration the appropriate identification of relevant disease-specific targets. Relevance has to be brought from the clinical setting pointing to specificity in disease stage and disease evolution, both from pathophysiological and cellular perspectives. A better integration of physiological dynamics with molecular accuracy of delivery systems is therefore needed.

A significant lesson arises therefore from the need of better integration between clinical and basic research teams, preferably in an adequate oncology clinical setting.

From a quality perspective, linking chemistry characterization and biological relevance, as well as updated production technologies (incorporating quality by design (QbD) strategies) are essential for paving the way for process analytical technologies (PAT) and more efficient industrial production lines.

6. Conclusions and future perspectives

Besides the strong demand to develop vaccines to address unmet clinical needs, the novel nanotechnology-based platforms have important underexplored challenges for drug delivery researchers, industry and government agencies [155]. Experimental design and risk analysis are central to provide the necessary requisites for accessing vaccine quality and safety to reduce to a minimum the product quality variations, but also any risks to the targeted

population (short and long term). Highly interconnected with this is the need to incorporate high-throughput methods coming from the PAT palette to allow a real-time and highly efficient control of possible changes in product(s) quality. These PAT devices are based on different concepts, as the use of Dynamic Light Scattering (DLS) and Quartz Crystal Microbalance with Dissipation Monitoring (QCM-D) for protein folding and aggregation monitoring, efficient robust total particle quantification techniques, characterization of ligands density at nanocarrier surface and exhaustive and tight control of all production raw material lots.

Acknowledgements

The authors thank to Fundação para a Ciência e Tecnologia, Ministério da Ciência e da Tecnologia, Portugal (PhD Grant SFRH/BD/78480/2011 to Eva Zupančič and SFRH/BD/87591/2012 to Carina Peres; research project PTDC/SAU-FAR/119389/2010 and Pest-OE/SAU/UI4013/2011).

Conflict of interest

All authors confirm that the content of this manuscript has no conflicts of interest.

Chapter 2

Chapter 2 - Development of a novel nanoparticle-based therapeutic vaccine for breast cancer immunotherapy

Eva Zupančič[a,b], Joana M Silva[a], Mafalda A Videira[a], João N Moreira[b,c], Helena F Florindo[a]*

[a]Research Institute for Medicines (iMed.ULisboa), Faculty of Pharmacy, Universidade de Lisboa, Lisbon, Portugal.

[b]CNC - Center for Neuroscience and Cell Biology, Unniversity of Coimbra, Portugal

[c]Faculty of Pharmacy (FFUC), University of Coimbra, Coimbra, Portugal

Published in Elsevier's Procedia in Vaccinology 2014;8:62-67

Abstract

Nanoparticles (NP) have great potential as advanced delivery systems for cancer immunotherapy. PEGylated-Poly-lactide-co-glycolic acid-based (PLGA-PEG) NP were prepared by double-emulsion solvent evaporation technique, using ovalbumin (OVA) as a model antigen. Glycol chitosan and block co-polymer Pluronic F127 were used in order to best attain the most efficient parameters for cancer immunotherapy. OVA-loaded PLGA-PEG NP presented a narrow size distribution with an average size of 167 nm with a polidisperity index (PDI) 0.167 and ζ potential values close to neutrality (-1.66 mV), which is desired for a particulate cancer vaccine to overcome their premature capture by macrophages. The encapsulation efficiency (EE) and loading capacity (LC) of these NP were 57.5 % and 29 μg/mg, respectively. PLGA-PEG NP modified with Pluronic F127 presented slightly higher average size (180 nm with a PDI 0.18), and ζ potential (-1.78 mV), but lower EE and LC (32 % and 16 μg/mg). The effect of NP on dendritic cell viability was evaluated using Alamar Blue® assays.

Keywords: nanoparticles; PLGA-PEG; Pluronic F127; ovalbumine; dendritic cells.

1. Introduction

Breast cancer is one of the most commonly diagnosed malignancies, being thus the leading cancer-related cause of death among women worldwide [1]. The conventional forms of treatment do not specifically target this tumor cells, leading to adverse effects that heavily decrease patient's quality of life. Therefore, there is an urgent and critical need for new therapeutic strategies against this disease. Therapeutic cancer vaccines are used to overcome host immunosupression, mostly induced by tumor cells. Nanomedicine-based systems have been emerging as promising tools to promote tumor associated antigens (TAA) recognition, capture and presentation by professional antigen presentation cells (APC), leading to an extensive, specific and long-lasting immune response, while the parenteral administration of soluble antigens would be rapidly removed from circulation [2]. A polymeric platform consisting on antigen-loaded PLGA-PEG-based nanoparticles (NP) is being developed to ultimately deliver breast cancer antigens to dendritic cells (DC) and improve their recognition by T cells within tumor microenvironment. This type of NP is appealing due to their biocompatibility, biodegradability and low toxicity [3].

2. Materials, Methods and Results

2.1. Preparation of nanoparticles

Polymeric NP were aseptically prepared by double emulsion (w/o/w) solvent evaporation method, described elsewhere4. Briefly, PLGA-PEG polymer was dissolved in dichloromethane (DCM) and emulsified by sonication (Sonifier Vibracell VC 375, Sonics & Materials Inc, USA) under continuous conditions for 15 s at 70 W with a glycol chitosan (CS) solution that contained OVA (5% $w_{OVA}/w_{polymer}$). A surfactant solution (internal aqueous phase; IP) was added to this o/w single emulsion and a second sonication was performed under the same conditions. The double emulsion w/o/w was added dropwise to a surfactant solution (external aqueous phase; EP), and magnetically stirred at 37°C during 1 h for organic solvent evaporation, thus enabling the formation of NP. The polymeric NP were harvested three times by centrifugation (22000 x g, 45 min, 4˚C; Beckman Coulter, lnc, Avanti® J-E Centrifuge JA-20, USA), and washed with ultrapure water to remove excess of surfactant and non-encapsulated antigen. NP were dispersed in phosphate buffered saline (PBS pH 7.4) and kept at 4˚C until analysis. Three groups of formulations were defined, depending on the nature of the surfactant used to stabilize both primary and second emulsions: i) sodium cholate as a surfactant in both IP and EP; ii) PVA in both IP and EP and iii) PVA in IP and Pluronic F127 (PF127) in EP.

Table 1: Composition of nanoparticles.

Formulation	Aqueous phase	Surfactant IP*	Surfactant EP**
NP_1b	CS ,PBS	1 % (w/v) Na-cholate	0.3 % (w/v) Na-cholate
NP_2b	CS ,PBS	2 % (w/v) Na-cholate	0.3 % (w/v) Na-cholate
NP_3b	CS, PBS	1 % (w/v) PVA	0.3 % (w/v) PVA
NP_4b	CS, PBS	2 % (w/v) PVA	0.3 % (w/v) PVA
NP_4OVA	CS, OVA	2 % (w/v) PVA	0.3 % (w/v) PVA
NP_5b	CS, PBS	4 % (w/v) PVA	0.3 % (w/v) PVA
NP_5OVA	CS, OVA	4 % (w/v) PVA	0.3 % (w/v) PVA
NP_6b	CS, PBS	10 % (w/v) PVA	0.3 % (w/v) PVA
NP_6OVA	CS, OVA	10 % (w/v) PVA	0.3 % (w/v) PVA
NP_7b	CS , PBS	2 % (w/v) PVA	0.3 % (w/v) PF127
NP_8b	CS , PBS	4 % (w/v) PVA	0.3 % (w/v) PF127
NP_8OVA	CS, OVA	4 % (w/v) PVA	0.3 % (w/v) PF127
NP_9b	CS, PBS	10 % (w/v) PVA	0.3 % (w/v) PF127
NP_9OVA	CS, OVA	10 % (w/v) PVA	0.3 % (w/v) PF127

* internal phase, ** external phase

OVA-loaded NP were prepared with a loading of 5 % $w_{OVA}/w_{polymer}$. All formulations described in Table 1 were prepared using PLGA-PEG polymer and 1 % ($w_{CS}/w_{polymer}$) CS in aqueous IP.

2.2. Physicochemical characterization of nanoparticles

NP mean size and polidispersity index (PDI) were determined by Dynamic Light Scattering (DLS) using the Malvern Nano S (Malvern Instruments, UK). NP surface charge in PBS (pH 7.4) was inferred from the determination of ζ potential that was assessed by Laser Doppler Velocimetry (LDV) with Malvern Nano Z (Malvern Instruments, UK). All measurements were performed in triplicate (Table 2).

Table 2. NP physicochemical properties. (Mean ± SD; n ≥ 3)

Formulation	Size (nm)	PDI	ζ ptential (mV)
NP_1b	NA	*Flocculated system*	NA
NP_2b	NA	2 % (w/v) Na-cholate	0.3 % (w/v) Na-cholate
NP_3b[1]	330 ± 2	0.239 ± 0.03	0.081 ± 0.87
NP_4b	263 ± 15	0.266 ± 0.021	-1.21 ± 0.87
NP_4OVA	247 ± 9	0.250 ± 0.012	-1.77 ± 0.80
NP_5b[*]	150 ± 9	0.166 ± 0.030	-1.27 ± 1.05
NP_5OVA[*]	167 ± 13	0.171 ± 0.022	-1.66 ± 0.79
NP_6b[*]	194 ± 17	0.162 ± 0.028	-0.90 ± 0.62
NP_6OVA[*]	227 ± 18	0.254 ± 0.032	-1.05 ± 0.82
NP_7b	360 ± 30	0.363 ± 0.043	-0.95 ± 0.49
NP_8b[*]	159 ± 9	0.189 ± 0.036	-1.17 ± 0.54
NP_8OVA[*]	180 ± 6	0.180 ± 0.019	-1.78 ± 0.93
NP_9b	219 ± 18	0.183 ± 0.003	-0.060 ± 0.21
NP_9OVA	NA	*Flocculated system*	NA

[*]n = 9; [1]n = 2

Overall, NP formulations were required to comply with two conditions: i) NP should present a mean size between 50 and 200 nm with a PDI below 0.2 and ii) NP surface charged should be close to neutrality, owing to lower toxicity and prevention of their premature phagocytosis by macrophages in circulation.

Formulations were divided into three groups based on the nature of the surfactant used to promote the stabilization of the double emulsion (w/o/w). The first group of formulations was developed using sodium cholate as a surfactant of both IP and EP. However, the system was not stable, due to the increased viscosity of the IP. Sodium cholate was not strong enough to lower the surface tension between organic and aqueous phases, and the coalescence of the droplets of this emulsion occurred immediately after its preparation. As a result, sodium cholate was replaced by the nonionic surfactant PVA, which is a strong colloidal stabilizer. In this second group, different concentrations (1, 2, 4 and 10% w/v) of surfactant on IP were used in order to assess its effect on NP physicochemical properties. Accordingly, higher concentrations of PVA have generally potentiated emulsion stability and thus the size of both plain and antigen-loaded NP decreased when higher concentrations of surfactant were used to emulsify aqueous and organic phases (Table 2). Moreover, the results also show that higher surfactant concentrations decreased NP polidispersity. On the other hand, OVA-loaded NP prepared with 4% (w/v) PVA solution had a average size significantly higher than NP without encapsulated antigen ($P = 0.074$). Based on these results, the 4% (w/v) PVA solution used in NP formulation also promoted the formation of a nanoparticulate population with lower polidispersity values. However, when higher amount of PVA (10% (w/v)) was used as IP, the NP size was higher by 50 nm than that presented by NP prepared with 4% (w/v) PVA solution (Table 2). This increase in average size occurred due to the higher viscosity of the 10% (w/v) PVA solution used as IP, leading to system instability having in consideration the small volume of this phase. All of these NP had ζ ptential close to neutrality, between -1.8 and 0.08 mV. However, ζ ptential of antigen-loaded NP was slightly lower, due to the fact that OVA is a negatively charged protein at pH 7.4, and if absorbed on the surface of particles can influence NP surface charge.

In the third group of NP formulations, PF127 was used as a surfactant in the EP (0.3% w/v) and different concentrations of PVA were tested as IP (2, 4, 10% w/v). These NP showed a similar trend as the second group. With increasing concentrations of surfactant in the IP (Table 2), plain NP showed lower mean diameters. Formulations obtained using 4% (w/v) of PVA solution (NP_8b and NP_8OVA) presented the best parameters among all formulated particles within this group. Those plain NP had an average size of 159 nm with

PdI of 0.19, and ζ ptential of -1.17 mV; while NP containing OVA presented a mean diameter of 180 nm, PdI of 0.18, and ζ ptential of -1.78 mV. Moreover, ζ ptential of antigen-loaded NP is slightly more negative, owing to the charge of the protein. Interestingly, when 10% (w/v) PVA solution was used (NP_9OVA), the system flocculated. This is likely due to the interactions between OVA, PF127 and increased concentration of PVA. However, this instability was not observed for plain particles (NP_9b), even if they showed higher mean diameter in comparison to the formulation prepared with 4% (w/v) PVA solution.

Overall, formulated nanosystems are expected to be suitable for parenteral administration and for the adjuvant effect needed to enhance host immune response, being possible to predict their extensively uptake by APC, namely DC [4].

2.3. Antigen loading

The amount of encapsulated protein OVA was quantified indirectly by the MicroBCATM assay [5]. Supernatants from each centrifugation were collected in triplicates. Plain NP were used as controls. The absorbances were determined using a Fluostar Omega microplate reader (BMG LAbtech, Germany) and cthe entrapment efficiency (EE% (w/w), Eq. (1)) and the loading capacity (LC μg/mg, Eq. (2)) of protein were calculated.

$$Entrapment\ Efficiency\ (EE\ \%) = \frac{initial\ amount\ of\ agent - amount\ of\ agent\ in\ the\ supernatant}{initial\ amount\ of\ agent} \times 100 \quad (1)$$

$$Loading\ Capacity\ (LC\ \mu g/mg) = \frac{initial\ amount\ of\ agent - amount\ of\ agent\ in\ the\ supernatant}{total\ amount\ of\ polymer} \quad (2)$$

Table 3. EE (%) and LC (μg/mg) of protein in formulated NP. (Mean ± SD; n ≥ 12)

Formulation	EE% (w/w)	LC (μg/mg)
NP_4OVA	44.5 ± 1.6	22.24 ± 0.82
NP_5OVA	57.5 ± 13.2	28.77 ± 6.61
NP_6OVA	59.4 ± 6.2	29.69 ± 3.10
NP_8OVA	31.8 ± 4.0	15.87 ± 1.10

*n = 3

CS polymer is able to protect biomolecules not only during particle formulation process, but also throughout release in physiologic media. The higher viscosity that is expected for IP after its dissolution may decrease the interaction between proteins and the interface of droplets of the primary (w/o) emulsion, promoting the maintenance of their structure and activity, as well as, enhancing NP LC by preventing protein leakage to the external aqueous phase. PLGA-PEG NP prepared using CS dissolved in 2% (w/v) PVA solution (NP_4OVA) presented an EE of 44.5% and a LC of 22 μg/mg. Higher concentration

of emulsifier (PVA) in the IP increased NP EE and thus led to higher LC (57.5% and 29 μg/mg for those formulated with 4% (w/v) PVA solution (NP_5OVA) and 59% and 30 μg/mg for 10% (w/v) PVA solution (NP_6OVA) as IP. It is important to emphasize however that the EE and LC obtained for those formulations were not statistically different, suggesting that the concentration of the emulsifier (PVA) and its increase from 4% (w/v) to 10 % (w/v) in the IP phase does not significantly contribute to higher entrapment efficiencies ($P > 0.05$). However, NP prepared with lower amounts of PVA in the IP (2% (w/v) PVA) showed significatively lower EE and LC.

In addition, when PVA was replaced by PF127 in EP (NP_8OVA), only 32% (w/w) of protein was found to be associated to polymer matrix (Table 3). This shows that the co-polymeric surfactant PF127 allowed an extensive leakage of OVA to this external phase probably due to its lower ability to decrease free energy at this specific emulsion droplets interface.

2.4. Evaluation of protein integrity by SDS PAGE

The assessment of protein integrity was determined by sodium dodecyl sulphate polyacrylamide gel electrophoresis (SDS-PAGE) using MW markers (Sigma Marker™, 6.5-200 kDa) and OVA standard solution (250 μg/ml) as controls [5]. Protein band patterns of migration obtained for OVA standard solution and those extracted from loaded NP (NP_OVA) are identical, suggesting that protein molecular weight had not be affected by NP formulation process. Additionally, these observations are corroborated by the absence of those bands at 45 kDa for control NP (NP_blank).

2.5. *In vitro* cell viability assay

The cytotoxicity of PLGA-PEG NP was inferred by the determination of cell viability using AlamarBlue® assay that was performed on immature murine DC (JAW SII). This cell line was incubated with increasing concentrations of three different PLGA-PEG-based NP: (i) NP with CS and PVA in IP and EP, (ii) NP with CS and PVA in IP and PF127 in EP, and (iii) NP without CS and with PVA in IP and PF127 in EF. DC viability was not affected by any type of NP.

These results support the safety and biocompatibility of PLGA-PEG and CS polymers used in the formulation of these polymeric NP [6-9]. It reinforces the fact that the organic solvent used in the formulation process might have been completely evaporated during the evaporation time, as verified previously in our laboratory [10], and thus no toxic residues

remain in NP. Also the excess of surfactants used in NP formulation might have been completely washed at the final stage of production process where three centrifugations and washings were performed. The presence of PEG on the surface of NP might also contribute to the absence of a cytotoxic effect, as this polymer is highly biocompatible due to its high hydrophilicity and due to particle surface charge close neutrality [11].

3. Conclusions

From NP physicochemical properties, LC and effect on cell viability we can conclude that the most promising formulations are NP_5 and NP_8. NPs within this size range are expected to stay longer time in circulation and be efficiently taken up by DC enhancing cross-presentation in mice. Moreover their average sizes and surface charge may prevent their premature capture by macrophages and also increases their ability to promote a tumor specific immune response. Having in consideration the results herein described, it is possible to state that the developed PLGA-PEG-based NP constitute a promising platform for the delivery of tumor associated antigens to DC, key players in tumor immunology.

Acknowledgements

The authors would like to thank for the financial support to the Fundação para a Ciência e a Technologia (FCT) Portugal, for the PhD grant (SFRH/BD/78480/2011) and for the project PTDC/SAU-FAR/119389/2010.

Chapter 3

Chapter 3 - Design of an optimal PLGA-PEG nanoparticulate vaccine for cancer immunotherapy

Eva Zupančič[a], Helena F. Florindo[a]

[a]Research Institute for Medicines (iMed.ULisboa), Faculty of Pharmacy, Universidade de Lisboa, Lisbon, Portugal.

Abstract

The major goal of this study was to demonstrate the complexity of developing a reproducible and stable colloidal nanoparticulate suspension with the desired physicochemical properties for an efficient immune cell targeting and activation. By controlling various parameters of the formulation process, the average size, polydispersity index, ζ potential, encapsulation efficiency and loading capacity were optimized to obtain highly reproducible Polyethylene glycol (PEG)-grafted poly(lactic-co-glycolic acid) (PLGA)-NP nanoparticles presenting the targeted features for the successful modulation of immune cells' activity.

Keywords: PLGA-PEG nanoparticles; cancer vaccine; antigen presenting cells; dendritic cells; tumor associated antigens (TAA)

1. Introduction

Recent advances in the fields of immunology and molecular oncology, combined with the knowledge raised from clinical and translational studies have provided deeper insights into the interaction between cancer and immune cells. Consequently newer forms of cancer treatments have been devised, including promising immunotherapeutic approaches [1]. These developments within tumor immunology have stemmed from the identification of tumor associated antigens (TAA) overexpressed in these malignant cells. Efficacious cancer vaccines potentiate the delivery of those TAA to dendritic cells (DC) to ultimately improve T cell efficiency within tumor microenvironment towards the induction of a specific and long-lasting anti-tumor immune response [2-4]. The specificity of the induced adaptive immunity is highly increased if tumor cells exclusively express those antigens delivered by the vaccine. However, these antigens are poorly immunogenic in solution and thus vaccines containing these entities generally require the use of potent immunological adjuvants in order to boost the anti-tumor immune responses.

The use of nanomedicine-based systems appears to be a promising strategy to achieve a strong and long-lasting immunity against cancer diseases. These carriers have many theoretical advantages over other conventional therapies like low toxicity, possible targeted delivery and thus high specificity. In addition, when used to deliver antigens, nanoparticles (NP) can lead to a continuous anti-tumor effect attributable to the successful induction of an immunologic memory. Moreover, it has been shown that the entrapment of both antigens and adjuvants by a singular carrier ensured an optimal processing and presentation of epitopes in a targeted and prolonged manner [5, 6].

The rate and extend of passive targeting towards DC are dictated by NP size, geometry, surface charge, hydrophobicity and hydrophilicity [7, 8].

NP size influences their endocytic pathways in antigen presenting cells (APC) and thus their accumulation and degradation [9]. Particles below 200 nm are usually transported through lymph drainage to lymph nodes (LN), where they are internalized by immature DC via classic clathrin-mediated endocytosis and tend to generate both cytotoxic T lymphocytes (CTL) and T helper (Th)1 immune responses [10-13]. Furthermore, NP within this size range are known to avoid the reticuloendothelial system (RES), such as liver and spleen, presenting then a prolonged circulation time in blood [14].

On the other side, larger NP (>0.5 μm) require peripheral immature DC and active cellular migration to the draining LN, where micropinocytosis occurs. This will preferentially

generate an immune response based on the activation of Th2 cells and production of antibodies [15, 16].

Furthermore, spherical-shaped NP display higher cellular uptake compared to non-spherical counterparts [17]. A number of studies have shown that positively charged NP present extended internalization profiles due to their ionic interactions with the negatively charged cell membrane [18-20]. Hence, negatively charged and neutral NP preferentially co-localize within the acidic pH at lysosomes, while positively charged NP could escape, being thus released into cell cytoplasm [21, 22]. Surface charge of NP mainly depends on the chemical nature of the polymer and stabilizing agent [23].

The poly(lactic-co-glycolic acid) (PLGA)-based NP are promising tools for the modulation of immune cells' activity. The properties of this aliphatic polyester polymer can be manipulated in order to control antigen release towards its extensive capture and prolonged presentation, promoting the expansion of effector T cells [24, 25].

Aliphatic copolymer PLGA is negatively charged at pH 7.4. Therefore, PLGA NP become positively charged in the endosomal and lysosomal compartments, due to their acidic pH, being thus released into the cytosol, where the antigen cross-presentation through the major histocompatibility complex (MHC) class I pathway promotes the generation of CTL [20, 26-28]. However, surface charge of aliphatic polyester-based NP can be easily shifted to the neutral or positive charges by using PEG-coated polymers or adding cationic polymers, such as chitosan (CS) [29-31]. All these advantages listed above make aliphatic polyester-based NP a promising cancer immunotherapeutic strategy.

The major goal of this work was the development of a colloidal suspension of polyethylene glycol (PEG)-grafted PLGA-NP for the passive targeting of APC, preferentially DC. Having in consideration previous evidences related to the interaction of nanocarriers with phagocytic cells, NP composition and formulation process were optimized in order to obtain NP with mean size below 200 nm, neutral surface charge and spherical shape. Nanosystems were developed by the double-emulsion solvent evaporation technique, using α-lactalbumin (LALBA) as an antigen. Other polymers (glycol CS, polyvinyl alcohol (PVA) and block co-polymer Pluronic® F127 (PF127)) were used in order to best attain the most efficient parameters for an optimal antigen delivery to APC. This chapter particularly explored the impact of surfactant physical and chemical properties, and concentration on the characteristics of those PLGA-PEG- NP, including batch stability. The optimal NP will be selected for *in vitro* and *in vivo* evaluation of the adjuvant effect of this novel nanoparticulate vaccine.

2. Materials and methods

2.1. Materials

Poly(lactic-co-glycolic acid) (PLGA) conjugated with polyethylene glycol (PEG), i.e. PLGA-PEG (5050 DLG mPEG 5000, 10 wt % PEG, molecular weight (MW) = 17 kDa), Alpha-lactoalbumin (LALBA, average MW = 14 kDa), Polyvinyl alcohol (PVA, MW = 13-23 kDa) with hydrolyzation 87-89 %, Pluronic® F127 (PF127, MW = 12.6 kDa), Glycol Chitosan (CS), and Dichloromethane (DCM) were purchased from Sigma-Aldrich (St. Louis, MO, USA). All other chemicals and reagent used in the study were of analytical grade.

Dulbecco's Phosphate Buffered Saline (PBS) (1×) was purchased to Life Technologies (Carlsbad, CA, USA).

Double distilled water was used after filtration in a Millipore® (Millipore, Billerica, MA) system.

2.2. Preparation process of PLGA-PEG nanoparticles

Biodegradable polymeric NP were prepared by the state of the art double emulsion solvent evaporation technique (w/o/w) [32], with specific modifications. This method is based on the emulsification of an aqueous phase into an organic polymeric solution, where NP result from single volume shrinkage of the initial emulsion droplet by ultrasonication. Accordingly, the aqueous solutions containing the antigen LALBA dispersed in PVA solutions at different concentrations (2, 4, 6, 8, 10, 12 or 14 % (v/v)) were added to the PLGA-PEG polymer solutions (50 mg/ml in DCM) and emulsified using an ultrasonic processor for 15 s at 70 W. A second emulsion was performed with 2 % (w/v) PVA aqueous solution under the same conditions. The double emulsion w/o/w was added dropwise to a surfactant solution containing 0.3 % (w/v) PVA or Pluronic F127 (PF127), the external aqueous phase (EP), and stirred at 37 °C for 1 h. The NP suspension was then washed twice with ultrapure water by centrifugation at 22000 × g for 45 min, 4 °C (Beckman Coulter Avanti® J-E Centrifuge JA-20) and finally re-suspended in phosphate buffered saline (PBS pH 7.4) and kept at 4 ˚C until further analysis.

2.3. Particle size and ζ potential analysis

NP size and polydispersity index (PDI) were determined by Dynamic Light Scattering (DLS) using the Malvern Nano S (Malvern Instruments, UK). Briefly, the final 20 mg/ml NP suspension was diluted to 1 mg/ml in PBS pH 7.4. Nanoparticles' surface charge was inferred by their ζ potential assessed by Laser Doppler Velocimetry (LDV) with Malvern Nano Z

(Malvern Instruments, UK). Each analysis was carried out in triplicate at 25 °C. The conditions were kept constant in order to have comparable results.

2.4. Protein loading assay

The supernatants obtained from NP centrifugation were collected and the entrapment efficiency (EE, %) and the loading capacity (LC, μg/ml) of proteins were quantified indirectly by a reverse-phase high-performance liquid chromatography (HPLC) (RP-HPLC) using Beckman System Gold: UV-Vis detector (Beckman 166) at 220 nm, Beckman 126 solvent module and Midas autosampler. Samples (20 μl) were injected onto a Shodex Protein KW-803 series column (8.0 mm ID x 300 mm, 5 μm particle size, 300 Å pore size) and eluted with 50 mM sodium phosphate buffer (pH 7.0) plus 0.3 M NaCl at 1 ml/min for 16 min at room temperature. Plain NP were used as controls and all measurements were performed in triplicate. The amount of protein in each sample was calculated using a linear standard curve generated in the range of 0.5 – 5.0 mg/ml, $r^2 = 0.9987$. The EE (%) and the LC (μg/mg) of the protein were calculated as indicated in Equations 1 and 2.

$$EE\ \% = \left(\frac{initial\ amount\ of\ antigen - amount\ of\ antigen\ in\ supernatant}{initial\ amount\ of\ antigen}\right) x\ 100 \quad (1)$$

$$LC\ \mu g\ /\ mg = \left(\frac{initial\ amount\ of\ antigen - amount\ of\ antigen\ in\ supernatant}{total\ amount\ of\ polymer}\right) x\ 100 \quad (2)$$

2.5. Determination of residual surfactant at nanoparticle vaccine

Surfactant washing efficiency was indirectly quantified HPLC using Beckman System Gold: UV-Vis detector (Beckman 166), Beckman 126 solvent module, Midas autosampler, and Shodex Protein KW-803 column (8.0 mm ID x 300 mm, 5 μm particle size, 300 Å pore size). The PVA washing efficiency was calculated as the percentage of PVA quantified in supernatants comparing to the total amount of surfactant used for NP formulation.

3. Results

The NP size distribution and surface charge are key parameters for carrier biodistribution and fate. In addition, the NP size also influences their EE and LC [10, 18, 25]. The major goal of this study was to develop NP smaller than 200 nm with uniform size distribution, PDI below 0.2, high LC and ζ potential close to neutrality, in order to potentiate NP-APC interaction.

Table 1: Composition of tested PLGA-PEG nanoparticles.

Formulation	Matrix polymer	Aqueous phase	Surfactant IP*	Surfactant EP**
F1	PLGA-PEG	2 % (w/v) PVA, CS, LALBA	2% (w/v) PVA	0.3 % (w/v) PVA
F2		4 % (w/v) PVA, CS, LALBA		
F3		6 % (w/v) PVA, CS, LALBA		
F4		8 % (w/v) PVA, CS, LALBA		
F5		10 % (w/v) PVA, CS, LALBA		
F6		12 % (w/v) PVA, CS, LALBA		
F7		14 % (w/v) PVA, CS, LALBA		
F8	PLGA-PEG	2 % (w/v) PVA, CS, LALBA	2% (w/v) PVA	0.3 % (w/v) PF127
F9		4 % (w/v) PVA, CS, LALBA		
F10		6 % (w/v) PVA, CS, LALBA		
F11		8 % (w/v) PVA, CS, LALBA		
F12		10 % (w/v) PVA, CS, LALBA		
F13		12 % (w/v) PVA, CS, LALBA		
F14		14 % (w/v) PVA, CS, LALBA		

* internal phase, ** external phase

All formulations described in Table 1 were developed using 0.5 % ($w_{CS}/w_{polymer}$) CS solution and 2.5 % ($w_{LALBA}/w_{polymer}$) LALBA solution in the aqueous phase. For each formulation, blank NP were formulated as controls.

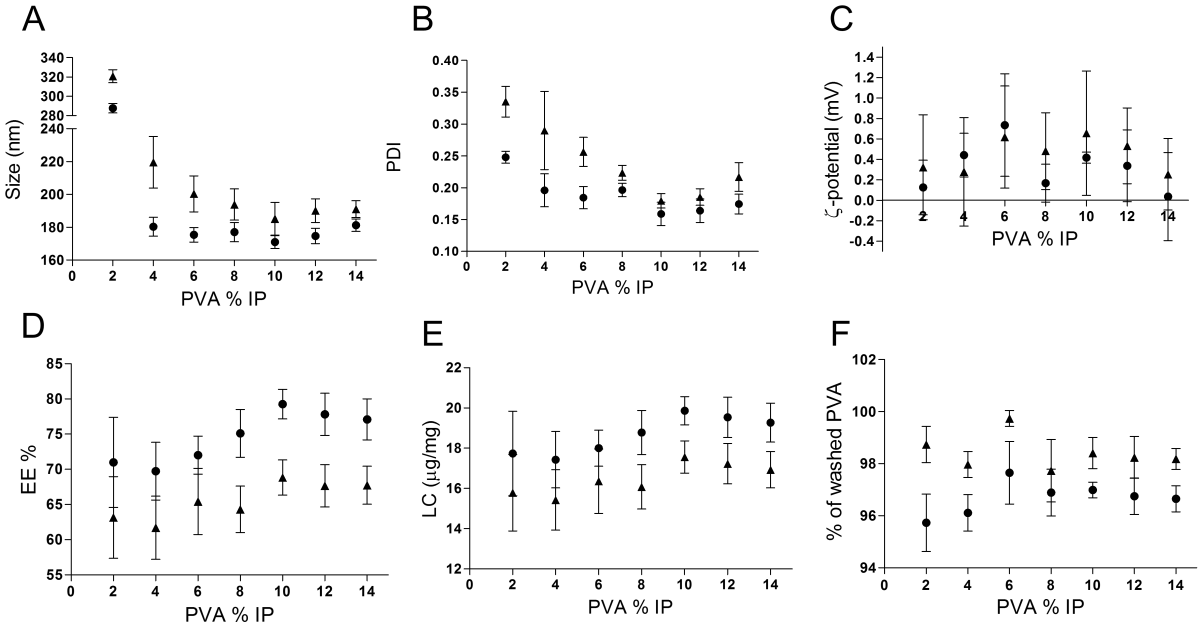

Figure 1: Circles (●) are for all the formulation (F1-F7), developed with PVA in the EP. Triangles (▲) are used for all formulations (F8-F14) prepared with Pluronic as EP. Average size (A), poydispersity index (PdI) (B), ζ potential (C), entrapment efficiency (EE) (D), loading capacity (LC) (E) and percent of washed PVA (F) were determine for all PLGA-PEG NP. All results are expressed as mean ± SD of three independent experiments of 3-5 formulations per group (n>3).

Various concentrations of PVA (2, 4, 6, 8, 10, 12 and 14% (w/v)) in the IP were tested to produce highly reproducible and stable NP, with the required physicochemical properties for DC targeting. The targeted NP size, surface charge and PDI were achieved with formulations F5 & F12. Even though, the effect of PVA higher concentrations in the IP on NP parameters and suspension overall stability was further evaluated.

PVA concentration influenced the average size of formulated NP and their EE (Figure 1). DLS results were recorded in triplicate (n = 3) of at least three independent batches of NP formulations (Figure 1). DLS studies yielded consistent and reproducible results. It is observed that higher concentrations of the PVA in aqueous phase led to smaller NP and lower PDI. The highest decrease on the average mean diameter of NP was determined when PVA concentration in the aqueous phase ranged from 2 % (w/v) to 4 % (w/v). However, NP with size bellow 200 nm were only obtained when the concentration of PVA was at least 8 % (w/v) in the primary aqueous phase (Figure 1A). PDI of the formulation F11 was still higher than 0.2 (Figure 1B), and therefore out of the targeted specifications.

ζ potential was determined by LDV of all formulated batches of NP (from F1 to F14). It was slightly positive (Figure 1C) but close to neutrality, despite the nature of the surfactant used at the external phase (PVA or PF127). This could be due to the PEG–chains expected to be on the surface of the NP and also to the presence of positively charged CS dispersed within the nanoparticulate matrix.

It is also possible to infer that smaller NP with low PDI, led to higher antigen EE and LC (Figure 1D & E), both validated by HPLC method. The best EE was determined for formulations F5, F6, and F7, being close to 80 %. Lower EE were presented by F12, F13, and F14 NP prepared with PF127 in EP, being close to 70 %.

At least 96 % (Figure 1F) of the surfactant was removed from NP during washing procedure.

4. Discussion

In this study we focused on the design of reproducible batches of NP vaccines with desirable physicochemical characteristics. To achieve this goal, it is important to understand the physical and chemical properties of raw materials and correlate those with critical parameters within formulation process.

A significant amount of research has been conducted on numerous nanoparticulate systems, which show that physical and chemical properties of NP are crucial for their biological outcome as delivery system [11, 33].

In this study, we developed and precisely characterized different nanoparticulate delivery systems for the systemic delivery of a protein antigen to DC, the key APC with a determinant role in the stimulation and enhancement of T cell immunity. Consequently, having in consideration previous evidences, we aimed to develop a highly stable and reproducible colloidal suspension of NP smaller than 200 nm with narrow size distribution, and ζ potential close to neutrality.

LALBA was selected as a model antigen to be associated to the modified DC-targeted polymeric NP. LALBA is a breast specific differentiation protein expressed at high levels in the majority of human breast carcinomas [34], expressed in 67 % of primary mammary carcinomas and in 62 % of their metastases, including lymph nodes, bone, liver, lung, skin, and subcutaneous tissue. In contrast, it is present only in mammary epithelial cells during lactation [34-36]. Due to its characteristics it is a perfect target for anti-cancer immunotherapeutic approach.

The aliphatic polyester copolymer PLGA-PEG has been chosen not only due to its biodegradable and biocompatible characteristics, but especially having in consideration the expected exposure of PEG chain at the surface of the resultant nanocarrier [7, 25]. The PEGylated layer will overcome the negative charge of PLGA carboxylic groups, leading to neutral nanoparticulate surfaces. PLGA-PEG NP are expected to present PEG-chains oriented towards the external aqueous phase, which will act as a barrier, by suppressing the adsorption of serum proteins and reducing the extent of cell recognition by steric and hydrated repulsion, leading to an enhanced shelf stability [37, 38]. It has been shown that the protein repellant ability of PEG-containing surfaces depends on PEG chain molecular weight, interfacial density and architecture [39]. Moreover, different works have evidenced that Pegylated PLGA NP presented smaller average size in comparison to the non-PEGylated ones. All of these parameters resulted in better release kinetics and reduction of systemic clearance rates *in vivo*, and prolonged the circulation time of formulated NP [30].

The production of the PLGA-PEG di-block (10% PEG with 5 kDa) co-polymer by Boehringer Ingelheim (Germany), used in chapter 2, was interrupted and therefore it was necessary to choose a different supplier. In fact, anticipating the possible changes in the properties of this polymer when produced by another company, it was necessary to ensure that a considerable amount would be available for the future studies. New PLGA-PEG polymer was thus purchased from Sigma-Aldrich and its effect on formulation physical and chemical properties was further evaluated.

PVA is a commonly used polymeric non-ionic surfactant with a HLB value of 18 [40]. Due to its ampiphilic character, it has excellent emulsifying properties, being commonly used for stabilization of w/o/w double emulsion at the formation of NP. However, EMA (European Medicines Agency) and FDA (Food and Drug Administration) attention has been attracted by several studies evidencing the possible effect of this surfactant in cell viability. We performed an indirect quantification of PVA by HPLC to determine the surfactant washing efficiency. Our data attested the successful removal of this surfactant.

PF127, on the other hand, is a triblock copolymer (polyoxyethylene-block–polyoxypropylene-block-polyoxyethylene; PEO-b-PPO-b-PEO), being the most cytocompatible polymer among the Pluronics. Thus, it has been widely applied in a variety of pharmaceutical formulations due to its surfactant (HBL value between 18 and 23) and protein stabilizing properties [41]. In our studies, PF127 was used to develop an alternative formulation with possible improved mechanisms of interaction *in vitro* and *in vivo* with immune cells.

The PVA surfactant concentration in IP dictated NP average mean diameter, PDI, ζ potential, EE and LC. All of the above mentioned parameters were monitored in order to select the best formulation composition.

NP based on the PLGA-PEG polymer, now supplied by Sigma Aldrich, were firstly developed using 2 and 4 % (w/v) PVA surfactant concentration in the internal aqueous phase (IP), as this was the concentration previously used with polymer perches from Boehringer Ingelheim (Chapter 2). The average size of these NP was not comparable to the previous ones obtained for NP developed in Chapter 2. Formulations F1 and F8 presented an average size above 300 nm when using 2 % (w/v) PVA, while it was dramatically increased in formulation F2 when a 4 % (w/v) PVA solution was used in the IP. However, this trend was not observed for formulation F9 when PF127 was used as a stabilizer of EP.

Having in consideration these results regarding NP size and low reproducibility, as anticipated, it was necessary to optimize the formulation by testing various concentrations of PVA (2, 4, 6, 8, 10, 12 and 14% (w/v)) in the IP, to produce highly reproducible and stable NP, with the required physicochemical properties for DC targeting.

Overall, NP presented neutral ζ potential, while DLS studies showed that higher concentration of the PVA surfactant in the IP led to lower particle size and size distribution. Moreover, NP with smaller size and PDI, resulted in more stable colloidal nanoparticulate suspensions and thus favored the entrapment of the model antigen. The highest EE was obtained for the formulations F5, F6 and F8, being close to 80 %. When using PF127 in the

EP, the EE was 70 % (F12, F13, and F14). However, the developed NP presented EE higher than those reported in recently published studies, despite the nature of surfactant present at the EP [27, 42, 43].

High EE and LC were also related to the presence of CS in the IP. CS increases the viscosity of this aqueous phase [44, 45] and it is also expected to potentiate protein entrapment due to the establishment of electrostatic interactions between the negative charge of the model protein at PBS pH 7.4 (isoelectric point 4.2) and CS positively charged amines at that pH. Both properties may thus be underlying an improved physical and chemical stability of the internal phase, and thus to the higher EE and LC obtained for NP prepared using CS in the IP (Figure 1).

Overall, according to these results, the physicochemical properties of developed PLGA-PEG NP are composition dependent, as expected. The formulations F5 and F12 best meet the criteria enlisted above. Both formulations presented high reproducibility and stability with NP smaller than 200 nm, with a uniformed size distribution and high LC and EE. The percentage of washed PVA, detected by HPLC, was higher than 97 % for both formulations.

5. Conclusions

The aim of this study was to develop a nanoparticulate delivery system with optimal physicochemical properties to passively target APC, principally DC. A reproducible formulation method has been developed using biodegradable and biocompatible aliphatic polyester copolymer PLGA-PEG to produce ~175 nm NP with narrow particle size distribution and ζ potential close to neutrality. This property constitutes a basic advantage to enhance the interaction of a vaccine delivery system with DC, by avoiding their premature recognition and capture by macrophages- the first line of body defence. These results highlight the importance of NP composition, as expected, as small differences in the surfactant concentration can may result in altered and unsuited NP average size, PDI and EE.

These optimal formulations were selected for further *in vitro* and *in vivo* evaluation of these vaccine carriers on the modulation of immune cells' activity.

Acknowledgement

The authors would like to thank for the financial support to the Fundação para a Ciência e a Technologia (FCT) Portugal, for the PhD grant (SFRH/BD/78480/2011) and for the project PTDC/SAU-FAR/119389/2010.

Chapter 4

Chapter 4 - A mechanistic approach for selecting nanoparticulate immunotherapeutic vaccines for systemic antigen delivery towards dendritic cells

Eva Zupančič[a,b,c], Caterina Curato[c], Maria Paisana[a], Catarina Rodrigues[a], Ziv Porat[d], Ana S Viana[e], Carlos A Afonso[a], João Pinto[a], João N Moreira[b,f], Rogério Gaspar[a], Ronit Satchi-Fainaro[g], Steffen Jung[c*], Helena F Florindo[a*]

[a]Research Institute for Medicines (iMed.ULisboa), Faculty of Pharmacy, Universidade de Lisboa, Lisbon, Portugal.

[b]Center for Neuroscience and Cell Biology (CNC), Unniversity of Coimbra, Portugal

[c]Immunology, The Weizmann Institute of Science, Rehovot, Israel

[d]Biological Services, The Weizmann Institute of Science, Rehovot, Israel

[e]Chemistry and Biochemistry Center, Sciences Faculty, Universidade de Lisboa, 1749-016 Lisbon, Portugal

[f]Faculty of Pharmacy (FFUC), University of Coimbra, Portugal

[g]Department of Physiology and Pharmacology, Sackler School of Medicine, Tel Aviv University, Israel

Submited to the Elsevier journal Biomaterials (under revision by September 2016)

Abstract

Vaccination is a promising strategy to trigger and boost immune responses against cancer. Here we designed biodegradable polymeric nanoparticles (NP) using different surfactants and polymers for particle stabilization to develop a nanoparticle delivery system with unique properties for clinical applications in immunotherapy and to optimize particle uptake by specific immune cells.

We report the design and development of safe and efficacious nanoparticulate vaccines including an extensive characterization of physiochemical NP parameters, such as average size, ζ potential, loading efficiency, thermodynamic stability, and protein integrity. *In vitro* uptake of these NP by murine bone marrow-derived dendritic cells (DC) was observed and quantified by imaging flow cytometry. *In vivo* activation of DC by NP was analyzed in lymph nodes (LN) of immunized animals. Induction of activation markers and upregulation of co-stimulatory molecules by specific NP was studied post-immunization. Antigen-specific immune responses towards ovalbumin (OVA)-loaded NP were monitored through analysis of proliferation and expansion of OVA-specific T cell receptor transgenic $CD4^+$ and $CD8^+$ LN T cells. We show how physicochemical properties of particle surfaces, dictated by surfactant selection or the antigen association method, can alter fundamental particle properties and thereby influence cellular uptake, leading to distinct antigen presentation efficacy and resultant antigen-specific responses.

Our studies highlight the need for comprehensive characterization of NP to optimize their use for vaccination strategies. These findings support the notion that the delivery system itself is a potential and versatile adjuvant platform.

Keywords: Dendritic cells; polymeric nanoparticles; PLGA; PLGA-PEG; vaccine; immunization

1. Introduction

Effective immune responses result from a complex interplay between the innate (antigen-nonspecific) and the adaptive (antigen-specific) immune cell compartments. Dendritic cells (DC) are the most potent antigen presenting cells (APC) and have, owing to this property, an important role in translating innate into adaptive immunity. Given their capacity to capture and process internalized antigens, DC efficiently prime naive T cells against foreign antigens and polarize them towards distinct effector fates [1-3]. Moreover, the specific DC subsets and their activation mode after antigen engulfment are pivotal steps that control whether clinically relevant responses are dominated by cytotoxic $CD8^+$ T cells, or $CD4^+$ T cells with helper activity [4].

Vaccination protocols that target DC are promising strategies for the initiation and enhancement of immune responses for cancer treatment [5, 6], as well as viral and microbial infections [7-9].

Specifically, the concept of the immunotherapeutic vaccination aims to harness the patients' own immune system to specifically target malignant or infected cells by activating *in vivo* immune effectors against specific tumor associated antigens (TAA) or microbes [5].

Nanoparticulate delivery systems have major potential as immunotherapeutic platform towards the tailored and effective targeting of immune cells, which have a pivotal role in enhancing the immune response towards a specific antigen. Nanoparticles (NP) can improve antigen stability and have high surface to volume ratios, thus improving loading capacity. NP often are biocompatible and biodegradable, with tunable sub-cellular size, and a possibility of controlled release [10, 11]. NP can therefore extend antigen exposure of immune cells, facilitate uptake and antigen access to DC, modulate the antigen presentation pathway, and enhance the subsequent antigen-specific immune responses.

Herein we describe the rational development of different nanoparticulate delivery systems with the ability of systemic antigen delivery to DC for potential anti-cancer treatment.

We address the reproducibility and stability of the colloid suspension with the targeted physicochemical parameters, by controlling various parameters of the formulation process of poly(lactic-co-glycolic acid) (PLGA)-based NP, using alpha-lactalbumin (LALBA) or ovalbumin (OVA) as antigens.

PLGA polymers have been chosen due to their biocompatibility and biodegradable properties [12, 13] Under physiological environment, PLGA matrix faces hydrolytic

degradation into the monomeric components, lactic and glycolic acid, [14] both compatible with cell proliferation. Pharmaceutical products containing PLGA have already been approved by EMA (European Medicines Agency) and FDA (Food and Drug Administration) for parenteral use [15, 16]. Poly(ethylene glycol) (PEG) was also used as a carrier surface modifier with hydrophilic shielding properties, to increase polymer water-solubility and thus biocompatibility, greatly reducing intrinsic immunogenicity and toxicity [17]. LALBA protein was selected as targeted vaccine antigen, since this breast specific protein is overexpressed in 67 % of primary breast carcinomas and in 62 % of metastatic ones [18-20], being only conditionally present in healthy breast tissue at the time of lactation [21, 22]. Thus, LALBA meets the criteria for antigen selection in the development of a cancer vaccine [19]. OVA is commonly used as a model antigen in preclinical studies and well characterized in studies, which focus on specifics of induced immune responses, not the least due the availability of OVA-specific T cell receptor (TCR) transgenic mice [23, 24].

Antigens can be either adsorbed or entrapped into NP. Entrapment allows stronger interaction between these carriers and the antigen, which may lead to prolong and controlled antigen release [25]; on the other hand, antigen adsorption based on charged and hydrophilic interactions is weaker and therefore antigen is expected to dissociate from the NP surface much faster. However, both high entrapment and adsorption strongly depend on the physicochemical properties of the nanoparticulate delivery system [26-29].

To develop a highly stable colloid suspension with the desired specifications for optimal vaccination purposes, we optimized the NP composition and formulation procedure in order to achieve an average size below 200 nm, ζ potential close to neutrality, high loading efficiency, thermodynamic stability, and ensure protein integrity [11, 30, 31].

This work explores the development of safe and efficacious nanoparticulate vaccines, which physicochemical properties were fully characterized in detail. In addition, we evaluated NP uptake by DC, both *in vitro* and *in vivo*, including effects on activation and maturation of these APC, which are critical checkpoints for effective immune responses. We report that immunization with antigen-loaded NP results in successful DC stimulation and extensive T cell expansion. Most importantly, our well-characterized nanosystem allowed to correlate NP functionality with major physicochemical properties, namely presence of antigen at the surface or antigen dispersion within the matrix.

2. Materials and methods

2.1. Materials

Poly(lactic-co-glycolic acid) (PLGA) conjugated with polyethylene glycol (PEG), i.e. PLGA-PEG (5050 DLG mPEG 5000, 10 wt % PEG, molecular weight (MW) = 17 kDa), Resomer® RG 502 Poly(lactic-co-glycolic acid) PLGA (MW = 7–17 kDa), Alpha-lactoalbumin (LALBA, average MW = 14 kDa), Ovalbumin (OVA, average MW = 45 kDa), Poly(vinil alcohol) (PVA, MW = 13-23 kDa) and hydrolyzation 87-89 %, Pluronic® F127 (MW = 12.6 kDa), Glycol Chitosan (CS), sucrose and Dichloromethane (DCM) were purchased from Sigma-Aldrich (St. Louis, MO, USA). Double distilled water was used after filtration in a Millipore® (Millipore, Billerica, MA) system. All other chemicals and reagent used in the study were of analytical grade.

MW markers for SDS PAGE (Thermo Fisher Scientific, PageRulerTM Prestained Protein Ladder 10-180 kDa #SM0671) were purchased from Thermo Fisher Scientific (MA, USA).

The Roswell Park Memorial Institute medium (RPMI 1640), heat inactivated fetal bovine serum (FBS), L-glutamine 200 mM, 0.25 % (w/v) Trypsin/ 0.53 mM ethylenediamine tetracetic acid (Trypsin-EDTA) solution penicillin/streptomycin (Pen-Strep) 10000 Unit/ml/10000 μg/ml and AlamarBlue® were purchased from Life Technologies (Carlsbad, CA, USA).

Granulocyte-macrophage colony stimulating factor (GM-CSF) and interleukine-4 (IL-4) were purchase from PeproTech Inc. (Rocky Hill, NJ, USA).

The CpG ODN 1826 VaccigradeTM (TCCATGACGTTCCTGACGTT) was purchased from the InvivoGen (San Diego, CA, USA).

Antibodies anti-mouse CD11c (clone: N418), CD11b (clone: M1/70), CD4 (clone: CK1.5), CD8α (clone: 53-6.7), I-Ab (MHCII; clone: AF6-120.1), H-2Kb (MHCI; clone: AF6-88.5), CD45.1 (clone: A20), TCRβ (clone: H57-597), TCRVα2 (clone: B20.1) and Carboxyfluorescein diacetate succinimidyl ester (CFSE) were purchased from BioLegend (San Diego, CA, USA).

2.2. Mice

Female OT-I (C57BL/6) TCR transgenic mice harboring OVA-specific CD8 T cells [23] and OT-II (C57BL/6) TCR transgenic mice harboring OVA-specific CD4 T cells [24] were in-house bred at the Weizmann Institute of Science (Rehovot, Israel), under conventional, specific pathogen-free (SPF) conditions. Female C57BL/6 mice (6 - 8 weeks

old) were purchased from the Envigo RMS LTD (Jerusalem, Israel). All animals were handled according to protocols approved by the Weizmann Institute Animal Care Committee (IACUC) as per international guidelines.

2.3. Preparation of NP

Polymeric NP were aseptically prepared by double emulsion (w/o/w) solvent evaporation method [32]. Briefly, the single emulsion (o/w) was formed emulsifying an organic solution of the polymer, which was dissolved in dichloromethane (DCM) with an aqueous solution (IP) using an ultrasonic processor (Sonifier Vibracell VC 375, Sonics & Materials Inc, USA) under continuous conditions for 15 s at 70 W in an ice bath. Two different types of NP were formulated: with antigen dissolved in the IP for future Entrapped (Entrap) protein NP or without a protein in IP, being rather adsorbed onto the surface of the NP for future Adsorbed (Ads) protein NP. Fluorescent NP were formulated by replacing one tenth of the polymer mass by Rho-PLGA, synthesized in-house as previously described [33], or by replacing 50 µL of organic polymer solution with (2 mg/mL) Rhodamine G6 (Sigma-Aldrich) solution in DCM. A 2 % (w/v) polyvinyl alcohol (PVA) solution was added to the o/w primary emulsion and a second sonication was performed under the same conditions. The double emulsion w/o/w was added dropwise to a surfactant solution containing 0.3 % (w/v) PVA or Pluronic F127 (PF127), which constituted an external aqueous phase (EP). Afterwards, the solvent evaporation was carried out by gentle magnetic stirring at 37 °C during 1 h, thus enabling the formation of NP. The polymeric NP were harvested by centrifugation (22000 x g, 45 min, 4 ˚C; Beckman Coulter, lnc, Avanti® J-E Centrifuge JA-20, USA), and rinsed with ultrapure water three times to remove excess of surfactant and non-associated antigen. NP were resuspended in phosphate buffered saline (PBS) pH 7.4 and kept at 4 ˚C until further analysis. 100 µl of LALBA solution (10 mg/ml) was adsorbed to NP by 1 h incubation at room temperature. Protein-adsorbed NP were washed with ultrapure water and centrifuged at 22000 x g for 20 min at 4 ˚C.

2.4. Characterization of NP size and ζ potential

NP size and polydispersity index (PDI) were determined by Dynamic Light Scattering (DLS) using the Malvern Nano S (Malvern Instruments, UK). Briefly, the final 20 mg/ml NP suspension was re-suspended in PBS pH 7.4 to prepare 1 mg/ml NP suspensions. The conditions were kept constant in order to have comparable results. Readings were obtained based on the scattering of laser light within the equipment by the Brownian motion of NP.

Each analysis was carried out in triplicate at 25°C. NP' surface charge was inferred by their ζ potential that was assessed by Laser Doppler Velocimetry (LDV) with Malvern Nano Z (Malvern Instruments, UK). Since ζ potential is highly dependent on measurement conditions, mainly pH and ionic strength of the dispersant and concentration of NP in the suspension, those conditions were always maintained. All measurements were performed at 25 °C in triplicate.

2.5. Atomic force microscopy

The morphology of formulated NP was investigated by Tapping mode atomic force microscopy (AFM) (Nanoscope IIIa Mulimode AFM, Digital Instruments, Veeco), using silicon tips (ca. 300 kHz) at a scan rate of ca. 1.6 Hz. Samples were diluted in purified water (10 mg/ml), a drop was placed onto freshly cleaved mica for 20 min, and dried with N2 prior to analysis.

2.6. Protein loading

The supernatants from NP centrifugation were collected and the entrapment efficiency (EE, %) and the loading capacity (LC, μg/mg) of proteins were quantified indirectly by a reverse-phase high-performance liquid chromatography (HPLC) (RP-HPLC) using Beckman System Gold: UV-Vis detector (Beckman 166) at 220 nm, Beckman 126 solvent module and Midas autosampler. Samples (20 μl) were injected onto a Shodex Protein KW-803 series column (8.0 mm ID x 300 mm, 5 μm particle size, 300 Å pore size) and eluted with 50 mM sodium phosphate buffer (pH 7.0) plus 0.3 M NaCl at 1 ml/min for 16 min at room temperature. Plain NP were used as controls and all measurements were performed in triplicate. The amount of protein in each sample was calculated using a linear standard curve generated in the range of 0.5 – 5.0 mg/ml, $r^2 = 0.9987$. The EE (%) and the LC (μg/mg) of protein were calculated as indicated in Equations 1 and 2.

$$EE\ \% = \left(\frac{initial\ amount\ of\ antigen - amount\ of\ antigen\ in\ supernatant}{initial\ amount\ of\ antigen}\right) x\ 100 \quad (1)$$

$$LC\ \mu g\ /\ mg = \left(\frac{initial\ amount\ of\ antigen - amount\ of\ antigen\ in\ supernatant}{total\ amount\ of\ polymer}\right) x\ 100 \quad (2)$$

2.7. PVA assay

To determine the residual amount of PVA at NP, PVA was indirectly quantified by HPLC using Beckman System Gold: UV-Vis detector (Beckman 166), Beckman 126 solvent module, Midas autosampler, and Shodex Protein KW-803 column (8.0 mm ID x 300 mm, 5 µm particle size, 300 Å pore size). The surfactant washing efficiency was calculated as the percentage of PVA quantified in the supernatants comparing to the total amount used for NP formulation.

2.8. Freeze-drying of NP

NP were freeze-dried in the presence of the 0.05 % (w/v) sucrose, which was used as a cryoprotectant. Prior to lyophilization, all samples were placed into glass vials and frozen at -80 °C. On the following day, samples were freeze-dried for 24 h at -45 °C, 0.2 mbar in a VirTis BenchTop L freeze-drier (SP Scientific, NY, US). Lyophilized NP were only used for FTIR and thermal characterization.

2.9. Integrity of the NP-entrapped protein (SDS-PAGE)

The assessment of protein integrity was determined by sodium dodecyl sulphate polyacrylamide gel electrophoresis (SDS-PAGE). LALBA standard solution (250 µg/mL) and NP suspension (20 mg/ml) were mixed with SDS-containing loading buffer and digested at 95 °C for 20 min. Samples were loaded at room temperature onto a 10 % (w/w) polyacrilamide mini-gel (20 µl for samples and 5µl for MW markers (Thermo Fisher Scientific, 10 - 180 kDa) and electrophoresis was then performed at a constant voltage of 170 V for 50 min using a Bio-Rad 300 power pack (Bio-Rad, Hercules, CA, USA). Gels were further stained with Coomassie Blue G250 0.025 % (w/v) to reveal protein bands [34].

2.10. FTIR characterization

Each sample was mixed with KBr at a concentration of 0.5 w/w. The mixtures (200 mg) were compressed into a tablet of 12 mm diameter. The infrared spectras were measured at the absorption mode (IR Affinity-1 Shimadzu spectrophotometer, Japan) with 64 scans with a resolution of 2 cm^{-1}.

2.11. Thermal characterization

The thermal properties of the samples were determined using a DSC (TA instruments, Q200, USA) after calibration with indium (TA instruments, USA; T_{fus} =156.55 °C, $\Delta_{fus}H$ = 28.51 J/g). Dry $N_{2(g)}$ was used as the purge gas (Air Liquide, 50 ml/min). Prior to the

experiment, all the samples were kept in dry atmosphere with only 11 % of humidity (Lithium chloride supersaturated solution) for one week. The samples (2 to 3 mg) were placed in hermetic crucibles and heated up at 5 °C/min from 0 °C to 100 °C. An empty crucible was used as reference.

2.12. Stability of NP

Aseptically prepared polymeric NP were dispersed in PBS pH 7.4 and kept at 4 ˚C. After predetermined periods of time over 3 months, samples were collected and particle size, PDI, and ζ potential were evaluated.

2.13. *In vitro* evaluation of target cell viability in the presence of NP

The murine immature DC line (JAW SII cell line, American Type Culture Collection, ATCC#CRL-11904) was cultured in RPMI medium1640 supplemented with GM-CSF (50 ng/mL) and IL-4 (50 ng/mL) in 5 % CO_2 at 37 °C. Cell viability of JAW SII DC was quantitatively evaluated by measuring metabolic activity of mitochondrial dehydrogenase by AlamarBlue®. DC were incubated with increasing concentrations of different nanoparticulate systems in a 96-well plate (Nunc®, Roshilda, Denmark). Cells were seeded with a total volume of 5000 cells/100 µl/well. Different concentrations of NP suspension (100, 125, 150, 200, 250, 500, 1000 µl/ml) were added to wells. Cells in culture medium were used as negative control, while the positive control was obtained after cell treatment with a solution of 0.5 % (v/v) Triton X-100 (Gibco®). After NP incubation for 21 h at 37 °C with 5 % CO2, 10 µl of AlamarBlue® reagent were added to each well and incubated for additional 3 h. After a total of 24 h of incubation, the absorbance of AlamarBlue® was determined with a Fluostar Omega microplate reader (BMG LAbtech, Ortenberg, Germany) at 570 nm, using 600 nm as a reference wavelength.

2.14. Internalization of antigen-loaded NP by bone marrow derived dendritic cells (BMDC)

DC were derived from bone marrow cells that were isolated from femura and tibiae of C57BL/6 mice and cultured in RPMI medium1640 supplemented with GM-CSF (50 ng/mL) and IL-4 (50 ng/mL) at 37 °C, 5 % CO_2. After 7 days, immature DC were harvested, washed, and used for *in vitro* experiments.

Cells were seeded in 24 well plate (1.5 × 105 cells per well) 24 h prior administration of fluorescent NP (250 µg/mL) to the culture. After incubation with NP for 3, 6, 16 or 24 h,

cells were harvested, rinsed three times with PBS and stained with anti-mouse CD11c, CD11b antibodies and DAPI (for dead cells exclusion). Cells were analyzed by ImageStreamX, as described below.

2.15. Multispectral imaging flow cytometry (ImageStreamX) analysis

Cells were imaged using multispectral Imaging Flow Cytometry (ImageStreamX markII flow cytometer; Amnis Corp, part of EMD millipore, Seattle, WA). A 60x magnification was used for all samples. At least 30,000 cells were collected for each sample. Data were analyzed using a dedicated image analysis software (IDEAS 6.2; Amnis Corp). Images were compensated for fluorescent dye overlap by using single-stain controls. Cells were gated for single cells using the area and aspect ratio features, and for focused cells using the Gradient RMS feature [35]. Cells were further gated using a bivariate plot for circularity (the degree of the mask's deviation from a circle) based on the Object mask (a segmentation mask that creates a tight fit on the cell morphology) and intensity of the side scatter channel (illuminated by the 785 nm laser and collected in channel 12).

Particle internalization was calculated by the Internalization feature, i.e. the ratio of the intensity inside the cell to the intensity of the entire cell, mapped to a log scale. To define the internal mask for the cell, the object mask of the bright field image was eroded by 5 pixels.

2.16. *In vivo* study of activation markers and co-stimulatory molecule expressed on DC in draining lymph nodes

Female C57BL/6 mice, 8-weeks-old (n = 3 / group) were injected into the right flank by subcutaneous (s.c.) hock immunization with 50 µl of one of the following fluorescent NP formulations (20 mg/ml): EntrapOVA(PVA), EntrapOVA(PF127), AdsOVA(PVA), and AdsOVA(PF127). Non-injected left flank served as negative control. All NP were labeled with Rhodamine G6 (Sigma-Aldrich). After 16 h post-immunization (p.i.), popliteal and inguinal lymph nodes (LN) were harvested and homogenized in a single cell suspension. Cells were then stained with fluorescent-labeled anti-mouse antibodies against CD11c, MHCII (I-Ab), MHCI (H-2Kb), CD80 and CD86 for 20 min at 4 °C. Samples were acquired with an LSR II Fortessa flow cytometer (BD Bioscience) and analyzed with FlowJo software (Treestar).

2.17. Analysis of *in vivo* T cell activation after NP immunization

Eight-week-old female C57BL/6 mice (n = 6 mice/group) were intravenously (i.v.) engrafted with $CD8^+$ OT-I and $CD4^+$ OT-II cells isolated by MACS from spleens and LN of the respective TCR transgenic mice. Prior to the transfer, both T cell populations were labeled with 5 mM CFSE, for tracking *in vivo* proliferation [36]. On the following day, animals were injected s.c. into the right flank (hock immunization) with 50 µl of NP suspension (20 mg/ml); EntrapOVA(PVA), EntrapOVA-CpG(PVA) and AdsOVA(PVA) and AdsOVA-CpG(PVA). Non-injected left flank served as negative control. OVA was used as an antigen and CpG as an adjuvant. Three days p.i. with NP, inguinal and popliteal LN were isolated. Single cell suspension was stained with CD4, CD8α, TCRβ, TCRVα2, and CD45.1 antibodies and analyzed by flow cytometry.

2.18. Statistics

All results are presented as mean ± standard deviation (SD). One-way ANOVA analysis, following by a Tukey-Kramer test was applied to demonstrate statistical differences ($p<0.001$ (***), $p<0.01$ (**), $p<0.05$ (*)). For direct comparison between two groups of data, t-student test was applied. All tests were performed in GraphPad Prism5® (GraphPad Software, Inc., La Jolla, CA) with a statistical significance level of 0.05 and 0.001 very significant.

3. Results

3.1. Physicochemical characterization of formulated NP

3.1.1. NP size and ζ potential

Biodegradable polymeric NP were prepared by the double emulsion solvent evaporation technique (w/o/w). This method is based on the emulsification of an organic and an aqueous phase where the NP result from single volume shrinkage of the initial emulsion droplet by ultrasonication [33]. Formulation parameters, including average size (Size), PDI, ζ potential, entrapment efficiency (EE) (%) and loading capacity (LC) (µg/mg) were monitored along the preparations with two different surfactants: PVA or Pluronic (PF127) (Table 1). All formulations described in Table 1 were developed using 0.5 % ($w_{CS}/w_{polymer}$) chitosan (CS) solution and antigen-loaded NP were formulated using 2.5 % ($w_{LALBA}/w_{polymer}$) LALBA solution as aqueous phase (IP). For antigen-adsorbed NP, empty PLGA NP were incubated with 5 % ($w_{LALBA}/w_{polymer}$) LALBA solution. For each formulation, blank NP were formulated as a control.

NP size distribution and surface charge are key parameters for preferential passive targeting of DC, adequate biodistribution profile and efficient immune response. In addition, the size also influences EE and LC [11, 28, 30, 31]. With these parameters in mind, our formulation process was adjusted in order to attain particles of a size smaller than 200 nm, PDI below 0.2, neutral ζ potential, high loading efficiency and a minimum surfactant residue, particularly important to guarantee NP safety and biocompatibility.

The PVA surfactant concentration in the aqueous phase (10% (w/v)) influences the average size of formulated NP and their entrapment capacity [37, 38]. DLS results were recorded as average of three independent NP formulations (Table 2). DLS studies yielded consistent and reproducible results. ζ potential was determined by LDV. All formulated batches of NP were close to neutrality, independent of the surfactant used in the external phase (PVA or PF127). This can be explained by the presence of the PEG–chains on the surface of the EntrapLALBA(PVA) and EntrapLALBA(PF127) NP, but also to the dispersion of the positively charged CS on NP matrix.

EE and LC were validated by HPLC. The best EE was obtained for the formulation EntrapLALBA(PVA), as close to 80 % of initial protein solution was entrapped within the PLGA-PEG NP. When PF127 as used at EP (EntrapLALBA(PF127)), the EE was close to 70 %. However, it is important to highlight that despite the surfactant used to ensure NP stability, the overall EE were much higher than those reported in other recently published studies [33, 39, 40]. The same profile was obtained for LC, which could be due to the CS used in the emulsion internal phase. CS increases the viscosity of the aqueous phase and also forms weak electrostatic and hydrophilic interactions with the protein [41, 42]. Therefore, both physical and chemical stabilities of the internal phase are thus enhanced. Moreover, the adsorption efficiency of AdsLALBA(PVA) and AdsLALBA(PF127) NP was considerable close to 40 or 50 %, respectively. The chemical structure of PF127 is branched, therefore AdsLALBA(PF127) NP were able to adsorb protein more efficiently and with higher stability than those NP prepared with PVA polymer.

It was important to assess the residual amount of PVA present within NP matrix by HPLC, as a considerable high concentration of PVA was used in the emulsion aqueous phase. The percentage of surfactant washing efficiency was higher than 96 % for all formulations.

Table 1: Composition of polymeric NP.

Formulation	Matrix polymer	Encapsulated aqueous phase	Surfactant IP*	Surfactant EP**	Protein adsorption
EntrapPROTEIN(PVA)	PLGA-	10 % (w/v) PVA, CS,	2% (w/v)	0.3 % (w/v)	-

	PEG	protein	PVA	PVA	
EntrapPROTEIN(PF127)		10 % (w/v) PVA, CS, protein		0.3 % (w/v) Pluronic	-
AdsPROTEIN(PVA)	PLGA	10 % (w/v) PVA, CS		0.3 % (w/v) PVA	protein
AdsPROTEIN(PF127)		10 % (w/v) PVA, CS		0.3 % (w/v) Pluronic	protein

* internal phase ** external phase

Table 2: Physicochemical characterization of polymeric NP.

Formulation	Size (nm)	PDI	ζ potential (mV)	Protein loading (µg/mg)	
				Loading capacity	Surface adsorption
EntrapLALAB(PVA)	171 ± 3	0.15 ± 0.02	0.51 ± 0.1	19.56	-
EntrapLALBA(PF127)	185 ± 4	0.17 ± 0.05	0.37 ± 0.4	16.96	-
AdsLALBA(PVA)	188 ± 11	0.18 ± 0.08	-1.89 ± 0.5	-	19.72
AdsLALBA(PF127)	195 ± 10	0.20 ± 0.09	-1.42 ± 0.2	-	25.10

3.1.2. Atomic force microscopy

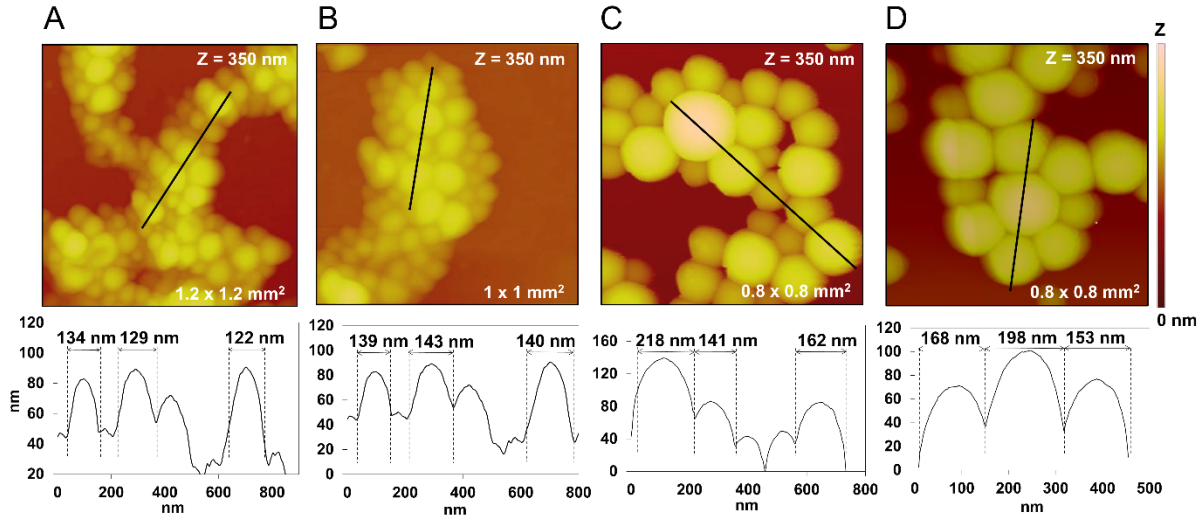

Figure 1: Size and morphology characterization of formulated NP by AFM. Section analysis of NP (A) EntrapLALBA(PVA) and (B) EntrapLALBA(PF127) with the matrix polymer PLGA-PEG and with entrapped antigen; (C) AdsLALBA(PVA) and (D) AdsLALBA(PF127) with PLGA polymer and adsorbed LALBA protein.

The size and surface morphology of NP was also determined by AFM (Figure 2). A drop of each sample was placed onto freshly cleaved mica and dried with $N_{2(g)}$ prior to examination. All NP had smooth surfaces and spherical topography. The section analyses of PLGA-PEG NP with entrapped antigen showed uniform size distributions, which correlated with the data measured by DLS analyzer. As the NP were dried and PEG chains could not form a corona around the NP, the average diameter was 30 nm smaller than the hydrodynamic diameter obtained by DLS. However, there were no considerable differences between the

formulations EntrapLALBA(PVA) (Figure 1A) and EntrapLALBA(PF127) (Figure 1B). Hence, the different surfactants present at the EP did not greatly influence the size or the morphology of the NP. On the other side, PLGA NP with adsorbed antigen demonstrated less uniformed size distribution, with an average diameter closer to the one determine by DLS. Also here we could not observe any differences between the AdsLALBA(PVA) (Figure 1C) and AdsLALBA(PF127) NP (Figure 1D), despite the use of different surfactants in the EP. However, with the AFM images we could clearly distinguish between the different polymers. Formulations with PLGA-PEG (EntrapLALBA(PVA) and EntrapLALBA(PF127)) show nicely spherical NP, which are stuck to each other forming clusters, due to the surrounding hydrophilic PEG chains, that tend to accommodate water molecules, precluding a sharp imaging of particles boundaries. This latter effect was not observed when only PLGA (AdsLALBA(PVA) and AdsLALBA(PF127)) was used for the matrix formation; here we got spherical shapes NP with good defined edges.

3.1.3. FTIR and DSC studies on lyophilized NP

FTIR spectroscopy is one of the important tools for the rapid and efficient identification of protein and polymers' integrity in lyophilized NP, after formulation. In addition, the differences related to the presence of the LALBA antigen entrapped into the polymeric matrix or adsorbed onto the surface of NP was also evaluated by FTIR (Figure 2A).

FTIR spectrum of both polymers (PLGA, PLGA-PEG) and all NP showed a strong stretching absorption at 1720 cm^{-1} (§) which corresponds to C=O bond, indicating the presence of a carboxylic acid. The band at 2950 cm^{-1} (ф) indicates the presence of C-H bonds (ethylene glycol) that is clearly more pronounced in $Entrap_{blank}$(PVA) and $Entrap_{blank}$(PF127), when PLGA-PEG was used as a matrix polymer [40]. From the LALBA spectrum, one can see two specific absorption bands at approximately 1600 cm^{-1}. One appears at 1662 cm^{-1} (*) and is specific for primary amides, while the peak at 1562 cm^{-1} (ϫ) is distinctive for $-NH_2$ groups. Both of these bands also appear on the FTIR of the samples AdsLALBA(PVA) and AdsLALBA(PF127), where LALBA is adsorbed onto the surface of the nanoparticulate delivery system. The slight shift to the higher wave numbers indicates changes of the hydrogen bonding strength between the protein and the polymer. The broad and strong band at 3400 cm^{-1} (‡) is related to the hydroxyl and amine groups overlapping each other. Also these bands are much more pronounced for NP with adsorbed LALBA [43]. The absence of these bands in the spectrum of EntrapLALBA(PVA) and EntrapLALBA(PF127) (Table 1)

suggests that when entrapped, protein is well protected within the matrix of the polymer, therefore this change is not visible on the FTIR spectrum.

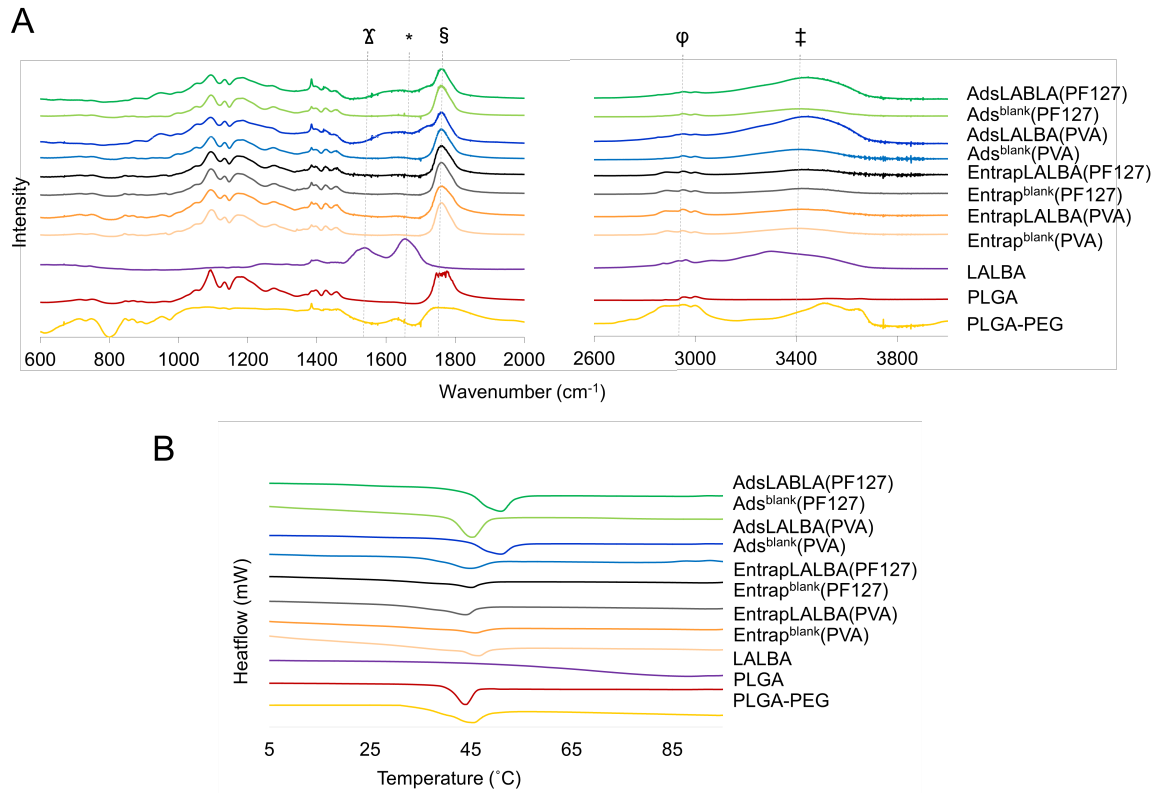

Figure 2: (A) FTIR spectrographs of NP and the components used for their formulations. The symbols on the top of the graph correspond to the specific band. Peak at 1720 cm^{-1} (§) is a specific band for C=O bond; 1662 cm^{-1} (*) is specific for primary amides; peak at 1562 cm^{-1} (ϰ) corresponds to vibration of -NH_2 groups; 2950 cm^{-1} (Φ) indicates the presence of C-H bond; 3400 cm^{-1} (‡) correlates to the hydroxyl and amine groups overlapping. (B) DSC specters of formulated NP and the components used for their formulations.

DSC studies were performed with lyophilized NP at a rate of 5 °C/min from 0 °C to 100 °C. This thermo-analytical technique provided information on the thermal transformations of biodegradable polymers and the LALBA protein in NP (Figure 2B). Analysis of PLGA and PLGA-PEG demonstrated, the presence of an endothermic event between 40 - 50 ºC. This endothermic band results from the glass transition of the polymers followed by an endothermic relaxation peak. The glass temperature (Tg) of polymers depends strongly on the MW and their composition. Results show that the Tg values of PLGA biodegradable copolymer were lower than those obtained for PLGA-PEG, due to the higher MW of PLGA–PEG [44].

When empty and LALBA entrapped NP were evaluated, their Tg were in the same range as the Tg of PLGA and PLGA-PEG, revealing that formulation process did not affect

the structure of these polymers. Moreover, no specific interactions between the polymers and protein were detected. However, when the protein was adsorbed onto the NP surface, a higher Tg was found, indicating that the adsorption of protein at the surface of the NP occured [43, 45].

From the LALBA thermogram there was no melting peak visible at 50 - 70 °C, in contrast to what has been previously reported in the literature [46, 47], suggesting that the protein is in an amorphous phase (which was confirmed by XRPD analysis, data not shown). Also, no melting peak of native LALBA was detected in all NP with entrapped protein, suggesting that the LALBA protein is in a disordered phase within the polymer matrix of NP [44].

3.1.4. Formulation procedures do not affect protein integrity

SDS-PAGE was used to assess protein integrity after incorporation into NP. Protein band patterns of migration obtained for LALBA standard solution and those extracted from loaded NP (EntrapLALBA(PVA), EntrapLALBA(PF127), AdsLALBA(PVA), and AdsLALBA(PF127)) are identical, suggesting that the MW and integrity of the protein is not affected by the NP formulation process (Figure 3). Additionally, these observations are corroborated by the absence of those bands next to 14 kDa of the gel in lanes 6, 8, 11 and 13.

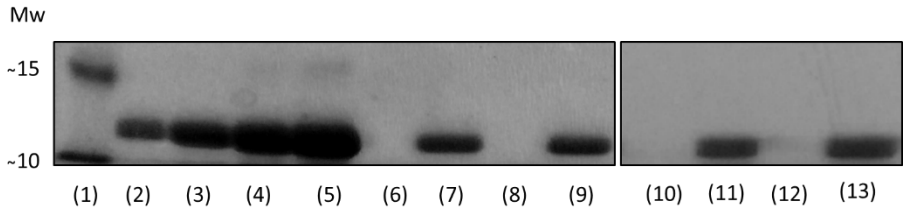

Figure 3: SDS–PAGE (12 % separating gel) of protein LALBA before and after entrapment in NP. Lanes: (1) standard molecular weight (MW) markers, wide range 10–180 kDa; (2) LALBA standard solution at 2 μg; (3) 4 μg; (4) 8 μg; (5) 16 μg all LALBA's bands may be seen at the 14 kDa; (6) $Entrap_{blank}$(PVA); (7) EntrapLALBA(PVA); (8) $Entrap_{blank}$(PF127); (9) EntrapLALBA(PF127); (10) Ads_{blank}(PVA); (11) AdsLALBA(PVA); (12) Ads_{blank}(PF127). (13) AdsLALBA(PF127); A representative image of 3 independent experiments is presented.

3.1.5. NP stability over 3 months

Average size, PDI, and ζ potential of polymeric NP were measured over 3 month period when dispersed in PBS pH 7.4 and kept at 4 ˚C. The main challenge of colloidal suspensions is to ensure their stability over time.

As it can be sen in Figure 4, the EntrapLALBA(PVA) and EntrapLALBA(PF127) formulations showed high stability over a period of 60 days. The size of the NP was

decreasing slowly from 182 to 170 nm for the formulation EntrapLALBA(PVA), and 192 to175 nm for EncLALBA(PF127), respectively. The ζ potential stayed close to neutrality; with a shift from slightly positive (0.3 mV) to negative (-1.2 mV). PDI started to increase only after 60 days, suggesting degradation of polymeric matrix through bulk erosion.

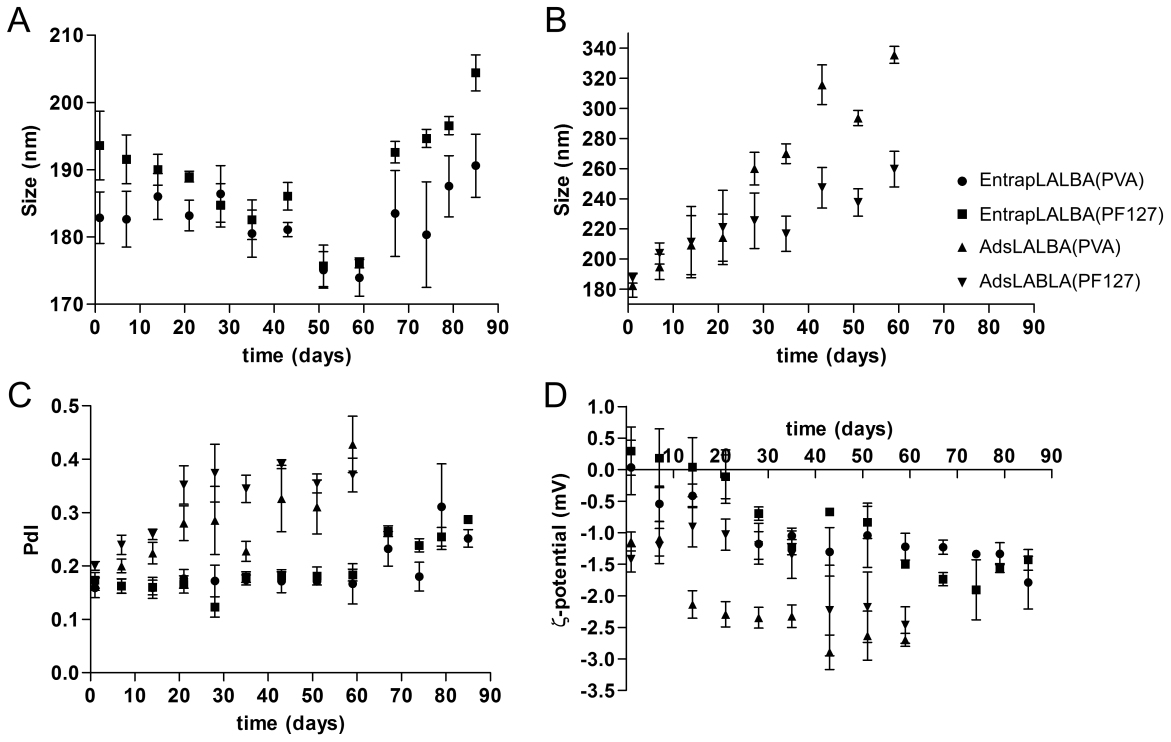

Figure 4: Circles (●) present formulation EntrapLALBA(PVA), squares (■) EntrapLALBA(PF127), triangles (▲) AdsLALBA(PVA) and diamonds (▼) AdsLALBA(PF127) F4. (Figure 1A and 1B) Average size, (Figure 1C) poydispersity index (PDI), and (Figure 1D) ζ potential of polymeric NP were measured over 3 month period when dispersed in PBS pH 7.4 and kept at 4 ˚C. All results are expressed as mean ± SD (n>3).

On the other side, the formulations AdsLALBA(PVA) and AdsLALBA(PF127) with adsorbed protein onto the surface of PLGA matrix, showed an increase in size for 80 and 40 nm, respectively, already after 30 days, suggesting aggregation. This was further supported by increased PDI (> 0.35) that occurs after 20 days of NP storage in aqueous suspension at 4 °C. Moreover, adsorbed protein may contribute to the rise of compelling forces leading to increase NP aggregation. It appears that the PF amphiphilic character and branched chemical structure, leads to the formulation of NP (AdsLALBA(PF127)) with higher stability over time and increased association affinity towards the protein.

Overall, the ζ potential for all formulations was close to neutrality, suggesting weak repulsive forces between NP. After 60 days even steric and hydrated barrier of PEG, in case

of formulations EntrapLALBA(PVA) and EntrapLALBA(PF), were not strong enough to maintain NP separated from each other [48, 49].

Taken together, we can conclude that all formulations of NP remain stable for a period that is relevant for their application as drug delivery systems. In addition, most probably the final product would become available as an extemporaneous vaccine, containing the NP in the lyophilized form and an adequate buffer for dispersion previous to administration.

3.2. NP have no cytotoxic effect on murine immature DC

NP cytotoxicity was studied *in vitro* on a murine immature DC cell line (JAWSII, ATCC®, #CRL-11904™). The cells were incubated for 24 h with increasing concentrations (100 – 1000 µg/ml) of NP. As shown in Figure 5, cell viability was not affected by any composition of NP, in a concentration up to 1000 µg/ml. This corroborates the safety of surfactants, polymers biocompatibility and evaporation of the organic solvent used in the formulation of NP [50].

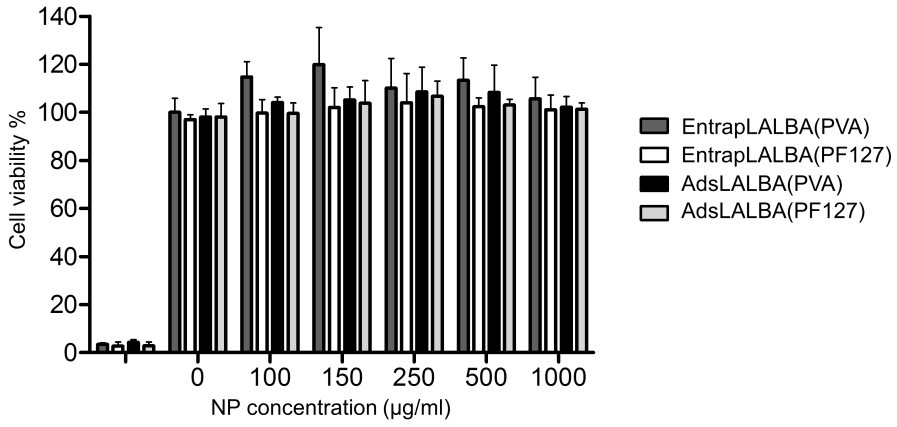

Figure 5: Cell viability (%) determined by the AlamarBlue® assay after 24 h incubation of murine immature BMDC with increasing concentrations of NP. Culture medium (0) and triton 0.5 % (w/v) were used as negative and positive controls, respectively (Mean ± SD; n = 6).

3.3. *In vitro* study of internalization of antigen loaded NP by bone marrow-derived DC

DC are the most potent APC, and form the interface of innate and adaptive immunity. Hence, NP uptake ability and internalization by DC are critical steps of the cascade towards an effective immune response. To study these parameters with antigen-loaded NP, we used mouse DC that had been generated from BM cells in the presence of GM-CSF and IL-4, for 7 days [51]. To analyze the NP-exposed BMDC with high throughput and spatial resolution nature, we used imaging stream flow cytometry (ImageStream™) (Suppl. Figure S1) [52].

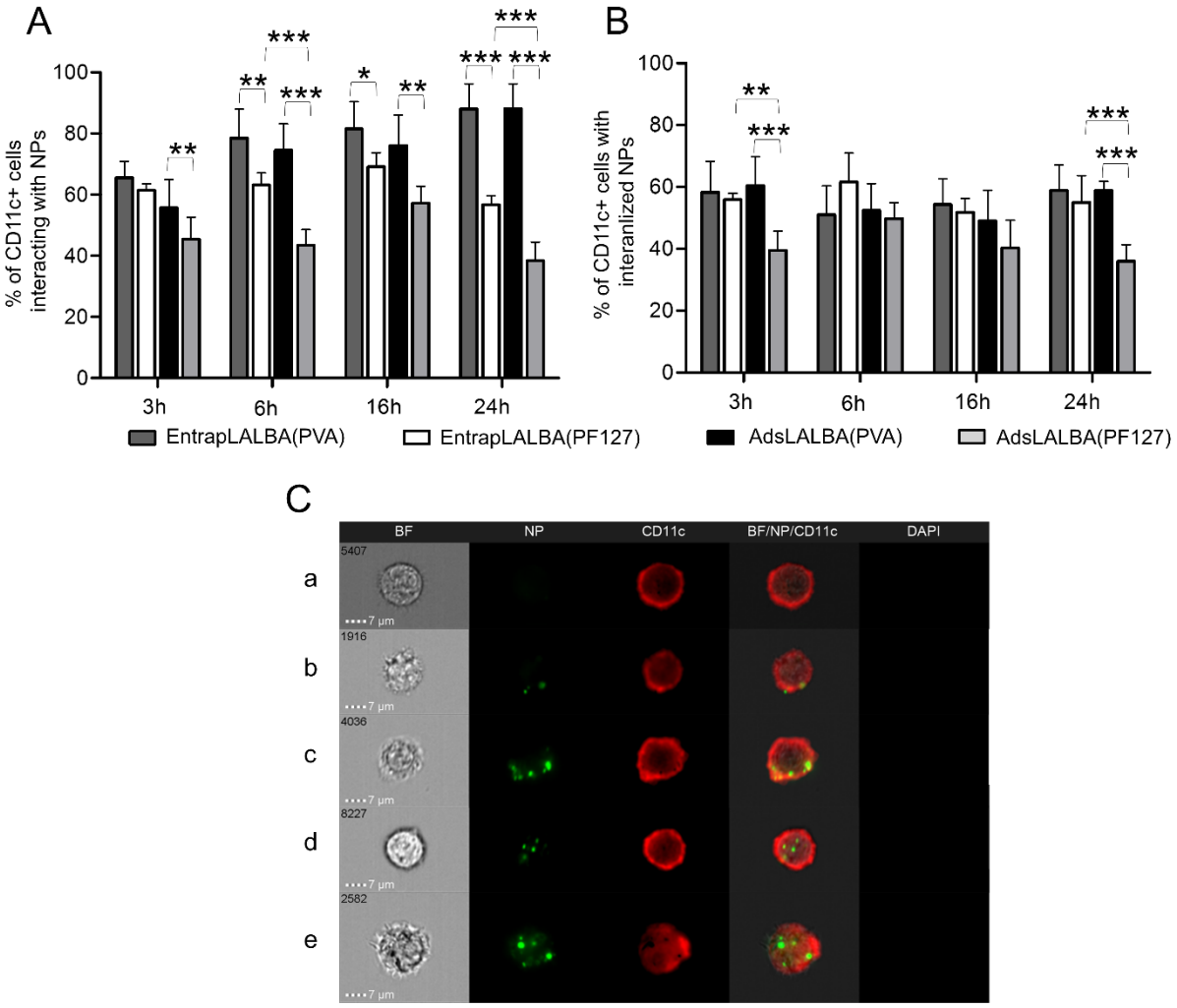

Figure 6: *In vitro* NP internalization by BMDC. ImageStream analysis was performed to detect PLGA-Rho labeled NP in BMDC; 3, 6, 16 and 24 h after the *in vitro* incubation. Distribution of at least 30,000 cells was calculated by Amnis IDEAS software and presented with the histograms showing the percentages of $CD11c^+$ cells interacting with NP (A) and of $CD11c^+$ cells with internalized NP (B). Examples of representative images captured by the Amnis ImageStreamX Flow Cytometer of DC incubated for 16 h at 37 °C with AdsOVA(PVA) (C). First column shows brightfield (BF) images of the cells, second column shows images of PLGA-Rho labeled NP (NP), third column shows APC-labeled $CD11c^+$ DC (CD11c), forth column shows merged images of the precedent fields (BF/NP/CD11c) and fifth column shows DAPI signal for dead cells. (C.a) CD11c without NP. (C.b) NP on the surface of the $CD11c^+$ cell. (C.c) Various NP, entering the cytoplasm of $CD11c^+$ cell. (C.d) DC with various NP. (C.e) DC with start morphology, indicator of the DC maturation process. Results are mean ± SD, normalized to that of control non-labeled cells, representative of three independent experiments (n = 3). Scale bar, 7 µm.

Overall, DC-NP interactions were observed to be time dependent, as total fluorescence, max pixel, and median pixel intensities of NP, increased with incubation time, as seen in Figure 6A for EntrapOVA(PVA) and AdsOVA(PVA). Percentages of DC with

internalized NP ranged from 50 - 60 % and cells with NP persisted for a 1 day period (Figure 6B).

Of note, EntrapOVA(PF127) and AdsOVA(PF127) did not show this time dependent increase in total fluorescence. Moreover, the percentage of DC interacting with AdsOVA(PF127) after 3 h incubation was significantly lower (~60 %) ($p < 0.01$ (**)) (Figure 6A) compared to the DC-EntrapOVA(PF127) interactions, with a slight increase after 16 h incubation.

3.4. *In vivo* impact of NP on DC in draining LN of challenged animals

The *in vitro* experiments established that all NP formulations that we developed were efficiently internalized by BMDC in the cultures. To test if this also holds for a physiological setting, we immunized C57BL/6 mice into a flank with NP and used the non-immunized contralateral flank as control. Popliteal and inguinal LN were isolated from both flanks 16 h after immunization, single cell suspensions were prepared and analyzed by flow cytometry, focusing on DC. First, we tested the expression of MHCI, MHCII, and the co-stimulatory molecules CD80 and CD86 on all DC (gated as $CD11c^+$, $MHCII^+$; gating strategy is provided in the Figure 7A). LN of animals immunized with empty NP (lacking antigen) were compared to non-immunized LN. No significant differences were observed between these samples. As shown in Figure 7B, there was no significant difference in the expression of CD80 between the formulations, but also between the formulations and the control group. However, after immunization with EntrapOVA(PVA) and AdsOVA(PVA) formulations, DC expressed significantly higher levels of the co-stimulatory molecule CD86, than after injection with other types of NP ($p < 0.001$ (***)). Moreover, AdsOVA NP with PVA in EP induced higher CD86 expression than formulation AdsOVA NP with PF as a surfactant in EP ($p < 0.001$ (***)). However, there was no significant difference between the NP with entrapped or NP with adsorbed antigen. Surface MHCII expression was significantly increased only in animals immunized with AdsOVA(PVA), compared to control ($p < 0.05$ (*)). Otherwise, there was no significant difference between the NP capture *in vivo* by DC of animals treated with formulations or between the different formulations and the control.

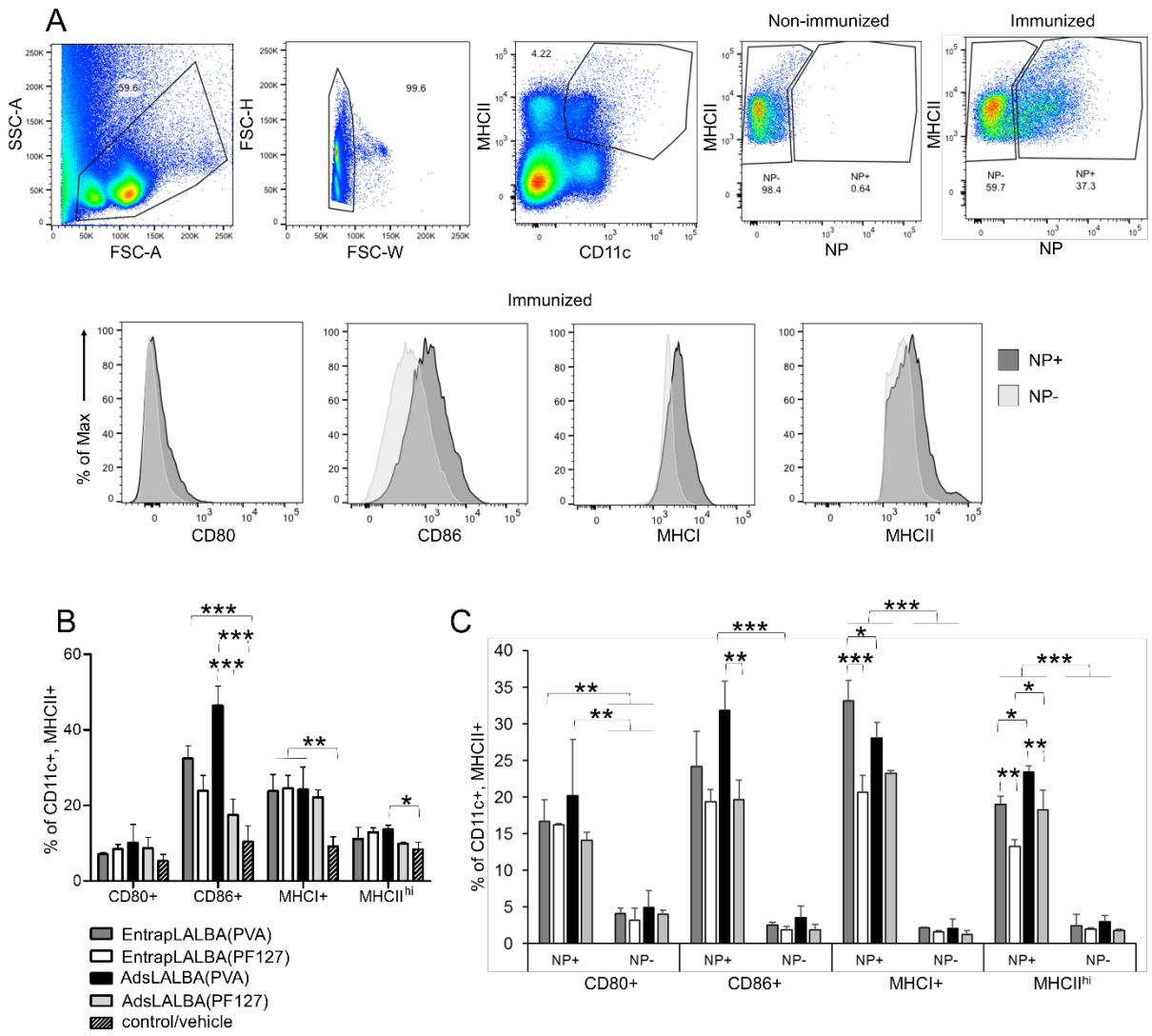

Figure 7: (A) Gating strategies for $CD11c^{+}/MHCII^{+}/NP^{+}$ or NP^{-} DC in immunized and non-immunized female C57BL/6 mice 16 h following immunization. Histograms of expressed activations markers on DC with and without NP after hock immunization. (B) Percentages of activated DC 16 h after immunization with different formulations of NP. (C) Expression of surface activation markers on DC with internalized NP and the DC without internalized NP in the same LN, 16 h after immunization with different formulation of NP.

Next we focused on differences in activation between DC with and without internalized NP in the same LN (Figure 7C). Rho-labeling of the NP allowed us to distinguish these populations by flow cytometry (Figure 7A). Statistical analysis showed generally a significantly higher expression of activation markers ($p < 0.001$ (***) for CD86, MHCI, MHCII, and $p < 0.01$ (**) in case of CD80) on the surface of DC with internalized NP compared to the DC lacking NP. DC expressed significantly higher CD86 and MHCII levels after vaccination with AdsOVA(PVA) formulation than after AdsOVA(PF127) ($p < 0.01$ (**)). Moreover, the activation markers MHCI ($p < 0.001$ (***)) and MHCII ($p < 0.01$ (**))

were significantly higher expressed after the immunization with EntrapOVA(PVA) NP than EntrapOVA(PF127) NP. Furthermore, a significant difference in the activation markers (MHCI and MHCII $p < 0.05$ (*)) for the formulations EntrapOVA(PVA) and AdsOVA(PVA) was observed. Collectively, this establishes that, rather surprisingly, the surfactant used in the EP has a major impact on the APC activation.

3.5. Characterization of the immune response to NP: T cell proliferation

Efficient adaptive immune responses are characterized by the stimulation of antigen-specific $CD4^+$ and $CD8^+$ T lymphocytes to rapidly proliferate and differentiate into effector T cells. Based on the above *in vitro* and *in vivo* results, we decided to test the efficiency of the two NP formulations that showed the best *in vitro* uptake profile and most efficient upregulation of activation markers on DC, i.e. EntrapOVA(PVA) and AdsOVA(PVA), to induce T cell proliferation. Specifically, we analyzed the expansion of antigen-specific $CD4^+$ and $CD8^+$ T cells in response to OVA antigen carrying NP with and without adjuvant (CpG). Therefore, we formulated the following NP: EntrapOVA(PVA), EntrapOVA-CpG(PVA), AdsOVA(PVA), and AdsOVA-CpG(PVA).

Proliferative responses were assessed according to the CFSE label dilution of the adoptively transferred OVA-specific T cells in response to different NP formulations. Specifically, the animals that had been engrafted with CFSE-labelled OT-I and OT-II T cell were immunized with 1 mg of NP s.c. into the right flank, while the left flank was challenged with PBS for control. Three days following immunization, inguinal and popliteal LN were collected and analyzed by flow cytometry (Suppl. Figure S2). $CD4^+$ OT-II and $CD8^+$ OT-I T cells extensively proliferated after immunization with EntrapOVA(PVA), with peaks of the divided daughter cells could be detected up to eight generations (Figure 8).

Interestingly, the formulation EntrapOVA-CpG(PVA) showed the most profound antigen-specific response, with $CD4^+$ OT-II and $CD8^+$ OT-I T cells approaching the autofluorescence level of unlabeled lymphocytes in the recipient animal. This confirms that adjuvant and the associated DC maturation as expected, significantly contributes to boost T cell stimulation.

The AdsOVA(PVA) and AdsOVA-CpG(PVA) formulations induced both $CD4^+$ and $CD8^+$ T cells to respond 3 days p.i. . However, no significant differences in the T cell proliferation efficiency between AdsOVA(PVA) and AdsOVA-CpG(PVA) were detected. Notably, in our experiment the CpG in the formulation AdsOVA-CpG(PVA) did not boost the

antigen-specific response. This deviation could be due to the low co-delivery of antigen and adjuvant into APC, leading to unaltered T cell proliferation.

Collectively, these results suggest that rapid and efficient antigen-specific immune responses can be elicited through co-delivery of antigen and adjuvant NP. Moreover, the importance of uniform delivery is a priority to ensure boost and expansion of the immune response.

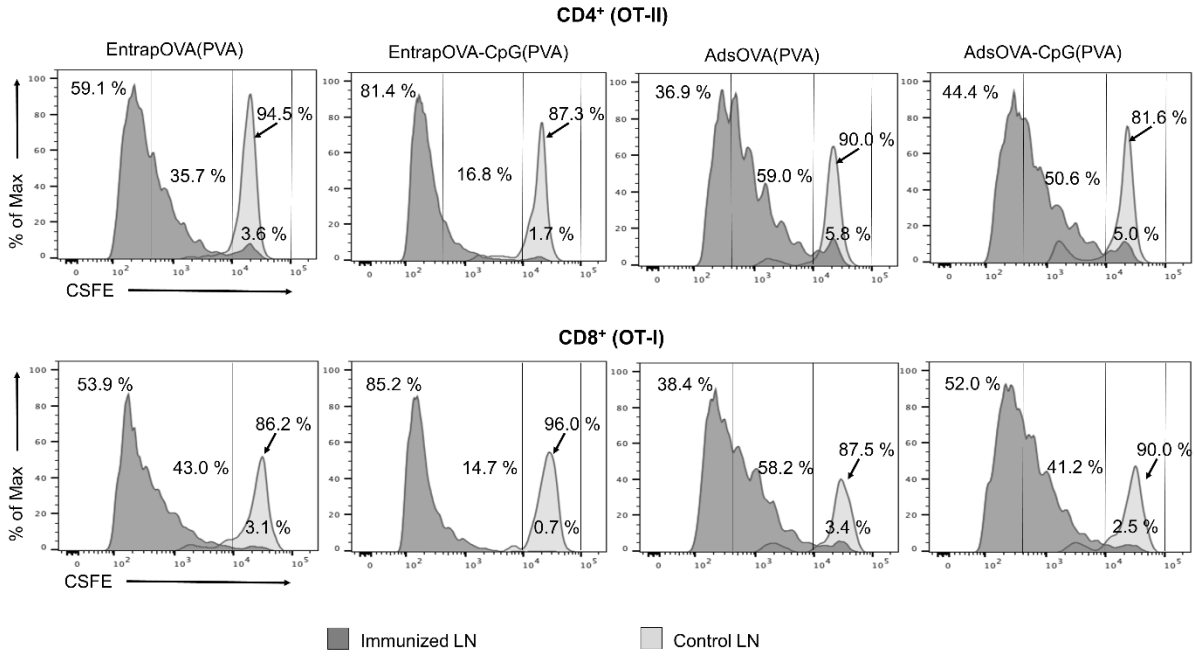

Figure 8: T cell proliferation was studied using dilution of CFSE fluorescence of OVA-specific TCR-transgenic $CD4^+$ OT-II and $CD8^+$ OT-I T cells *in vivo* 3 days post-immunization with NP. The histogram plots show the CFSE profiles of viable $CD4^+$ OT-II and $CD8^+$ OT-I T cells after the immunization with different NP (dark gray histogram) relative to the generation zero CFSE profile of viable transferred $CD4^+$ OT-II and $CD8^+$ OT-I T cells in the absence of OVA NP (light gray histogram). Representative histogram plots were selected from tree independent experiments (n = 6).

4. Discussion

Designing safe and efficacious NP vaccines requires a thorough understanding of the physical and chemical features of the carrier and their interaction with biological systems. The unique properties of NP, such as chemical composition, size, surface charge, shape, and hydrophobicity, impart their characteristics in the interaction and uptake efficiency by APC that elicit T cell immunity [31, 53].

In this study, we focused on the reproducibility and stability of the colloid suspension with different types of protein association to NP and their chemical composition. The latter

was influenced by using either PLGA-PEG or PLGA polymers in combination with two different non-ionic surfactants, PVA and PF127, respectively.

PLGA-PEG and PLGA have been chosen for their biodegradability [11-13] and excellent biocompatibility with immune cells. PLGA is contained in medicinal products approved by EMA (European Medicines Agency) and FDA (Food and Drug Administration) for the topical, oral and parenteral usage [29]. PEG was used to modify PLGA hydrophobic surface with a hydrophilic shielding properties that increase polymer water-solubility, and thus biocompatibility, and greatly reduce immunogenicity and toxicity [17].

PVA is a commonly used polymeric emulsifier with amphiphilic properties [37]. PF127 on the other hand is a triblock copolymer (polyoxyethylene-block–polyoxypropylene-block-polyoxyethylene; PEO-b-PPO-b-PEO) and the most cytocompatible among the Pluronics. Both surfactants have non-ionic and amphiphilic character and obtain quite similar MW, PVA with 13 - 23 kDa and PF127 with 13 kDa, respectively [54, 55].

For NP to act as immune potentiators, presence of the antigen either entrapped within or adsorbed onto NP surface can be expected to be an important factor of delivery. Hence, we developed various NP platforms to address this factor. Entrapment ensures antigen release only after NP uptake and degradation inside the APC [31]; therefore it may lead to slower antigen release or longer preservation of antigen stability [25]. Additionally, entrapment could also represent an efficient way of delivering of antigens that are highly degradable, cause tissue necrosis or would change/ reduce their effectiveness in immune response upon the injection [11, 29].

On the other hand, antigens can be adsorbed onto NP surface based on charge and hydrophilic interactions, which are usually much weaker. Adsorbed antigen is expected to dissociate from the NP faster and to a higher extent. Thus, antigen adsorption may simulate/emulate pathogen presentation to immune systems [11]. However, both high entrapment and adsorption strongly depend on physicochemical properties of the nanoparticulate delivery system [26, 28, 29].

A wealth of research explored numerous nanoparticulate systems and has shown that size and surface charge of NP are the most pivotal and critical factors for their application as drug delivery system. NP smaller than 200 nm [28, 31] can be directly transported by lymph drainage to lymphoid organs, where they are internalized by immature DC, while larger NP require peripheral immature DC and active cellular migration to the draining LN [27-29, 33]. Surface charge of NP, on the other hand, profoundly influences the internalization capability

by APC, as the negative charge of the cell membrane has higher affinity for positively charged particles [11, 30].

In this study, we developed and precisely characterized four different NP delivery systems for a systemic delivery of protein antigen to DC, the key APC that trigger T cell immunity. We aimed to develop a highly stable and reproducible colloidal suspension of NP smaller than 200 nm with narrow size distribution, PDI below 0.2 and ζ potential close to neutrality, in order to potentiate NP-APC interaction. Therefore we used biodegradable aliphatic polyester copolymers PLGA-PEG or PLGA, together with CS, to form a polymeric matrix; and two different stabilizers, PVA or PF127, to ensure NP best physical and chemical characteristics, including size, surface charge and antigen association.

Four highly reproducible and homogeneous nanoplatforms have been developed, all with narrow particle size distribution (Table 2), which was also confirmed by AFM. EntrapLALBA(PVA) and EntrapLALBA(PF127) with entrapped antigen presented an average size ranging from 171 and 185 nm, respectively. While NP with adsorbed LALBA protein, AdsLALBA(PVA) and AdsLALBA(PF127), were slightly bigger, showing 188 nm and 195 nm, respectively.

CS was used in the IP in all formulations, due to its positive charge (+30 mV) [56, 57] to establish electrostatic interactions with the negatively charged groups of biodegradable polymers, thus increasing the ζ potential of NP. Many research studies have used PLGA or PLGA-PEG polymers in the past. However, most of the reported formulations, despite their high biocompatibility, displayed quite negative surface charge, from -5.2 to -20 mV for PLGA NP [58, 59] and −2.8 mV to −5.3 mV [60] for PLGA-PEG NP, as the PEGylation reduces the overall negative surface charge of PLGA. Overall, the amount of CS (0.5 % (wcs/wploymer)) used in all our formulated NP was enough to display surface charge close to neutrality. This was especially important for PLGA NP (AdsLALBA(PVA) and AdsLALBA(PF127)) to augment the electrostatic bonds and therefore affinity of the adsorbed antigen onto the surface of the polymeric matrix. NP with adsorbed protein, AdsLALBA(PVA) and AdsLALBA(PF127), had ζ potential 1.89 and -1.42 mV, respectively. With an isoelectric point (pI) at 4.2, LALBA (and OVA at pI = 4.5) protein exhibit negative charge under physiological pH (7.4) and thus could be adsorbed more efficiently onto the positively surface of PLGA-CS NP.

In the formulations EntrapLALBA(PVA) and EntrapLALBA(PF127), CS not only contributed to the increase of surface charge, but also raises the viscosity of the IP and is

expected to establish electrostatic interactions with negatively charged protein, which may explain the obtained higher EE values.

In order to verify if the protein is degraded during the NP formulation process, SDS-PAGE was performed. LALBA-loaded NP (EntrapLALBA(PVA), EntrapLALBA(PF127), AdsLALBA(PVA) and AdsLALBA(PF127)) their plain control NP (Entrapblank(PVA), Entrapblank(PF127), Adsblank(PVA) and Adsblank(PF127)) were applied together with LALBA standard solutions and commercial MW standards, which were used as a control. Overall, in all formulations of NP where LALBA was used, entrapped or adsorbed, its MW was identical to the ones obtained for LALBA standard solutions (14 kDa). Moreover, no other bands were detected with a different MW (Figure 3), supporting the absence of protein fragmentation or aggregation. Therefore, the integrity of the LALBA protein was maintained after the NP formulation.

The stability of the NP was followed for 3 months in PBS at 4 °C. Such robust stability of EntrapLALBA(PVA) and EntrapLALBA(PF127) NP could be explained by steric hindrance and repulsion of hydrophilic PEG chains, also known as a “stealth” effect [61, 62]. Therefore the stability study does not show any significant changes and deviation in size or PDI of NP over a period of 2 months. However, following 2 months a drastic increase in size andI was detected, while ζ potential was decreased. These data demonstrate the PLGA-PEG bulk erosion, swelling and degradation of NP, which is in accordance with the characteristics of these aliphatic polyesters [63].

In case of AdsLALBA(PVA) and AdsLALBA(PF127) NP, PLGA polymer was used and therefore these NP lack PEG stealth effect [32]. However, adsorbed protein on the hydrophobic polymeric matrix may form a protein corona that probably prevents NP aggregation, thus contributing to their stabilization via steric repulsion. Clustering and aggregation of AdsLALBA(PVA) and AdsLALBA(PF127) NP has been detected after 14 days, which is relatively late taking into consideration the time lag between the preparation of the extemporaneous suspension and their administration to the patients. Given the fact that the adsorption of antigens onto NP is based simply on charge and hydrophobic interaction, the interaction between NP and antigen is relatively weak. A size increase was obviously due to the long incubation time in PBS that resulted in an increase of electrostatic repulsion and therefore influenced the protein affinity and redistribution.

The influence of NP different chemical composition on their interaction with targeted cells was investigated on a murine immature DC line. A wide range of concentrations was screened for the toxicity of the NP over a 24 h of incubation time No significant differences

were observed as a function of NP concentration. None of the NP formulations led to a reduction in cell viability.

However, a number of challenges remain, not only related to the lack of fundamental understanding of how the physicochemical properties of NP affect their uptake, and how these properties influence their interactions with the biological system, but also due to the lack of adequate *in vitro* and *in vivo* models to support the evaluation of immune-adjuvant potential, ensuring an antigen-specific induction. Presently, in the area of immunotherapy, we have a well-established animal model to help us to study the effect of a model antigen – the highly immunogenic protein ovalbumin (OVA). In order to ensure reliable results, all *in vitro* and *in vivo* experiments were performed with OVA as model antigen [64, 65]. Subsequently our findings will be extrapolated to other antigenic system.

To verify, if the produced NP were internalized by BMDC *in vitro*, and were able to efficiently induce the activation and maturation of DC *in vivo* with subsequent T cell proliferation, we formulated the nanoplatforms with OVA. All formulations presented a uniform size distribution, below 200 nm, and ζ potential close to neutrality. There was no significant difference between the chemical and physical properties of formulated NP, when LABLA was replaced with OVA. Despite their difference in MW, both proteins possess quite similar chemical characteristics, such as pI, solubility (10 mg/mL) and expected amphiphilic properties [66].

The efficacy of immuno-nanotherapeutics is contingent on particle uptake and internalization by DC. The NP we developed in this study have all the advantageous characteristics, such as narrow size distribution, rounded shape, and ζ potential, for a highly efficient uptake by APC. To verify this prediction, we incubated BMDC with rhodamine-tagged, fluorescent NP up to 24 h. The influence of surface chemistry and charge of NP on BMDC uptake was then investigated in living cells by image flow cytometry. Overall, we would expect that the uptake of antigen-adsorbed NP would allow faster internalization, due to the similarity to the pathogens [11]. However, the slightly negative charge of protein covering the NP surface can influence the endocytosis of NP [67]. Our *in vitro* studies demonstrate that the interaction profile between the BMDC with NP with adsorbed antigen (AdsOVA(PVA) and AdsOVA(PF127)) was slower and time dependent, especially for the NP formulation AdsOVA(PVA). After 3 h of incubation, only 55 percent of $CD11c^+$ cells were interacting with the AdsOVA(PVA), while this amount almost doubled after 24 h (~90%). In addition, no significant difference could be observed for AdsOVA(PF127) NP and different incubation times. This suggested that NP with antigen adsorbed on the surface, do

not necessarily emerge with higher interaction and phagocytosis by APC. On the other hand, NP with entrapped antigen were covered with the hydrophilic PEG, which contributes to the "stealth-like" effect which should delay their internalization by DC [68], exhibiting a higher phagocytic uptake. This could be explained by the slightly positively charge NP (EntrapOVA(PVA) and EntrapOVA(PF127), which can facilitate the interaction with the negative cell membrane. Overall, we can conclude that the chemical difference of NP influences their internalization by BMDC. All of the formulations with the PF127 emulsifier in the EP, present steady interaction and phagocytic uptake by $CD11c^+$ cells, which is time independent. This could be explained not only by the influence of more negative surface charge of NP, but also by the steric repulsion effect of PF127 triblock copolymer (PEO-b-PPO-b-PEO). PPO polymer present the hydrophobic chain which is normally oriented to the matrix of the NP, while PEO the two edges of the polymer is hydrophilic, and is similar to PEG, usually oriented away from the core of NP [69, 70].

This phenomenon cannot be observed in NP formulations EntrapOVA(PVA) and AdsOVA(PVA), when PVA is used in the EP. The interaction and internalization of latter NP was time dependent. Despite their different surface properties, and their divergent tendency of interaction, all formulated NP were efficiently internalized by BMDC.

Physiological activation of DC populations in organism context was examined in skin-draining LN of wild-type mice upon a single immunization with NP injection. Rho-labeled NP allowed us to distinguish and compare subpopulations of DC with and without internalized NP. Vehicles (empty NP) by themselves did not induce immune responses. DC with internalized NP expressed significantly higher levels of the co-stimulatory molecule CD86, especially after the immunization with EntrapOVA(PVA) and AdsOVA(PVA) formulations. Furthermore, there was no significant difference between the NP with encapsulated and NP with adsorbed antigen. Formulation AdsOVA NP with PVA in EP induced higher expression of the co-stimulatory molecule CD86 and activation marker MHCII than AdsOVA NP with PF127 as a surfactant in EP. This demonstrates that more than antigen association into the NP (entrapment vs. adsorbed), the chemical composition of NP is a pivotal parameter that determines the activation of DC after NP uptake. From these results, we can conclude that not only the size and charge, but also a slight change in the composition of NP has an extensive impact on the DC uptake following their maturation. Phagocytic uptake of AdsOVA(PVA) NP resulted in upregulation of the MHCII activation marker which presents the peptides that can be recognized by the TCR, leading to the $CD4^+$ T cell activation and boosting humoral immune responses [29, 71].

On the other side, internalized EntrapOVA(PVA) NP preferentially led to upregulation of MHCI on the DC, driving the antigen processing and presentation pathway towards the activation of a cytotoxic phenotype of $CD8^+$ T cells which is essential for the control of tumor and infectious diseases. [72, 73]. Nanoparticulate vaccines for immunotherapy can drive the immune response toward exogenous antigens through the cross-presentation pathway by MHCI complexes after their internalization by DC [29, 72, 74]. Although a certain NP formulation has a preferential pathway, it does not mean the exclusion of the other antigen presentation pathway.

Among all NP, those without PF127 in their composition were far more efficient, thus showing the highest activation levels of co-stimulatory molecules and activation markers. This could be explained by the observation that NP EntrapOVA(PF127) and AdsOVA(PF127) show very slow or no increase in NP-DC interaction during incubation time. It could mean that the NP were internalized and degraded inside the DC much slower and therefore, overall activation markers are not upregulated.

Our *in vitro* study and the *in vivo* experiment on DC activation were conclusive in showing that minor differences in the chemical composition of the NP and protein affinity (entrapped or adsorbed) in the NP can have an extensive impact on their uptake and activation of DC. It has been demonstrated before, that the NP uptake by DC, antigen processing and presentation is essential parameter for the activation and differentiation of T cells [75]. The expansion of T cells is also dictated by the affinity of the TCR for its MHC-peptide ligand [76]. Therefore we went a step further and studied the T cell response. We chose the best two PVA formulations, that drove the most efficient upregulation and activation of DC (EntrapOVA(PVA) and AdsOVA(PVA)). For this study we engrafted mice with antigen-specific OT-I $CD8^+$ and OT-II $CD4^+$ T cell, one day prior the immunization with the nanoparticulate vaccine, which allow us to follow the cell proliferation and expansion in draining LN of the wild type C57BL/6 mice.

We were interested to improve potential of the vaccination with the boost in the primary T cell responses, therefore we incorporated adjuvant, CpG oligodeoxynucleotide, a toll-like receptor 9 (TLR9) agonists in the matrix of the NP. Specifically, we formulated the following NP: EntrapOVA(PVA), EntrapOVA-CpG(PVA), AdsOVA(PVA), and AdsOVA-CpG(PVA). Immunization with EntrapOVA(PVA), resulted in very balanced expansion and proliferation of $CD4^+$ OT-II and $CD8^+$ OT-I T cells. For a potent $CD8^+$ T cell activation and clonal expansion, efficient support of $CD4^+$ T cells is needed [77, 78]. Interestingly the formulation EntrapOVA-CpG(PVA) showed the fastest antigen-specific response, as the

fluorescence of CFSE-labeled $CD4^+$ OT-II and $CD8^+$ OT-I T cells were mainly concentrated at the autofluorescence level of unlabeled lymphocytes in the recipient animal [36]. The percentage of proliferating OT-II $CD4^+$ and OT-I $CD8^+$ T cells was lower for EntrapOVA-CpG(PVA) NP, compared to immune responses of other NP formulations (EntrapOVA(PVA), AdsOVA(PVA), and AdsOVA-CpG(PVA)). EntrapOVA-CpG(PVA) enhanced both uptake of antigen and adjuvants effect on DC and augmented vigorously the nascent adaptive immune response, which implicates that incorporation of adjuvant contributes to the boost of the T cell proliferation and expansion.

The variation of proliferated T cells, 3 days after the immunization with the AdsOVA(PVA) or AdsOVA-CpG(PVA) NP, was minor, compared to the difference between EntrapOVA(PVA) and EntrapOVA-CpG(PVA). Remarkably, CpG in the formulation AdsOVA-CpG(PVA) could not boost the antigen-specific response as powerful as when entrapped into the EntrapOVA-CpG(PVA) NP. This deviation could be due to a lower co-delivery of antigen and adjuvant into APC by AdsOVA-CpG(PVA), as in this formulation CpG is entrapped inside the NP and OVA is adsorbed onto the surface of the polymeric matrix. Therefore, it is possible that DC do not process the antigen and adjuvant together, leading to comparable T cell clonal expansion.

Taken together, our results suggest that fast and efficient antigen-specific specific primary T cell responses occur upon co-delivery of antigen and adjuvant. Moreover, the importance of uniform delivery is a priority to ensure boost and expansion of immune response.

5. Conclusions

In this study, we aimed to develop simple, highly reproducible and highly efficient uniformed delivery system to target DC. Designing safe and efficacious nanoparticulate vaccines requires a thorough understanding of physiochemical characteristics of NP, their composition and also each individual component. The combination of all of these parameters determines the fate and efficiency of NP.

Our study highlights the importance of composition and physicochemical properties of nanoparticulate vaccines that are absolutely essential for good cellular uptake which generate prompt and efficient immune response. Developed NP possess desirable physicochemical properties, with good loading capacity, colloidal stability in biological media. All NP showed prompt and efficient DC activation and maturation, following by $CD4^+$ T OT-II and $CD8^+$

OT-I cell proliferation and activation through the antigen-specific immune response. These are pivotal steps in the immunology that leads to a complete and effective immune response.

Therefore, this type of nanoparticulate system could potentially be more widely applied *in vivo*; from prophylactic to therapeutic cancer vaccines to the vaccines for infectious and viral diseases.

Acknowledgements

This research work was funded by Fundação para a Ciência e a Technologia (FCT), Ministério da Educação e Ciência, Portugal for the PhD Grant SFRH/BD/78480/2011 and Research projects UTAP-ICDT/DTP-FTO/0016/2014 and ENMed/0003/2015, under the framework of EuroNanoMed-II; iMed.ULisboa grant UID/DTP/04138/2013. The Jung laboratory is supported by the European Research Council (340345). The authors are grateful to the EMBO for the Short Term Fellowship (ASTF 277-2015). The authors have no other relevant affiliations or financial involvement with any organization or entity with a financial interest or financial conflict with the subject matter or materials discussed in the manuscript.
The authors would like to thank Sigalit Boura-Halfon, PhD, and Ana Salgado for technical assistance.

Declaration of interest

The authors report no conflicts of interest. The authors alone are responsible for the content and writing of this article.

Ethical conduct of research

Animals were maintained and treated according to the Weizmann Institute of Science animal facility and National Institutes of Health guidelines, Israel. Procedures with animal subjects have been approved by Institutional Animal Care and Use Committee (IACUC) at the Weizmann Institute of Science, Israel.

Supplementary material

In vitro study of internalization of antigen loaded nanoparticles by bone marrow-derived DC:

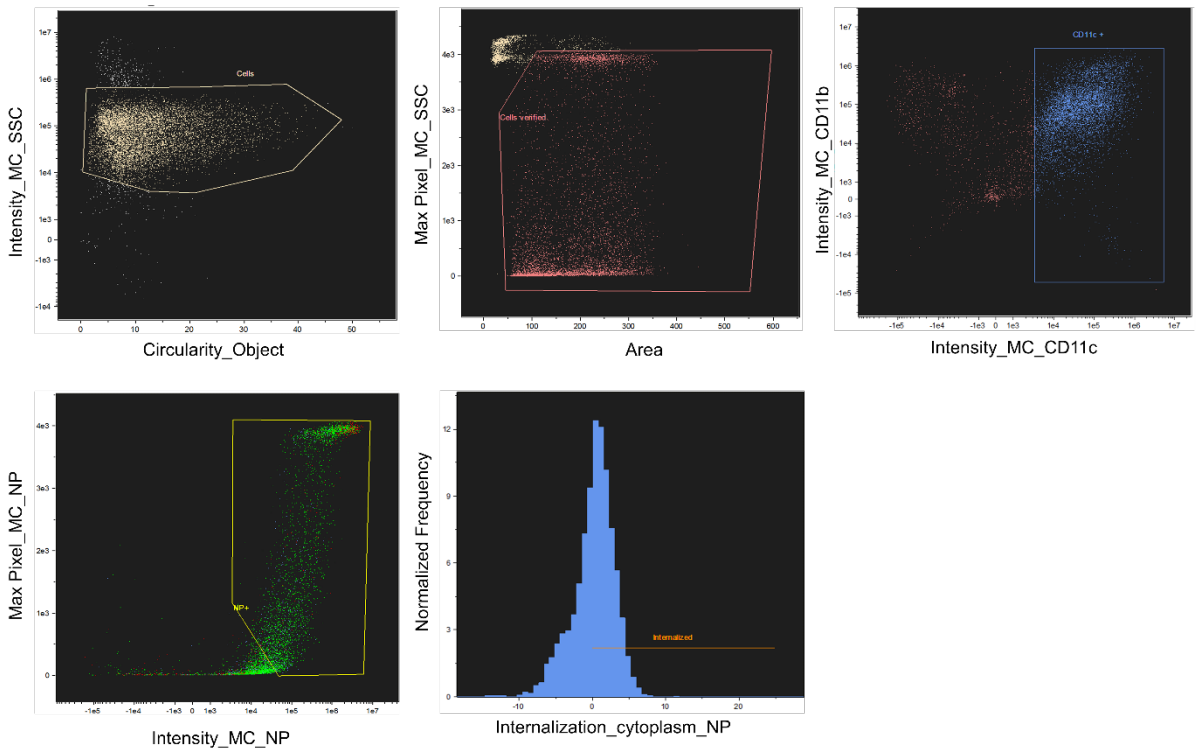

Figure S1: Gating strategy of *in vitro* experiment on BM-derived DC with GM-CSF and IL-4. ImageStream analysis was performed to detect PLGA-Rho labeled NP internalized by DC; 3, 6, 16 and 24h after the *in vitro* incubation. At least 30,000 cells were collected for each sample. Data were analyzed using a dedicated image analysis software (IDEAS 6.2; Amnis Corp). Images were compensated for fluorescent dye overlap by using single-stain controls. Cells were first gated for single cells using the area and aspect ratio features, and for focused cells using the Gradient RMS feature [35]. Cells were further gated using a bivariate plot for circularity (the degree of the mask's deviation from a circle) based on the Object mask (a segmentation mask that creates a tight fit on the cell morphology) and intensity of the side scatter channel (illuminated by the 785 nm laser and collected in channel 12). Particle internalization was calculated by the Internalization feature, i.e. the ratio of the intensity inside the cell to the intensity of the entire cell, mapped to a log scale. To define the internal mask for the cell, the object mask of the bright field image was eroded by 5 pixels. Data are representative of tree independent experiments after the 16 h incubation of DC with NP. Scale bar, 7 µm.

In vivo characterization of immune response to the NP: T cell proliferation

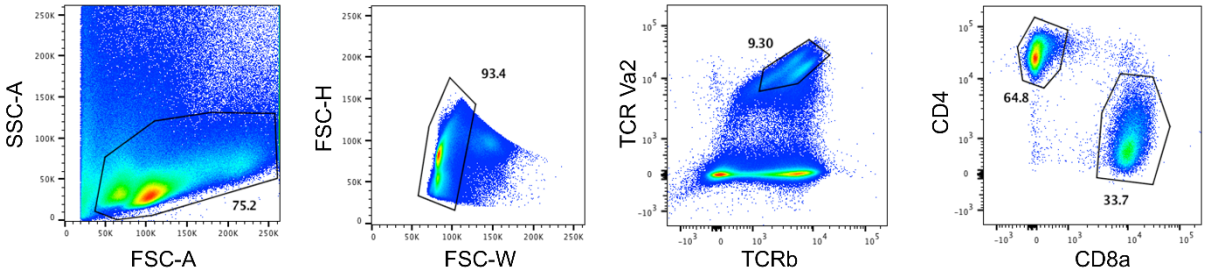

Figure S2: Gating strategies for expression of TCRβ, TCRVα2, CD8α or CD4 of T cells isolated from immunized and non-immunized LN, 3 days following immunization. Data shown are representative of three different animals and three independent experiments.

Chapter 5

Chapter 5 - Anti-tumor efficacy of a nanotechnology-based immunotherapeutic approach

Eva Zupančič[a,b,c], Caterina Curato[b], Jung-Seok Kim[b], Eilam Yeini[d], Ziv Porat[e], Ana S Viana[f], Anat Globerson-Levin[b,g], Tova Waks[b,g], Eshhar Zelig[b,g], João N Moreira[c,h], Ronit Satchi-Fainaro[d], Lea Eisenbach[b], Steffen Jung[b*], Helena F Florindo[a*]

[a]Research Institute for Medicines (iMed.ULisboa), Faculty of Pharmacy, Universidade de Lisboa, Avenida Gama Pinto, 1649-003 Lisbon, Portugal.

[b]Department of Immunology, Weizmann Institute of Science, Rehovot 76100, Israel

[c]Center for Neuroscience and Cell Biology (CNC), University of Coimbra, Faculty of Medicine (Polo I), Rua Larga, Coimbra 3004-504, Portugal

[d]Department of Physiology and Pharmacology, Sackler School of Medicine, Room 607, Tel Aviv University, Tel Aviv 69978, Israel

[e]Flow Cytometry unit, Biological Services Department, Weizmann Institute of Science, Rehovot 76100, Israel

[f]Chemistry and Biochemistry Center, Sciences Faculty, Universidade de Lisboa, 1749-016 Lisbon, Portugal

[g]Center of Cancer Research, Ichilov Hospital, Tel Aviv Sourasky Medical Center, Tel Aviv 64239, Israel

[h]Faculty of Pharmacy (FFUC), University of Coimbra, Pólo das Ciências da Saúde, Azinhaga de Santa Comba, Coimbra 3000-548, Portugal

(Article to be submitted to ACS Nano Journal)

Abstract

Nanoparticulate vaccines present a promising strategy to activate and generate anti-tumor immune responses. Here we designed an aliphatic polyester-based nanoparticle (NP) vaccine as a potential effective anti-tumor strategy aiming for co-delivery of antigens, as ovalbumin (OVA) and tumor associated antigens, and the Toll-like receptor (TLR) ligands oligodeoxynucleotide cytosine-phosphate-guanine motifs (CpG) and Monophosphoryl lipid A (MPLA). Two classes of NP have been developed to investigate the effect of antigen-loading method on the nature of ensuing immune responses. Accordingly, the antigen was adsorbed onto NP surface (Ads NP), or entrapped within the polymeric matrix (Entrap NP).

This work evidences the development of safe, biocompatible and effective nanoparticulate vaccines both under steady-state conditions and in tumor-bearing mice. In fact, this novel antigen-loaded PLGA nanoparticulate vaccine successfully triggered OVA-specific T cell cytotoxicity, T helper (Th)1-type cytokine production and consequent tumor growth reduction in OVA expressing B16.MO5 melanoma tumor-bearing mice. Most importantly, the induced activation and expansion of different immune cells was further confirmed at lymphoid organs and tumor site. This deeper understanding of the effect of antigen-loaded method on the overall immune-modulatory ability of these PLGA-based cancer vaccines is particularly important to design future treatment schedules to ensure optimal and prolonged efficacy, while preventing unexpected side effects related to their mechanisms of action.

Keywords PLGA nanoparticles; cancer vaccine; antigen presenting cells (APC); dendritic cells (DC); cytotoxic T cells (CTL); melanoma; tumor-infiltrating lymphocytes (TIL)

1. Introduction

One of the fundamental roles of the immune system is the immunosurveillance and the maintenance of tissue homeostasis, thereby detecting and destroying foreign invaders, such as pathogens. This process actively involves the coordination of innate and adaptive immunity and the discrimination between self and non-self-antigens [1-3].

Dendritic cells (DC) are the most important antigen presenting cells (APC) and play a prominent role in bridging innate and adaptive immune responses [4-6]. DC ingest foreign antigens and present them in an immunostimulatory context as major histocompatibility complex (MHC)-peptide complexes (MHCp) to the $CD8^+$ cytotoxic T lymphocytes (CTL) and $CD4^+$ T helper (Th) cells, respectively [7]. This cell-mediated immunity is pivotal, and has been widely investigated and exploited for vaccine benefit as cancer immunotherapies. Vaccination with tumor-associated antigens (TAA) is a promising approach to boost tumor-specific CTL, which are crucially dependent on the adequate delivery of the vaccine to DC [8-10]. Consequently, vaccine delivery systems can improve the outcome of antigen-specific T cell mediated immunotherapy in the destruction of cancer cells [11]. For T cells to become activated, next to the antigen presentation through MHCp, two additional signals need to be guaranteed, namely co-stimulation molecules and cytokine signals [12]. Accordingly, it has been shown that efficient immunity requires the simultaneous co-delivery of antigens and adjuvants, such as the Toll-like receptor (TLR) ligands, to DC [13, 14].

Nanoparticle (NP)-based vaccines with well-defined physicochemical properties are versatile delivery platforms that can improve the targeted delivery of TAA, amplify immune activation and augment the efficacy of anti-cancer therapies [15]. Generally, major advantages of NP include the stability of entrapped antigen, as well as heightened immunogenicity, bioavailability and efficacy, by enhancing their recognition and internalization by APC. In fact, the controlled release of NP payloads can be influenced and dictated by carrier physicochemical parameters, such as chemical composition, size, surface charge, geometry and hydrophobicity. These properties can be relatively easy to manipulate on aliphatic polyester-based particulate delivery systems [16, 17]. Among aliphatic polyester polymers, poly(lactic-co-glycolic acid) (PLGA)-based carriers have shown a high immunomodulation capacity, mostly related to the passive targeting of immune cells. Their particulate nature and versatile physicochemical characteristics resulting from the manipulation of polymer properties are fundamental to increase antigen capture, but also to modify the antigen release

kinetics within the targeted immune cells, thus prolonging antigen presentation and resultant expansion of effector T cells [18, 19].

The major goal of this research work was to characterize the immune modulatory effect of a novel vaccine based on PLGA nanodelivery systems. These particulate vaccines have been designed to potentiate the systemic delivery of antigens to DC, under both steady state and cancer disease. Therefore, to further assess their potential as an effective anti-tumor strategy, it was important to analyze the levels of internalization of antigen-associated PLGA NP by distinct APC subpopulations, as well as their effect on the activation of effector immune responses. Accordingly, these studies evaluated their impact on the activation and proliferation of T cells at different time points, as well as on priming antigen-specific cytotoxic T cells and inducing a long-lasting memory CTL response, 8 weeks after immunization. These studies indicated the most efficient and thus most promising anti-cancer vaccine, which immune therapeutic efficacy was further evaluated in melanoma tumor-bearing mice. Accordingly, the effect of PLGA NP entrapping a combination of ovalbumin (OVA) and TLR ligands (oligodeoxynucleotide cytosine-phosphate-guanine motifs (CpG) and monophosphoryl lipid A (MPLA)) on immune cells and overall tumor growth and mice survival was studied. Nanoparticulate vaccines were able to induce an effective anti-tumor immune response in this melanoma-bearing mice model, after a single or triple vaccination. We further investigated multiple factors known to have a critical impact on the efficacy of a therapeutic cancer vaccine, focusing on the characterization of antigen-specific CTL cells, which are crucial for the control or rejection of malignancies [20]. Various techniques have been used to provide detailed information about these antigen-specific T cells, namely regarding their frequency, phenotype and/or functionality. Of particular interest was the evaluation of the cell surface activation marker on $CD8^+$ T cells, the selective expression of cytotoxic T-lymphocyte-associated-antigen 4 (CTLA-4) receptors and the cytokine production by effector cells at different organs, namely spleen, lymph nodes (LN) and tumor microenvironment. In addition, these studies also explored the frequency of tumor-infiltrating lymphocytes (TIL) induced after the animals' immunization with one or three doses of PLGA NP.

2. Materials and methods

2.1. Materials

Poly(lactic-co-glycolic acid) (PLGA) conjugated with polyethylene glycol (PEG), i.e. PLGA-PEG (5050 DLG mPEG 5000, 10 wt % PEG, molecular weight (MW) = 17 kDa),

Resomer® RG 502 Poly(lactic-co-glycolic acid) PLGA (MW = 7–17 kDa), Ovalbumin (OVA, average MW = 45 kDa), Poly(vinyl alcohol) (PVA, MW = 13-23 kDa and hydrolyzation 87-89 %), Glycol Chitosan (CS), and Dichloromethane (DCM) were purchased from Sigma-Aldrich (St. Louis, MO, USA). All other chemicals and reagents used in the study were of analytical grade.

The adjuvants (Adjs) CpG ODN 1826 (TCCATGACGTTCCTGACGTT) and MPLA-SM Vaccigrade™ were purchased from InvivoGen (San Diego, CA, USA).

Double distilled water (DDW) was used after filtration in a Millipore® (Millipore, Billerica, MA) system.

Dulbecco's Phosphate Buffered Saline (PBS) (1×), RPMI® medium, fetal bovine serum (FBS), trypsin EDTA 0.05 %, penicilin/streptomycin (PenStrep) 10,000 Unit/ml/10,000 µg/ml, sodium pyruvate 100 mM, HEPES 1 M, non-essential amino acids and ACK lysing buffer were purchased from Life Technologies (Carlsbad, CA, USA).

Fixation/Permeabilization Kit (BD Cytofix/Cytoperm™ Cat: 554714) was purchased from BD Bioscineces, San Diego, CA, USA.

Proteome Profiler Mouse XL Cytokine Array Kit was purchased from R&D Systems, Inc (Minneapolis, MN, USA).

Matrigel Matrix (Cat. no. 356234) was purchased from BD Biosciences- Discovery Labware, Erembodegem, Europe.

Paraformaldehyde (PFA) 4 % (v/v) was purchased from Fisher Scientific.

Antibodies anti-mouse CD11c (clone: N418), CD11b (clone: M1/70), CD45.1 (clone: A20), TCRβ (clone: H57-597), TCR Vα2 (clone: B20.1), CD3e (clone: 145-2C11), CD4 (clone: CK1.5), CD8α (clone: 53-6.7), CD107 (clone: 1D4B), PD-1 (clone: 29F.1A12), CTLA-4 (clone: UC10-4B9), CD62L (clone: MEL-14), CD44 (clone: IM7), CD69 (clone: H1.2F3), CD25 (clone: PC61.5), IL-4 (clone: 11B11), IFN-g (clone: XMG1.2), TNF-a (MP6-XT22), I-Ab (MHCII; clone: AF6-120.1), and Carboxyfluorescein diacetate succinimidyl ester (CFSE) and DAPI were purchased from BioLegend (San Diego, CA, USA).

2.2. Cell line

OVA transfected, highly metastatic B16.MO5 melanoma cell line [21] was cultured in RPMI 1640 with 10 % (v/v) heat-inactivated FCS, 2 mmol/L glutamine, 1 % (v/v) sodium pyruvate, 25 mM HEPES, 1 % (v/v) nonessential amino acids and combined antibiotics 10,000 Unit/ml/10,000 µg/ml PenStrep (Invitrogen Life Technologies).

2.3. Mice

Female C57BL/6 mice (6-8 weeks old) were purchased from the Envigo RMS LTD (Jerusalem, Israel). Female OT-I (C57BL/6) TCR transgenic mice harboring OVA-specific $CD8^+$ T cells [22] and OT-II (C57BL/6) TCR transgenic mice harboring OVA-specific $CD4^+$ T cells [23] were in-house bred at the Weizmann Institute of Science (Rehovot, Israel), under conventional, specific pathogen-free (SPF) conditions. All animals were handled according to protocols approved by the Weizmann Institute Animal Care Committee as per international guidelines.

2.4. Preparation of NP

Biodegradable polymeric NP were prepared by the double emulsion solvent evaporation technique (w/o/w), as previously reported with modifications [24]. Briefly, the aqueous solution was added to the polymer previously dissolved in the organic solvent DCM. The single emulsion (o/w) was formed using an ultrasonic processor (Sonifier Vibracell VC 375, Sonics & Materials Inc, USA) at 70 W for 15 s. Two different types of NP were formulated: 1) the antigen dissolved in the internal aqueous solution (IP) (Entrapped (Entrap) protein-NP) and 2) antigen adsorbed onto the surface of the NP (Adsorbed (Ads) protein NP). Fluorescent NP were formulated by replacing 50 μL of organic polymer solution with Rhodamine 6G (Sigma-Aldrich, St. Louis, MO, USA) solution (2 mg/mL) in DCM. A 2 % (w/v) PVA solution was added to the (o/w) primary emulsion, and a second sonication was performed under the same conditions. The double emulsion (w/o/w) was added dropwise to the external surfactant phase (EP) with 0.3 % (w/v) PVA, and stirred at 37 °C for 1 h. The NP suspension was washed twice with ultrapure water by centrifugation (22000 x g, 45 min, 4 ˚C; Beckman Coulter, lnc, Avanti® J-E Centrifuge JA-20, USA). Final pellet of NP was resuspended in phosphate buffered saline (PBS) pH 7.4 and kept at 4 ˚C for further analysis. OVA was adsorbed onto NP after 1 h of incubation at room temperature. NP were washed with ultrapure water and centrifuged for 20 min (22000 x g, 4 ˚C; Beckman Coulter, lnc, Avanti® J-E Centrifuge JA-20, USA).

2.5. Physicochemical characterization of NP

NP size and polydispersity index (PDI) were inferred by Dynamic Light Scattering (DLS) using the Malvern Nano S (Malvern Instruments, UK). Nanoparticles' surface charge was determined by their ζ potential, assessed by Laser Doppler Velocimetry (LDV) with Malvern Nano Z (Malvern Instruments, UK). Since ζ potential is highly dependent on

measurement conditions, NP suspension (20 mg/ml) was re-suspended in PBS to the final concentration 1 mg/ml and all measurements were performed at 25°C in triplicate.

2.6. Atomic force microscopy

The morphology of formulated NP was investigated at room temperature by tapping mode atomic force microscopy (AFM) (Nanoscope IIIa Mulimode AFM, Digital Instruments, Veeco), using silicon tips (ca. 300 kHz) at a scan rate of ca. 1.6 Hz. Prior to examination, all samples were diluted in DDW to the concentration 10 mg/ml. A drop of sample was placed onto freshly cleaved mica for 20 min, and dried with $N_{2(g)}$.

2.7. Determination of antigen and adjuvants loading

The supernatants obtained from NP centrifugations were collected to quantify indirectly the entrapped agents. The entrapment efficiency (EE % (w/w), Eq. (1)) and the loading capacity (LC μg/mg, Eq. (2)) of OVA were determined by the MicroBCA™ assay according to the manufacturer's instructions [14, 25]. CpG was quantified by the Oligreen® ssDNA quantitation kit [14]. RFU were measured using the fluorometer at 485 nm excitation and 530 nm emission wavelengths.

$$EE\ \% = \left(\frac{initial\ amount\ of\ antigen - amount\ of\ antigen\ in\ supernatant}{initial\ amount\ of\ antigen}\right) x\ 100 \quad (1)$$

$$LC\ \mu g\ /\ mg = \left(\frac{initial\ amount\ of\ antigen - amount\ of\ antigen\ in\ supernatant}{total\ amount\ of\ polymer}\right) x\ 100 \quad (2)$$

2.8. *In vivo* study of antigen-loaded NP internalization by DC in draining LN

Female C57BL/6, 8 weeks old mice (n = 6 / group) were injected into the right flank by the subcutaneous (s.c.) hock immunization with one of the Rhodamine 6G fluorescently-labeled NP formulations: EntrapOVA or AdsOVA. Left non-injected flank served as negative control. All formulations contained OVA as the antigen. Popliteal and inguinal LN were harvested 16 h post-immunization (p.i.). A single-cell suspension was stained with fluorescent-labeled anti-mouse antibodies against CD11c, MHCII (I-Ab), CD11b and PDCA for 20 min at 4 °C and cells were analyzed by multispectral imaging flow cytometry (ImageStreamX markII flow cytometer; Amnis Corp, part of EMD millipore, Seattle, WA), as described below.

2.9. Multispectral imaging flow cytometry analysis

Cells were imaged using Multispectral Imaging Flow Cytometry (ImageStreamX markII flow cytometer; Amnis Corp, part of EMD millipore, Seattle, WA). A 60 x magnification was used for all analyzed samples. At least 30,000 cells were collected for each sample. Data were analyzed using a dedicated image analysis software (IDEAS 6.2; Amnis Corp). Images were compensated for fluorescent dye overlap by using single-stain controls. Cells were gated for single cells using the area and aspect ratio features, and for focused cells using the Gradient RMS feature [26]. Cells were further gated using a bivariate plot for circularity (the degree of the mask's deviation from a circle) based on the Object mask (a segmentation mask that creates a tight fit on the cell morphology) and intensity of the side scatter channel (illuminated by the 785 nm laser and collected in channel 12). Particle internalization was calculated by the Internalization feature, i.e. the ratio of the intensity inside the cell to the intensity of the entire cell, mapped to a log scale. To define the internal mask for the cell, the object mask of the bright field image was eroded by 5 pixels.

2.10. Adoptive cell transfer of T cells

For adoptive cell transfer of $CD8^+$ cells and $CD4^+$ T cells, spleens from 6 - 8 weeks old naïve OT-I and OT-II mice were positively selected for CD45.1 donor spleens, using anti-CD8α and anti-CD4 MACS Antibody-labeled microbeads (Miltenyi Biotec, Bergisch Gladbach), respectively. Cells were counted and mixed in ratio 1:1, and a total volume of 200 µL in PBS was injected intravenously (i.v.) into the tail vein, if not stated otherwise.

2.11. *In vivo* T cell activation and proliferation at 6, 16, 24 and 48 h after immunization with NP

Female mice C57BL/6, 8 weeks old (n = 6 mice/ group) had an i.v. graft of $CD8^+$ OT-I and $CD4^+$ OT-II cells. Prior to the cell transfer, both populations of cells were labeled with 5 mM CFSE, for tracking *in vivo* proliferation [27]. On the following day, animals were injected s.c. into the right flank (hock immunization) with 50 µl of NP (20 mg/ml), EntrapOVA or AdsOVA. Left non-injected flank served as negative control. At the previous determined time points (6, 16, 24 and 48 h) after p.i. with NP, inguinal and popliteal LN were isolated. Cells were stained with fluorescent-labeled antibodies against CD4, CD8α, TCRβ, TCRVα2, CD45.1, CD25, CD69, and CD44 for 20 min at 4 °C, protected from light. Samples were acquired with an LSR II Fortessa flow cytometer (BD Bioscience) and analyzed with FlowJo software (Treestar).

2.12. *In vivo* cytotoxicity assay

The *in vivo* killing assay was performed as described before [28]. Briefly, OT-I T cells were transfer into naive C57BL/6 mice on the first day. On the following day, mice were s.c. immunized with 2 mg of NP (AdsOVA, AdsOVA-Adjs, EntrapOVA, EntrapOVA-Adjs), OVA and Adjs in solution or PBS. Seven days following the immunization, splenocytes were isolated from $CD45.1^+$ donor mice. Half of the cells were pulsed with 10 μg/ml of the OVA peptide SIINFEKL for 2 h at 37 °C. Un-pulsed cells served as control. Un-pulsed and pulsed cells were stained with 0.5 $CSFE^{low}$ or 5 μM $CFSE^{hi}$, respectively. A mixture of both cells in the ratio 1:1 was transferred i.v. to C57BL/6 mouse. The differential clearance of both target cell populations was evaluated 16 h later in single-cell suspensions collected from LN and spleens. OT-I-specific CTL activity was evaluated by flow cytometry. T cells were gated for $CD45.1^+$, TCR $V\alpha2^+$, $CD8\alpha^+$ based OT-I-specific, and diluted series of CFSE fluorescence per cells were analyzed.

2.13. Assessment of T cell memory

C57BL/6 female mice were grouped into 7 groups of 5 animals. CFSE labeled $CD8^+$ OT-I and $CD4^+$ OT-II cells in ratio 1:1 were transferred i.v. one day prior to hock immunization with one of the following treatments: (1) PBS, (2) OVA & Adjs in solution, (3) AdsOVA, (4) AdsOVA-Adjs, (5) EntrapOVA. Two groups were treated with (6) EntrapOVA-Adjs. Seven weeks after the immunization with one of the treatments, all animals were re-stimulated i.v. with the 100 μg of OVA, except one of the EntrapOVA-Adjs group that served as a control. Seven days after the re-stimulation, spleens were collected and analyzed by flow cytometry. Antigen specific CTL were gated for $DAPI^-$, $CD45.1^+$, $TCR\beta^+$ and $CD8\alpha^+$.

2.14. Therapeutic efficacy of the nanoparticulate vaccines against B16.MO5 melanoma challenge

Female C57BL/6 mice (8 weeks old) were randomized into one of the following treatment groups (n=7): (1) PBS, (2) Empty NP, (3) AdsOVA-Adjs NP, (4) EntrapOVA-Adjs NP, (5) AdsOVA-Adjs NP (3 x immunization), (6) EntrapOVA-Adjs NP (3 x immunization). All animals were s.c. challenged with 2 x 10^5 B16.MO5 tumor cells in 200 μL of sterile PBS. Weight of the animals was monitored twice a week and tumor growth was followed every 2 days with a caliper. When tumors reached the size of 3 mm in diameter (day 10 post tumor inoculation), 1 x 10^6 splenocytes from OT-I and OT-II CD45.1 naïve donor spleens were

administered i.v.. To explore anti-tumor therapeutic efficacy of the NP, a single vaccination or a 3-time immunization treatment, seven days apart (Figure 4A) were performed on these B16.MO5 melanoma tumor-bearing mice.

Final mean tumor volumes were calculated using the equation: $V = ½ \times (L \times W^2)$, where V is the volume (mm^3), L the length (mm) and W the width (mm) of the tumor. Mice were sacrificed on day 31. Blood, spleens, LN and tumors were collected. Serum from the blood samples was separated by centrifugation (1,000 × g, 10 min at 22 °C, Allegra 64R, Beckman, USA) and stored at -20 °C until further quantification. A single cell suspension from spleens, draining LN and tumors of five animals from each treatment group was prepared and analyzed for infiltrated lymphocytes (CD45.1, CD3e, CD8α, CD4, CD44, CD62L, PD-1, CTLA-4) and cytokines (IFN-γ, TNF-α, IL-4) by flow cytometry.

2.15. Therapeutic efficacy of the nanoparticulate vaccines without a transfer of transgenic T cells

A second experiment was performed without the transfer of OT-I splenocytes. Eight weeks old female C57BL/6 mice were randomized and s.c. challenged with 2×10^5 B16.MO5 melanoma cells. Ten days after tumor inoculation animals were immunized with a single dose of one of the treatments: (1) PBS, (2) Empty NP, (3) AdsOVA-Adjs NP, and (4) EntrapOVA-Adjs NP. Tumor growth and mice weight were monitored as mentioned before (section 2.14).

2.16. Cytokine quantification in spleens and tumors of treated mice

Intracellular cytokine staining was performed using the Cytofix/Cytoperm plus kit (PharMinigen) [29]. Briefly, single-cell suspensions of splenocytes were treated with ACK lysis buffer for 1 min at 37 °C to remove red blood cells. Splenocytes were washed with PBS and resuspended in 1 mL of RPMI. The tumors obtained from five mice in each treatment groups were processed into the single-cell suspension, washed with PBS and resuspended in 1 ml of RPMI. Two aliquots of 500 µL for each sample were prepared in FACS tubes and incubated for 2 h at 37 °C and 5 % CO_2 with media alone (for the negative control) or with Phorbol 12-myristate 13-acetate (PMA; 25 µL/mL) and ionomycin (25 µL/mL). After incubation, a secretion inhibitor brefeldin A (Sigma, Steinheim, Germany), at a final concentration of 3 µg/mL was added and incubated for additional 4 h to block the secretory pathways and to keep the cytokines trapped intracellularly. Extracellular antigens ($CD3e^+$, $CD4^+$, $CD8\alpha^+$) were stained, prior to the cell fixation and permeabilization with 250 µL Cytofix/Cytoperm permealized/wash solution for 20 min. The staining of the intracellular

cytokine was performed with anti-cytokine fluorescent antibody conjugates to detect accumulated IFN-γ, TNF-α and IL-4 cytokines. Cells were washed in permealized/wash solution and resuspended in 400 μL of FACS buffer prior to flow cytometry analysis. All samples were analyzed by FlowJo software (TreeStar, San Carlos, CA, USA).

2.17. Tumor histology

From each group of C57BL/6J tumor bearing mice, two of the removed tumors were fixed for 24 h in 4 % (v/v) paraformaldehyde (PFA) at 4 °C, washed with PBS (pH 7.4) and stored into 70 % (v/v) ethanol (EtOH) for processing in paraffin-embedded blocks. Samples were cut in 2 μm thick slices. After the deparaffinization in xylene and rehydratation by sequential incubation in EtOH/water solutions, the samples were stained with both hematoxylin and eosin (H&E) staining, and fluorescent antibodies for detection via immunofluorescence. The latter was done by an overnight incubation with primary CD3 (1:50), CD8 (1:50), CD4 (1:100) antibodies (R&D Systems, Minneapolis, MN) in cold room. Slides were washed with PBS three times for 15 min and stained with biotinylated secondary antibodies (1:50) for 60 min at the room temperature in a humidified atmosphere. After incubation, slides were washed and rabbit streptavidin antibodies were applied to enhance biding affinity of antibodies, thus improving the overall staining. After rinsing with PBS, sections were stained with DAPI (1:1000) and mounting medium (Invitrogen) was applied for cover slipping. The images were acquired with Nikon Eclipse Ni fluorescent microscope using Carl Zeiss Axioskp 2 mot plus and their analysis to quantify the immunofluorescence staining was performed using AxioVision microscope software. A single operator acquired all images.

2.18. Statistics

All results are presented as mean ± standard deviation (SD). One-way ANOVA analysis, following by a Tukey-Kramer test was applied to demonstrate statistical differences ($p < 0.001$ (***), $p < 0.01$ (**), $p < 0.05$ (*)). For direct comparison between two groups of data, t-student test was applied. All tests were performed in GraphPad Prism 5® (GraphPad Software, Inc., La Jolla, CA) with a statistical significance level of 0.05 and 0.001 very significant.

3. Results

3.1. Characterization of developed NP

Polymeric NP were prepared by the double emulsion solvent evaporation technique (w/o/w), using PLGA or PLGA-PEG aliphatic polyester copolymers [24]. Formulation parameters such as average size, PDI, ζ potential, EE (%) and LC (μg/mg) were monitored for both types of antigen-loaded NP: Entrap NP or Ads NP (Table 1). EntrapOVA NP presented a size range between 188 ± 8 nm with a narrow particle size distribution (PDI range 0.16 ± 0.05). When the antigen was adsorbed onto the surface of the NP (AdsOVA NP), these carriers presented size of 195 ± 14 nm and PDI of 0.19 ± 0.10 (Table 2). Thus, regardless of the type of antigen association to the nanoparticulate formulation, both NP presented similar sizes. All formulations were developed using 0.5 % ($w_{CS}/w_{polymer}$) CS solution. NP with entrapped antigen were formulated using 2.5 % ($w_{OVA}/w_{polymer}$) OVA solution as the aqueous phase (IP), while for antigen-adsorbed NP, empty PLGA NP were incubated with 5 % ($w_{OVA}/w_{polymer}$) OVA solution. The amount of PVA present in the supernatants obtained from NP washing procedures was quantified by HPLC. It was observed that 96 ± 2.1 % of the PVA initially used for the emulsification process was efficiently removed during NP isolation.

The ζ potential was measured in PBS (pH 7.4) mimicking the intracellular cytosolic environments. Although the ζ potential varied between 0 to -1.5 mV in all formulations, it was still close to neutrality (Table 2). The slightly lower surface charge obtained for AdsOVA NP may be due to the negative charge of the OVA protein, which is expected to be on the surface of NP, when compared to its dispersion within the polymeric matrix in the EntrapOVA NP. Moreover, the presence of PEG chains shields the negative charge of PLGA at NP surface in these EntrapOVA NP.

Both EE and LC were validated with two different methods: MicroBCA and HPLC. EntrapOVA NP showed 80 % entrapment of the initial protein solution, while the adsorption efficiency of AdsOVA NP was close to 50 %.

Atomic force microscopy (AFM) was used to further characterize the size, shape and surface morphology of NP (Figure 1). Both NP had a smooth surface and spherical topography with uniform size distribution, which correlated with the data obtained by DLS analyzer. Section analysis of PLGA-PEG NP with entrapped antigen demonstrated an average diameter of 30 nm smaller than the hydrodynamic diameter obtained by DLS. This can be explained by the fact that for dried NP, the PEG chains were not in a hydrated state, hence not being extended in the form of corona as they were during the DLS measurements.

Table 1: NP composition.

NP formulation	Matrix polymer	Entrapped aqueous phase	Surfactant IP*	Surfactant EP**	Protein adsorption
EntrapOVA	PLGA-PEG	10 % PVA, CS, OVA	2% (w/v) PVA	0.3 % (w/v) PVA	-
EntrapOVA-Adjs	PLGA-PEG, MPLA	10 % PVA, CS, CpG, OVA			-
AdsOVA	PLGA	10 % PVA, CS,			OVA
AdsOVA-Adjs	PLGA, MPLA	10 % PVA, CS, CpG			OVA

* internal phase, ** external phase

Table 2: Physicochemical characterization of OVA-loaded NP. (Mean ± SD; n ≥ 5).

Formulation	Size (nm)	PdI	ζ-potential (mV)	Protein loading (µg/mg)	
				Loading capacity	Surface adsorption
EntrapOVA	188 ± 8.0	0.160 ± 0.05	0.41 ± 0.20	19.56	-
EntrapOVA-Adjs	198 ± 7.0	0.180 ± 0.03	0.66 ± 0.30	18.97	-
AdsOVA	195 ± 14	0.190± 0.10	-1.15 ± 0.50	-	19.72
AdsOVA-Adjs	197 ± 12	0.200 ± 0.04	-1.32 ± 0.40	-	21.17

3.2. *In vivo* uptake study of antigen loaded NP by APC

DC and macrophages are both very effective APC [30]. However, macrophages are large phagocytic cells that play a critical role in the innate immune response [31]. On the other side, DC are considered the bridge between the innate and adaptive immunity, as they initiate innate immune responses and control critical steps in the cascade of adaptive immunity, thereby contributing to the initiation and regulation of specific T cell responses [32, 33]. Moreover, DC have an extensive capacity for NP internalization in the periphery. They migrate to draining LN where they process and present antigenic peptides to naïve T cells.

For the *in vivo* uptake study of antigen-loaded NP, female C57BL/6 mice (8 weeks old) were injected s.c. with one of the fluorescent-labeled NP formulations: EntrapOVA or AdsOVA. The contralateral non-immunized flank served as negative control, lacking both NP and antigen. NP-internalized APC were analyzed with high throughput and spatial resolution, by imaging stream flow cytometry (Suppl. Figure S1) [34]. We isolated popliteal and inguinal LN, prepared single cell suspensions and analyzed $CD11b^+$, $CD11c^+CD11b^-$ and $CD11c^+CD11b^+$ cells, as representatives of the LN myeloid compartment [35].

No significant difference in the total fluorescence was detected 16 h upon administration of EntrapOVA or AdsOVA NP. This indicated that the same cell populations internalized a similar amount of NP (Figure 1C-D). Among all studied cells, the $CD11c^+CD11b^+$ population internalized the highest amount of NP. Both EntrapOVA and AdsOVA NP were also equally taken up by $CD11b^+$ cells. On the other side, $CD11c^+CD11b^-$ cells presented slightly lower NP internalization (30-35 %) (Figure 1C). Additional surface

markers for plasmacytoid DC (pDC; anti-PDCA-1) were used to discern differences in the uptake of EntrapOVA or AdsOVA NP. Interesting, AdsOVA NP yielded significantly higher number of pDC in the draining LN, than EntrapOVA NP (Figure 1F).

To address the changes of the activation molecule MHCII, before and after NP internalization, the total fluorescence and median pixel intensities of the MHCII fluorescent signal was quantified for each studied cell population (Figure 1E). As shown in Figure 1E, a significant increase of the MHCII activation marker occurred after the internalization of EntrapOVA NP and AdsOVA NP in all of studied cell populations ($CD11b^+$, $CD11c^+CD11b^-$, and $CD11c^+CD11b^+$).

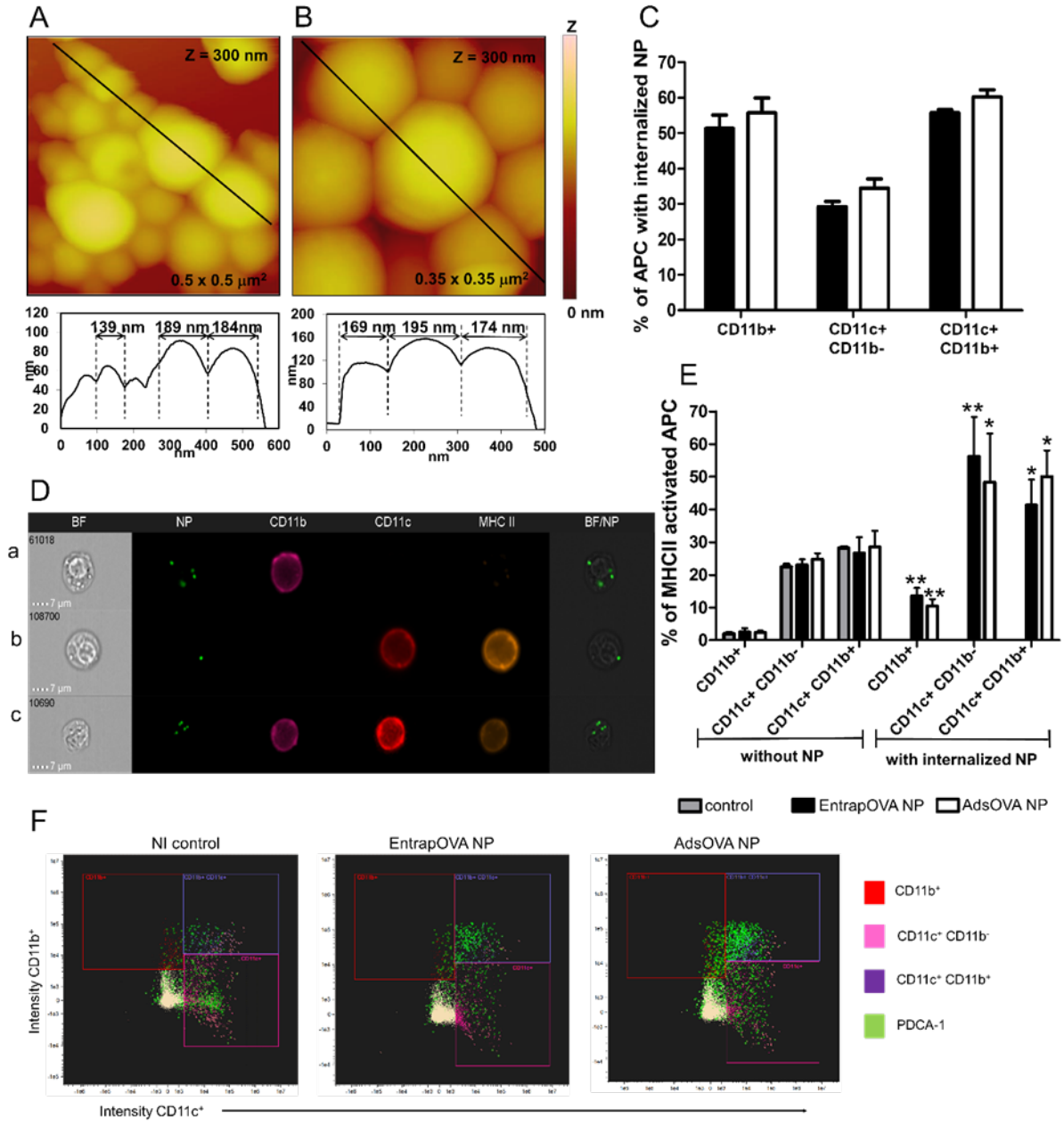

Figure 1: Section analysis and diameter distribution of nanoparticle by atomic force microscopy. (A) PLGA-PEG NP with entrapped OVA protein (EntrapOVA NP), (B) PLGA NP with adsorbed OVA protein (AdsOVA

NP). ImageStream analysis was performed to detect *in vivo* Rho labeled NP internalization by APC 16 h p.i. at 37 °C. Distribution of at least 30,000 cells was calculated by Amnis IDEAS software and presented with the histograms showing the percentages of APC with internalized NP (C) and % of MHCII activated APC (E). Examples of representative images with AdsOVA NP (D). First column shows brightfield (BF) images of the cells, second column shows images of Rho labeled NP (NP), third column shows $CD11b^+$ cells (CD11b), forth column $CD11c^+$ cells (CD11c), fifth column shows $MHCII^+$ cells (MHCII), sixth column presents merged images of the precedent fields (BF/NP). (D.a) $CD11c^+$ with upregulated MHCII. (D.b) NP internalized by $CD11b^+$ cell. (D.c) NP taken up by double positive cells $CD11b^+CD11c^+$ cell. Results are represented as mean ± SD, normalized to that of control non-labeled cells, representative of three independent experiments (n = 3). Scale bar, 7 μm. (F) ImageStream representative plots showing the gating of cells with surface makers CD11b, CD11c and PDCA-1.

3.3. *In vivo* T cell activation and proliferation at 6, 16, 24 and 48 h after NP immunization

This study focused on the *in vivo* kinetics of the activation and proliferation capacity of antigen-specific $CD4^+$ and $CD8^+$ T lymphocytes, first step towards an effector T cell phenotype. Different time points were assessed by flow cytometry after hock immunization with PBS, EntrapOVA NP or AdsOVA NP. To determine the activation profiles of $CD4^+$ (OT-II) and $CD8^+$ (OT-I) T cells in draining LN, the phenotypic changes in the expression of surface molecules (CD25, CD69, and CD44) were measured in combination with CFSE (Suppl. Figure S2). CD25 and CD69 are early activation markers [36, 37]. Conversely, CD44 is upregulated on activated T cells, firstly more gradually but persists at high levels on memory T cells [38, 39].

After immunization with EntrapOVA NP and AdsOVA NP, the percentages of $CD4^+$ and $CD8^+$ T cells expressing CD25 and CD69 increased exponentially over time (Figure 2A-B). The number of $CD25^+$ $CD4^+$ and $CD25^+$ $CD8^+$ T cells increased 3- or 4-fold respectively, within 48 h p.i.. Compared to other time points, a modest decline in the percentage of $CD69^+$ $CD8^+$ T cells was observed in the LN 24 and 48 h after immunization. Consistent with the results observed for $CD25^+$ and $CD69^+$ T cells, the percentage of $CD4^+$ and $CD8^+$ T cells expressing CD44 activation marker was gradually upregulated over time. However, there was not only an increase in the percentage of activated T cells, but also an increase in the absolute number of activated T cells, as shown by the serial dilution of CFSE dye indicating new generation of activated T cells (Figure 2A-B).

Overall, the activation and expansion of antigen-specific $CD4^+$ and $CD8^+$ T lymphocytes into effector T cells represent key steps in the development of an efficient adaptive immune response [40].

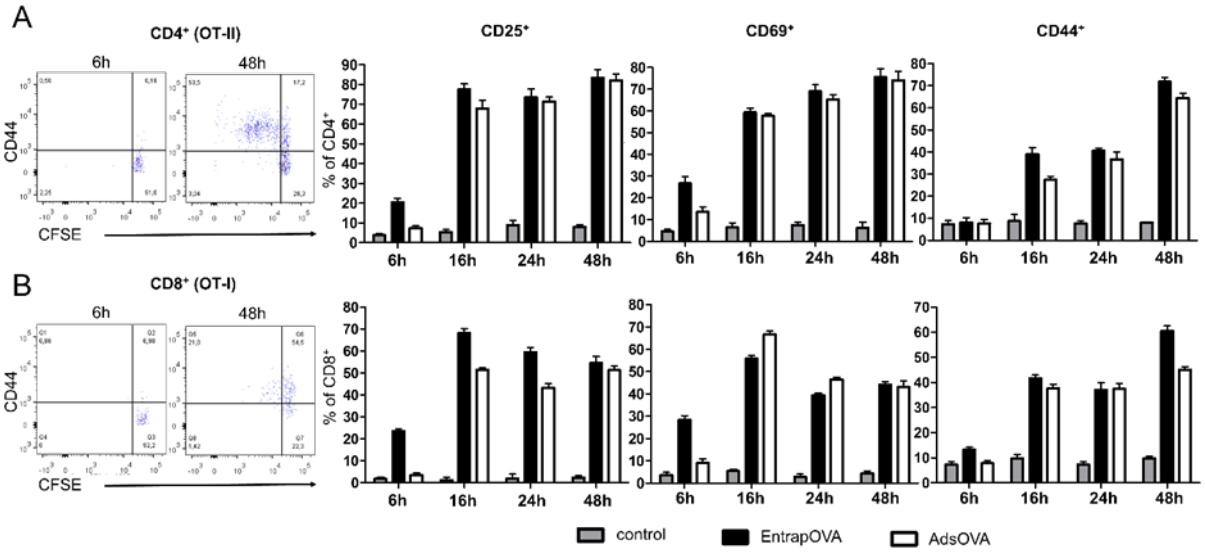

Figure 2: Activation profiles of T cells isolated from the draining LN. Time dependent phenotypic changes in the expression of activation surface molecules (CD25, CD69, and CD44) on $CD4^+$ (A) and $CD8^+$ (B) transgenic T cell stimulated *in vivo*. The expression of CD25, CD69, and CD44, was measured on freshly isolated cells by flow cytometry. Histograms present the mean values of three independent experiments, each with n=3 mice per time point.

3.4. *In vivo* cytotoxicity assay

The aim of every successful vaccination is an effective activation and priming of antigen-specific cytotoxic $CD8^+$ T (CTL) cells that recognize and kill target cells. To explore whether the immunization with formulated NP results in efficient cross-priming, an *in vivo* cytotoxicity assay was performed. Naïve C57BL/6 mice were engrafted with $CD8^+$ (OT-I) cells and 24 h later immunized with PBS, OVA & Adjs in solution, AdsOVA NP, AdsOVA-Adjs NP, EntrapOVA NP or EntrapOVA-Adjs NP. Five days after immunization, mice were injected with $CD45.1^+$ splenocytes. The graft consisted of an equal mix (1:1) of target cells: pulsed with the OT-I specific OVA-derived peptide (SIINFEKL) pulsed cells labeled with higher dose of CFSE ($CFSE^{hi}$) and un-pulsed control cells labeled with a lower dose of CFSE ($CSFE^{low}$). The differential *in vivo* clearance of both target cell populations was evaluated 16 h later in single-cell suspensions collected from LN (Figure 3, Suppl. Figure S3) and spleens by flow cytometry.

Antigen-specific OT-I CTL with acquired cytotoxic function selectively kill SIINFEKL-pulsed target cells and do not affect the proliferation of un-pulsed target T cells [41]. The results from the isolated LN (Figure 3), demonstrated that all immunizations with NP formulations, with or without adjuvants, generated the most efficient *in vivo* killing activity towards the SIINFEKL-pulsed cells, as shown by the disappearance of the $CFSE^{hi}$ peak of cells [28]. Likewise, OVA & Adjs in solution induced a moderate cytotoxicity. The control group without OVA antigen did not display detectable killing activity. Similar data was obtained for the cytotoxic ability of T cells in spleens of the animals (data not shown), indicating the successful induction of a systemic immune response.

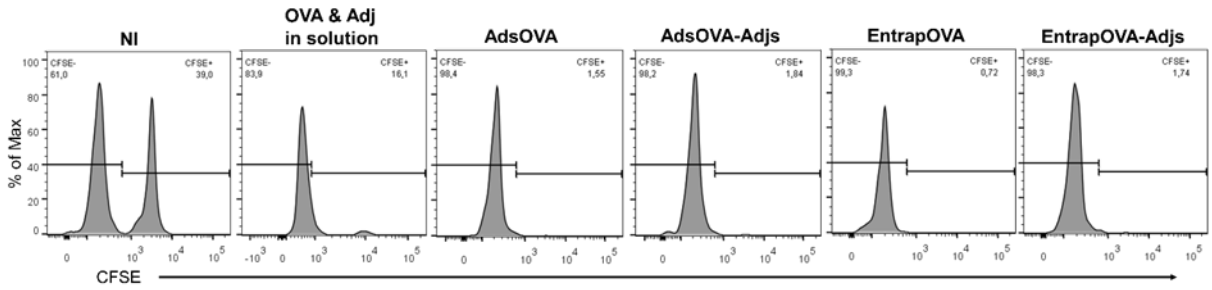

Figure 3: Cytotoxicity ability of antigen-specific cytotoxic T lymphocytes (CTL) in LN from naïve C57BL/6 mice seven days after treatment with PBS, OVA & Adjs in solution, AdsOVA NP, AdsOVA-Adjs NP, EntrapOVA, or EntrapOVA-Adjs.

3.5. Establishment of memory CTL cells

Immunological memory is the prime feature of adaptive immunity and guaranty rapid and effective response to foreign antigens that have been previously encountered. Therefore, long-lasting and stable memory is essential for successful vaccination. We evaluated the long-lasting memory of CTL eventually induced 8 weeks after the first immunization in response to the different ways of antigen delivery. Naïve C57BL/6 mice were immunized with PBS, OVA in solution, OVA & Adjs in solution, AdsOVA NP, AdsOVA-Adjs NP, EntrapOVA NP, or EntrapOVA-Adjs NP after engraftment with $CD8^+$ (OT-I) cells. Seven weeks p.i., animals were re-stimulated i.v. with 100 µg of OVA, except for one EntrapOVA-Adjs group, which served as a control. One week later, spleens were isolated, and the presence of antigen-specific $CD8^+$ (OT-I) CTL was assessed by flow cytometry (defined as $DAPI^-$, $TCR\beta^+$, $CD45.1^+$, and $CD8\alpha^+$ cells, Suppl. Figure S4).

Antigen recall induced a remarkable proliferation of $CD8^+$ (OT-I) in mice that had been immunized with EntrapOVA-Adjs NP 8 weeks earlier (Figure 4). Interestingly, re-

stimulation did not induce efficient CTL recall after immunization with AdsOVA-Adjs NP, AdsOVA NP, EntrapOVA NP or OVA & Adjs in solution.

Two groups, PBS and EntrapOVA-Adjs NP without re-stimulation, were used as controls and did not show expansion of $CD8^+$ (OT-I) T cells. All memory cells uniformly expressed high levels of CD44 and low levels of CD62L (data not showed) as previously reported [42].

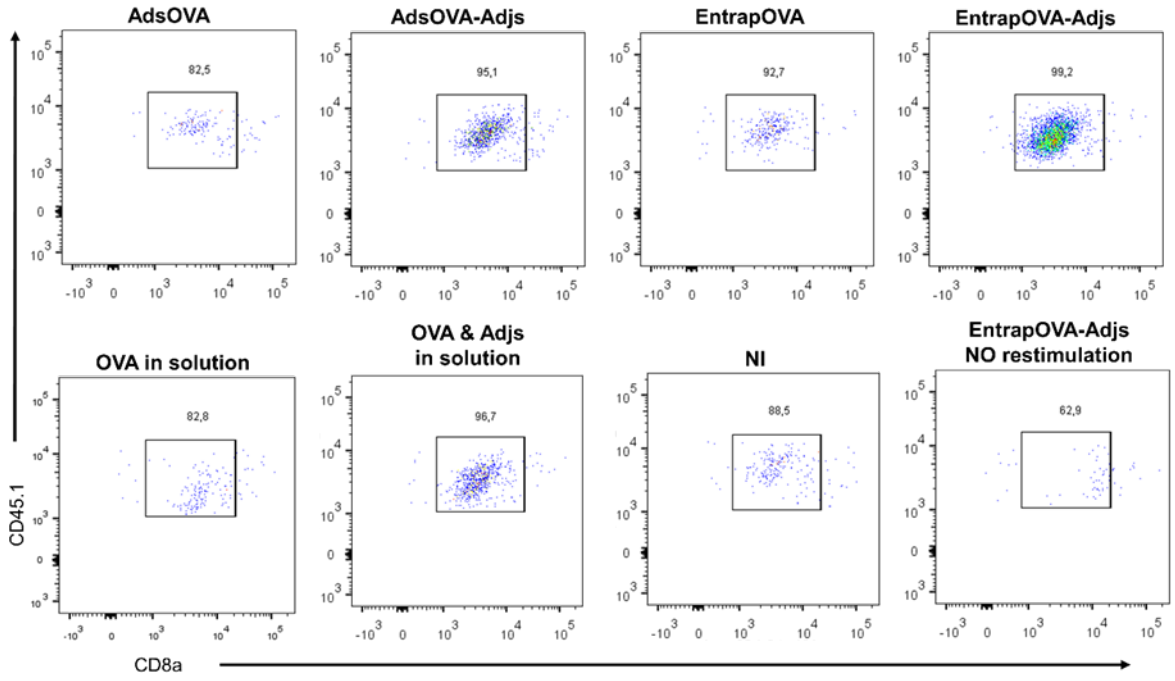

Figure 4: Immunization with protein and adjuvant in the uniformed delivery system drives development of memory CTL. Proliferation of antigen-specific memory T cells was determined by flow cytometry 8 weeks p.i. FACS plots are representative of at least three independent experiments with 2-3 mice per group.

3.6. Therapeutic efficacy of the nanoparticulate vaccines against B16.MO5 melanoma challenge

Two treatment schedules were followed to explore the therapeutic efficacy of the anti-tumor nanoparticulate vaccines in B16.MO5 melanoma tumor-bearing mice: single vaccination and 3-time immunization treatment, seven days apart (Figure 5A). B16.MO5 are characterized by a constitutive production of OVA protein, which render them targetable by immune cells instructed to recognize OVA as antigen. Nine days after tumor inoculation, 1 x 10^6 CD45.1 OT-I and 1 x 10^6 CD45.1 OT-II splenocytes were engrafted into tumor-bearing mice to follow an antigen-specific immune response against tumor cells. Mice were then randomized into one of the following treatment groups: (1) PBS, (2) Empty NP, (3) AdsOVA-

Adjs NP, (4) EntrapOVA-Adjs NP, (5) AdsOVA-Adjs NP (3x immunization), (6) EntrapOVA-Adjs NP (3x immunization).

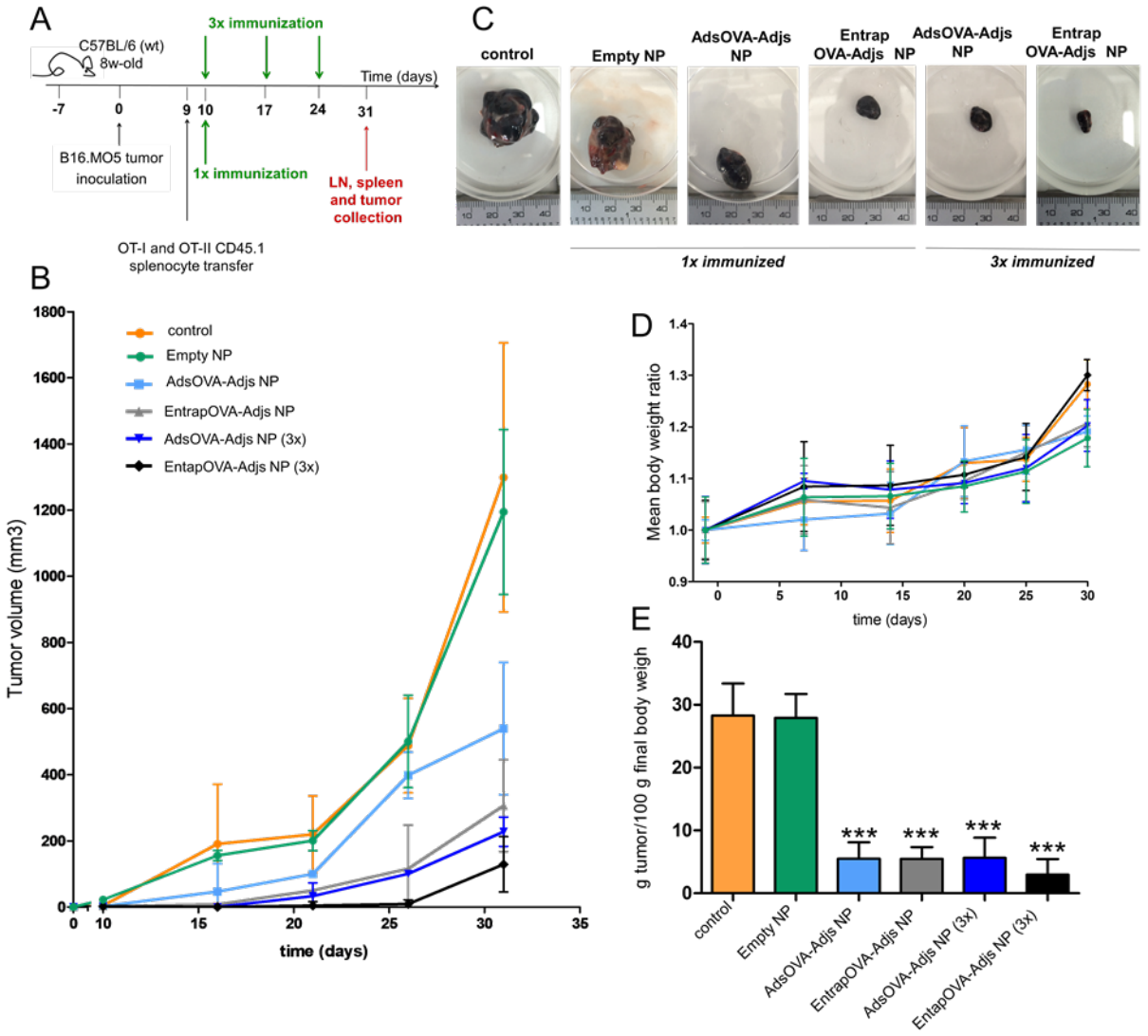

Figure 5: Anti-tumor therapeutic efficacy of the nanoparticulate vaccines. (A) Schedule of the assay. (B) Mean tumor growth curves given by mean tumor volume over time, determined by $V = ½ \times (L \times W^2)$, where L (length) is the longest dimension and W (width) is the perpendicular dimension to the length. (C) Representative images of removed melanoma tumors from each treatment group at the end of the assay. (D) The tolerability of the vaccine was evaluated by monitoring body weight of the treated mice. (E) Mean final tumor weight per 100 g of final body weight. Mean ± SD, n = 6, ***$p < 0.001$.

The groups immunized with PBS and Empty NP served as a control and presented similar tumor growth. All treated groups showed a significant reduction in tumor growth, compared to control groups ($p < 0.001$) (Figure 5B). EntrapOVA-Adjs NP (3x immunization) presented the slowest tumor growth, followed by the group immunized with AdsOVA-Adjs

NP (3x immunization) and EntrapOVA-Adjs NP. This can be also appreciated in the representative images of removed melanoma from each treatment group at the end of the assay (Figure 5C). The mean mass of tumors per 100 g of final body weight are presented on Figure 5E. The mean mass of tumors was in accordance with the obtained mean tumor growth curves, with the group 3-times immunized with EntrapOVA-Adjs NP presenting the lowest mean tumor mass per 100 g of final body weight.

The vaccine tolerability and safety *in vivo* were evaluated by monitoring body weight of the treated animals and further calculated by the mean ratios of body weight to the initial body weight of mice. Body weights in all groups increased during the treatment, therefore no abrupt weight loss was observed (Figure 5D).

3.7. T cell infiltration in the tumor microenvironment

It has been previously reported that tumor-infiltrating lymphocytes (TIL) confer a positive prognostic value [43-45].

To identify the immune cells infiltrating the B16.MO5 melanoma-bearing mice, a single cell suspension of tumors was prepared, and the presence of antigen-specific (CD3e) TIL was assessed by flow cytometry (Figure 6A & B; Suppl. Figure S5 show a representative plots of gating strategy, cells were gated by TCRβ$^+$, CD45.1$^+$,CD3e$^+$, CD4$^+$ and CD8α$^+$). It was observed an increased level of TIL in all treated groups. Moreover, besides that increase in the percentage of intra-tumoral T cells, there was also a dramatic increase in the absolute number of T cells, as shown by the flow cytometry plots (Figure 6A).

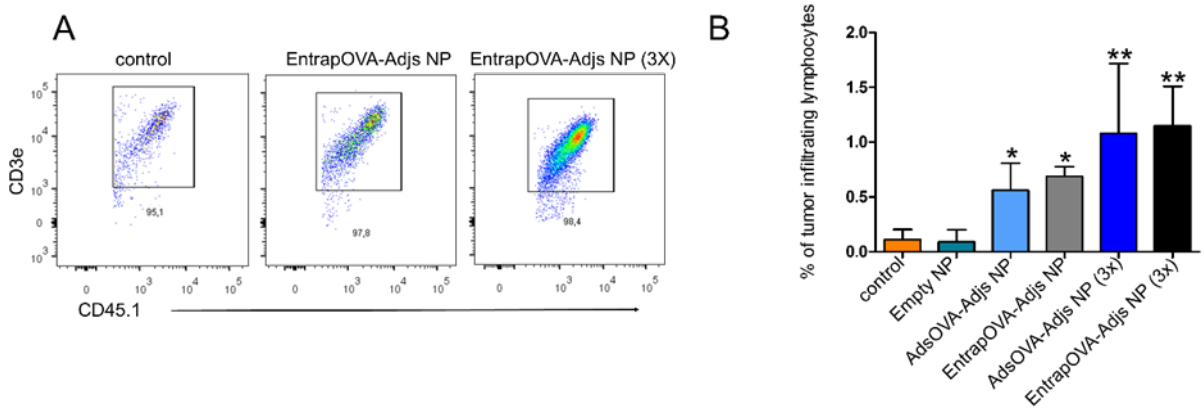

Figure 6: (A) Representative flow cytometry plots of the percentages of tumor infiltrated lymphocyte (TIL) CD45.1$^+$ versus CD3e$^+$ T cells. (B) Mean percentages of TIL present on tumor suspensions obtained from each treatment group. Mean ± SD, n = 6. *p < 0.05, **p < 0.01

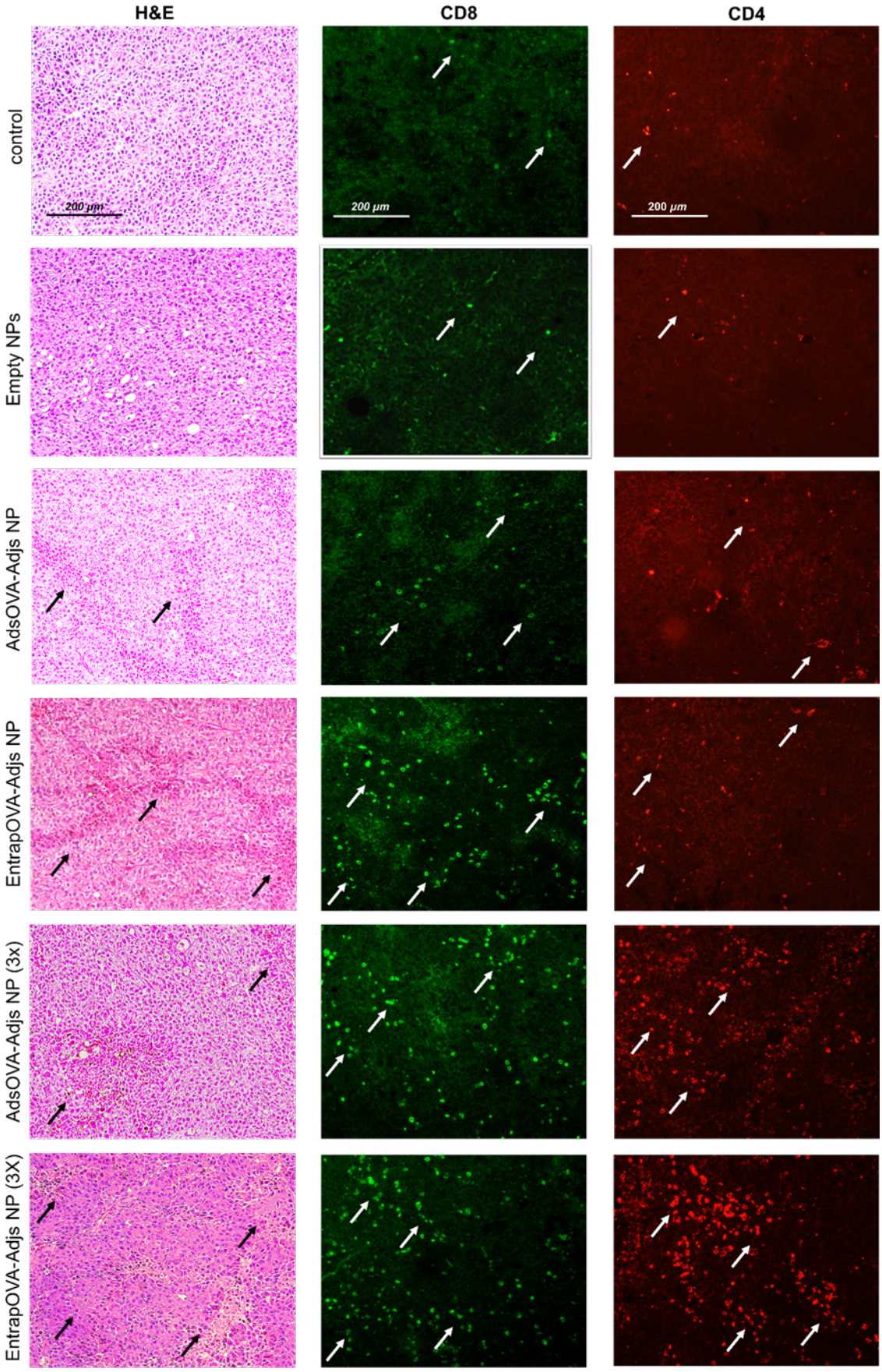

Figure 7: Images are representative histology sections with H&E staining and immunohistochemistry staining for CD8 and CD4, of multiple fields and magnifications in a three independent experiments. Bars, 200 µm.

The 3-time immunization with AdsOVA-Adjs NP or EntrapOVA-Adjs ($p < 0.01$) was more efficient in supporting T cell recruitment into tumor tissues than a single vaccination ($p < 0.05$), when compared to the control group (Figure 6B).

Hematoxylin and eosin (H&E)-stained sections were prepared for diagnostic purposes of stromal TIL, which are usually dispersed in the spaces between the carcinoma nests and do not directly contact carcinoma cells (Figure 7; first column with H&E staining) [2]. Generally, the H&E-stained sections showed that vaccination with the nanoparticulate vaccine generated the formation, growth and high density of stromal TIL (Figure 7; indicated with the arrow), compared to the groups treated with PBS or empty NP.

Figure 7 with CD8-staining shows a generally increase of $CD8^+$ TIL levels after a single dose of the nanoparticulate vaccines, particularly after immunization with EntrapOVA-Adjs. Finally, 3-time immunization with AdsOVA-Adjs NP or EntrapOVA-Adjs led to an increased infiltration of both $CD8^+$ and $CD4^+$ TIL.

3.8. Flow cytometry analysis of antigen-specific T cells

To characterize activation of antigen-specific T cell response to the tumor, we measured cell surface expression of the: i) activation marker CD107a (also known as lysosomal-associated membrane glycoproteins; LAMP-1) ii) inhibitory receptor programmed death-1 (PD-1) and iii) cytotoxic T-lymphocyte-associated-antigen 4 (CTLA-4) on antigen-specific $CD8^+$ (OT-I) T cells of different organs, namely spleen, LN and tumor, by flow cytometry (Supp. Figure S6).

CD107a has been described as a marker of $CD8^+$ T-cell degranulation upon its stimulation [46]. The results showed CD107a upregulation after immunization with one of the formulated NP (AdsOVA-Adjs NP or EntrapOVA-Adjs NP) ($p < 0.001$), while the CD107a levels in the control groups were below 5 % (Figures 8A-C). Interestingly, no differences were detected in the levels of CD107a after single or 3-time vaccinations. However, the overall number of antigen-specific cells was higher after the 3-time immunization. Therefore, one would predict higher mediated cytotoxic activity in animals immunized with three doses of the nanoparticulate vaccines.

CTLA-4 recruitment antagonizes the activation of T cell at the initiation of an immune response in the draining LN, while PD-1 mainly regulates effector T cell activity in response to tumor progression [1, 47, 48].

Interestingly, our study showed that the 3-time vaccination protocol with AdsOVA-Adjs NP or EntrapOVA-Adjs NP induced the expression of CTLA-4 in T cells isolated from the spleen and LN (Figure 8D-E). A significant upregulation was observed in the group vaccinated with AdsOVA-Adjs NP, compared to mice immunized with EntrapOVA-Adjs NP ($p < 0.05$).

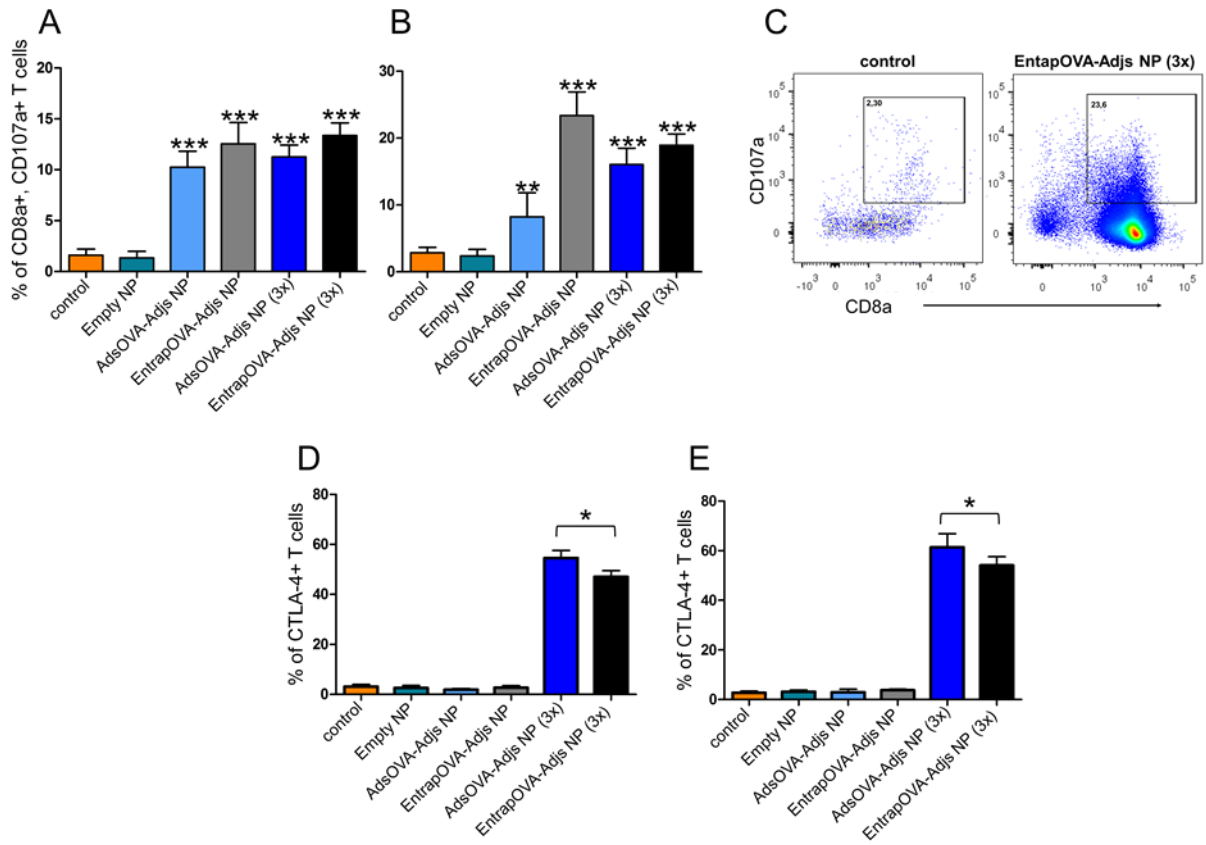

Figure 8: Activation of cytotoxic $CD8^+$ (OT-I) T lymphocytes in (A) spleen and (B) LN. (A & B) Histograms show frequency of the activated $CD107a^+$ $CD8^+$ CTL. (C) Representative flow cytometry plots of LN single–cell suspension from the control and EntrapOVA-Adjs NP (3x) groups, gated for CD45.1, CD3e, TCR Vα2 cells. (D & E) Histograms show frequency of the activated CTLA-4 T cells in (D) spleens and (E) LN in tumor-bearing mice. Mean ± SD, n = 6, *$p < 0.05$, **$p < 0.01$, ***$p < 0.001$

3.9. Cytokine quantification in spleens and tumors of treated mice

In order to understand the type of the immune response induced by the different nanoparticulate vaccines and tested schedules, the levels of IFN-γ, TNF-α and IL-4 cytokines were determined by intracellular staining (Figure 9). For the detection of produced cytokines, single cell suspension of tumors and spleens were gated for $CD45.1^+$, $CD3e^+$ and $CD8\alpha^+$, which includes engrafted antigen-specific OT-I T cells (Suppl. Figure S7).

The groups vaccinated with single dose of AdsOVA-Adjs NP or EntrapOVA-Adjs presented the highest levels of the splenic IFN-γ-producing ($p < 0.001$) and TNF-α-producing ($p < 0.001$) $CD8^+$ (OT-I) T cells, compared to the control and 3-time vaccination groups. Surprisingly, the 3-time immunization protocol, with the same nanoparticulate vaccine, did not induce further the secretion of either IFN-γ or TNF-α by T cells. This could be due to the compromised activation or exhaustion of T cells.

Tumor infiltrating $CD8^+$ (OT-I) T cells (TIL) secrete/produced significantly higher levels of TNF-α upon one immunization with EntrapOVA-Adjs and 3-time immunizations with both NP formulations, compared to control groups. Levels of IFN-γ^+ $CD8^+$ TIL cells are increased only upon one application of the NP vaccination, whereas upon 3-time application they return to the same level as in the control groups.

No differences were observed between IL-4 cytokine levels detected in different groups, which were in fact undetectable (data not shown).

3.10. Therapeutic efficacy of the nanoparticulate vaccines without a transfer of transgenic T cells

To explore the intrinsic potential of the developed anti-cancer nanoparticulate vaccine, a new group of animals was challenged with B16.MO5 melanoma, and treated without any engraftment of antigen-specific (OT-I) cells. After a single immunization, both AdsOVA-Adjs NP and EntrapOVA-Adjs NP delayed tumor growth ($p < 0.001$, Figure 10A-C). However, EntrapOVA-Adjs NP were more efficient, which is in accordance with the results reported with the previous experiment. These results indicate that the presence of previously transfer antigen-specific OT cells did not influence the outcome of the treatment. Even in the absence of OT-I cells, the vaccination with NP was efficient and led to the development of an adaptive immune response starting with the endogenous pool of T cells. Therefore, with this study we have confirmed the efficacy and safety of the developed nanoparticulate vaccine.

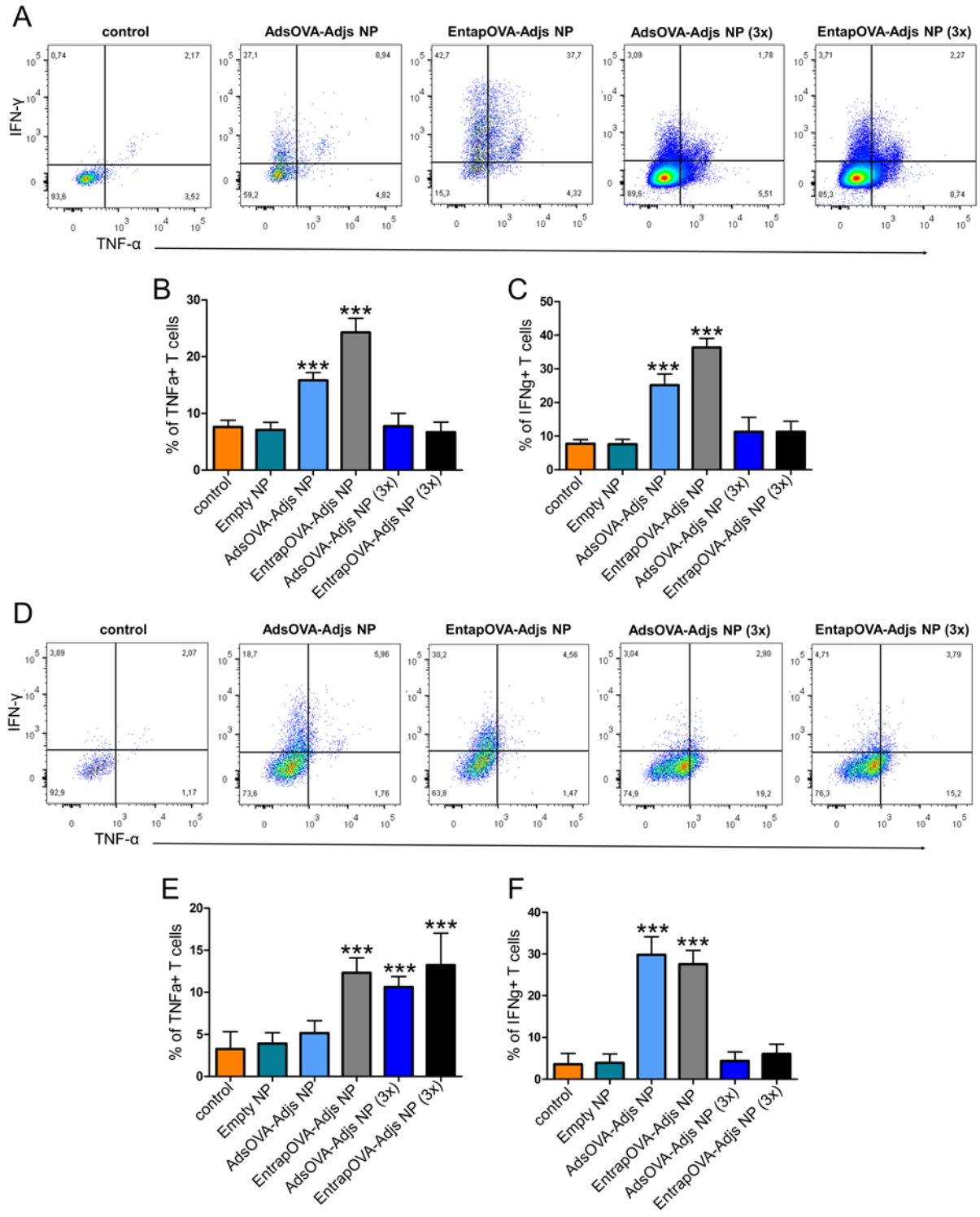

Figure 9: Intracellular staining of $CD8^{+}$ T cells and cytokine levels in (A-C) spleens and (D-F) tumors. Representative flow cytometry plots of TNF-α and IFN-γ in (A) spleens and (D) tumors from the control, AdsOVA-Adjs NP EntrapOVA-Adjs NP, AdsOVA-Ajs NP (3x), and EntrapOVA-Adjs NP (3x) groups. (B & E) Histograms show frequency of the activated TNF-α T cells in (B) spleens and (E) tumors. (C & F) Histograms show frequency of the activated IFN-γ T cells in (C) spleens and (E) tumors. Mean ± SD, n = 6, ***p < 0.001.

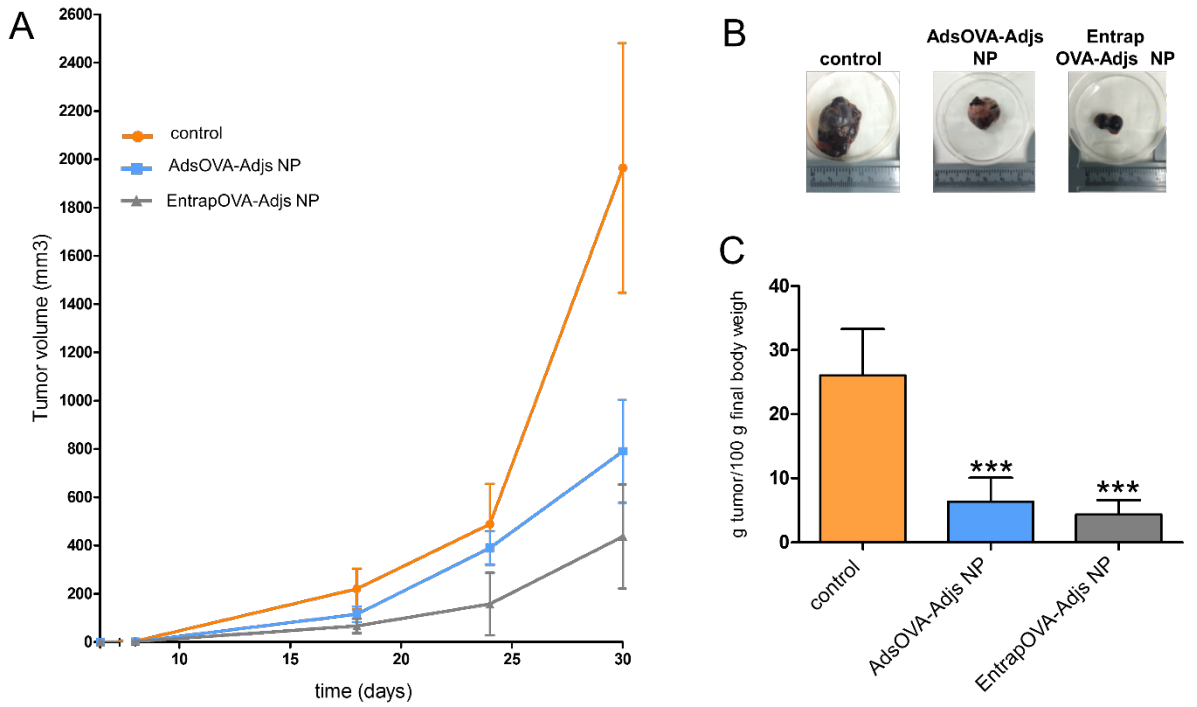

Figure 10: Anti-tumor therapeutic efficacy of the nanoparticulate vaccines without the previous transfer of transgenic T cells. (A) Mean tumor growth curves given by mean tumor volume over time. (B) Representative images of removed melanoma tumors from each treatment group at the end of the assay. (C) Mean final tumor weight per 100 g of final body weight. Mean ± SD, n = 6, ***p < 0.001.

4. Discussion

Nanodelivery systems are promising platforms for cancer immunotherapy due to their nanoscale size, successful co-entrapment of various active agents, and intrinsic biocompatibility [49]. In addition, nanosystems have extensively shown to positively alter payload biodistribution and increase therapeutic efficiency, while reducing a nonspecific toxicity [50].

Here, we report the use of PLGA NP as an antigen delivery carrier to investigate how different antigen-loading nanovaccines affect antigen uptake by APC and generation of DC-mediated antigen-specific immune responses. We developed two highly reproducible and homogeneous nanoplatforms - AdsOVA NP and EntrapOVA NP – based on the hydrophobic aliphatic polyester PLGA which allows the association of the antigen (OVA) and incorporation of adjuvants (CpG and MPLA) into the core of the its matrix. The presence of PEG polymer on the surface of EntrapOVA NP may be responsible for the similar size distribution, polarity of ζ potential and hydrophobicity presented by both OVA adsorbed and entrapped formulations. Narrow particle size distribution, mean diameter close to 190 nm and spherical geometry were also confirmed by AFM. The two classes of NP allowed us to

investigate the affect of antigen-loading method on the nature of ensuing immune responses. We hypothesize that the resulting immune responses would be significantly affected by the different nature of initial antigen exposure to APC.

To test this hypothesis, we firstly evaluated the *in vivo* uptake profile of NP by APC at predetermined time points (6 h, 16 h and 24 h). At 6 h, the amount of NP in the draining LN was too low to be detected. However, it has been reported before that it usually takes 8-16 h for pathogens to migrate within the lymph drainage or be actively transported by DC [51,52]. It was visible a peak in the fluorescence 16 h p.i, indicating the presence of the highest amount of Rhodamine-6G labeled NP in the draining LN. The fluorescence peak decreased at 24 h, which may suggests that a certain amount of Rhodamine-6G NP was already digested and degraded inside the APC. In addition, it can also indicate a possible release of this probe from the carrier. Therefore, we selected the time point 16 h p.i. for the *in vivo* uptake studies analyzed by imaging stream flow cytometry. We explored the myeloid compartment of the LN subdivided into different APC populations: macrophages, classical DC (cDC) and plasmacytoid DC (pDC) [35].

The *in vivo* kinetic study of NP internalization clearly indicated the efficient ability of APC to capture both types of NP, despite the antigen association method. In fact, no significant difference was detected in the total fluorescence for EntrapOVA or AdsOVA NP once internalized by the $CD11b^{+}$, $CD11c^{+}CD11b^{-}$ and $CD11c^{+}CD11b^{+}$. On the other side, pDC yielded significantly higher uptake of AdsOVA NP than EntrapOVA NP. Antigen presented on the NP surface (AdsOVA NP) may have enhanced affinity for pDC, whereas EntrapOVA NP may have rapidly escaped peripheral internalization by pDC, most probably due to the PEG present on the outer surface of NP. It is widely known that PEG "stealth" effect prevents NP premature capture [53,54], and thus prolongs their circulation under *in vivo* conditions.

To verify the specificity of DC-mediated antigen-specific activation and characterize the proliferation of T cells induced by the antigen-associated NP, a well-established animal model within the immunology field was used. Accordingly, a highly immunogenic protein, OVA, served as an antigen, in combination with the engraftment of $CD4^{+}$ (OT-II) and $CD8^{+}$ (OT-I) T cell, carrying a transgenic OVA-responding T cell receptor to better trace and characterize antigen-specific immune response upon NP vaccination.

To test the cytotoxic nature of the immune response developed in immunized animals, an *in vivo* killing assay was carried out. Vaccination with developed OVA-loaded NP (AdsOVA NP, Entrap OVA NP, AdsOVA-Adjs NP or EntrapOVA-Adjs NP) was efficient in

activating antigen-specific OT-I CTL and selective killing of SIINFEKL-pulsed targeted cells. Interestingly, the nature of antigen delivery, entrapped vs. adsorbed, in the presence or absence of the Adjs, did not have a significant influence on the resultant primary immune response. Therefore, both delivery systems efficiently drove the immune system towards a cross-presentation and cross-priming of antigen-specific cytotoxic $CD8^+$ T (CTL) cells, which is especially important in cancer immunotherapy [55].

To obtain deeper insight into the nature of immune response and better understand the effect of antigen association and combination with adjuvants, it was further important to characterize expansion of different subpopulations of T lymphocytes. Thus, in the *in vivo* kinetic study, we focused on the activation profile and proliferation capacity of antigen-specific $CD4^+$ (OT-II) and $CD8^+$ (OT-I) T lymphocytes in draining LN. We observed that the activation of $CD8^+$ T cells upon EntrapOVA NP was more prominent compared to the quantified in animals immunized with AdsOVA NP. This data suggested that EntrapOVA NP can generate stronger antigen-specific $CD8^+$ immune responses towards an effective memory T cells [40], even if no differences were previously observed in the *in vivo* killing assay for both Entrap and Ads NP.

These evidences were further supported by the long-lasting memory study, where a remarkable proliferation of $CD8^+$ (OT-I) was induced in mice that had been immunized with EntrapOVA-Adjs NP and re-stimulated with antigen (OVA boost) 7 weeks after treatment. A recall of antigen-specific CTL was not so efficient after immunization with AdsOVA-Adjs NP or OVA & Adjs in solution. Although all AdsOVA-Adjs NP were efficient internalized by APC and led to an equally strong OVA-specific cytotoxic immune response, these NP were not able to generate long-lasting effector memory, in contrast to EntrapOVA NP. This observation may be explained by an absent or delayed TLR signal. OVA is adsorbed on the NP surface through the establishment of weak electrostatic interactions, while the Adjs (CpG and MPLA) are dispersed into the matrix of the nanoparticulate vehicle. Therefore, OVA can be desorbed from NP surface prior to the release of Adjs, which will be rather controlled by the digestion and erosion of NP matrix. Consequently, the administration of AdsOVA-Adjs NP may not guarantee the co-stimulatory signal essential for an efficient generation of activated and long-lasting memory $CD8^+$ T cells. In addition, animals immunized with vaccines free of Adjs (AdsOVA NP, EntrapOVA NP or OVA in solution) failed to generate memory $CD8^+$ (OT-I) T cells. To the best of our knowledge, with this study we are the first to report the induction of a long-lasting effector memory CTL, even 8 weeks after a single immunization with a nanoparticulate vaccine. Thus, this long-term memory study provides

important insights into the effect of antigen delivery on the overall nanovaccine efficiency. Our findings have important implications for future vaccine development, as they suggest that protein boosting with adjuvant in a uniformed and unique delivery system (EntrapOVA-Adjs NP) can generate long-term functional memory CTL.

Having in consideration the above discussed promising effects on immune cells, it was important to clarify if the induced immune response would be able to fight against cancer growth. Therefore, the anti-tumor therapeutic efficacy of the developed nanovaccines (AdsOVA-Adjs NP and EntrapOVA-Adjs NP) has been tested on B16.MO5 melanoma-bearing C57BL/6 mice. When choosing this tumor model, authors were aware of the severity of its epigenetic phenotype, high enzymatic activity and multiple immune escape tumor-mediated mechanisms [56]. However, there is an important advantage of this system mostly related to the xenograft nature of the OVA antigen, constituting a clean and distinct read-out model that allows detailed and controlled characterization of the antigen-specific nature of the overall immune response. This model thus constitutes a perfect intermediate that may support a possible correlation of the data obtained under steady-state conditions and later evidenced in a proof of concept study using a cancer mouse model expressing an immunodominant TAA, such as the Her2-expressing cancer model.

Tumor growth was significantly delayed by the administration of the developed nanovaccines. The slowest tumor growth was achieved after the 3-dose immunization schedule with EntrapOVA-Adjs NP, followed by the group that has been vaccinated 3-times with AdsOVA-Adjs NP and once with EntrapOVA-Adjs NP. Both control groups (PBS and Empty NP) presented similar tumor growth, indicating that the nanoparticulate-vehicle itself did not possess an immunotherapeutic effect. As nanovaccine efficacy could be attributed to the adoptive transfer of OT-I ($CD8^+$) and OT-II ($CD4^+$) T cells, we addressed this hypothesis by triggering the immune response with only developed nanoparticulate vaccine. Similar immunotherapeutic efficiency was obtained in animals vaccinated with the antigen-associated NP (AdsOVA-Adjs and EntrapOVA-Adjs NP) without previous transfer of the antigen-specific splenocytes. A single vaccination with EntrapOVA-Adjs NP or AdsOVA-Adjs NPs was able to significantly decrease mean tumor development and growth, when compared to control group. The strongest effect was observed in animals treated with EntrapOVA-Adjs NP thus attesting the prominent anti-tumor immunity induced by this particular nanovaccine.

Next to the phenotypic determination and quantification of the therapeutic efficacy of developed nanovaccines, the presence and the activation of TIL were further addressed following two immunization protocols: single vaccination or 3-time vaccination with

AdsOVA-Adjs or EntrapOVA-Adjs NP. Our studies suggest that a repetitive immunization was more efficient than a single vaccination in promoting lymphocyte recruitment into tumor microenvironment, as both $CD8^+$ and $CD4^+$ T cells were infiltrated at the tumor site, thus anticipating a more efficient tumor rejection. After a single vaccination with either AdsOVA NP or EntrapOVA NP, mainly $CD8^+$ T cells were infiltrated at the tumor sites, suggesting a low infiltration of $CD4^+$ T cells after a single dose of antigen-associated NP.

The activation of $CD8^+$ T cells was also studied in the spleens and LN of tumor-bearing animals. Interestingly, the upregulation of CD107a activation marker was detected after a single and 3-dose vaccination. On the other side, the expression levels of the immune-checkpoint receptor CTLA-4 were upregulated on T cells isolated from the spleens and LN after the 3-time immunization with AdsOVA-Adjs or EntrapOVA-Adjs NP, indicating lower T cell priming. Moreover, we detected altered cytokine production. Tumor infiltrating $CD8^+$ T cells secrete significantly high levels of TNF-α but not IFN-γ upon 3-time immunizations. High levels of TNF-α in tumor microenvironment kept the tumor growth under control. However, splenic $CD8^+$ T cells of these immunized animals presented low levels of IFN-γ and TNF-α secretion, indication an abasance of any systemic inflammation. On the other side, single vaccination with EntrapOVA-Adjs upregulated both TNF-α and IFN-γ in the spleens and in tumor microenvironment. However, it was more efficient after the immunization with AdsOVA-Adjs NP. Moreover, lymphoid organs removed from animals treated with single dose of NP did not express upregulated levels of CTLA-4.

Overall, the anti-tumor therapeutic efficacy presented the best outcomes in tumor-bearing mice immunized 3-times with EntrapOVA-Adjs NP. However, based on these cytokine results and levels of immune-check point receptors at T cells, we anticipate that the schedule of 3-time immunization may soon led to the anergy and exhaustion of the antigen-specific T cells. Consequently, having in consideration the above results, alterations in the vaccination schedule may be suggested.

5. Conclusions

In this study we present the successful development of a cancer immunotherapeutic strategy by using biodegradable polymeric NP. This nanovaccine was able to efficiently co-entrap various TAA and immunoadjuvants, such as TLR to enhance their co-delivery towards APC, and consequently induce an antigen-specific anti-tumor immune response. Several *in vivo* studies under steady-state conditions and cancer disease have been performed, to evaluate vaccine efficacy.

Altogether, the results lead us to the following conclusions; APC, particularly DC, efficiently internalized both types of nanovaccines: EntrapOVA NP and AdsOVA NP. Differences in antigen-loading nanovaccines did not significantly alter their uptake by APC and the overall antigen-specific T cell activation within first 48 h p.i.. However, in a wider timeframe functional memory CTL were generated only when the antigen and adjuvants were co-delivered within the NP matrix (EntrapOVA-Adjs NP). The anti-tumor therapeutic efficacy of EntrapOVA-Adjs NP was also superior comparing to the vaccination with antigen adsorbed onto the surface of NP (AdsOVA-Adjs NP). These results highlight the importance of understanding the *in vivo* behavior of NP under both steady-state and tumor environment, providing important insights into the effect of antigen and adjuvant delivery on the overall nanovaccine efficiency.

Acknowledgements

This research work was funded by Fundação para a Ciência e a Technologia (FCT), Ministério da Educação e Ciência, Portugal (PhD Grant SFRH/BD/78480/2011 and Research projects UTAP-ICDT/DTP-FTO/0016/2014 and ENMed/0003/2015, under the framework of EuroNanoMed-II; iMed.ULisboa grant UID/DTP/04138/2013). The Jung laboratory is supported by the European Research Council (340345). The authors are grateful to the EMBO for the Short Term Fellowship (ASTF 277-2015). The authors have no other relevant affiliations or financial involvement with any organization or entity with a financial interest or financial conflict with the subject matter or materials discussed in the manuscript.

Declaration of interest

The authors report no conflicts of interest. The authors alone are responsible for the content and writing of this article.

Ethical conduct of research

Animals were maintained and treated according to the Weizmann Institute of Science animal facility and National Institutes of Health guidelines, Israel. Procedures with animal subjects have been approved by Institutional Animal Care and Use Committee (IACUC) at the Weizmann Institute of Science, Israel.

Supplementary material

Gating strategy for in vivo determination of antigen loaded nanoparticle uptake by APC with ImageStreamX:

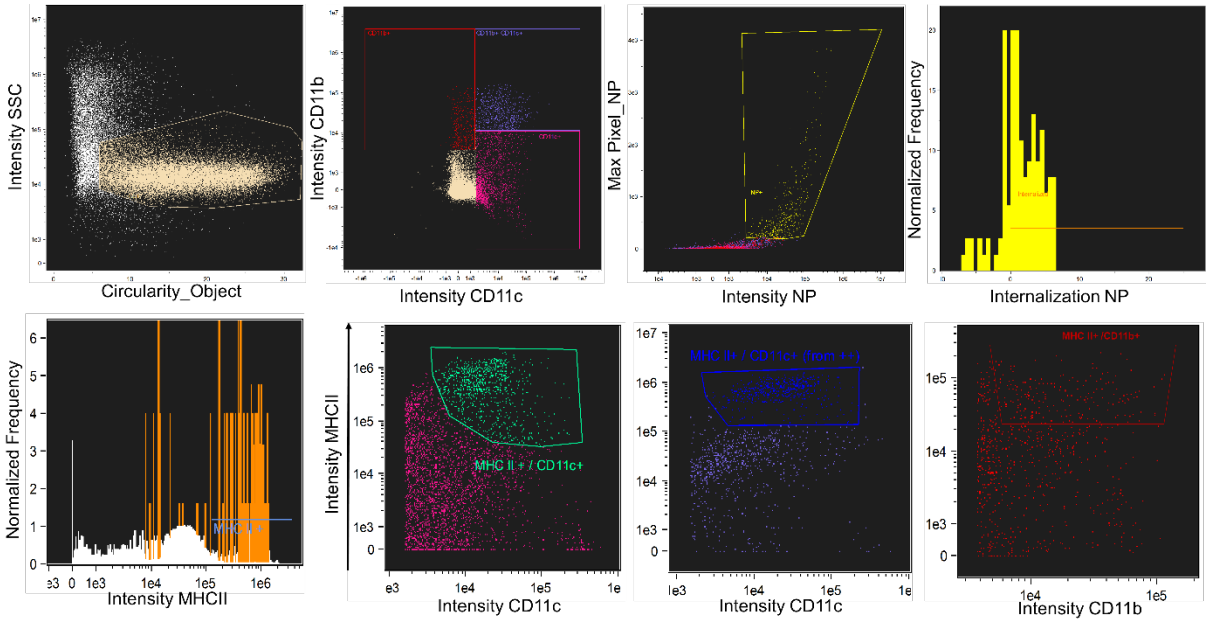

Figure S1: Gating strategy of the *in vivo* experiment of antigen-loaded nanoparticle uptake by APC. At least 30,000 cells were collected for each sample. ImageStream analysis was performed to detect Rho-labeled NP internalized by DC 16 h after the immunization. Images were compensated for fluorescent dye overlap by using single-stain controls. Cells were gated for single cells using the area, aspect ratio features, and bivariate plot for circularity (the degree of the mask's deviation from a circle) based on the Object mask (a segmentation mask that creates a tight fit on the cell morphology) and intensity of the side scatter channel (illuminated by the 785 nm laser and collected in channel 12). Particle internalization was calculated by the Internalization feature, i.e. the ratio of the intensity inside the cell to the intensity of the entire cell, mapped to a log scale. To define the internal mask for the cell, the object mask of the bright field image was eroded by 5 pixels. To measure the activation of $CD11b^{+}$, $CD11c^{+}CD11b^{+}$, and $CD11c^{+}CD11b^{-}$, intensity of MHCII was compared against the intensity of CD11c or CD11b, respectively. Data are representative of tree independent experiments after the 16 h incubation of DC with NP. Scale bar, 7 µm.

T cell activation:

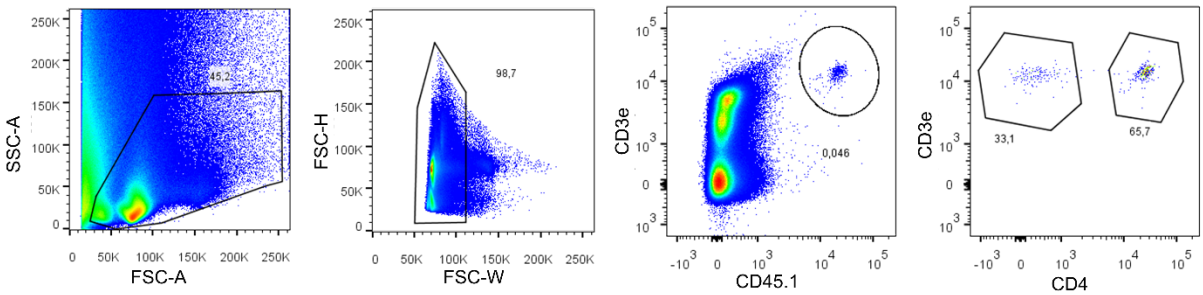

Figure S2: Gating strategies for the expression of CD45.1, TCRVα2, CD3e or CD4 of T cells isolated from

immunized and non-immunized LN, 6, 16, 24 and 48 h following immunization. Data shown are representative of three different animals and three independent experiments form the 16 h p.i..

In vivo cytotoxic assay:

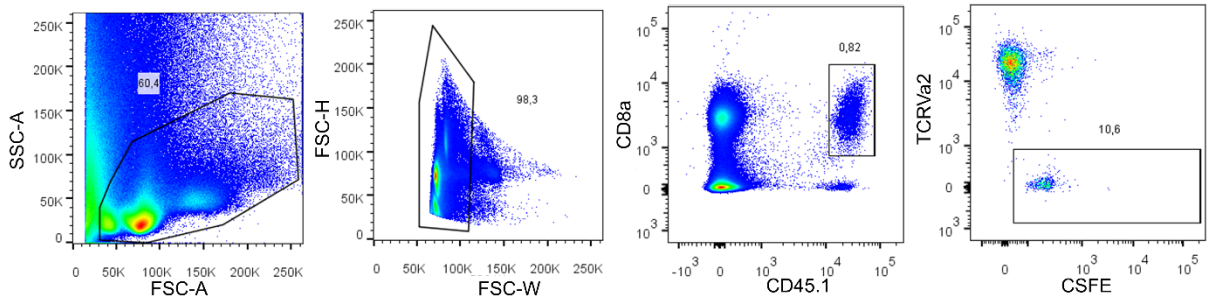

Figure S3: Gating strategies for the expression of CD45.1, TCRVα2, CD8α or CD4 of T cells isolated from immunized and non-immunized LN. Data shown are representative of three different animals and three independent experiments.

Memory CTL cells undergo an effective and rapid activation of naïve T cells 8 weeks after first immunization:

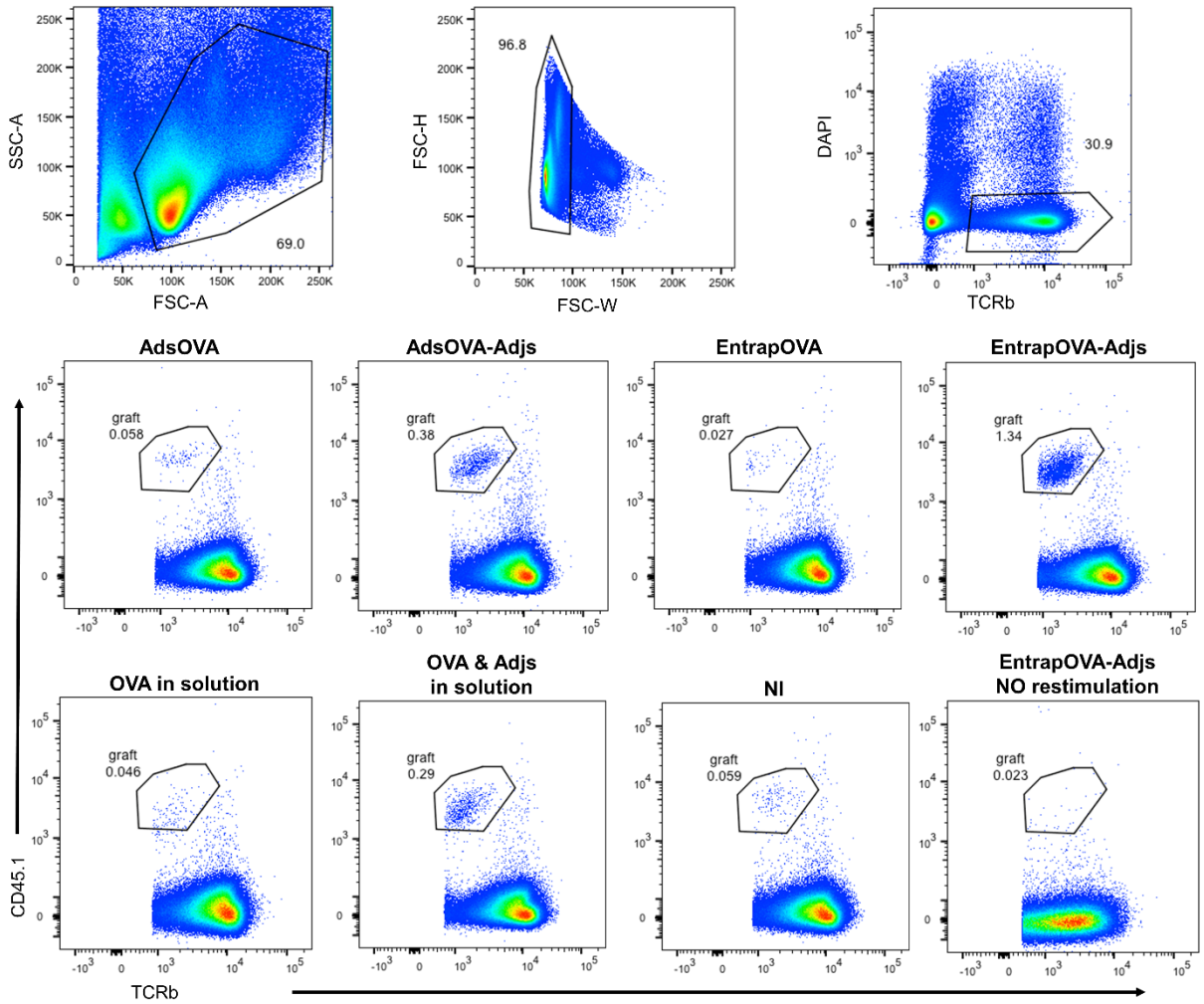

Figure S4: (A) Single-suspension of LN was gated for DAPI$^-$, TCRβ$^+$, CD45.1$^+$, and CD8α$^+$. (B) Representative FACS plots 8 weeks p.i. after the immunization. Protein and adjuvant in the uniformed delivery system drives

development of memory CTL. Data shown are representative of at least three independent experiments with 2-3 mice per group.

Gating strategy of T cell infiltration in the tumor microenvironment:

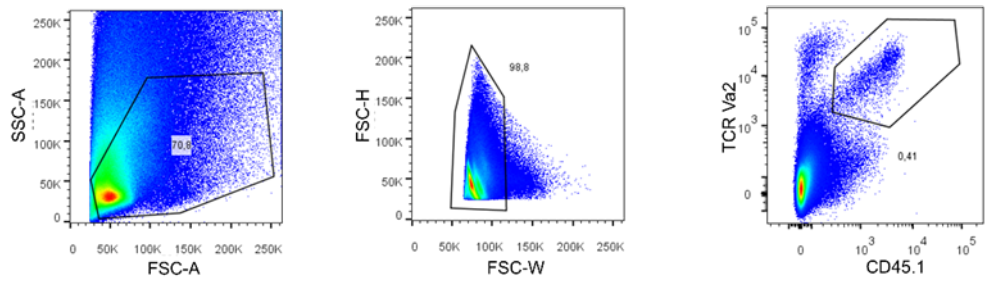

Figure S5: Extracellular staining of tumors infiltrated lymphocytes (TIL). This is a representative gating strategy for the analyzed tumor cell suspensions from two independent experiments, n = 6-8 animals/group.

Gating strategy of CD8α T cells for CD107a and expression of PD-1 and CTLA-4:

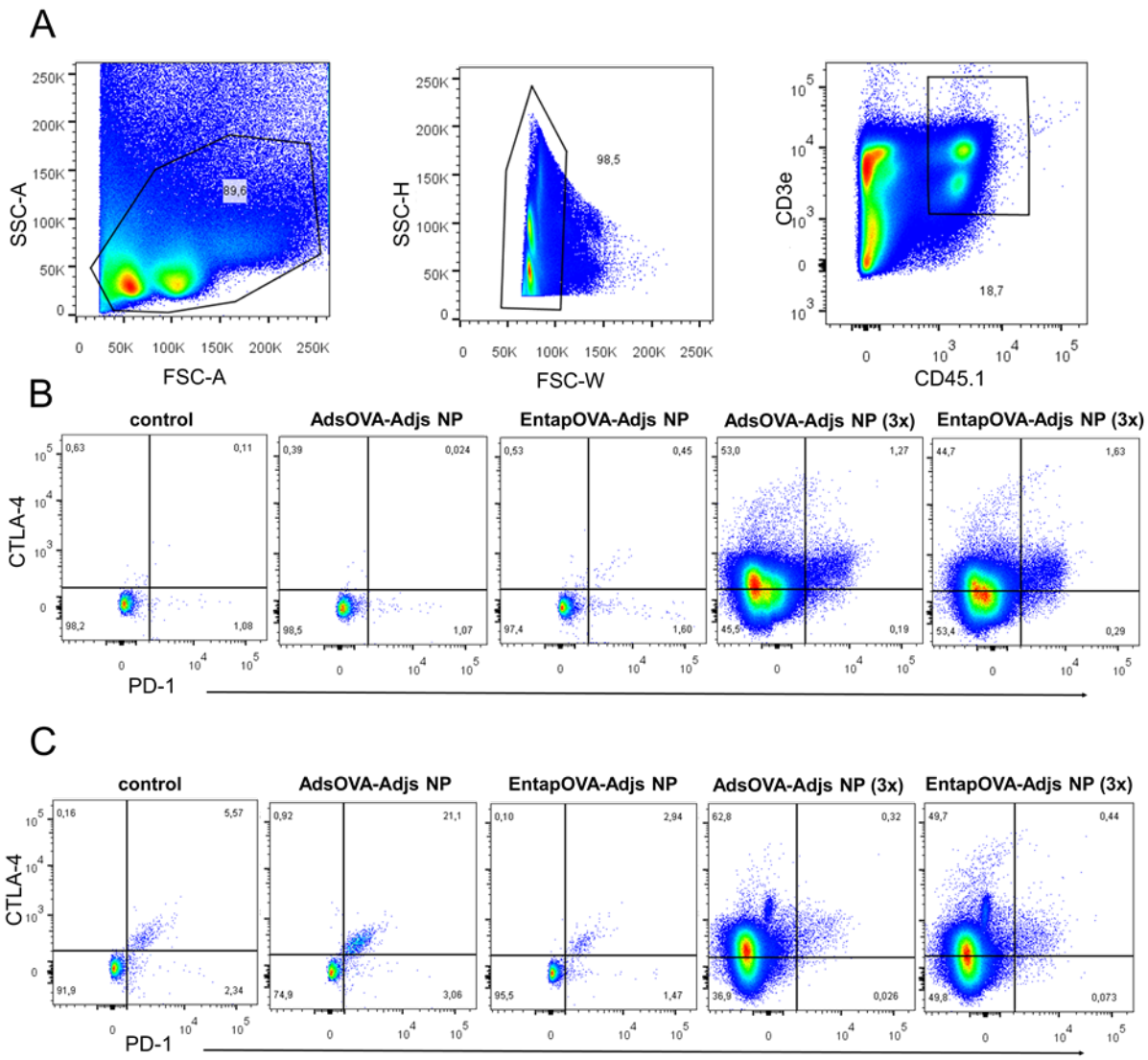

Figure S6: (A) Representative gating strategy for CD45.1, CD3, CD8, PD-1, CTLA-4 and CD107a in spleens

and LN (B & C) Representative flow cytometry plots of PD-1 and/or CTLA-4 upregulation in spleens (B) and LN (C) from the control, AdsOVA-Adjs NP EntrapOVA-Adjs NP, AdsOVA-Ajs NP (3x), and EntrapOVA-Adjs NP (3x) groups in tumor-bearing mice. Representitive FACS plots were chosen from two independent experiments, n = 6-8 animals/group

Gating strategy of cytokine quantification in spleens and tumors of treated mice:

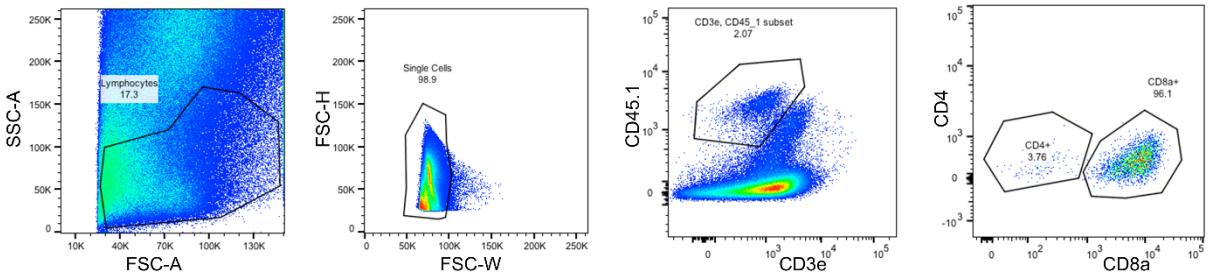

Figure S7: Intracellular staining of tumor and splenic IL-4, TNF-α, IFN-γ producing cells. This is a representative gating strategy for tumor $CD45.1^{+}$, $CD3e^{+}$, $CD8\alpha^{+}$ or $CD4^{+}$ cells from two independent experiments, n = 6-8 animals/group.

Chapter 6

Chapter 6 – General discussion and conclusions

Cancer remains one of the most challenging diseases. Among the treatment modalities, immunotherapy and particularly the cancer vaccines are among the most challenging but promising tools for the successful eradication of malignant cells. Generally, cancer vaccines are envisioned to be administered after the disease detection of thus to treat patients rather than protect individuals from the cancer development [1-3]. These vaccines present multiple theoretical advantages over other conventional therapies like low toxicity, high specificity, and prolonged anti-tumor effect associated to the effective induction of an immunologic memory. The successful use of cancer vaccines allows one to target TAA expressed by tumor cells to induce a specific and long-lasting anti-tumor immune response that would specifically target and destroy malignant cells [4, 5]. TAA may be tumor restricted or widely expressed; mutated, overexpressed or aberrantly expressed; and may be derived from proteins usually expressed on cell surface, secreted or exclusively present at intracellular level. Antigens are chosen based on their ability to induce robust anti-tumor immune responses, including cellular ($CD4^+$ and $CD8^+$ T cell) and humoral (B cell) responses. The antigens should be immunogenic in a broad range of Human Leukocyte Antigen (HLA) types and effector responses should be followed by long-lasting memory responses, while causing minimum or no side effects in normal tissues [6-8]. The recent developments in tumor immunology have stemmed from the identification of TAA overexpressed in these malignant cells, as well as the deeper understanding of the interplay between the immune system and cancer cells.

Effective immune responses result from a complex interplay between the innate (antigen-nonspecific) and the adaptive (antigen-specific) immune cell compartments. DC are the most potent APC and have, owing to this property, an important role in translating innate into adaptive immunity. Given their capacity to capture and process internalized antigens, DC efficiently prime naïve T cells against foreign antigens and polarize them towards distinct effector fates [8-10]. Moreover, antigen engulfment and the mode of DC activation are pivotal steps for clinically relevant responses which are dominated by cytotoxic $CD8^+$ T cells, or $CD4^+$ T cells with helper activity, and determines tolerance/immunity balance [2, 6, 11]. Thus, vaccination protocols that target DC are promising strategies for the initiation and enhancement of immune responses for cancer treatment.

The use of nanotechnology in cancer immunotherapy gives many advantages over the delivery of the immunotherapeutic agents in solution. Therefore, nanoparticulate delivery

systems have been widely explored as promising platforms for cancer vaccination. Major advantages of the NP are a large surface area to volume ratio, with well-defined physicochemical properties, improved antigen stability, immunogenicity, bioavailability and efficacy, and possibility for control release and targeted delivery. In addition to their tunable sub-cellular size, these nanoparticulate systems are able to improve antigen stability of different types of molecules, including drugs, polypeptides, proteins and oligonucleotides [10,12-14] and, thus increase their loading capacity. The major advantage of the NP vaccines is the recognized versatility of formulation procedures and raw materials, leading to carriers with physicochemical properties best suited to the *in vivo* effective targeting of different immune cells within TME [6, 15]. Therefore, these NP are potential systems to amplify the immune activation and augment the efficacy of anti-tumor therapies [3]. The success of the nanoparticulate vaccines as a cancer immunotherapeutic strategy strongly depends on the composition, size, geometry, hydrophobicity and surface properties of the system [16].

An ideal nanoparticulate cancer vaccine designed for the systemic delivery of payloads to DC, must comprise three main components: antigen, adjuvant, and a delivery system. Targeting antigen is defined as a protein, preferentially exclusively expressed on tumor cells, against which adaptive immune responses will be induced. An adjuvant acts as a "danger" signal stimulating the innate immune system. On the other hand, a delivery system is a vehicle with a well-established and defined physicochemical properties that enhances the delivery of single or multiple vaccine antigens and/or adjuvants to DC, and ensures optimal presentation in a targeted and prolonged manner [17, 18]. Moreover, a cancer vaccine has to be easy to manufacture and effective in all vaccinated population [4, 19].

The main goal of the research work presented in this thesis was the rational development of different nanoparticulate platforms with the ability to deliver TAA and immunoadjuvant molecules to DC as potential toold for anti-cancer treatment. Designing safe and efficacious NP vaccines requires a thorough understanding of the physical and chemical features of the carrier and their interaction with the biological systems. The unique properties of NP potentiate their interaction and uptake efficiency by APC that elicits T cell immunity [19, 20]. We aimed to develop a highly stable and reproducible colloidal suspension of NP smaller than 200 nm with narrow size distribution, PDI below 0.2 and ζ potential close to neutrality, in order to potentiate NP-APC interaction.

Extensive research, including the development and optimization of experimental protocols were carried out towards the development of a novel nanoparticulate vaccine. CS was a promising material to be included into the NP formulation due to its positive charge,

which was expected to increase NP LC through the electrostatic interactions established between cationic amines and negatively charged antigens dispersed in the IP. This was of particular importance when entrapping MHC I and MHC II peptides. However, the high viscosity of this polysaccharide constituted a challenge for the development of a stable NP formulation. Therefore, in Chapters 2 and 3 various combinations of surfactant at different percentages were explored to produce a highly stable and reproducible colloid system. Sodium-cholate, an anionic emulsifier could not stabilize the double emulsion w/o/w, leading to the flocculation of this emulsion prior to NP sedimentation. On the other side, PF127 possess good amphiphilic properties and lead to stable formulations when used as a stabilizer of both internal and external phases. Nevertheless, NP size was outside the specifications previously defined for the optimal NP-induced immune modulatory effect. PF127 has a complex branched triblock structure. The optimal NP were produced using PVA as an emulsifier of the internal aqueous phase (IP). However, the concentration of PVA solution had to be optimized in order to a reproducible NP formulation procedure, while leading to optimized physicochemical parameters, namely size, PDI, ζ potential with high yield. The NP that best fitted the previously established specifications for these targeted nanoparticulate vaccine were developed using 10% (w/v) PVA solution at IP, and PVA or PF127 in the external phase.

Particularly interesting was to investigate how different methods of antigen association to the developed particulate carriers could affect the antigen uptake by APC and modulate the overall antigen-specific immune responses. As described in Chapter 4, four highly reproducible and homogeneous nanoplatforms have been developed, two of those presented the antigen adsorbed onto NP surface (AdsPROTEIN NP), while the other two had the antigen entrapped ((EntrapPROTEIN NP) within NP matrix NP. All NP were based on the hydrophobic aliphatic polyester PLGA that forms a matrix of a nanoparticulate vehicle and allows the incorporation of chitosan (CS), antigens (LALBA; a breast cancer antigen) and adjuvants. CpG ODN stimulates TLR9 and was entrapped into the core of the polymeric matrix of NP. Two different stabilizers (PVA or PF127,) of the external aqueous phase were tested, to ensure NP best physical and chemical characteristics, including size, surface charge and antigen association. PEG polymer was used for the formulation of EntrapOVA NP in contrast to AdsOVA NP to improve the stability of the emulsion, thus leading to NP with similar size distribution, polarity of ζ potential and hydrophobicity, despite the method used for the association of the antigen. The similarity between the physical and chemical properties of both types of NP was particularly important in order to allow the rational characterization

of the effect of the method of antigen delivery on the overall efficacy of the developed cancer vaccine. If the nanoparticulate systems presented distinct properties, than the eventual different activity on immune cells could not be clearly associated to the adsorbed or entrapped antigen. An extensive characterization of the experimental parameters, such as nature of protein association (adsorbed vs. entrapped), polymers and surfactant concentrations were investigated for their effect on particle size, polydispersity index, ζ potential, EE, LC, protein integrity, percentage of surfactant residual amount, and formulation stability. These study allowed the identification of the best formulations to attain the previously described NP specification for the optimal modulation of immune cells owards the destruction of cancer cells.

Spherical NP with an average size between 170-180 nm were produced in a reproducible way and were highly stable over a period of 3 moths in suspension. Antigen-loading efficiency of developed nanovaccines was similar despite the entrapment or adsorption of the antigens, which was ideal for further evaluation of the immune response. Moreover, the protein integrity, investigated by SDS-PAGE, indicated that protein molecular weight was not affected by NP formulation process. However, a western-blot could have been performed in order to assess the maintenance of the antigen activity after the formulation procedure. Even though, having in consideration the data reported for *in vitro* and *in vivo* studies, it is now possible to state that the different antigens associated to the developed NP maintained their activity after the formulation. The *in vitro* studies on BMDC provided a better understanding on the importance of the chemical composition of the developed NP on their interaction with APC. This research data definitely evidenced the potential of the optimal nanoparticulate vaccine for targeting and modulating DC, prompted the evaluation of the efficacy of the two best formulation candidates as a potential cancer immunotherapeutic approaches at preclinical settings.

Chapter 5 describes the development of the best two PVA formulations (AdsOVA NP and EntrapOVA NP) that drove the most efficient upregulation and activation of DC *in vitro* (chapter 4). Developed NP presented an average mean diameter close to 190 nm, with a uniformed size distribution, ζ potential close to neutrality and high loading efficiency. Both AdsOVA NP and EntrapOVA NP were investigated *in vivo*, with or without adjuvants. Next to the CpG ODN, the lipophilic adjuvant MPLA (TLR4 agonist), was introduced into the NP scaffold. Herein, several factors that could affect the performance of the vaccine and could potentially have an impact on the anti-tumor immune response were addressed, such as (i) the advantage of using a carrier for vaccine delivery; (ii) the impact of antigen delivery by

different means on the systemic internalization by APC, principally DC; (iii) the influence of the simultaneous delivery of antigens with co-stimulatory TLR ligands; (iv) the ability of the delivery system to allow the antigen active cross-presentation, thus promoting the active generation of CTL; (v) the impact of the antigen and adjuvant co-delivery on long-lasting memory; (vi) the impact of single vs. three-dose immunization schedule in a tumor-bearing mice; and (vii) the effect of antigen-associated particulate vaccines on the cytokine production and TIL trafficking into the tumors of B16.MO5 challenged mice.

APC, particularly classical DC, presented a good internalization profile for both classes of NP (AdsOVA NP and EntrapOVA NP), despite the difference in the initial antigen exposure to APC, thus anticipating similarity in the overall triggered immune response. However, this hypothesis was not confirmed as AdsOVA NP were extensively engulf by pDC, while EntrapOVA NP escaped this rapid peripheral internalization by pDC, most probably due to the presence of PEG at EntrapOVA NP and its "stealth" effect that protects NP from premature capture [60, 61 in EVA1]. The further identification of DC-mediated antigen-specific T cell cytotoxicity was accomplished through the *in vivo* kinetic evaluation of the levels of the activation molecules CD25, CD69, and CD44. These studies indicated that the DC-T cell interactome at the LN is already activated 16 h p.i.. Moreover, EntrapOVA NP were more efficient in the upregulation of CD44 activation marker on $CD8^+$ T cells, suggesting the induction of a stronger antigen-specific immune response towards an effective memory immunity. EntrapOVA NP without adjuvants were not efficient in inducing long-lasting memory. However, the inclusion of adjuvants in EntrapOVA-Ajds NP lead to the expansion of a long-lasting memory, which was superior to that obtained in all of the remaining treated animals.

Prior to the tumor challenge, nanovaccines were tested for their ability to drive cross-presentation and cross-priming. During the short-time experiment (7 day), all NP were able to induce the effective activation and priming of antigen-specific cytotoxic $CD8^+$ T (CTL) cells that will thus recognize and kill targeted cells.

Anti-tumor therapeutic efficacy of developed nanovaccines (AdsOVA-Adjs NP and EntrapOVA-Adjs NP) co-delivering OVA antigen and adjuvants (CpG and MPLA) has been tested on OVA transfected melanoma B16.MO5 bearing C57BL/6 mice. Mice immunized with three-dose schedule for EntrapOVA-Adjs NP presented the slowest tumor growth, with the highest amount of TIL in the tumors, suggesting a good prognosis for vaccine outcome. However, the secretion of cytokines was lower in animals treated with the three doses of the

vaccine, when compared with those quantified in animals immunized with the single dose of EntrapOVA-Adjs NP.

Taken together, our studies highlight the importance of the composition and related physicochemical properties of nanoparticulate vaccines for their cellular uptake by APC, and overall nature of induced immune response. Developed NP possess the desirable physicochemical properties, with good LC and colloidal stability in biological media. All antigen-associated NP promptly induced the efficient DC activation and maturation. However, animals immunized with EntrapOVA NP and EntrapOVA-Adjs NP presented higher $CD8^+$ OT-I cell proliferation and activation through the antigen-specific immune response. These are pivotal steps in the immunology that leads to a complete and effective immune response. In addition, the immune response induced by the delivery of both OVA and Adjs by these optimal PLGA carriers was able to decrease tumor growth and therefore additional studies can clarify their ability to improve animal survival. One can expect this overall output, having in consideration the evidenced ability of the developed nanovaccine to induce a long-lasting memory immune response.

Therefore, the developed nanovaccine definitely has a promising potential for therapeutic cancer vaccines.

Massive data have been released from clinicals trials focused on the evaluation of the effect of the combination of different cancer treatment modalities of cancer treatments in the reduction of tumor growth, overall side effect and prolonged disease-free survival. Therefore, having in consideration the promising effect of the developed nanovaccine in the modulation of immune cells both at under steady-state and cancer disease, future studies should assess the overall therapeutic effect of its combination with the currently most promising alternative cancer treatment options, such as the administration of immune check points. Of particular interest would be the assessment of their ability to reduce the dose of the administered antibodies and thus decrease the reported developed resistance or severe side-effects.

Chapter 7

Chapter 7 – Future perspectives

Improved understanding on the role of the immune system in controlling tumor growth and recent developments in the field of nanoparticulate cancer vaccines have triggered scientific community attention towards a novel anti-tumor immunotherapeutic approach.

However, it is clear that preclinical tumor model systems are poorly predictive for clinical trials. This is not only due to the highly tumor heterogeneity, but also considerable differences between the rapidly growing transplantable tumors in murine models compare to usually slow-growing clinical disease [1]. Thus, a great demand for novel preclinical models for better prediction and detailed characterization of tumor treatments are needed.

The work described in this doctoral thesis highlights and characterizes the potential of nanoparticles (NP) as cancer vaccines to target tumor antigens and adjuvants to DC for priming antigen-specific cytotoxic T lymphocytes (CTL). Despite the potential recognized for these particulate vaccines, there is still limited knowledge underlying their biological effect on immune cells, and on cancer-immune cell interactions within tumor microenvironment. Deeper understanding on the impact of NP properties on those signaling mechanisms can rationally guide the selection of treatment schedules, as well as, the best combination approaches to achieve a long period of disease-free survival.

Due to tumors' heterogeneity and phenotypic diversity, targeting of a single antigen may not be sufficient for the induction of an immune response capable of destroying cancer cells. As a result, it is anticipated that effective cytotoxic immune responses may be obtained with multivalent cancer vaccines rather than monovalent. The immune system will be able to generate strong and long-lasting anti-tumor responses against each antigen. Therefore, this type of vaccine is expected to target a higher number of cancer cells in comparison with single-antigen containing vaccine. However, a potential problem that may arise from the use of a multivalent vaccine may be the stimulation of a dominant response against one particular antigen, due to steric hindrance [2, 3].

In addition, it must be kept in mind that tumor vaccines capacity to combat an already established malignant disease, will correlate with the stage of the disease. Ideally, cancer vaccine would be the first choice of treatment, when the tumor is in stage I/II, inducing an immune response that would have a fair chance to prevent tumor relapse. Moreover, evaluation of individual host immunity should be considered in the selection of the most appropriate treatment protocols. Even though, the use of cancer vaccines at clinical settings

has been mainly restricted to advanced stages of the disease, due to the limited therapeutic options still available for those patients.

However, the strategy to use two immunotherapeutic approaches to achieve immune-mediated tumor cell killing, looks promising, to shift favorably the balance between anti-cancer effector cells and tumor-induced immune suppression. We observed that the three-dose schedule treatment using the antigen-entrapped NP induced the overexpression of Cytotoxic T-Lymphocyte Associated Protein 4) CTLA4 and programmed cell death 1 (PD-1) immune checkpoints at tumor infiltrated T lymphocytes. Therefore, the combination of the cancer vaccine and monoclonal antibodies blocking the CTLA-4 and PD-1 may function synergistically and thus induce more effective anti-tumor immune responses, leading to promising clinical outcomes.

References

Chapter 1

[1] Marusyk A, Polyak K. Tumor heterogeneity: causes and consequences. Biochim Biophys Acta. 2010;1805(1):105-117.

[2] Fernald K, Kurokawa M. Evading apoptosis in cancer. Trends Cell Biol. 2013;23(12):620-633.

[3] Aly HA. Cancer therapy and vaccination. J Immunol Methods. 2012;382(1-2):1-23.

[4] Wu D, Gao Y, Qi Y et al. Peptide-based cancer therapy: Opportunity and challenge. Cancer Lett. 2014;351:13-22.

[5] Jemal A, Bray F, Center MM et al. Global cancer statistics. CA - Cancer J Clin. 2013;61:69-90.

[6] Xu Z, Wang Y, Zhang L et al. Nanoparticle-Delivered Transforming Growth Factor-β siRNA Enhances Vaccination against Advanced Melanoma by Modifying Tumor Microenvironment. ACS Nano. 2014;8(4):3636-3645.

[7] Kirkwood JM, Butterfield LH, Tarhini AA et al. Immunotherapy of cancer in 2012. CA - Cancer J Clin. 2012;62(5):309-335.

[8] Klebanoff C, Acquavella N, Yu Z et al. Therapeutic cancer vaccines: are we there yet? Immunol Rev. 2011;239(1):27-44.

[9] Rosenberg SA. Progress in human tumour immunology and immunotherapy. Nature. 2001;411:380-384.

[10] Palucka K, Banchereau J. Cancer immunotherapy via dendritic cells. Nat Rev Cancer. 2012;12(4):265-277.

[11] Henderson RA, Mossman S, Nairn N et al. Cancer vaccines and immunotherapies: emerging perspectives. Vaccine. 2005;23(17):2359-2362.

[12] Bringmann A, Held SA, Heine A et al. RNA vaccines in cancer treatment. J Biomed Biotechnol. 2010;2010:1-12.

[13] Bolhassani A, Safaiyan S, Rafati S. Improvement of different vaccine delivery systems for cancer therapy. Mol Cancer. 2011;10:1-3.

[14] Slingluff CL, Jr. The present and future of peptide vaccines for cancer: single or multiple, long or short, alone or in combination? Cancer J. 2011;17(5):343-350.

[15] Krishnamachari Y, Salem AK. Innovative strategies for co-delivering antigens and CpG oligonucleotides. Adv Drug Deliv Rev. 2009;61(3):205-217.

[16] Rosenberg SA, Yang, JC, Restifo NP. Cancer immunotherapy: moving beyond current vaccines. Nat Med. 2004;10:909-915.

[17] Silva JM, Videira M, Gaspar R et al. Immune system targeting by biodegradable nanoparticles for cancer vaccines. J Control Release. 2013;168(2):179-199.

[18] Nagata Y, Ono S, Matsuo M et al. Differential presentation of a soluble exogenous tumor antigen, NY-ESO-1, by distinct human dendritic cell populations. Proc Natl Acad Sci USA. 2002;99:10629-10634.

[19] Baumgartner CK, Malherbe LP. Regulation of CD4 T-cell receptor diversity by vaccine adjuvants. Immunology. 2010;130:16-22.

[20] Conti L, Ruiu R, Barutello G et al. Microenvironment, Oncoantigens, and Antitumor Vaccination: Lessons Learned from BALB-neuT Mice. BioMed Res Int. 2014;2014: 1-16.

[21] Mamo T, Moseman EA, Kolishetti N et al. Emerging nanotechnology approaches for HIV/AIDS treatment and prevention. Nanomedicine. 2010;5(2):269-285.

[22] Xu CF, Wang J. Delivery systems for siRNA drug development in cancer therapy. Asian J Pharm Sci. 2014;10:1-12.

23] Rosenberg SA, Yang JC, Sherry RM et al. Durable complete responses in heavily pretreated patients with metastatic melanoma using T-cell transfer immunotherapy. Clin Cancer Res. 2011;17:4550-4557.

[24] Yu MK, Park J, Jon S. Targeting strategies for multifunctional nanoparticles in cancer imaging and therapy. Theranostics. 2012;2:3-44.

[25] Desgrosellier JS, Cheresh DA. Integrins in cancer: biological implications and therapeutic opportunities. Nat Rev Cancer. 2010;10(1):9-22.

[26] Kumar H, Kawai T, Akira S. Pathogen recognition in the innate immune response. Biochem J. 2009;420(1): 1-16.

[27] Ito T, Connett JM, Kunkel SL et al. The linkage of innate and adaptive immune response during granulomatous development. Front Immunol, 2013;4:1-10.

[28] Kadowaki N. Dendritic cells: a conductor of T cell differentiation. Allergol Int. 2007;56:193-199.

[29] Awada A, Bozovic-Spasojevic I, Chow, L. New therapies in HER2-positive breast cancer: a major step towards a cure of the disease? Cancer Treat Rev. 2012;38(5):494-504.

[30] Harding CV, Canaday D, Ramachandra L. Choosing and preparing antigen□presenting cells. Curr Protoc Immunol. 2010;16(1):1-16.

[31] Lin KW, Jacek T, Jacek R. Dendritic cells heterogeneity and its role in cancer immunity. J Cancer Res Ther. 2006;2(2):35-40.

[32] Fajardo-Moser M, Berzel S, Moll H. Mechanisms of dendritic cell-based vaccination against infection. Int J Med Microbiol. 2008;298(1-2):11-20.

[33] Faith A, Hawrylowicz CM. Targeting the dendritic cell: the key to immunotherapy in cancer? Clin Exp Immunol. 2005;139(3):395-397.

[34] O'Neill DW, Adams S, Bhardwaj N. Manipulating dendritic cell biology for the active immunotherapy of cancer. Blood. 2004;104(8):2235-2246.

[35] Bachmann MF, Jennings GT. Vaccine delivery: a matter of size, geometry, kinetics and molecular patterns. Nat Rev Immunol. 2010;10(11):787-796.

[36] Garg NK, Dwivedi P, Prabha P et al. RNA pulsed dendritic cells: an approach for cancer immunotherapy. Vaccine. 2013;31(8):1141-1156.

[37] Schnorrer P, Behrens GM, Wilson NS et al. The dominant role of CD8+ dendritic cells in cross-presentation is not dictated by antigen capture. Proc Natl Acad Sci USA. 2006;103(28):10729-10734.

[38] Skokos D, Nussenzweig MC. CD8− DCs induce IL-12–independent Th1 differentiation through Delta 4 Notch-like ligand in response to bacterial LPS. J Exp Med. 2007;204(7):1525-1531.

[39] Schettini J, Mukherjee P. Physiological role of plasmacytoid dendritic cells and their potential use in cancer immunity. Clin Dev Immunol. 2008;2008:1-10.

[40] Liu YJ. IPC: professional type 1 interferon-producing cells and plasmacytoid dendritic cell precursors. Annu Rev Immunol. 2005;23:275-306.

[41] McKenna K, Beignon AS, Bhardwaj N. Plasmacytoid dendritic cells: linking innate and adaptive immunity. J Virol. 2005;79(1):17-27.

[42] Morva A, Lemoine S, Achour A et al. Maturation and function of human dendritic cells are regulated by B lymphocytes. Blood. 2012;119(1):106-114.

[43] Kumar H, Kawai T, Akira S. Pathogen recognition by the innate immune system. Int Rev Immunol. 2011;30(1):16-34.

[44] Adams S, O'Neill DW, Bhardwaj N. Recent advances in dendritic cell biology. J Clin Immunol. 2005;25(2):87-98.

[45] Gajewski TF, Schreiber H, Fu YX. Innate and adaptive immune cells in the tumor microenvironment. Nat Immunol. 2013;14(10):1014-1022.

[46] Rabinovich GA, Gabrilovich D, Sotomayor EM. Immunosuppressive strategies that are mediated by tumor cells. Ann Rev Immunol. 2007;25:255-267.

[47] Ali OA, Verbeke C, Johnson C et al. Identification of immune factors regulating antitumor immunity using polymeric vaccines with multiple adjuvants. Cancer Res. 2014;74(6):1670-1681.

[48] Riboldi E, Musso T, Moroni E et al. Cutting edge: proangiogenic properties of alternatively activated dendritic cells. J Immunol. 2005;175(5):2788-92.

[49] Benencia F, Sprague L, McGinty J et al. Dendritic cells the tumor microenvironment and the challenges for an effective antitumor vaccination. J Biomed Biotechnol. 2012;2012:1-15.

[50] Blum JS, Wearsch PA, Cresswell P. Pathways of antigen processing. Ann Rev Immunol. 2013;31:443-73.

[51] Buckwalter MR, Albert ML. Orchestration of the immune response by dendritic cells. Curr Biol. 2009;19(9):R355-R361.

[52] Amigorena S, Savina A. Intracellular mechanisms of antigen cross presentation in dendritic cells. Curr Opin Immunol. 2010;22(1):109-117.

[53] Ackerman AL, Cresswell P. Cellular mechanisms governing cross-presentation of exogenous antigens. Nat Immunol. 2004;5(7):678-684.

[54] Vyas JM, Van der Veen AG, Ploegh HL. The known unknowns of antigen processing and presentation. Nat Rev Immunol. 2008;8(8):607-618.

[55] Hubbell JA, Thomas SN, Swartz MA. Materials engineering for immunomodulation. Nature. 2009; 462(7272): 449-460.

[56] Kim J, Mooney DJ. In Vivo Modulation of Dendritic Cells by Engineered Materials: Towards New Cancer Vaccines. Nano Today. 2011;6(5):466-477.

[57] Markovic SN, Erickson LA, Rao RD et al. Malignant Melanoma in the 21st Century, Part 2: Staging, Prognosis, and Treatment. Mayo Clin. Proc. 2007;82:490-513.

[58] Bode U, Lörchner M, Ahrendt M et al. Dendritic cell subsets in lymph nodes are characterized by the specific draining area and influence the phenotype and fate of primed T cells. Immunology. 2008;123(4):480-490.

[59] Kalinski P. Dendritic cells in immunotherapy of established cancer: Roles of signals 1, 2, 3 and 4. Curr Opin Investig Drugs. 2009;10(6):526.

[60] Hwang I, Ki D. Receptor-mediated T cell absorption of antigen presenting cell-derived molecules. Front Biosci. 2011;16:411-21.

[61] Arens R, Schoenberger SP. Plasticity in programming of effector and memory CD8+ T□cell formation. Immunol Rev. 2010;235(1):190-205.

[62] Klebanoff CA, Gattinoni L, Restifo NP. CD8+ T□cell memory in tumor immunology and immunotherapy. Immunol Rev. 2006;211(1):214-224.

[63] Jaini R, Kesaraju P, Johnson JM et al. An autoimmune-mediated strategy for prophylactic breast cancer vaccination. Nat Med. 2010;16(7):799-803.

[64] Toubi E, Shoenfeld Y. Protective autoimmunity in cancer. Oncol Rep. 2007;17(1):245-251.

[65] Shedlock DJ, Shen H. Requirement for CD4 T cell help in generating functional CD8 T cell memory. Science. 2003;300(5617):337-339.

[66] Bourgeois C, Veiga□Fernandes H et al. CD8 lethargy in the absence of CD4 help. Eur J Immunol. 2002;32(8): 2199-2207.

[67] Luckheeram RV, Zhou R, Verma AD et al. CD4+T Cells: Differentiation and Functions. Clin Dev Immunol. 2012;2012:1-12.

[68] Takeuchi S, Furue M. Dendritic Cells-Ontogeny. Allergol Int. 2007;56(3):215-223.

[69] MacLeod MK, Kappler JW, Marrack P. Memory CD4 T cells: generation, reactivation and re□assignment. Immunology. 2010;130(1):10-15.

[70] Ma B, Roden R, Wu T. Current status of HPV vaccines. J Formos Med Assoc. 2010;109(7):481-483.

[71] Kirby T. FDA approves new upgraded Gardasil 9. Lancet Oncol. 2014;16(2):e56.

[72] Chen X. Molecular Imaging Probes for Cancer Research, 1st ed.; World Scientific, 2012.

[73] Cheever MA, Higano CS. PROVENGE (Sipuleucel-T) in prostate cancer: the first FDA-approved therapeutic cancer vaccine. Clin Cancer Res. 2011;17(11):3520-3526.

[74] Snook AE, Waldman SA. Advances in cancer immunotherapy. Discov Med. 2013;15(81):120-5.

[75] Sims RB. Development of sipuleucel-T: autologous cellular immunotherapy for the treatment of metastatic castrate resistant prostate cancer. Vaccine. 2012;30(29):4394-4397.

[76] Ahmad M, Rees RC, Ali SA. Escape from immunotherapy: possible mechanisms that influence tumor regression/progression. Cancer Immunol Immunother. 2004;53(10):844-854.

[77] Hamdy S, Haddadi A, Hung RW et al. Targeting dendritic cells with nano-particulate PLGA cancer vaccine formulations. Adv Drug Deliv Rev. 2011;63(10-11):943-955.

[78] Bodles-Brakhop AM, Draghia-Akli R. DNA vaccination and gene therapy: optimization and delivery for cancer therapy. Vaccines. 2008;7:1085-1101.

[79] Palena C, Abrams SI, Schlom J et al. Cancer vaccines: preclinical studies and novel strategies. Adv Cancer Res. 2006;95:115-145.

[80] Fioretti D, Iurescia S, Fazio VM et al. DNA vaccines: developing new strategies against cancer. J Biomed Biotechnol. 2010;2010:1-17.

[81] Tabi Z, Man S. Challenges for cancer vaccine development. Adv Drug Deliv Rev. 2006;58(8):902-915.

[82] Escors D. Tumour immunogenicity, antigen presentation, and immunological barriers in cancer immunotherapy. New J Sci. 2014;2014:1-26.

[83] Davis ID, Jefford M, Parente P et al. Rational approaches to human cancer immunotherapy. J Leukoc Biol. 2003;73(1):3-29.

[84] Buonaguro L, Petrizzo A, Tornesello ML et al. Translating tumor antigens into cancer vaccines. Clin Vaccine Immunol. 2011;18(1):23-34.

[85] Novellino L, Castelli C, Parmiani G. A listing of human tumor antigens recognized by T cells. Cancer Immunol Immunother. 2005;54(3):187-207.

[86] Slansky JE, Rattis FM, Boyd LF et al. Enhanced antigen-specific antitumor immunity with altered peptide ligands that stabilize the MHC-peptide-TCR complex. Immunity. 2000;13(4):529-538.

[87] Wang AZ, Gu F, Zhang L et al. Biofunctionalized targeted nanoparticles for therapeutic applications. Biol Ther. 2008;8(8):1063-70.

[88] Bhutia SK, Maiti TK. Targeting tumors with peptides from natural sources. Trends Biotechnol. 2008;26(4):210-217.

[89] Kummar S, Chen HX, Wright J et al. Utilizing targeted cancer therapeutic agents in combination: novel approaches and urgent requirements. Nat Rev Drug Discov. 2010;9(11):843-856.

[90] Thundimadathil J. Cancer treatment using peptides: current therapies and future prospects. J Amino Acids. 2012;2012:1-13.

[91] Margus H, Padari K, Pooga M. Cell-penetrating peptides as versatile vehicles for oligonucleotide delivery. Mol Ther. 2012:20(3):525-533.

[92] Singh V, Ji Q, Feigenbaum L et al. Melanoma progression despite infiltration by in vivo-primed TRP-2-specific T cells. J Immunother. 2009;32(2):129-39.

[93] Slingluff Jr CL, Petroni GR, Smolkin ME et al. Immunogenicity for CD8+ and CD4+ T cells of two formulations of an incomplete Freund's adjuvant for multipeptide melanoma vaccines. J Immunother. 2010;33(6):630-8.

[94] Curiel TJ, Curiel DT. Tumor immunotherapy: inching toward the finish line. J Clin Invest. 2002;109(3):311-312.

[95] Kanzler H, Barrat FJ, Hessel EM et al. Therapeutic targeting of innate immunity with Toll-like receptor agonists and antagonists. Nat Med. 2007;13(5):552-559.

[96] Dinarvand R, Sepehri N, Manoochehri S et al. Polylactide-co-glycolide nanoparticles for controlled delivery of anticancer agents. Int J Nanomedicine. 2011;6:877-895.

[97] Peer D, Karp JM, Hong S et al. Nanocarriers as an emerging platform for cancer therapy. Nat Nanotechnol. 2007;2(12):751-760.

[98] Davis ME, Chen ZG, Shin DM. Nanoparticle therapeutics: an emerging treatment modality for cancer. Nat Rev Drug Discov. 2008;7(9):771-782.

[99] Markman JL, Rekechenetskiy A, Holler E et al. Nanomedicine therapeutic approaches to overcome cancer drug resistance. Adv Drug Deliv Rev. 2013;65(13-14):1866-1879.

[100] Milani A, Sangiolo D, Montemurro F et al. Active immunotherapy in HER2 overexpressing breast cancer: current status and future perspectives. Ann Oncol. 2013;24(7):1740-1748.

[101] Kim MG, Park JY, Shon Y et al. Nanotechnology and vaccine development. Asian J Pharm Sci. 2014;9(5):227-235.

[102] Conniot J, Silva JM, Fernandes JG et al. Cancer immunotherapy: nanodelivery approaches for immune cell targeting and tracking. Front Chem. 2014;2:105-32.

[103] Mahapatro A, Singh DK. Biodegradable nanoparticles are excellent vehicle for site directed in-vivo delivery of drugs and vaccines. J Nanobiotechnology. 2011; 9:55-66.

[104] Shiao SL, Ganesan AP, Rugo HS et al. Immune microenvironments in solid tumors: new targets for therapy. Genes Dev. 2011;25(24):2559-2572.

[105] Heit A, Schmitz F, Haas T et al. Antigen co-encapsulated with adjuvants efficiently drive protective T cell immunity. Eur J Immunol. 2007;37(8):2063-2074.

[106] Schlosser E, Mueller M, Fischer S et al. TLR ligands and antigen need to be coencapsulated into the same biodegradable microsphere for the generation of potent cytotoxic T lymphocyte responses. Vaccine. 2008;26(13):1626-1637.

[107] Alexandrakis G, Brown EB, Tong RT et al. Two-photon fluorescence correlation microscopy reveals the two-phase nature of transport in tumors. Nat Med. 2004;10(2):203-207.

[108] Geng Y, Dalhaimer P, Cai S et al. Shape effects of filaments versus spherical particles in flow and drug delivery. Nat Nanotechnol. 2007;2(4):249-255.

[109] Oliveira MF, Guimaraes PP, Gomes AD et al. Strategies to target tumors using nanodelivery systems based on biodegradable polymers, aspects of intellectual property, and market. J Chem Biol. 2012;6(1):7-23.

[110] Garg A, Visht S, Sharma PK et al. Formulation, Characterization and Application on Nanoparticle. Pelagia Res Libr Der Pharmacia Sinica. 2011;2(2):17-26.

[111] Na JH, Lee SY, Lee S et al. Effect of the stability and deformability of self-assembled glycol chitosan nanoparticles on tumor-targeting efficiency. J Control Release. 2012;163(1):2-9.

[112] Petros RA, DeSimone JM. Strategies in the design of nanoparticles for therapeutic applications. Nat Rev Drug Discov. 2010;9(8):615-627.

[113] Akagi T, Baba M, Akashi M. Polymers in Nanomedicine. Kunugi, S.; Yamaoka, T., Eds.; Springer Berlin Heidelberg, 2012; Vol. 247, pp 31-64.

[114] Mattheolabakis G, Rigas B, Constantinides PP. Nanodelivery strategies in cancer chemotherapy: biological rationale and pharmaceutical perspectives. Nanomedicine. 2012;7(10):1577-1590.

[115] Gong J, Chen M, Zheng Y et al. Polymeric micelles drug delivery system in oncology. J Control Release. 2012;159(3):312-323.

[116] Torchilin VP. Micellar nanocarriers: pharmaceutical perspectives. Pharm Res. 2007;24(1):1-16.

[117] Mansour HM, Sohn M, Al-Ghananeem A et al. Materials for pharmaceutical dosage forms: molecular pharmaceutics and controlled release drug delivery aspects. Int J Mol Sci. 2010;11(9):3298-3322.

[118] Mohamed F, van der Walle CF. Engineering biodegradable polyester particles with specific drug targeting and drug release properties. J Pharm Sci. 2008;97(1):71-87.

[119] Jain RA. The manufacturing techniques of various drug loaded biodegradable poly (lactide-co-glycolide) (PLGA) devices. Biomaterials. 2000;21(23):2475-2490.

[120] van Vlerken LE, Vyas TK, Amiji MM. Poly (ethylene glycol)-modified nanocarriers for tumor-targeted and intracellular delivery. Pharm Res. 2007;24(8):1405-1414.

[121] Hines DJ, Kaplan DL. Poly (lactic-co-glycolic) -acid Controlled-Release Systems: Experimental and Modeling Insights. Crit Rev Ther Drug Carrier Syst. 2013;30(3):257-276.

[122] Makadia HK, Siegel SJ. Poly Lactic-co-Glycolic Acid (PLGA) as Biodegradable Controlled Drug Delivery Carrier. Polymers. 2011;3(3):1377-1397.

[123] Fahmy TM, Samstein RM, Harness CC et al. Surface modification of biodegradable polyesters with fatty acid conjugates for improved drug targeting. Biomaterials. 2005;26(28):5727-5736.

[124] Silva JM, Vandermeulen G, Oliveira VG et al. Development of functionalized nanoparticles for vaccine delivery to dendritic cells: a mechanistic approach. Nanomedicine. 2014;9(17):2639-2656.

[125] Silva JM, Zupancic E, Vandermeulen G et al. In vivo delivery of peptides and Toll-like receptor ligands by mannose-functionalized polymeric nanoparticles induces prophylactic and therapeutic anti-tumor immune responses in a melanoma model. J Control Release. 2015;198:91-103.

[126] Ma W, Chen M, Kaushal S et al. PLGA nanoparticle-mediated delivery of tumor antigenic peptides elicits effective immune responses. Int J Nanomedicine. 2012;7:1475-1487.

[127] Clawson C, Huang CT, Futalan D et al. Delivery of a peptide via poly (d, l-lactic-co-glycolic) acid nanoparticles enhances its dendritic cell–stimulatory capacity. Nanomedicine. 2010;6(5):651-661.

[128] Hamdy S, Molavi O, Ma Z et al. Co-delivery of cancer-associated antigen and Toll-like receptor 4 ligand in PLGA nanoparticles induces potent CD8+ T cell-mediated anti-tumor immunity. Vaccine. 2008;26(39):5046-5057.

[129] Tan S, Sasada T, Bershteyn A et al. Combinational delivery of lipid-enveloped polymeric nanoparticles carrying different peptides for anti-tumor immunotherapy. Nanomedicine. 2014;9(5):635-647.

[130] Wu XL, Kim JH, Koo H et al. Tumor-targeting peptide conjugated pH-responsive micelles as a potential drug carrier for cancer therapy. Bioconjugate Chem. 2010;21(2):208-213.

[131] Gao H, Zhang Q, Yu Z et al. Cell-penetrating peptide-based intelligent liposomal systems for enhanced drug delivery. Curr Pharm Biotechnol. 2014;15(3):210-219.

[132] Fahmy TM, Fong PM, Park J et al. Nanosystems for simultaneous imaging and drug delivery to T cells. AAPS J. 2007;9(2):E171-E180.

[133] Akbarzadeh A, Rezaei-Sadabady R, Davaran S et al. Liposome: classification, preparation, and applications. Nanoscale Res Lett. 2013;8(1):102-11.

[134] Kraft JC, Freeling JP, Wang Z et al. Emerging research and clinical development trends of liposome and lipid nanoparticle drug delivery systems. J Pharm Sci. 2014;103(1):29-52.

[135] Çağdaş M, Sezer AD, Bucak S. Application of Nanotechnology in Drug Delivery; Ali Demir Sezer, Ed.; InTech, 2014; Vol. 1, pp. 1-50.

[136] Laouini A, Jaafar-Maalej C, Limayem-Blouza I et al. Preparation, characterization and applications of liposomes: state of the art. J Colloid Sci Biotechnol. 2012;1(2):147-168.

[137] Periyasamy PC, Leijten JC, Dijkstra PJ et al. Nanomaterials for the local and targeted delivery of osteoarthritis drugs. J Nanomater. 2012;2012:1-13.

[138] Cruz LJ, Rueda F, Cordobilla B et al. Targeting nanosystems to human DCs via Fc receptor as an effective strategy to deliver antigen for immunotherapy. Mol Pharm. 2010;8(1):104-116.

[139] Cruz LJ, Rueda F, Simón L et al. Liposomes containing NY-ESO-1/tetanus toxoid and adjuvant peptides targeted to human dendritic cells via the Fc receptor for cancer vaccines. Nanomedicine. 2014;9(4):435-449.

[140] Sangha R, Butts C. L-BLP25: a peptide vaccine strategy in non small cell lung cancer. Clin Cancer Res. 2007;13:4652-4654.

[141] Sarkar S, Salyer AC, Wall KA et al. Synthesis and immunological evaluation of a MUC1 glycopeptide incorporated into l-rhamnose displaying liposomes. Bioconjugate Chem. 2013;24(3):363-375.

[142] Mansourian M, Badiee A, Jalali SA et al. Effective induction of anti-tumor immunity using p5 HER-2/neu derived peptide encapsulated in fusogenic DOTAP cationic liposomes co-administrated with CpG-ODN. Immunol Lett. 2014;162(1):87-93.

[143] Cheng Y, Zhao L, Li Y et al. Design of biocompatible dendrimers for cancer diagnosis and therapy: current status and future perspectives. Chem Soc Rev. 2011;40(5):2673-2703.

[144] Gillies ER, Frechet JM. Dendrimers and dendritic polymers in drug delivery. Drug Discov Today. 2005;10(1):35-43.

[145] Khandare J, Calderon M, Dagia NM et al. Multifunctional dendritic polymers in nanomedicine: opportunities and challenges. Chem Soc Rev. 2012;41(7):2824-2848.

[146] Martinho N, Florindo H, Silva L et al. Molecular Modeling to Study Dendrimers for Biomedical Applications. Molecules. 2014;19(12):20424-20467.

[147] Liu TY, Hussein WM, Jia Z et al. Self-adjuvanting polymer-peptide conjugates as therapeutic vaccine candidates against cervical cancer. Biomacromolecules. 2013;14(8):2798-2806.

[148] Schuster M, Nechansky A, Kircheis R. Cancer immunotherapy. Biotechnol J. 2006;1(2):138-147.

[149] Danhier F, Feron O, Preat V. To exploit the tumor microenvironment: Passive and active tumor targeting of nanocarriers for anti-cancer drug delivery. J Control Release. 2010;148(2):135-146.

[150] Bertrand N, Wu J, Xu X et al. Cancer nanotechnology: the impact of passive and active targeting in the era of modern cancer biology. Adv Drug Deliv Rev. 2014;66:2-25.

[151] Peer D, Karp JM, Hong S et al. Nanocarriers as an emerging platform for cancer therapy. Nat Nanotechnol. 2007;2(12):751-760.

[152] Wang M, Thanou M. Targeting nanoparticles to cancer. Pharm Res. 2010; 62(2):90-99.

[153] Iyer AK, Khaled G, Fang J et al. Exploiting the enhanced permeability and retention effect for tumor targeting. Drug Discov Today. 2006;11(17-18):812-818.

[154] Schutz CA, Juillerat-Jeanneret L, Mueller H et al. Therapeutic nanoparticles in clinics and under clinical evaluation. Nanomedicine (Lond). 2013;8(3):449-467.

[155] Ehmann F, Sakai-Kato K, Duncan R et al. Next-generation nanomedicines and nanosimilars: EU regulators' initiatives relating to the development and evaluation of nanomedicines. Nanomedicine (Lond). 2013;8(5):849-856.

[156] Black M, Trent A, Tirrell M et al. Advances in the design and delivery of peptide subunit vaccines with a focus on toll-like receptor agonists. Vaccines. 2010;9(2):157-73.

[157] van Broekhoven CL, Parish CR, Demangel C et al. Targeting Dendritic Cells with Antigen-Containing Liposomes A Highly Effective Procedure for Induction of Antitumor Immunity and for Tumor Immunotherapy. Cancer Res. 2004;64(12):4357-4365.

[158] Daftarian PM, Serafini P, Lemmon VP et al. Compositions, kits and methods for in vitro antigen presentation, assessing vaccine efficacy, and assessing immunotoxicity of biologics and drugs. U.S. Patent 2012/0129199, May 24, 2012.

[159] Daftarian PM, Serafini P, Lemmon VP et al. Vaccine compositions and methods of use thereof. U.S. Patent 2012/0093761, April 19, 2012.

[160] Daftarian P, Kaifer AE, Li W et al. Peptide-conjugated PAMAM dendrimer as a universal DNA vaccine platform to target antigen-presenting cells. Cancer Res. 2011;71(24):7452-7462.

[161] Espuelas S, Roth A, Thumann C et al. Effect of synthetic lipopeptides formulated in liposomes on the maturation of human dendritic cells. Mol Immunol. 2005;42(6):721-729.

[162] Zaks K, Jordan M, Guth A et al. Efficient immunization and cross-priming by vaccine adjuvants containing TLR3 or TLR9 agonists complexed to cationic liposomes. J Immunol. 2006;176(12):7335-7345.

[163] Varypataki EM, van der Maaden K, Bouwstra J et al. Cationic liposomes loaded with a synthetic long Peptide and poly(i:C): a defined adjuvanted vaccine for induction of antigen-specific T cell cytotoxicity. AAPS J. 2015;17(1):216-226.

[164] Thomann JS, Heurtault B, Weidner S et al. Antitumor activity of liposomal ErbB2/HER2 epitope peptide-based vaccine constructs incorporating TLR agonists and mannose receptor targeting. Biomaterials. 2011;32(20):4574-4583.

[165] Lakshminarayanan V, Thompson P, Wolfert MA et al. Immune recognition of tumor associated mucin MUC1 is achieved by a fully synthetic aberrantly glycosylated MUC1 tripartite vaccine. Proc Natl Acad Sci USA. 2012;109(1):261-266.

[166] Mizuuchi M, Hirohashi Y, Torigoe T et al. Novel oligomannose liposome-DNA complex DNA vaccination efficiently evokes anti-HPV E6 and E7 CTL responses. Exp Mol Pathol. 2012;92(1):185-190.

[167] Chang JS, Choi MJ, Cheong HS et al. Development of Th1-mediated CD8+ effector T cells by vaccination with epitope peptides encapsulated in pH-sensitive liposomes. Vaccine. 2001;19(27):3608-3614.

[168] Faham A, Altin JG. Ag-bearing liposomes engrafted with peptides that interact with CD11c/CD18 induce potent Ag-specific and antitumor immunity. Int J Cancer. 2011;129(6):1391-1403.

[169] Zhang Z, Tongchusak S, Mizukami Y et al. Induction of anti-tumor cytotoxic T cell responses through PLGA-nanoparticle mediated antigen delivery. Biomaterials. 2011;32(14):3666-3678.

[170] Yamaguchi S, Tatsumi T, Takehara T et al. EphA2-derived peptide vaccine with amphiphilic poly (γ-glutamic acid) nanoparticles elicits an anti-tumor effect against mouse liver tumor. Cancer Immunol Immunother. 2010;59(5):759-767.

[171] Gallois A, Bhardwaj N. Dendritic cell-targeted approaches to modulate immune dysfunction in the tumor microenvironment. Front Immunol. 2013;4:436.

[172] Banchereau J, Briere F, Caux C et al. Immunobiology of dendritic cells. Ann Rev Immunol. 2000;18:767-811.

[173] Steinman RM. Decisions about dendritic cells: past, present, and future. Ann Rev Immunol. 2012;30:1-22.

[174] Chatterjee B, Smed-Sorensen A, Cohn L et al. Internalization and endosomal degradation of receptor-bound antigens regulate the efficiency of cross presentation by human dendritic cells. Blood. 2012;120(10):2011-2020.

[175] Cohn L, Chatterjee B, Esselborn F et al. Antigen delivery to early endosomes eliminates the superiority of human blood BDCA3+ dendritic cells at cross presentation. J Exp Med. 2013;210(5):1049-1063.

[176] Heath WR, Belz GT, Behrens GM et al. Cross-presentation, dendritic cell subsets, and the generation of immunity to cellular antigens. Immunol Rev. 2004;199:9-26.

[177] Villadangos JA, Shortman K. Found in translation: the human equivalent of mouse CD8+ dendritic cells. J Exp Med. 2010;207(6):1131-1134.

[178] Scarlett UK, Rutkowski MR, Rauwerdink AM et al. Ovarian cancer progression is controlled by phenotypic changes in dendritic cells. J Exp Med. 2012;209(3):495-506.

[179] Randolph GJ, Angeli V, Swartz MA. Dendritic-cell trafficking to lymph nodes through lymphatic vessels. Nat Rev Immunol. 2005;5(8):617-628.

[180] Adams S, O'Neill DW, Bhardwaj N. Recent advances in dendritic cell biology. J Clin Immunol. 2005;25(2):87-98.

[181] Florindo HF, Pandit S, Goncalves LM et al. Antibody and cytokine-associated immune responses to S. equi antigens entrapped in PLA nanospheres. Biomaterials. 2009;30(28):5161-5169.

[182] Rock KL, Shen L. Cross□presentation: underlying mechanisms and role in immune surveillance. Immunol Rev. 2005;207(1):166-183.

[183] Kazzaz J, Singh M, Ugozzoli M et al. Encapsulation of the immune potentiators MPL and RC529 in PLG microparticles enhances their potency. J Control Release. 2006;110(3):566-573.

[184] Wilson NS, El-Sukkari D, Belz GT et al. Most lymphoid organ dendritic cell types are phenotypically and functionally immature. Blood. 2003;102(6):2187-2194.

[185] Reddy ST, Swartz MA, Hubbell JA. Targeting dendritic cells with biomaterials: developing the next generation of vaccines. Trends Immunol. 2006;27(12):573-579.

[186] Paulis LE, Mandal S, Kreutz M et al. Dendritic cell-based nanovaccines for cancer immunotherapy. Curr Opin Immunol. 2013;25(3):389-395.

[187] Bachmann MF, Jennings GT. Vaccine delivery: a matter of size, geometry, kinetics and molecular patterns. Nat Rev Immunol. 2010;10(11):787-796.

[188] Gamvrellis A, Leong D, Hanley JC et al. Vaccines that facilitate antigen entry into dendritic cells. Immunol Cell Biol. 2004;82(5):506-516.

[189] Cruz LJ, Tacken PJ, Fokkink R et al. The influence of PEG chain length and targeting moiety on antibody-mediated delivery of nanoparticle vaccines to human dendritic cells. Biomaterials. 2011;32(28):6791-6803.

[190] Tacken PJ, Ginter W, Berod L et al. Targeting DC-SIGN via its neck region leads to prolonged antigen residence in early endosomes, delayed lysosomal degradation, and cross-presentation. Blood. 2011;118(15):4111-4119.

[191] Cruz LJ, Rueda F, Simon L et al. Liposomes containing NYESO1/tetanus toxoid and adjuvant peptides targeted to human dendritic cells via the Fc receptor for cancer vaccines. Nanomedicine (Lond). 2014;9(4):435-449.

[192] Kazzaz J, Singh M, Ugozzoli M et al. Encapsulation of the immune potentiators MPL and RC529 in PLG microparticles enhances their potency. J Control Release. 2006;110(3):566-573.

[193] Blander JM, Medzhitov R. Regulation of phagosome maturation by signals from toll-like receptors. Science. 2004;304(5673):1014-1018.

[194] Diebold SS. Activation of dendritic cells by toll-like receptors and C-type lectins. Handb Exp Pharmacol. 200;188:3-30.

[195] Chaturvedi A, Pierce SK. How location governs Toll like receptor signaling. Traffic. 2009;10(6):621-8.

[196] Celis E. Toll-like receptor ligands energize peptide vaccines through multiple paths. Cancer Res. 2007;67(17):7945-7947.

[197] Beutler B. Microbe sensing, positive feedback loops, and the pathogenesis of inflammatory diseases. Immunol Rev. 2009;227(1):248-263.

[198] Medzhitov R. Toll-like receptors and innate immunity. Nat Rev Immunol. 2001;1(2):135-145.

[199] Ameres SL, Martinez J, Schroeder R. Molecular basis for target RNA recognition and cleavage by human RISC. Cell. 2007;130(1):101-112.

[200] Jérôme V, Graser A, Müller R et al. Cytotoxic T lymphocytes responding to low dose TRP2 antigen are induced against B16 melanoma by liposome-encapsulated TRP2 peptide and CpG DNA adjuvant. J Immunother. 2006;29(3):294-305.

[201] de Jong S, Chikh G, Sekirov L et al. Encapsulation in liposomal nanoparticles enhances the immunostimulatory, adjuvant and anti-tumor activity of subcutaneously administered CpG ODN. Cancer Immunol Immunother. 2007;56(8):1251-1264.

[202] Diwan M, Elamanchili P, Cao M et al. Dose sparing of CpG oligodeoxynucleotide vaccine adjuvants by nanoparticle delivery. Curr Drug Deliv. 2004;1(4):405-412.

[203] Bauer S, Kirschning CJ, Häcker H et al. Human TLR9 confers responsiveness to bacterial DNA via species-specific CpG motif recognition. Proc Natl Acad Sci USA, 2001;98(16):9237-9242.

[204] Hemmi H, Takeuchi O, Kawai T et al. A Toll-like receptor recognizes bacterial DNA. Nature. 2000;408(6813):740-745.

[205] Banchereau J, Paczesny S, Blanco P et al. Dendritic cells: controllers of the immune system and a new promise for immunotherapy. Ann NY Acad Sci. 2003;987:180-187.

[206] Schreibelt G, Tel J, Sliepen KH et al. Toll-like receptor expression and function in human dendritic cell subsets: implications for dendritic cell-based anti-cancer mmunotherapy. Cancer Immunol Immunother. 2010;59(10):1573-1582.

[207] Matsumoto M, Kikkawa S, Kohase M et al. Establishment of a monoclonal antibody against human Toll-like receptor 3 that blocks double-stranded RNA-mediated signaling. Biochem Biophys Res Commun. 2002;293(5):1364-1369.

[208] Alexopoulou L, Holt AC, Medzhitov R et al. Recognition of double-stranded RNA and activation of NF-κB by Toll-like receptor 3. Nature. 2001;413(6857):732-738.

[209] Zaks K, Jordan M, Guth A et al. Efficient immunization and cross-priming by vaccine adjuvants containing TLR3 or TLR9 agonists complexed to cationic liposomes. J Immunol. 2006;176(12):7335-7345.

[210] Takeda K, Akira S. Toll-like receptors in innate immunity. Int Immunol. 2005;17(1):1-14.

[211] Radford KJ, Caminschi I. New generation of dendritic cell vaccines. Hum Vaccin Immunother. 2013;9(2):259-264.

[212] Pasare C, Medzhitov R. Toll pathway-dependent blockade of CD4+ CD25+ T cell-mediated suppression by dendritic cells. Science. 2003;299(5609):1033-1036.

[213] Heil F, Hemmi H, Hochrein H et al. Species-specific recognition of single-stranded RNA via toll-like receptor 7 and 8. Science. 2004;303(5663):1526-1529.

[214] Sioud M. Innate sensing of self and non-self RNAs by Toll-like receptors. Trends Mol Med. 2006;12(4):167-176.

[215] Sabbatini P, Tsuji T, Ferran L et al. Phase I trial of overlapping long peptides from a tumor self-antigen and poly-ICLC shows rapid induction of integrated immune response in ovarian cancer patients. Clin Cancer Res. 2012;18(23):6497-6508.

[216] Liu YJ. IPC: professional type 1 interferon-producing cells and plasmacytoid dendritic cell precursors. Ann Rev Immunol. 2005;23:275-306.

[217] Krug A, Rothenfusser S, Hornung V et al. Identification of CpG oligonucleotide sequences with high induction of IFN-alpha/beta in plasmacytoid dendritic cells. Eur J Immunol. 2001;31(7):2154-2163.

[218] Ito T, Amakawa R, Kaisho T et al. Interferon-alpha and interleukin-12 are induced differentially by Toll-like receptor 7 ligands in human blood dendritic cell subsets. J Exp Med. 2002;195(11):1507-1512.

[219] Warger T, Osterloh P, Rechtsteiner G et al. Synergistic activation of dendritic cells by combined Toll-like receptor ligation induces superior CTL responses in vivo. Blood. 2006;108(2):544-550.

[220] Kaisho T, Akira S. Toll-like receptors as adjuvant receptors. Biochim Biophys Acta. 2002;1589(1):1-13.

[221] Heikenwalder M, Polymenidou M, Junt T et al. Lymphoid follicle destruction and immunosuppression after repeated CpG oligodeoxynucleotide administration. Nat Med. 2004;10(2):187-192.

[222] He LZ, Crocker A, Lee J et al. Antigenic targeting of the human mannose receptor induces tumor immunity. J Immunol. 2007;178(10):6259-6267.

[223] Avraméas A, McIlroy D, Hosmalin A et al. Expression of a mannose/fucose membrane lectin on human dendritic cells. Eur J Immunol. 1996;26(2):394-400.

[224] Kreutz M, Tacken PJ, Figdor CG. Targeting dendritic cells--why bother? Blood. 2013;121(15):2836-2844.

[225] Unger WW, van Kooyk Y. 'Dressed for success' C-type lectin receptors for the delivery of glyco-vaccines to dendritic cells. Curr Opin Immunol. 2011;23(1):131-137.

[226] Brunner R, Jensen-Jarolim E, Pali-Scholl I. The ABC of clinical and experimental adjuvants--a brief overview. Immunol Lett. 2010;128(1):29-35.

[227] Burgdorf S, Kautz A, Bohnert V et al. Distinct pathways of antigen uptake and intracellular routing in CD4 and CD8 T cell activation. Science. 2007;316(5824):612-616.

[228] Woof JM, Burton DR. Human antibody-Fc receptor interactions illuminated by crystal structures. Nat Rev Immunol. 2004;4(2):89-99.

[229] Hangalapura BN, Oosterhoff D, de Groot J et al. Potent antitumor immunity generated by a CD40-targeted adenoviral vaccine. Cancer Res. 2011;71(17):5827-5837.

[230] Kwon YJ, James E, Shastri N et al. In vivo targeting of dendritic cells for activation of cellular immunity using vaccine carriers based on pH-responsive microparticles. Proc Natl Acad Sci USA. 2005;102(51):18264-18268.

[231] Conroy H, Galvin KC, Higgins SC et al. Gene silencing of TGF-beta1 enhances antitumor immunity induced with a dendritic cell vaccine by reducing tumor associated regulatory T cells. Cancer Immunol Immunother. 2012;61(3):425-431.

[232] Lee H, Jang IH, Ryu SH et al. N-terminal site-specific mono-PEGylation of epidermal growth factor. Pharm Res. 2003;20(5):818-825.

[233] Betancourt T, Byrne JD, Sunaryo N et al. PEGylation strategies for active targeting of PLA/PLGA nanoparticles. J Biomed Mater Res Part A. 2009;91(1):263-276.

[234] Brocchini S, Godwin A, Balan S et al. Disulfide bridge based PEGylation of proteins. Adv Drug Deliv Rev. 2008;60(1):3-12.

[235] Freichels H, Pourcelle V, Auzely-Velty R et al. Synthesis of poly(lactide-co-glycolide-co-epsilon-caprolactone)-graft-mannosylated poly(ethylene oxide) copolymers by combination of "clip" and "click" chemistries. Biomacromolecules. 2012;13(3):760-768.

[236] Devaud C, John LB, Westwood JA et al. Immune modulation of the tumor microenvironment for enhancing cancer immunotherapy. Oncoimmunology. 2013;2(8):e25961.

[237] Junttila MR, de Sauvage FJ. Influence of tumour micro-environment heterogeneity on therapeutic response. Nature. 2013;501(7467):346-354.

[238] Ding ZY, Zou XL, Wei YQ. Cancer microenvironment and cancer vaccine. Cancer Microenviron. 2012;5(3):333-344.

[239] Quante M, Tu SP, Tomita H et al. Bone marrow-derived myofibroblasts contribute to the mesenchymal stem cell niche and promote tumor growth. Cancer Cell. 2011;19(2):257-272.

[240] Pietras K, Östman A. Hallmarks of cancer: interactions with the tumor stroma. Exp Cell Res. 2010;316(8):1324-1331.

[241] Zhang J, Liu J. Tumor stroma as targets for cancer therapy. Pharmacol Ther. 2013;137(2):200-215.

[242] Zou W. Immunosuppressive networks in the tumour environment and their therapeutic relevance. Nat Rev Cancer. 2005;5(4):263-274.

[243] Stewart TJ, Smyth MJ. Improving cancer immunotherapy by targeting tumor-induced immune suppression. Cancer Metast Rev. 2011;30(1):125-140.

[244] Flavell RA, Sanjabi S, Wrzesinski SH et al. The polarization of immune cells in the tumour environment by TGFβ. Nat Rev Immunol. 2010;10(8):554-567.

[245] Zitvogel L, Apetoh L, Ghiringhelli F et al. Immunological aspects of cancer chemotherapy. Nat Rev Immunol. 2008;8(1):59-73.

[246] Pham NLL, Pewe LL, Fleenor CJ et al. Exploiting cross-priming to generate protective CD8 T-cell immunity rapidly. Proc Natl Acad Sci USA. 2010;107(27):12198-12203.

[247] Wang LCS, Lo A, Scholler J et al. Targeting fibroblast activation protein in tumor stroma with chimeric antigen receptor T cells can inhibit tumor growth and augment host immunity without severe toxicity. Cancer Immunol Res. 2013;2(2):154-66.

[248] Spaeth EL, Dembinski JL, Sasser AK et al. Mesenchymal stem cell transition to tumor associated fibroblasts contributes to fibrovascular network expansion and tumor progression. PloS ONE. 2009;4(4):e4992.

[249] Rubtsov YP, Rudensky AY. TGFβ signalling in control of T-cell-mediated self-reactivity. Nat Rev Immunol. 2007;7(6):443-453.

[250] Massagué J. TGFβ in cancer. Cell. 2008;134(2):215-230.

[251] Nagaraj NS, Datta PK. Targeting the transforming growth factor-β signaling pathway in human cancer. Expert Opin Investig Drugs. 2010;19(1):77-91.

[252] Ellermeier J, Wei J, Duewell P et al. Therapeutic efficacy of bifunctional siRNA combining TGF-β1 silencing with RIG-I activation in pancreatic cancer. Cancer Res. 2013;73(6):1709-1720.

[253] Oh YK, Park TG. siRNA delivery systems for cancer treatment. Adv Drug Deliv Rev. 2009;61(10):850-862.

[254] Folkman, J. What is the evidence that tumors are angiogenesis dependent? J Natl Cancer Inst. 1990;82(1):4-7.

[255] Weidner N, Semple JP, Welch WR et al. Tumor angiogenesis and metastasis—correlation in invasive breast carcinoma. N Engl J Med. 1991;324(1):1-8.

[256] Weidner N, Folkman J, Pozza F et al. Tumor angiogenesis: a new significant and independent prognostic indicator in early-stage breast carcinoma. J Natl Cancer Inst. 1992;84(24):1875-1887.

[257] Ellis L, Fidler I. Angiogenesis and metastasis. Eur J Cancer. 1996;32(14):2451-2460.

[258] Hervé MA, Buteau-Lozano H, Vassy R et al. Overexpression of vascular endothelial growth factor 189 in breast cancer cells leads to delayed tumor uptake with dilated intratumoral vessels. Am J Pathol. 2008;172(1):167-178.

[259] Tuomela J, Valta M, Seppänen J et al. Overexpression of vascular endothelial growth factor C increases growth and alters the metastatic pattern of orthotopic PC-3 prostate tumors. BMC Cancer. 2009;9(1):355-362.

[260] Moon WS, Rhyu KH, Kang MJ et al. Overexpression of VEGF and angiopoietin 2: a key to high vascularity of hepatocellular carcinoma? Mod Pathol. 2003;16(6):552-557.

[261] Tokunaga T, Oshika Y, Abe Y et al. Vascular endothelial growth factor (VEGF) mRNA isoform expression pattern is correlated with liver metastasis and poor prognosis in colon cancer. Br J Cancer. 1998;77(6):998-1002.

[262] Wang X, Chen X, Fang J et al. Overexpression of both VEGF-A and VEGF-C in gastric cancer correlates with prognosis, and silencing of both is effective to inhibit cancer growth. Int J Clin Exp Pathol. 2013;6(4):586-97.

[263] Saharinen P, Eklund L, Pulkki K et al. VEGF and angiopoietin signaling in tumor angiogenesis and metastasis. Trends Mol Med. 2011;17(7):347-362.

[264] Zhang C, Tan C, Ding H et al. Selective VEGFR inhibitors for anticancer therapeutics in clinical use and clinical trials. Curr Pharm Des. 2012;18(20):2921-2935.

[265] Poindessous V, Ouaret D, El Ouadrani K et al. EGFR-and VEGF (R)-targeted small molecules show synergistic activity in colorectal cancer models refractory to combinations of monoclonal antibodies. Clin Cancer Res. 2011;17(20):6522-6530.

[266] Pestourie C, Tavitian B, Duconge F. Aptamers against extracellular targets for in vivo applications. Biochimie. 2005;87(9):921-930.

[267] Zhang Y, Schwerbrock NM, Rogers AB et al. Codelivery of VEGF siRNA and gemcitabine monophosphate in a single nanoparticle formulation for effective treatment of NSCLC. Mol Ther. 2013;21(8):1559-1569.

[268] Wang J, Lu Z, Wientjes MG et al. Delivery of siRNA therapeutics: barriers and carriers. AAPS J. 2010;12(4):492-503.

[269] Yang XZ, Dou S, Sun TM et al. Systemic delivery of siRNA with cationic lipid assisted PEG-PLA nanoparticles for cancer therapy. J Control Release. 2011;156(2):203-211.

[270] Xue HY, Liu S, Wong HL. Nanotoxicity: a key obstacle to clinical translation of siRNA-based nanomedicine. Nanomedicine. 2014;9(2):295-312.

[271] Schiffelers RM, Ansari A, Xu J et al. Cancer siRNA therapy by tumor selective delivery with ligand-targeted sterically stabilized nanoparticle. Nucleic Acids Res. 2004;32(19):e149-e149.

[272] Pittella F, Miyata K, Maeda Y et al. Pancreatic cancer therapy by systemic administration of VEGF siRNA contained in calcium phosphate/charge-conversional polymer hybrid nanoparticles. J Control Release. 2012;161(3):868-874.

[273] Li SD, Chono S, Huang L. Efficient oncogene silencing and metastasis inhibition via systemic delivery of siRNA. Mol Ther. 2008;16(5):942-946.

[274] Pardoll DM. The blockade of immune checkpoints in cancer immunotherapy. Nat Rev Cancer. 2012;12(4):252-264.

[275] Naidoo J, Page D, Wolchok J. Immune modulation for cancer therapy. Br J Cancer. 2014;111:2214-2219.

[276] Weber J. In Seminars in oncology; Michele Maio, Ed.; Elsevier, 2010; Vol. 37, pp. 430-439.

[277] O'Day SJ, Hamid O, Urba WJ. Targeting cytotoxic T□lymphocyte antigen□4 (CTLA□4). Cancer. 2007;110(12):2614-2627.

[278] Vanneman M, Dranoff G. Combining immunotherapy and targeted therapies in cancer treatment. Nat Rev Cancer. 2012;12(4):237-251.

[279] Hodi FS, O'Day SJ, McDermott DF et al. Improved survival with ipilimumab in patients with metastatic melanoma. N Engl J Med. 2010;363(8):711-723.

[280] Topalian SL, Drake CG, Pardoll DM. Targeting the PD-1/B7-H1 (PD-L1) pathway to activate anti-tumor immunity. Curr Opin Immunol. 2012;24(2):207-212.

[281] Brahmer JR, Tykodi SS, Chow LQ et al. Safety and activity of anti–PD-L1 antibody in patients with advanced cancer. N Engl J Med. 2012;366(26):2455-2465.

[282] Boyle GM, Woods SL, Bonazzi VF et al. Melanoma cell invasiveness is regulated by miR□211 suppression of the BRN2 transcription factor. Pigment Cell Melanoma Res. 2011;24(3):525-537.

[283] Pichon C, Billiet L, Midoux P. Chemical vectors for gene delivery: uptake and intracellular trafficking. Curr Opin Biotechnol. 2010;21(5):640-645.

[284] Viola JR, Rafael DF, Wagner E et al. Gene therapy for advanced melanoma: selective targeting and therapeutic nucleic acids. J Drug Deliv. 2013;2013:1-15.

[285] Lu Y, Kawakami S, Yamashita F et al. Development of an antigen-presenting cell-targeted DNA vaccine against melanoma by mannosylated liposomes. Biomaterials. 2007;28(21):3255-3262.

[286] Patil Y, Panyam J. Polymeric nanoparticles for siRNA delivery and gene silencing. Int J Pharm. 2009;367(1):195-203.

[287] Duncan R, Gaspar R. Nanomedicine(s) under the microscope. Mol Pharm. 2011;8(6):2101-2141.

Chapter 2

[1] Jemal A, Bray F, Center MM et al. Global cancer statistics. CA Cancer J Clin. 2013;61:69-90.

[2] Park YM, Lee SJ, Kim YS et al. Nanoparticle-based vaccine delivery for cancer immunotherapy. Immune Netw. 2013;13:177-183.

[3] Vert M, Li S, Spenlehauer G et al. Bioresorbability and biocompatibility of aliphatic polyesters. J Mater Sci Mater. 1992;3:432-46.

[4] Garinot M, Fievez V, Pourcelle V et al. PEGylated PLGA-based nanoparticles targeting M cells for oral vaccination. J Control Release. 2007;120:195-204.

[5] Florindo H, Pandit S, Lacerda L et al. The enhancement of the immune response against S. equi antigens through the intranasal administration of poly-caprolactone-based naoparticels. Biomaterials. 2009;30:879-891.

[6] Dash M, Chiellini F, Ottenbrite RM et al. Chitosan-A versatile semi-synthetic polymer in biomedical applications. Prog Polym Sci. 2011;36:981-1014.

[7] Park JH, Saravanakumar G, Kim K et al. Targeted delivery of low molecular drugs using chitosan and its derivatives. Adv Drug Deliv Rev. 2010;62:28-41.

[8] Chua BY, Al Kobaisi M, Zeng W et al. Chitosan microparticles and nanoparticles as biocompatible delivery vehicles for peptide and protein-based immunocontraceptive vaccines. Mol Pharm. 2012;9:81-90.

[9] Athanasiou KA, Niederauer GG, Agrawal CM. Sterilization, toxicity, biocompatibility and clinical applications of polylactic acid / polyglycolic acid copolymers. Biomaterials. 1996;17:93-102.

[10] Florindo HF, Pandit S, Goncalves L et al. Streptococcus equi antigens absorbed onto surface modified poly-e-caprolactone microspheres induce humural and cellular specific immune responses. Vaccine. 2008;26:4168-4177.

[11] Moffatt S, Cristiano RJ. Uptake characteristics of NGR-coupled stealth PEI/pDNA nanoparticles loaded with PLGA-PEG-PLGA tri-block copolymer for targeted delivery to human monocyte-derived dendritic cells. Int J Pharm. 2006;321:143-154.

Chapter 3

[1] Davis I, Jefford M, Parente P et al. Rational approaches to human cancer immunotherapy. J Leukoc Biol. 2003;73:3-29.

[2] Bringmann A, Held SA, Heine A et al. RNA vaccines in cancer treatment. J Biomed Biotechnol. 2010;2010:623687.

[3] Mossman SP, Evans LS, Fang H et al. Development of a CTL vaccine for Her-2/neu using peptide-microspheres and adjuvants. Vaccine. 2005;23:3545-54.

[4] Ahmad M, Rees R, Ali S. Escape from immunotherapy: possible mechanisms that influence tumor regression/progression. Cancer Immunol Immunothe. 2004;53:844-54.

[5] Pashine A, Valiante N, Ulmer J. Targeting the innate immune response with improved vaccine adjuvants. Nat Med. 2005;11(4):63-8.

[6] Hamdy S, Molavi O, Ma Z et al. Co-delivery of cancer-associated antigen and Toll-like receptor 4 ligand in PLGA nanoparticles induces potent CD8+ T cell-mediated anti-tumor immunity. Vaccine. 2008;26:5046-57.

[7] Jain RA. The manufacturing techniques of various drug loaded biodegradable poly(lactide-co-glycolide) (PLGA) devices. Biomaterials. 2000;21:2475–90.

[8] Bachmann M, Jennings G. Vaccine delivery: a matter of size, geometry, kinetics and molecular patterns. Nat Rev Immunol. 2010;10(11):787-96.

[9] Mottram P, Leong D, Crimeen-Irwin B et al. Type 1 and 2 immunity following vaccination is influenced by nanoparticle size: formulation of a model vaccine for respiratory syncytial virus. Mol Pharm. 2007;4(1):73-84.

[10] Reddy ST, Swartz MA, Hubbell JA. Targeting dendritic cells with biomaterials: developing the next generation of vaccines. Trends Immunol. 2006;27(12) 573-9.

[11] Zhao L, Seth A, Wibowo N et al. Nanoparticle vaccines. Vaccine. 2014;32:327- 37.

[12] Ehrlich M, Boll W, van Oijen A et al. Endocytosis by random initiation and stabilization of clathrin-coated pits. Cell. 2004;118(5):591-605.

[13] Wang Z, Tiruppathi C, Minshall R et al. Size and dynamics of caveolae studied using nanoparticles in living endothelial cells. ACS Nano. 2009;3(12):4110-6.

[14] Na JH, Lee SY, Lee S et al. Effect of the stability and deformability of self-assembled glycol chitosan nanoparticles on tumor-targeting efficiency. J Control Release. 2012;163:2-9.

[15] Atri MS, Saboury AA, Moosavi-Movahedi AA et al. Effects of zinc binding on the structure and thermal stability of camel alpha-lactalbumin. J Therm Anal Calorim. 2015;120:481-8.

[16] Manolova V, Flace A, Bauer M et al. Nanoparticles target distinct dendritic cell populations according to their size. Eur J Immunol. 2008;38:1404-13.

[17] Venkataraman S, Hedrick J, Ong Z et al. The effects of polymeric nanostructure shape on drug delivery. Adv Drug Deliv Rev. 2011;63(14-15):1228-46.

[18] Foged C, Brodin B, Frojkaer S et al. Particle size and surface charge affect particle uptake by human dendritic cells in an in vitro model. Int J Pharm. 2005;298(2):315-22.

[19] Vasir J, Labhasetwar V. Quantification of the force of nanoparticle-cell membrane interactions and its influence on intracellular trafficking of nanoparticles. Biomaterials. 2008;29(31):4244-52.

[20] Thurn K, Brown E, Wu A et al. Nanoparticles for applications in cellular imaging. NanoscaleRes Lett. 2007;2(9):430-41.

[21] Liu J, Bauer H, Callahan J et al. Endocytic uptake of a large array of HPMA copolymers: Elucidation into the dependence on the physicochemical characteristics. J Control Release. 2010;143(1):71-9.

[22] Yue Z, Wei W, Lv P et al. Surface Charge Affects Cellular Uptake and Intracellular Trafficking of Chitosan-based Nanoparticles. Biomacromolecules. 2011;12(7):2440-6.

[23] Silva JM, Videira M, Gaspar R et al. Immune system targeting by biodegradable nanoparticles for cancer vaccines. J Control Release. 2013;168(2):179-99.

[24] Krishnamachari Y, Geary S, Lemke C et al. Nanoparticle Delivery Systems in Cancer Vaccines. Pharma Res. 2011;28(2):215-36.

[25] Park YM, Lee SJ, Kim YS et al. Nanoparticle-based vaccine delivery for cancer immunotherapy. Immune Netw. 2013;13:177-83.

[26] Shen H, Ackerman AL, Cody V et al. Enhanced and prolonged cross-presentation following endosomal escape of exogenous antigens encapsulated in biodegradable nanoparticles. Immunology. 2005;117(1):78–88.

[27] Silva JM, Vandermeulen G, Oliveira VG et al. Development of functionalized nanoparticles for vaccine delivery to dendritic cells: a mechanistic approach. Nanomedicine (Lond). 2014;9(17):2639-56.

[28] Panyam M, Zhou W, Prabha S et al. Rapid endo-lysosomal escape of poly (DL-lactide-co-glycolide) nanoparticles: implications for drug and gene delivery. FASEB J. 2002;16(10):1217-26.

[29] Danhier F, Lecouturier N, Vroman B et al. Paclitaxel-loaded PEGylated PLGA-based nanoparticles: in vitro and in vivo evaluation. J Control Release. 2009;133(1):11-7.

[30] Van den Berg J, Oosterhuis K, Hennink W et al. Shielding the cationic charge of nanoparticle-formulated dermal DNA vaccines is essential for antigen expression and immunogenicity. J Control Release. 2010;141(2):234-40.

[31] Tahara K, Sakai T, Yamamoto H et al. Improved cellular uptake of chitosan-modified PLGA nanospheres by A549 cells. Int J Pharm. 2009;382(1-2):198-204.

[32] Garinot M, Fiévez V, Pourcelle V et al. PEGylated PLGA-based nanoparticles targeting M cells for oral vaccination. J Control Release. 2007;120(3):195-204.

[33] Albanese A, Tang PS, Chan WC. The effect of nanoparticle size, shape, and surface chemistry on biological systems. Ann Rev Biom Eng. 2012;14:1-16.

[34] Jaini R, Kesaraju P, Johnson JM et al. An autoimmune-mediated strategy for prophylactic breast cancer vaccination. Nat Med. 2010;16:799-803.

[35] Vilotte JL, Soulier S, Mercier JC. Sequence of the murine α-lactalbumin-encoding cDNA: interspecies comparison of the coding frame and deduced pre-protein. Gene. 1992;112:251-5.

[36] Li X, Zhang J, Gao H et al. Transcriptional targeting modalities in breast cancer gene therapy using adenovirus vectors controlled by alpha-lactalbumin promoter. Mol Cancer Ther. 2005;4:1850-9.

[37] Makadia HK, Siegel SJ. Poly Lactic-co-Glycolic Acid (PLGA) as Biodegradable Controlled Drug Delivery Carrier. Polymers. 2011;3:1377-97.

[38] Tobio M, Gref R, Sanchez A et al. Stealth PLA-PEG nanoparticles as protein carriers for nasal administration. . Pharm Res. 1998;15:270-5.

[39] Cruz LJ, Tacken PJ, Fokkink R et al. The influence of PEG chain length and targeting moiety on antibody-mediated delivery of nanoparticle vaccines to human dendritic cells. Biomaterials. 2011;32:6791-803.

[40] Turk CT, Oz UC, Serim TM et al. Formulation and optimization of nonionic surfactants emulsified nimesulide-loaded PLGA-based nanoparticles by design of experiments. AAPS PharmSciTech. 2014;15:161-76.

[41] Coeshott CM, Smithson SL, Verderber E et al. Pluronic F127-based systemic vaccine delivery systems. Vaccine. 2004;22:2396-405.

[42] Alimohammadi S, Salehi R, Amini N et al. Synthesis and Physicochemical Characterization of Biodegradable PLGA-based Magnetic Nanoparticles Containing Amoxicilin. Bull Korean Chem Soc. 2012;33:3225-32.

[43] Mukherjee B, Santra K, Pattnaik G et al. Preparation, characterization and in-vitro evaluation of sustained release protein-loaded nanoparticles based on biodegradable polymers. Int J Nanomedicine. 2008;3(4):487-96.

[44] Pereira P, Morgado D, Crepet A et al. Glycol chitosan-based nanogel as a potential targetable carrier for siRNA. Macromol Biosci. 2013;13(10):1369-78.

[45] Pereira P, Pedrosa SS, Correia A et al. Biocompatibility of a self-assembled glycol chitosan nanogel. Toxicol In Vitro. 2015;29:638-46.

Chapter 4

[1] Banchereau J, Steinman R. Dendritic cells and the control of immunity. Nature. 1998;19(392):245-52.

[2] Howard CJ, Charleston B,Stephens SA et al. The role of dendritic cells in shaping the immune response. Anim Health Res Rev. 2004;5(2):191-5.

[3] Mellman I. Dendritic Cells: Master Regulators of the Immune Response. Cancer Immunol Res. 2013;1(3):145-9

[4] Saluja SS, Hanlon DJ, Sharp FA et al. Targeting human dendritic cells via DEC-205 using PLGA nanoparticles leads to enhanced cross-presentation of a melanoma-associated antigen. Int J Nanomedicine. 2014;9(1):5231-46.

[5] Silva JM, Videira M, Gaspar R et al. Immune system targeting by biodegradable nanoparticles for cancer vaccines. J Control Release. 2013;168(2):179-99.

[6] Palucka K, Banchereau J. Cancer immunotherapy via dendritic cells. Nat Rev Cancer. 2012;12:265-77.

[7] Zhou Y, Zhang Y, Zhiqiang Y et al. Dendritic cell-based immunity and vaccination against hepatitis C virus infection. Immunology. 2012;136(4):385–96.

[8] Finlay BB, McFadden G. Anti-Immunology: Evasion of the Host Immune System by Bacterial and Viral Pathogens. Cell. 2006;124(4):767–82.

[9] Kumar H, Kawai T, Akira S. Pathogen recognition in the innate immune response. Biochem J. 2009;420:1-16.

[10] Prasad S, Cody V, Saucier-Sawyer JK et al., Polymer nanoparticles containing tumor lysates as antigen delivery vehicles for dendritic cell-based antitumor immunotherapy. Nanomedicine. 2011;7(1):1-10.

[11] Park YM, Lee SJ, Kim YS et al. Nanoparticle-based vaccine delivery for cancer immunotherapy. Immune Netw. 2013;13:77-83.

[12] Jain RA. The manufacturing techniques of various drug loaded biodegradable poly(lactide-co-glycolide) (PLGA) devices. Biomaterials. 2000;21:2475–90.

[13] Semete B, Booysen L, Lemmer Y et al. In vivo evaluation of the biodistribution and safety of PLGA nanoparticles as drug delivery systems. Nanomedicine. 2010;6(5):662-71.

[14] Muthu M. Nanoparticles based on PLGA and its co-polymer: an overview. Asian J Pharm. 2009;3:266–73.

[15] Mansour HM, Sohn M, Al-Ghananeem A et al. Materials for pharmaceutical dosage forms: molecular pharmaceutics and controlled release drug delivery aspects. Int J Mol Sci. 2010;1(9):3298-322.

[16] Mohamed F, van der Walle CF. Engineering biodegradable polyester particles with specific drug targeting and drug release properties. J Pharm Sci. 2008;97(1):71-87.

[17] Jeong J, Lim D, Han D et al. Synthesis, characterization and protein absorption behaviors of PLGA-PEG di-block co-polymer blend film. Colloids Surf B. 2000;8(3-4):371-9.

[18] Lee AK, Rosen PP, DeLellis RA et al. Tumor marker expression in breast carcinomas and relationship to prognosis: an immunohistochemical study. Am J Clin Pathol. 1985;84:687–96.

[19] Jaini R, Kesaraju P, Johnson JM et al. An autoimmune-mediated strategy for prophylactic breast cancer vaccination, Nat Med. 2010;16:799-803.

[20] Cohen C, Sharkey FE, Shulman G et al. Tumor associated antigens in breast carcinomas: Prognostic significance. Cancer. 1987;60:1294-8.

[21] Nagamatsu Y, Oka T. Purification and characterization of mouse alpha-lactalbumin and preparation of its antibody Biochem J. 1980;185:227-37.

[22] Vilotte JL, Soulier S, Mercier JC. Sequence of the murine α-lactalbumin-encoding cDNA: interspecies comparison of the coding frame and deduced pre-protein. Gene. 1992;112:251-5.

[23] Hogquist KA, Jameson SC, Heath WR et al. T cell receptor antagonist peptides induce positive selection, Cell. 1994;76:17–27.

[24] Robertson JM, Jensen PE, Evavold BD. DO11.10 and OT-II T cells recognize a C-terminal ovalbumin 323-339 epitope. J Immunol. 2000;164(9):4706-12.

[25] Zhang W, Wang L, Liu Y et al. Immune responses to vaccines involving a combined antigen-nanoparticle mixture and nanoparticle-encapsulated antigen formulation. Biomaterials. 2014;35(23):6086-97.

[26] Athar M, Das AJ. Therapeutic nanoparticles: State-of-the-art of nanomedicine. Adv Mater Rev. 2014;1(1):25-37.

[27] Manolova V, Flace A, Bauer M et al. Nanoparticles target distinct dendritic cell populations according to their size. Eur J Immunol. 2008;38:1404-13.

[28] Reddy ST, Swartz MA, Hubbell JA. Targeting dendritic cells with biomaterials: developing the next generation of vaccines. Trends Immunol. 2006;27(12):573-9.

[29] Zupančič E, Peres C, Matos AI et al. Translational Peptide-associated Nanosystems: Promising Role as Cancer Vaccines. Curr Top Med Chem. 2016;16(3):291-313.

[30] Foged C, Brodin B, Frojkaer S et al. Particle size and surface charge affect particle uptake by human dendritic cells in an in vitro model. Int J Pharma. 2005;298(2):315-22.

[31] Zhao L, Seth A, Wibowo N et al. Nanoparticle vaccines. Vaccine. 2014;32:327- 37.

[32] Garinot M, Fiévez V, Pourcelle V et al. PEGylated PLGA-based nanoparticles targeting M cells for oral vaccination. J Control Release. 2007;120(3):195-204.

[33] Silva JM, Vandermeulen G, Oliveira VG et al. Development of functionalized nanoparticles for vaccine delivery to dendritic cells: a mechanistic approach. Nanomedicine (Lond). 2014;9(17):2639-56.

[34] Florindo HF, Pandit S, Lacerda L et al. The enhancement of the immune response against S. equi antigens through the intranasal administration of poly-epsilon-caprolactone-based nanoparticles. Biomaterials. 2009;30:879-91.

[35] George TC, Fanning SL, Fitzgerald-Bocarsly P et al. Quantitative measurement of nuclear translocation events using similarity analysis of multispectral cellular images obtained in flow. J Immunol Methods. 2006;311(1-2):117-29.

[36] Quah BJC, Warren HS, Parish CR. Monitoring lymphocyte proliferation in vitro and in vivo with the intracellular fluorescent dye carboxyfluorescein diacetate succinimidyl ester. Nat Protoc 2. 2007;2(9):2049-56.

[37] Turk CT, Oz UC, Serim TM et al. Formulation and optimization of nonionic surfactants emulsified nimesulide-loaded PLGA-based nanoparticles by design of experiments. AAPS Pharm Sci Tech. 2014;15:161-76.

[38] Sharma N, Madan P, Lin S. Effect of process and formulation variables on the preparation of parenteral paclitaxel-loaded biodegradable polymeric nanoparticles: A co-surfactant study. Asian J Pharm Sci. 2016;11(3):404-16.

[39] Mukherjee B, Santra K, Pattnaik G et al. Preparation, characterization and in-vitro evaluation of sustained release protein-loaded nanoparticles based on biodegradable polymers. Int J Nanomedicine. 2008;3(4):487-96.

[40] Alimohammadi S, Salehi R, Amini N et al. Synthesis and Physicochemical Characterization of Biodegradable PLGA-based Magnetic Nanoparticles Containing Amoxicilin. Bull Korean Chem Soc. 2012;33:3225-32.

[41] Hosseinzadeh H, Atyabi F, Dinarvand R et al. Chitosan-Pluronic nanoparticles as oral delivery of anticancer gemcitabine: preparation and in vitro study. Int J Nanomedicine. 2012;7:1851-63.

[42] Park MH, Baek JS, Lee CA et al. Effect of chitosan on physicochemical properties of exenatide-loaded PLGA nanoparticles. J Pharm Investig. 2013;43(6):489-97.

[43] Amjadi I, Rabiee M, Hosseini MS. Anticancer activity of NPs based on PLGA and co-polymer in vitro evaluation. Iran J Pharm Res. 2013;12(4):623-34.

[44] Kulinski Z, Piorkowska E, Gadzinowska K et al. Plasticization of poly(l-lactide) with poly(propylene glycol). Biomacromolecules. 2006;7:2128-35.

[45] Dubernet C. Thermoanalysis of microspheres. Termochim Acta. 1995;248:259-69.

[46] Atri MS, Saboury AA, Moosavi-Movahedi AA et al. Effects of zinc binding on the structure and thermal stability of camel alpha-lactalbumin. J Therm. Anal Calorim. 2015;120:481-8.

[47] Hendrix T, Griko YV, Privalov PL. A calorimetric study of the influence of calcium on the stability of bovine a-lactalbumin. Biophys Chem. 2000;84(1):27-34.

[48] Makadia HK, Siegel SJ. Poly Lactic-co-Glycolic Acid (PLGA) as Biodegradable Controlled Drug Delivery Carrier. Polymers. 2011;3:1377-97.

[49] Tobio M, Gref R, Sanchez A et al. Stealth PLA-PEG nanoparticles as protein carriers for nasal administration. Pharm Res. 1998;15:270-5.

[50] Athanasiou KA, Niederauer GG, Agrawal CM. Sterilization, toxicity, biocompatibility and clinical applications of polylactic acid / polyglycolic acid copolymers. Biomaterials. 1996;17(2):93-102.

[51] Naik SH. Dendritic Cell Protocols, second ed., Humana Press, New York, 2010.

[52] Rodriguez-Lorenz L, Fytianos K, Blank F et al. Fluorescence-Encoded Gold Nanoparticles: Library Design and Modulation of Cellular Uptake into Dendritic Cells. Small. 2014;10(7):1341–50.

[53] Albanese A, Tang PS, Chan WC. The effect of nanoparticle size, shape, and surface chemistry on biological systems. Annu Rev Biomed Eng. 2012;14:1-16.

[54] Derakhshandeh K, Fashi M, Seifoleslami S. Thermosensitive Pluronic® hydrogel: prolonged injectable formulation for drug abuse. Drug Des Devel Ther. 2010;4:255-62.

[55] Menon JU, Kona S, Wadajkar AS et al. Effects of surfactants on the properties of PLGA nanoparticles. J Biomed Mater Res A. 2012;100:1998-2005.

[56] Pereira P, Pedrosa SS, Correia A et al. Biocompatibility of a self-assembled glycol chitosan nanogel. Toxicol in vitro. 2015;29:638-46.

[57] Pereira P, Morgado D, Crepet A et al. Glycol chitosan-based nanogel as a potential targetable carrier for siRNA. Macromol Biosci. 2013;13(10):1369-78.

[58] Mura S, Hillaireau H, Nicolas J et al. Influence of surface charge on the potential toxicity of PLGA nanoparticles towards Calu-3 cells. Int J Nanomedicine. 2011;6:2591-605.

[59] Manoochehri S, Darvishi B, Kamalinia G et al. Surface modification of PLGA nanoparticles via human serum albumin conjugation for controlled delivery of docetaxel. DARU J Pharm Sci. 2013;21(1):58.

[60] Pamujula S, Hazari S, Bolden G et al. Cellular delivery of PEGylated PLGA nanoparticles. J Pharm Pharmacol. 2012;64:61-7.

[61] Butcher NJ, Mortimer GM, Minchin RF. Drug delivery: Unravelling the stealth effect. Nat Nanotechnol. 2016;11:310–311.

[62] Amoozgar Z, Yeo Y, Recent advances in stealth coating of nanoparticle drug delivery systems. Wiley Interdiscip Rev Nanomed Nanobiotechnol. 2012;4(2):219-33.

[63] Mollica F, Biondi M, Muzzi S et al. Mathematical modelling of the evolution of protein distribution within single PLGA microspheres: prediction of local concentration profiles and release kinetics. J Mater Sci Mater Med. 2008;19:1587-93.

[64] Schijns V, O'Hagan D. Immunopotentiators in Modern Vaccines. first ed., Elsevier Academic Press, New York, 2005.

[65] Acton QA. Advances in Active Immunotherapy Research and Application. 2011 ed., A Schoolarly EditionTM Schoolarly BreifTM, Atlanta, 2011.

[66] Kramer RM, Shende VR, Motl N et al. Toward a Molecular Understanding of Protein Solubility: Increased Negative Surface Charge Correlates with Increased Solubility. Biophys J. 2012;102(8):1907-15.

[67] Oh N, Park JH. Endocytosis and exocytosis of nanoparticles in mammalian cells. Int J Nanomedicine. 2014;9(Suppl 1):51-63.

[68] Shan X, Yuan Y, Liu C et al. Influence of PEG chain on the complement activation suppression and longevity in vivo prolongation of the PCL biomedical nanoparticles. Biomed Microdevices. 2009;11(6):1187-94.

[69] Miyazaki S, Tobiyama T, Takada M et al. Percutaneous Absorption of Indomethacin from Pluronic F127 Gels in Rats. J Pharm Pharmacol. 1995;47(6):455-7.

[70] Escobar-Chávez JJ, López-Cervantes L, Naïk A et al. Applications of Thermo-reversible Pluronic F-127 Gels in Pharmaceutical Formulations. J Pharm Pharmaceut Sci. 2006;9(3):339-58.

[71] Norbury CC. Drinking a lot is good for dendritic cells. Immunology. 2006;117(4):443-51.

[72] Danhier F, Ansorena E, Silva JM et al. PLGA-based nanoparticles: an overview of biomedical applications. J Control Release. 2012;161:505-22.

[73] Arens R, Schoenberger SP. Plasticity in programming of effector and memory CD8+ T-cell formation, Immunol Rev. 2012;235(1):190–205.

[74] Shen H, Ackerman AL, Cody V et al. Enhanced and prolonged cross-presentation following endosomal escape of exogenous antigens encapsulated in biodegradable nanoparticles. Immunology. 2005;117(1):78–88.

[75] Silva AL, Rosalia RA, Varypataki E at al. Poly-(lactic-co-glycolic-acid)-based particulate vaccines: Particle uptake by dendritic cells is a key parameter for immune activation. Vaccine. 2015;33(7):847–54.

[76] Zehn D, Lee SY, Bevan MJ. Complete but curtailed T-cell response to very low-affinity antigen. Nature. 2009;458(7235):211-4.

[77] Bevan MJ. Helping the CD8+ T-cell response. Nat Rev Immunol. 2004;4:595-602.

[78] Rabenstein H, Behrendt AC, Ellwart JW et al. Differential kinetics of antigen dependency of CD4+ and CD8+ T cells. J Immunol. 2014;192(8):3507-17.

Chapter 5

[1] Fife B, Bluestone J. Control of peripheral T-cell tolerance and autoimmunity via the CTLA-4 and PD-1 pathways. Immunol Rev. 2008;224:166-82.

[2] Salgado R, Denkert C, Demaria S et al. The evaluation of tumor-infiltrating lymphocytes (TILs) in breast cancer: recommendations by an International TILs Working Group 2014. Ann Oncology. 2014;26 (2):259-71.

[3] Demaria S, Pikarsky E, Karin M et al. Cancer and inflammation: promise for biologic therapy. J Immunother. 2010;33:335-51.

[4] Silva AL, Rosalia RA, Varypataki E et al. Poly-(lactic-co-glycolic-acid)-based particulate vaccines: Particle uptake by dendritic cells is a key parameter for immune activation. Vaccine. 2015;33(7):847–54.

[5] Palucka AK, Ueno H, Fay J et al. Dendritic cells: a critical player in cancer therapy? J Immunother. 2008;31:793-805.

[6] Banchereau J, Steinman R. Dendritic cells and the control of immunity. Nature. 1998;19(392):245-52.

[7] Lesterhuis W, Haanen J, Punt C. Cancer immunotherapy-revisited. Nat Rev Drug Discov. 2011;10(8):591-600.

[8] Palucka K, Banchereau J. Cancer immunotherapy via dendritic cells. Nat Rev Cancer. 2012;12:265-77.

[9] Tacken PJ, Zeelenberg IS, Cruz LJ et al. Targeted delivery of TLR ligands to human and mouse dendritic cells strongly enhances adjuvanticity. Blood. 2011;118:6836-44.

[10] Cruz LJ, Rueda F, Cordobilla B et al. Targeting Nanosystems to Human DCs via Fc Receptor as an Effective Strategy to Deliver Antigen for Immunotherapy. Mol Pharm. 2011;8:1-13.

[11] Bolhassani A, Safaiyan S, Rafati S. Improvement of different vaccine delivery systems for cancer therapy. Mol Cancer. 2011;10:1-3.

[12] Zaritskaya L, Shurin M, Sayers T et al. New flow cytometric assays for monitoring cell-mediated cytotoxicity Expert Rev Vaccines. 2010;9(6):601-16.

[13] Heit A, Schmitz F, Haas T et al. Antigen co-encapsulated with adjuvants efficiently drive protective T cell immunity. Eur J Immunol. 2007;37:2063-74.

[14] Silva J, Zupancic E, Vandermeulen G et al. In vivo delivery of peptides and Toll-like receptor ligands by mannose-functionalized polymeric nanoparticles induces prophylactic and therapeutic anti-tumor immune responses in a melanoma model. J Control Release. 2015;28(198):91-103.

[15] Fan Y, Moon J. Nanoparticle Drug Delivery Systems Designed to Improve Cancer Vaccines and Immunotherapy. Vaccines. 2015;3(3):662-85.

[16] Jain RA. The manufacturing techniques of various drug loaded biodegradable poly(lactide-co-glycolide) (PLGA) devices. Biomaterials. 2000;21:2475–90.

[17] Bachmann M, Jennings G. Vaccine delivery: a matter of size, geometry, kinetics and molecular patterns. Nat Rev Immunol. 2010;10(11):787-96.

[18] Krishnamachari Y, Geary S, Lemke C et al. Nanoparticle Delivery Systems in Cancer Vaccines. Pharma Res. 2011;28(2):215-36.

[19] Park YM, Lee SJ, Kim YS et al. Nanoparticle-based vaccine delivery for cancer immunotherapy. Immune Netw. 2013;13:177-83.

[20] Thompson E, Enriquez H, Fu Y et al. Tumor masses support naive T cell infiltration, activation, and differentiation into effectors. J Exp Med. 2010;207(8):1791-804.

[21] Falo LJ, Kovacsovics-Bankowski M, Thompson K et al. Targeting antigen into the phagocytic pathway in vivo induces protective tumour immunity. Nat Med 1995;1(7):649-53.

[22] Hogquist KA, Jameson SC, Heath WR et al. T cell receptor antagonist peptides induce positive selection. Cell. 1994;76:17–27.

[23] Robertson JM, Jensen PE, Evavold BD. DO11.10 and OT-II T cells recognize a C-terminal ovalbumin 323-339 epitope. J Immunol. 2000;164(9):4706-12.

[24] Garinot M, Fiévez V, Pourcelle V et al. PEGylated PLGA-based nanoparticles targeting M cells for oral vaccination J Control Release. 2007;120(3):195-204.

[25] Florindo HF, Pandit S, Lacerda L et al. The enhancement of the immune response against S. equi antigens through the intranasal administration of poly-epsilon-caprolactone-based nanoparticles. Biomaterials. 2009;30:879-91.

[26] George TC, Fanning SL, Fitzgerald-Bocarsly P et al. Quantitative measurement of nuclear translocation events using similarity analysis of multispectral cellular images obtained in flow. J Immunol Methods. 2006;311(1-2):117-29.

[27] Quah BJC, Warren HS, Parish CR. Monitoring lymphocyte proliferation in vitro and in vivo with the intracellular fluorescent dye carboxyfluorescein diacetate succinimidyl ester. Nat Protoc 2. 2007;2(9):2049-56.

[28] Barber D, Wherry E, Ahmed R. Cutting edge: rapid in vivo killing by memory CD8 T cells. J Immunol Methods. 2003;171:27-31.

[29] Badovinac V, Harty J. Intracellular staining for TNF and IFN-γ detects different frequencies of antigen-specific CD8+ T cells. J Immunol Methods. 2000;238(1-2):107-17.

[30] Hume D. Macrophages as APC and the Dendritic Cell Myth. J Immunol Methods. 2008;181:5829-35.

[31] Aderem A. Phagocytosis and the Inflammatory Response. J Infect Dis. 2003;187(2):340-5.

[32] de Jong EC, Smits HH, Kapsenberg ML. Dendritic cell-mediated T cell polarization. Springer Semin Immunopathol. 2005;26:289-307.

[33] Fajardo-Moser M, Berzel S, Moll H. Mechanisms of dendritic cell-based vaccination against infection. Int J Med Microbiol. 2008;298:11-20.

[34] Rodriguez-Lorenzo L, Fytianos K, Blank F et al. Fluorescence-Encoded Gold Nanoparticles: Library Design and Modulation of Cellular Uptake into Dendritic Cells. Small. 2014;10(7):1341–50.

[35] Merad M, Sathe P, Helft J et al. The dendritic cell lineage: ontogeny and function of dendritic cells and their subsets in the steady state and the inflamed setting. Ann Rev Immunol. 2013;31:563-604.

[36] Malek T, Robb R, Shevach E. Identification and initial characterization of a rat monoclonal antibody reactive with the murine interleukin 2 receptor-ligand complex. Proc Natl Acad Sci USA. 1983;80(18):5694-8.

[37] Ziegler S, Ramsdell F, Alderson M. The activation antigen CD69. Stem Cells. 1994;12:456-65.

[38] Budd R, Cerottini J, Horvath C et al. Distinction of virgin and memory T lymphocytes. Stable acquisition of the Pgp-1 glycoprotein concomitant with antigenic stimulation. J Immunol. 1987;138:3120-9.

[39] Miyake K, Underhill C, Lesley J et al. Hyaluronate can function as a cell adhesion molecule and CD44 participates in hyaluronate recognition. J Exp Med. 1990;172:69-75.

[40] Lindell D, Moore T, McDonald R et al. Distinct Compartmentalization of CD4+ T-Cell Effector Function Versus Proliferative Capacity during Pulmonary Cryptococcosis. Am J Pathol.168(3):847-55.

[41] Oehen S, Brduscha-Riem K. Differentiation of Naive CTL to Effector and Memory CTL: Correlation of Effector Function with Phenotype and Cell Division. J Immunol. 1998;161:5338−46.

[42] Cho B, Wang C, Sugawa S et al. Functional differences between memory and naive CD8 T cells,. Proc Natl Acad Sci USA. 1999;96(6):2976-81.

[43] Zhang L, al. e. Intratumoral T cells, recurrence, and survival in epithelial ovarian cancer. N Engl J Med. 2003;348:203-13.

[44] Prall F et al. Prognostic role of CD8+ tumor-infiltrating lymphocytes in stage III colorectal cancer with and without microsatellite instability. Hum Pathol. 2004;35:808-16.

[45] Elder D. Tumor progression, early diagnosis and prognosis of melanoma. Acta Oncol. 1999;38:535-47.

[46] Wolint P, Betts M, Koup R et al. Immediate cytotoxicity but not degranulation distinguishes effector and memory subsets of CD8+ T cells. J Exp Med. 2004;199(7):925-36.

[47] He J, Hu Y, Hu M et al. Development of PD-1/PD-L1 Pathway in Tumor Immune Microenvironment and Treatment for Non-Small Cell Lung Cancer. Sci Rep. 2015;5:13110.

[48] Pardoll DM. The blockade of immune checkpoints in cancer immunotherapy. Nat Rev Cancer. 2012;12:252-64.

[49] Danhier F, Ansorena E, Silva JM et al. PLGA-based nanoparticles: an overview of biomedical applications. J Control Release. 2012;161:505-22.

[50] Babu A, Templeton A, Munshi A et al. Nanoparticle-Based Drug Delivery for Therapy of Lung Cancer: Progress and Challenges. J Nanomaterials. 2013;2013:11.

[51] Cahalan M, Parker I. Choreography of Cell Motility and Interaction Dynamics Imaged by Two-Photon Microscopy in Lymphoid Organs. Ann Rev Immunol. 2008;26:585–626.

[52] Radtke A, Kastenmüller W, Espinosa D et al. Lymph-Node Resident CD8α+ Dendritic Cells Capture Antigens from Migratory Malaria Sporozoites and Induce CD8+ T Cell Responses. PLoS Pathog. 2015;11(2):1-23.

[53] Pamujula S, Hazari S, Bolden G et al. Cellular delivery of PEGylated PLGA nanoparticles. J Pharm Pharmacol. 2012;64:61-7.

[54] Butcher NJ, Mortimer GM, Minchin RF. Drug delivery: Unravelling the stealth effect. Nat Nanotechnology. 2016;11.

[55] Hadrup S, Donia M, Thor Straten P. Effector CD4 and CD8 T cells and their role in the tumor microenvironment. Cancer microenviron. 2013;6:123-33.

[56] Goldberger O, Volovitz I, Machlenkin A, Vadai E, Tzehoval E, Eisenbach L. Exuberated Numbers of Tumor-Specific T Cells Result in Tumor Escape. Cancer Res. 2008;68(9):3450-7.

Chapter 6

[1] Knutson KL, Schiffman K, Disis ML. Immunization with a HER-2/neu helper peptide vaccine generates Her-2/neu CD8 T-cell immunity in cancer patients. J Clin Invest. 2001;107:8.

[2] Fioretti D, Iurescia S, Fazio VM, Rinaldi M. DNA vaccines: developing new strategies against cancer. J Biomed Biotechnol. 2010;2010:174378.

[3] Milani A, Sangiolo D, Montemurro F et al. Active immunotherapy in HER2 overexpressing breast cancer: current status and future perspectives. Ann Oncol. 2013;24:1740-8.

[4] Conniot J, Silva JM, Fernandes JG et al. Cancer immunotherapy: nanodelivery approaches for immune cell targeting and tracking. Front Chem. 2014;2:105.

[5] Bringmann A, Held SA, Heine A, Brossart P. RNA vaccines in cancer treatment. J Biomed Biotechnol. 2010;2010:623687.

[6] Thundimadathil J. Cancer treatment using peptides: current therapies and future prospects. J Amino Acids. 2012;2012:967347.

[7] Bei R, Scardino A. TAA polyepitope DNA-based vaccines: a potential tool for cancer therapy. J Biomed Biotechnol. 2010;2010:102758.

[8] Tabi Z, Man S. Challenges for cancer vaccine development. Adv Drug Deliv Rev. 2006;58:902-15.

[9] Banchereau J, Steinman R. Dendritic cells and the control of immunity. Nature. 1998;19(392):245-52.

[10] Howard CJ, Charleston B, Stephens SA et al. The role of dendritic cells in shaping the immune response. Anim Health Res Rev. 2004;5(2):191-5.:191-5.

[11] Mellman I. Dendritic Cells: Master Regulators of the Immune Response. Cancer Immunol Res. 2013;1(3):145-9.

[12] Saluja SS, Hanlon DJ, Sharp FA et al. Targeting human dendritic cells via DEC-205 using PLGA nanoparticles leads to enhanced cross-presentation of a melanoma-associated antigen. Int J Nanomedicine. 2014;9(1):5231-46.

[13] Garg NK, Dwivedi P, Prabha P et al. RNA pulsed dendritic cells: an approach for cancer immunotherapy. Vaccine. 2013;31:1141-56.

[14] Ali OA, Verbeke C, Johnson C et al. Identification of immune factors regulating antitumor immunity using polymeric vaccines with multiple adjuvants. Cancer Res. 2014;74:1670-81.

[15] Markman JL, Rekechenetskiy A, Holler E et al. Nanomedicine therapeutic approaches to overcome cancer drug resistance. Adv Drug Deliv Rev. 2013;65:1866-79.

[16] Silva JM, Videira M, Gaspar R et al. Immune system targeting by biodegradable nanoparticles for cancer vaccines. J Control Release. 2013;168(2):179-99.

[17] Palucka K, Banchereau J. Cancer immunotherapy via dendritic cells. Nat Rev Cancer. 2012;12:265-77.

[18] Dinarvand R, Sepehri N, Manoochehri S et al. Polylactide-co-glycolide nanoparticles for controlled delivery of anticancer agents. Int J Nanomedicine. 2011;6.

[19] Peer D, Karp J, Hong S et al. Nanocarriers as an emerging platform for cancer therapy. Nat Nanotechnol. 2007;2(12):751-60.

[20] Park YM, Lee SJ, Kim YS et al. Nanoparticle-based vaccine delivery for cancer immunotherapy. Immune Netw. 2013;13:177-83.

[21] Kim M-G, Park JY, Shon Y et al. Nanotechnology and vaccine development. Asian J Pharm Sci. 2014;9:227-35.

[22] Zupančič E, Peres C, Matos AI et al. Translational Peptide-associated Nanosystems: Promising Role as Cancer Vaccines. Curr Top Med Chem. 2016;16(3):291-313.

[23] Davis M, Chen Z, Shin D. Nanoparticle therapeutics: an emerging treatment modality for cancer. Nat Rev Drug Discov. 2008;7(9):771-82.

[24] Bolhassani A, Safaiyan S, Rafati S. Improvement of different vaccine delivery systems for cancer therapy. Mol Cancer. 2011;10:3.

[25] Fan Y, Moon J. Nanoparticle Drug Delivery Systems Designed to Improve Cancer Vaccines and Immunotherapy. Vaccines. 2015;3(3):662-85.

[26] Jain RA. The manufacturing techniques of various drug loaded biodegradable poly(lactide-co-glycolide) (PLGA) devices. Biomaterials. 2000;21:2475–90.

[27] Bachmann M, Jennings G. Vaccine delivery: a matter of size, geometry, kinetics and molecular patterns. Nat Rev Immunol. 2010;10(11):787-96.

[28] Hamdy S, Molavi O, Ma Z et al. Co-delivery of cancer-associated antigen and Toll-like receptor 4 ligand in PLGA nanoparticles induces potent CD8+ T cell-mediated anti-tumor immunity. Vaccine. 2008;26:5046-57.

[29] Pashine A, Valiante N, Ulmer J. Targeting the innate immune response with improved vaccine adjuvants. Nat Med. 2005;11(4):63-8.

[30] Zhao L, Seth A, Wibowo Net al. Nanoparticle vaccines. Vaccine. 2014;32:327- 37.

[31] Albanese A, Tang PS, Chan WC. The effect of nanoparticle size, shape, and surface chemistry on biological systems. Ann Rev Biomed Eng. 2012;14:1-16.

[32] Manolova V, Flace A, Bauer M et al. Nanoparticles target distinct dendritic cell populations according to their size. Eur J Immunol. 2008;38:1404-13.

[33] Park JH, Lee S, Kim J-H, et al. Polymeric nanomedicine for cancer therapy. Prog Polym Sci. 2008;33:113-37.

Chapter 7

[1] Liu J, Blake S, Smyth M et al. Improved mouse models to assess tumour immunity and irAEs after combination cancer immunotherapies. Clin Transl Immunol. 2014;3:e22.

[2] Knutson KL, Schiffman K, Disis ML. Immunization with a HER-2/neu helper peptide vaccine generates Her-2/neu CD8 T-cell immunity in cancer patients. J Clin Invest. 2001;107:1-8.

[3] Feng D, Shaikh A, Wang F. Recent Advance in Tumor associated Carbohydrate Antigens (TACAs)-based Antitumor Vaccines. ACS Chem Biol. 2016;11 (4):850-63.